Process Design and Integration of Refuse Derived Fuel (RDF) Gasification in Cement Manufacturing Process

THESIS

Submitted in partial fulfillment

of the requirements for the degree of

DOCTOR OF PHILOSOPHY

by

PRATEEK SHARMA

2018PHXF0501P

Under the supervision

of

Dr. PRATIK N SHETH

and Co-supervision of

Dr. B N MOHAPATRA

BIRLA INSTITUTE OF TECHNOLOGY AND SCIENCE

PILANI (RAJASTHAN) INDIA

2023

ॐ सर्वे भवन्तु सुखिनः ।
सर्वे सन्तु निरामयाः ।।
सर्वे भद्राणी पश्यन्तु ।
मा कश्चित् दुःख भाग्भवेत् ।।
ॐ शान्तिः शान्तिः शान्तिः ।।

May all be prosperous and happy.
May all be free from illness.
May all see what is spiritually uplifting.
May no one suffer.
Om peace, peace, peace !

Dedicated to

My Grandparents
Parents
Wife
&
My Loving Daughter

Birla Institute of Technology & Science, Pilani
Pilani Campus

CERTIFICATE

This is to certify that the thesis titled **"Process Design and Integration of Refuse Derived Fuel (RDF) Gasification in Cement Manufacturing Process,"** submitted by **Mr. Prateek Sharma** ID No **2018PHXF0501P for** the award of Ph.D. Degree of the Institute embodies original work done by him under my supervision.

Signature (Supervisor):____________________

Prof. PRATIK N SHETH

Professor and Head, Department of Chemical Engineering,

BITS Pilani, Pilani campus, India

Date: 25/9/23

Signature (Co-supervisor):____________________

Dr. BIBEKANANDA MOHAPATRA

Former Director General,

National Council for Cement and Building Materials, Ballabgarh, Haryana, India

Date: 25/09/2023

Acknowledgements

This thesis is the culmination of four years of intensive work. It embodies the work carried out during this period as a PhD scholar. This thesis would not have seen the light of day without the help available to me from various quarters. At the very outset, I am pleased to express my deep gratitude to my guide, Prof. Pratik N Sheth, (Professor and Head-Chemical Engineering Department), for his constant encouragement and valuable suggestions. He has been of immense moral support throughout this research work. I have been truly privileged to have the opportunity to work under his continuous supervision. I would also like to thank my co-guide Dr. B.N. Mohapatra, (Former Director General – National Council for Cement and Building Materials), for his support throughout this work. He introduced me and highlighted the work carried out in this research at various national and international forums, which is of immense importance.

I sincerely thank the Doctoral Advisory Committee members of BITS Pilani- Prof. Suresh Gupta, Professor (Chemical Engineering Department) and Prof. Manoj Kumar Soni, Professor (Mechanical Engineering Department) for their support and suggestions during this research period. Their advice has been of great significance. Their experience enriched my work and paved the way to move ahead.

My sincere thanks go to Prof. V. Ramgopal Rao, Vice-Chancellor, BITS Pilani, for allowing me to carry out the PhD work in BITS. I am thankful to Prof. Sudhir kumar Barai, Director (Pilani Campus), Prof. Suman Kundu, Director (Goa Campus), Prof. G Sundar, Director (Hyderabad Campus), Prof. Srinivasan Madapusi, Director (Dubai Campus), Prof. Sanjay Kumar Verma, Dean (Administration), Prof. M. B. Srinivas Dean, Academic – Graduate Studies & Research and Prof. Shamik Chakraborty, Associate Dean, Academic – Graduate Studies & Research, for providing the necessary facility and infrastructure to carry out this work.

I extend my special thanks to Prof. Hare krishna Mohanta, Prof Banasri Roy, Prof. Arvind Kumar Sharma, Dr Amit Jain, Dr Srinivas Appari, Dr Pradipta Chattopadhyay, Dr Ajaya Kumar Pani, Dr. Smita Raghuvanshi and other members of Chemical Engineering Department for their valuable advice and moral support throughout the work.

I wish to thank Dr. D K Panda (Joint Director and Head of Centre- Centre for Mining, Environment, Plant Engineering, and Operation, NCCBM) for his guidance and advice during difficult junctures. My special thanks and appreciation are also due to Mr K P K Reddy for arranging RDF samples and Mr Anand Bohra for providing technical input throughout the work. I would also like to mention my senior colleague, Mr Kapil Kukreja, who supported me at every stage. I extend thanks to Ms Moon Chourasia for her support in RDF characterization work. I am also grateful to Mr Subhadip Sen for supporting me in modelling work. For the paucity of space, I cannot name all my colleagues but their help is sincerely acknowledged.

Besides all the faculty members and other friends, I would also take this opportunity to thank Mr. Ashok Saini, Mr. Kuldeep Kumar, Mr. Jeevan Verma, Mr Suresh Kumar Sharma and Mr Jangvir for their help in carrying out the experimental work. Mr. Ashok Saini also supported me a lot during the palletization work.

I am short of words to express my gratitude to my parents, Dr. Satish Chandra Sharma and Smt. Roopa Sharma, for having stood by me through the thick and thin of every aspect of my life, this thesis is no exception. This work could not be possible without their constant help and cooperation.

This journey would have been incomplete without my wife Mansi Sharma and daughter Krisha Sharma who has been my source of inspiration and motivation.

Last but not least, I pray and thank ALMIGHTY GOD for showering HIS blessings and giving me inner strength and patience.

PRATEEK SHARMA

Abstract

Municipal solid waste (MSW) disposal is considered one of the potential problems worldwide. The global MSW generation is more than 2.1 billion tonnes annually, of which 16% is recycled and 46% is disposed of unsustainably. It is expected to increase to 3.4 billion tonnes by 2050. It is to be noted that the top ten cement-producing nations are also top solid waste-producing countries. The combustible fraction (15-20%) consists of paper, textiles, polyethene, rags, leather, rubber, non-recyclable plastic, and other non-biodegradable fraction of MSW, which is processed into Refuse Derived Fuel (RDF). The energy-intensive cement industry utilizes conventional fuels like coal and petcoke for clinkerisation. Hence, tremendous potential lies in the cement sector of these nations to utilize RDF as an alternative fuel. As per the current scenario, the availability of RDF, considering the proximity of cement plants in India, is estimated to be around 13600 tonnes of RDF per day, equivalent to 4.96 million tonnes per annum.

RDF has been identified as one of the major potential fuels for the Indian cement industry to achieve a thermal substitution rate (TSR) of around 30% by 2030. The current TSR is at 6%. The 24% jump in TSR can support decarbonization in the cement industry in a big way. After consistent efforts of the Indian cement industry, government, and other stakeholders, % TSR based on RDF is picking up. However, cement plants utilizing RDF directly as a fuel face operational issues due to heterogeneity, high ash, high chloride etc. In this regard, RDF gasification as a thermochemical technology can be a game-changer in tackling some of these issues. The producer gas generated may be directly burned in the calciner/kiln without gas cleaning. Although gasification technology is not new, its application in cement manufacturing is still developing. The cement plant needs an entirely new set up of gasifiers to be integrated with its existing pyro-processing system. Some patents and articles reported in the literature ideated several gasifier-calciner integration configurations that may require cement plant retrofit. However, some modelling and experimental studies are needed to establish RDF-based producer gas as an alternative fuel.

In the present work, the characterization of six RDF samples (A, B, C, D, E and F) from different sources is performed, followed by RDF gasification experimental studies and model development of the RDF gasifier and calciner. RDF characterization has been done using TGA and Py-GC/MS. The experimental runs were carried out in a downdraft gasifier for RDF gasification and RDF-biomass mix co-gasification. To study the integration of gasification with calciner, stoichiometric and Aspen Plus-based models have been developed for calciner along with material and energy balance which predicted calciner outlet temperature, gas composition, SO_2 and CO_2 for co-processing of producer gas as an alternative fuel in white cement plant. Later, techno-economic feasibility is carried out to co-process producer gas via RDF gasification in a white cement plant to achieve 15% TSR.

Gasification experiments were performed with RDF fluff and RDF pellets as feedstock and air as gasifying agents. The gas yield ranges from 2.43-3.65 Nm^3/kg RDF with LHV of 1.87-2.24 MJ/Nm^3 RDF and CGE of 44-60%. It is observed that RDF containing high ash content in the range of ~31-51% is quite challenging to gasify in a downdraft-type gasifier with operational bridging and clinker formation issues. Upon adding O_2 to air as a gasifying agent, LHV and CGE increased by 78%and 30%, respectively. Further, more experimental runs were carried out using RDF and biomass mix in different ratios using air as a gasifying agent. The results indicated the gas yield in the 2.42-3.27 Nm^3/kg fuel range with LHV of 2.46-3.88 MJ/Nm^3 RDF and CGE of 46.83-77.65%. Upon adding O_2 to air as a gasifying agent for a 50:50 RDF-biomass mix, LHV and CGE increased by 35.5% and 8.35%, respectively. It can be inferred that RDF-biomass mix co-gasification results are better than RDF gasification in terms of LHV and CGE.

The proposed multizone gasifier model for RDF gasification has four zones, i.e., drying, pyrolysis, oxidation/combustion and reduction/gasification. In each zone, different thermochemical phenomena occur. A stoichiometric approach is followed for modelling the drying, pyrolysis and combustion zone. The reduction zone is modelled as a cylindrical fixed bed reactor with a uniform cross-sectional area. The developed differential equations are solved using MATLAB to predict the producer gas properties. The model can predict the output of each zone satisfactorily since the model assumptions are more realistic and cater to the heterogeneous nature of RDF. The impact of equivalence ratio (ER), moisture content and reduction zone length on the performance of the gasifier are evaluated. For calciner modelling, at 15% TSR, both the models (stoichiometric and Aspen Plus-based) predicted the calciner outlet temperature accurately compared to the baseline scenario (100% petcoke firing). Considering the biogenic content, CO_2 mitigation potential due to RDF utilization as producer gas is estimated to be 10.5% of the baseline scenario at 15% TSR.

The economic feasibility for 15% TSR in calciner through co-processing of producer gas has been commenced for ten years of plant operation. It has been chalked out in two phases; 8% TSR during phase I (three years) and 15% TSR during the next seven years of plant operation (phase II). An MS Excel model has been developed to evaluate economic performance. The capital cost investment is estimated to be Rs 71.6 million. The projected revenue is in terms of fuel savings, power savings and savings under the BEE-PAT scheme. The IRR is calculated to be 18.30% with a discounted payback period of five years and seven months.

Keywords: *Refuse derived fuel; Biomass; White cement; Calciner; MATLAB; Gasification; Techno-economic feasibility.*

Contents

List of Figures

List of Tables

Nomenclature

A	Gasifier bed cross-sectional area (m^2)
A_i	Frequency factor for reaction i (1/s)
ANFIS	Adaptive neuro-fuzzy inference system
c_x	Molar heat capacity of the species x (kJ/mol/k)
$C_{p,w}$	Specific heat of water
CRF	Char reactivity factor
DD	Down draft
E_i	Activation energy of species (kJ/mol)
ER	Equivalence ratio
FCM	Fuzzy c-means
ΔH_R	Heat of reaction
$\Delta h_{v,w}$	Latent heat of the vaporization of water
IFRF	International flame research foundation
K_i	Equilibrium constant
MC	Moisture content
MTN	Multi-dimensional taylor network
MW_{H_2O}	Molecular weight of H_2O
MW_{RDF}	Molecular weight of RDF
p	Total pressure (Pa)
PTG	Plasma torch gasification
Q_l	Latent heat required for moisture vaporization
Q_s	Sensible heat required to reach the drying temperature
r_i	Rate of reaction i ($mol/m^3/s$)
R_x	Net rate of creation of species x by chemical reactions
R	Gas constant (kJ/mol/k)

v	Superficial gas velocity (m/s)
w	Moisture content per mole of the fuel
x	Stoichiometric amount of air
y	Actual amount of air supplied

Greek letters

$\emptyset$	Equivalence ratio
ρ	Mass density of the fluid

Subscripts

AF	Alternative fuel
CI	Calciner inlet
FG	Flue gas
FG-K	Kiln exit gas
M	Hot meal
nj	Number of moles of constituents of combustion zone output
PF	Primary fuel
TA	Tertiary air
TR	Transport air

CHAPTER – 1

INTRODUCTION

1.0 Introduction

Cement is one of the key essentials in the construction sector and forms the backbone of a nation's economy. The total world cement production was around 4.1 billion tonnes in 2019, with India being the second-largest cement producer after China [1, 2]. The installed capacity and production of the Indian cement industry are 594.14 million tonnes and 361 million tonnes in the year 2021-22. There are 333 cement manufacturing units in India comprising 150 integrated cement plants, 116 grinding units, 5 clinkerization units, and 62 mini cement plants [3]. The cement consumption in India is around 260 kg per capita compared to the global average of 540 kg per capita, which shows significant potential for industry growth [3]. According to the technology roadmap by the international energy agency [4], global cement production is also poised to grow by 12-23% from 2014 to 2050. Globally, the cement sector leads to around 7% of the annual anthropogenic greenhouse gas emissions [5].

Cement manufacturing is an energy-intensive process that requires ~3.3 GJ/tonne of clinker [6], with a significant share of heat input from the combustion of fossil fuels. Waste utilization as an alternative fuel (AF) for co-processing in the cement industry has gained popularity due to its key advantage of complete waste destruction in a rotary kiln at 1400-1450°C without impacting clinker quality [7]. The utilization of AF in the cement industry is measured in terms of the thermal substitution rate (TSR), the rate of substitution of fossil fuels by alternative fuels in terms of thermal energy. Waste utilization as an alternative fuel has been identified as a key lever in mitigating CO_2 emissions in cement plants. The percentage of fossil fuel utilization in global cement production is expected to reduce from 94% (2014 as the baseline year) to 67-70% in 2050. It will lead to a reduction in direct CO_2 intensity to the tune of 32-38% [4]. The following section describes the status of alternative fuel utilization in the cement industry.

1.1 Status of waste co-processing as an alternative fuel in the cement industry

The TSR for alternative fuel utilization in the Indian cement industry in 2022 is around 6%, which is very low compared to the European nations, of approximately 46%, and the world average of 18%, as shown in Fig 1.1.

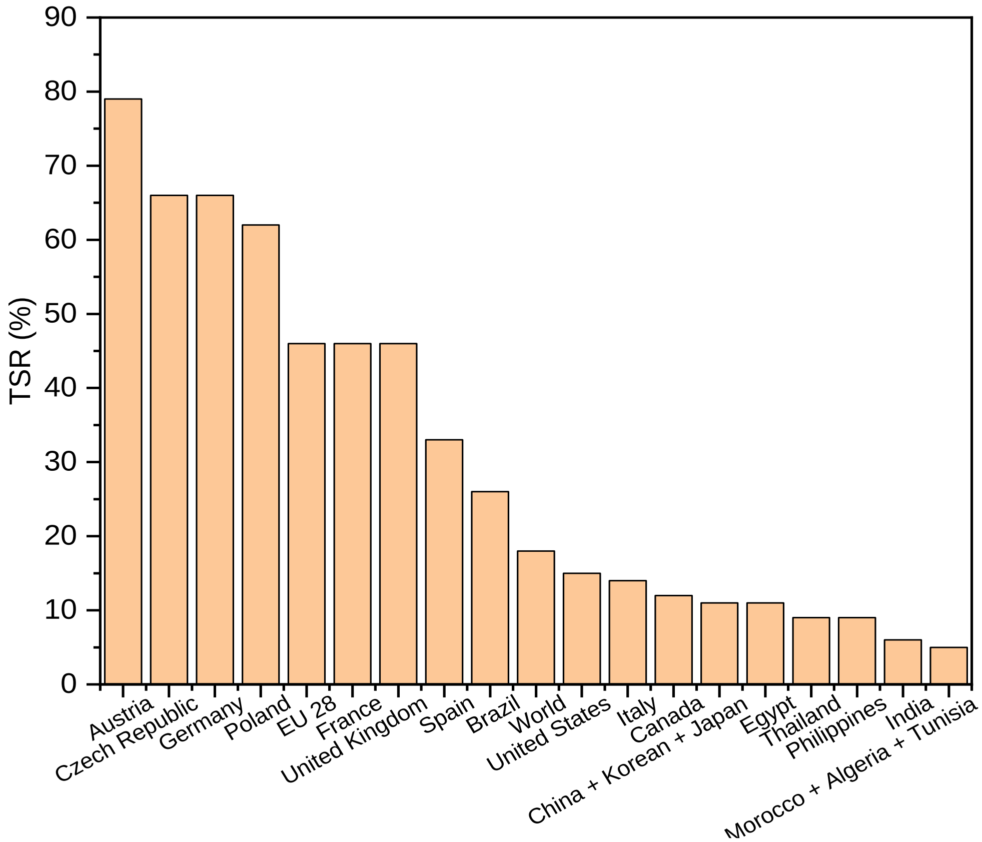

Fig. 1.1 Status of % TSR of the cement industry for different nations [8]

The major cement companies in India, Ambuja Cements Limited, ACC Limited, Ultratech Cement Limited and Shree Cement Limited, had TSR of 4.6, 6.9, 3.1 and 5.0%, respectively, in FY 2020-21 [9]. Dalmia Cement Limited stands at 12.45% TSR for FY 2020-21, with a significant share from RDF, plastics and biomass [10]. Few cement plants have achieved TSR in the range of 25-30% on a month average [11, 12]. The type of waste utilized as an alternative fuel, along with the source of generating industry and quantity, is given in Table 1.1.

Table 1.1 Type of waste utilized as AF in the Indian cement industry [7, 13-15]

Source Industry	Type of waste generated	Generation quantity (million tonnes per annum)
Urban local bodies	Refuse-derived fuel from municipal solid waste (MSW)	10.47 [16]
Agricultural	*Biomass (Rice husk, cotton stalk, etc.)	230 [17]
Woods and related	Wood chips	
Automobile	ETP Sludge, paint sludge, oily rags	7.17[18]
Paints and related	Paint sludge, chemical sludge, process waste	
Petroleum	Oil sludge spent catalyst	
Pharmaceutical	Expired medicines, Process/distillation residue, organic spent solvent, spent carbon	
Beverage	Spent Carbon, Effluent treatment plant (ETP) Sludge	
Textile	ETP Sludge	
Paper, Plastics	Plastic waste	3.47 [19]
Tyres	Tyre-derived fuel (TDF), Carbon black	0.60 [20, 21]
FMCG, Footwear	Expired products, plastics	3.30 (E)[22, 23]

*Surplus, E: Estimated

It can be inferred from Table 1.1 that RDF and biomass are the two most potential alternative fuels for the cement industry. The surplus biomass generation is 230 million tonnes, the highest of all the wastes with the maximum potential for fuel use. However, biomass has several other uses, and its availability is uncertain. On the contrary, MSW-based RDF is available round the year. Moreover, RDF utilization as a fuel can also be considered a waste management solution reducing waste going to landfills and mitigating environmental hazards. The next section describes RDF application in the cement industry.

1.1.1 RDF utilization in the Indian cement industry

1.1.1.1 Municipal Solid Waste (MSW)

Municipal solid waste (MSW) is defined as household waste, commercial and market area waste, slaughterhouse waste, institutional waste (e.g., from schools and community halls), horticultural waste, waste from road sweeping, and silt from drainage. MSW management is one of the most challenging problems for countries all around the globe. The global municipal solid waste generation is more than 2.1 billion tonnes annually, of which 16% is recycled, and 46% is disposed off unsustainably [24]. It is expected to increase to 3.4 billion tonnes by 2050. The top ten cement-producing nations are also top solid waste-producing countries; thereby, the tremendous potential lies in the cement sector of these nations to utilize this waste [25]. It is anticipated that MSW co-processing in cement kilns in China can replace 75% of landfills and have substantial environmental benefits [26].

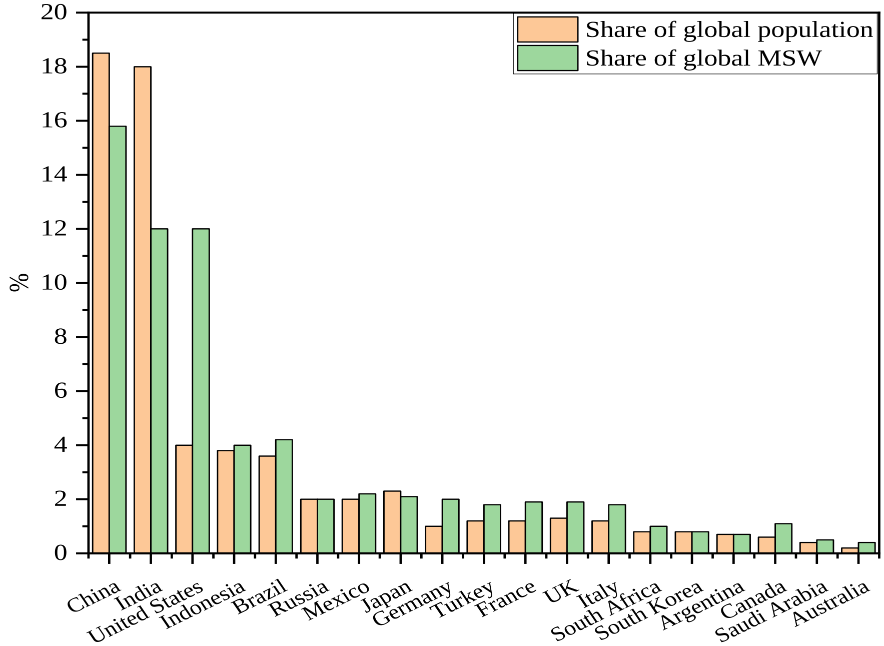

Fig. 1.2 Status of global municipal solid waste generation [24]

In India, MSW generation is around 62-65 million tonnes, estimated to be 130 million tonnes by 2031 [16, 27]. The quantity and characteristics of solid waste may vary from place to place depending upon the type of population and their living style.

1.1.2 Treatment and disposal of MSW

The disposal of MSW is still an issue of concern in India despite enacting various legislations. There are mainly six types of MSW disposal practices in India; open area landfilling, sanitary landfills properly designed with lining and leachate collection wells, composting, waste to energy, and RDF as fuel. Composting and waste to energy (WTE) are significant waste disposal methods in India. The combustibles consisting of paper, textile, polyethene, diapers, sanitary napkins, rags, leather, rubber, non-recyclable plastic, and other non-biodegradable fraction of MSW is processed into Refuse Derived Fuel (RDF). The RDF obtained from MSW is generally 15-20%, excluding compostable and inert fractions. As per the current scenario, the availability of RDF, considering the proximity of cement plants in India, is estimated to be around 13600 tonnes of RDF per day, equivalent to 4.96 million tonnes per annum [16]. A guideline has been developed by the ministry of housing and urban affairs (MoHUA), where Indian RDF grading has been done based on the quality of RDF [16].

1.1.3 Utilization in the Indian cement industry

The cement industry has always acted as a backbone for using industrial waste like fly ash from thermal power plants, slag from steel plants, and other hazardous/non-hazardous wastes. Still, the same is not happening in the case of RDF. After consistent efforts of the cement industry, government, and other stakeholders,% TSR based on RDF is picking up. The industry aims to achieve a total TSR of around 30% by 2030 [28], which looks daunting. As per CII estimates, RDF is the most potential waste to achieve 25% TSR by 2025 in the Indian cement industry, and 14.27% TSR of the total is envisaged from RDF [29].

1.1.4 Global Scenario

Co-processing in cement plants has been practised since 1970 in developed countries. Countries like Germany, Poland, and Austria have vast experience in RDF utilization. Some European countries like the UK and Ireland have high landfill taxes, thus exporting RDF to other countries. In Germany, landfilling was banned in 2005, and by 2008, Germany had replaced 54% of conventional fuel usage with RDF in cement plants. The thermal substitution rate of Poland's cement industry is very high at above 60% and some plants have a TSR of more than 85% with a significant share of RDF [16]. The Kujawy Cement Plant in Poland of 4500 tpd has achieved 75% TSR by solid alternative fuels. The plant is receiving pre-processed RDF. The plant adopted the latest lab facilities for quick and accurate assessment of key parameters i.e. Hg, Cl, moisture, size, etc., for acceptance of RDF. A company called Novago has an annual RDF production capacity of 200,000 tonnes, and the fuel is supplied to cement plants & power plants. CBR Heidelberg Cement at Lixhe, Belgium, uses 35% coal and 65% alternative fuel. RDF is received from M/s Recyfuel in processed form and utilized in kiln and calciner burners. The Austrian cement industry also has a high %TSR to the tune of 80%. Legal compliance, quality checks, and quality assurances have helped increase RDF utilization in cement plants. Japan has a different scenario. Due to land scarcity, landfill is not a valid option; hence Japan primarily relies on the thermal treatment of RDF. Around 43 million tonnes of MSW were generated in 2015, and 81% was incinerated or gasified [16].

1.1.5 Status of CO_2 emissions for the Indian cement industry

Cement, steel, chemicals, etc., are considered hard-to-abate sectors, and it is technologically challenging to reduce process-related CO_2 emissions. The Indian cement industry has brought down its CO_2 emission factor from 1.12 t CO_2/t cement in 1996 to 0.670 t of CO_2/t cement in 2017 [30]. The proactive steps taken by the Indian cement industry have contributed to achieving the goal of a reduction in carbon intensity. The present specific direct CO_2 emissions of major cement companies vary in the range of 488-589 kg CO_2/t cement [9]. Further, to achieve the target of Net Zero by 2070, decarbonization of the Indian cement industry is required. The identified levers in the low carbon technology roadmap of the Indian cement industry are (i) Substitution of Clinker, (ii) **Alternative Fuel** and Raw Materials, (iii)

Improving Energy Efficiency, (iv) Installation of Waste Heat Recovery, and (v) Newer technologies like Renewable Energy, Novel Cement, Carbon Capture and Storage/Utilization. Out of all, alternative fuel utilization is emerging as one of the biggest contributors in abating CO_2 emissions in the Indian cement industry, as the waste being dumped or burnt earlier is being utilized in cement rotary kiln for clinker production.

1.1.6 Challenges related to RDF utilization in the cement industry

RDF utilization as an alternative fuel has its challenges. The poor quality of waste, improper segregation, low calorific value, high chloride content, cost fluctuations, inadequate characterization facilities, system design flaws, operational issues, etc., are some of the challenges faced by the Indian cement industry during RDF utilization. The ineffective shredding, absence of cost-effective moisture drying technology, and screening are the key bottlenecks when utilizing waste like RDF, plastics and mixed type of waste, etc. The wear and tear of shredding blades and feeding systems are also bottlenecks in some cases. The presence of high chloride and alkalis in RDF gets combined with conventional fuel petcoke sulphur resulting in coating formation. High volatility of chloride results in its circulation inside kiln system. Thus, clogging takes place in lower preheater cyclones.

Sharma et al. [31] and Kukreja et al. [32, 33] highlighted several issues related to pre-processing and co-processing faced by cement plants in India during RDF utilization. The lower heat value of 7.53 MJ/kg with 25% moisture and odour are some of the major challenges observed by Dalmia Cement Ltd.-Dalmiapuram during RDF utilization, as reported by Rajamohan et al. [34]. One of the most common issues highlighted is the high chloride content in RDF, leading to operational challenges. Abbas and Akritopoulos [35] reported that some

European cement plants achieved a TSR of 80-100% through RDF in the calciner. However, some operational challenges, like hot spots and high CO emissions, need further optimization. The plants in European nations have well-established pre-processing and co-processing facilities and kiln bypass systems that facilitate high TSR in their plants. China has 8% TSR with co-processing in more than 100 cement plants. It co-processes 3.5 million tonnes of municipal solid waste annually, with 10-15% plastic and 2 million tonnes of RDF containing 30-40% plastic [36]. Out of 150 integrated cement plants in India, 96 plants are co-processing hazardous waste, mainly in the calciner [37]. Only a few cement plants achieved a TSR of more than 15% [11]. Two Indian cement plants have recently installed a kiln bypass and are operating at 35% TSR using RDF sustainably as the calciner's primary alternative fuel. Therefore, more plants have to opt for the kiln bypass to sustainably reach the value of 25% TSR throughout the year. One of the environmental issues associated with kiln bypass is the disposal of kiln bypass dust as it may contain high concentration of chlorides, alkalis and other deleterious elements. In view of above, creating an enabling infrastructure for the collection, segregation, and transportation of alternative fuels and handling of bypass dust is also required. Cement plants that have achieved 15-20% TSR and aiming to increase their TSR need to invest in pre-processing and co-processing systems to maximize utilization in the calciner and kiln.

RDF producers process MSW and segregation, shredding, and screening of the waste to make it worth utilization for industries. It becomes part of the RDF production cost. Cement plants are mostly located far from cities, while RDF is mostly available near cities resulting in the high cost of transportation. These factors bring the overall cost close to the price of conventional fuel in India and sometimes even higher in cement plants. RDF is generally associated with high ash content which has no heating value and is undesirable for the user.

Further, to be utilized as fuel, replacing conventional fuel, cement plants have to make a certain investment for handling, storage, and feeding of RDF. Ministry of environment, forest, and climate change (MoEFCC) notified emission norms for the co-processing of waste by cement plants vide Gazette Notification dated 10th May 2016 [38]. Apart from the parameter's criteria for pollutants like PM, SO_2, and NO_X, emission limits for other pollutants, i.e. HCl, SO_2, CO, TOC, HF, NO_X, dioxins and furans, and heavy metals were also notified. The real challenge lies in meeting these emission norms and consistent clinker quality during higher percentage TSR from RDF with high chloride content.

Hence, it is the need of the hour that the cement industry, particularly in India, looks for other options of thermochemical treatment like waste gasification to overcome the challenges mentioned above. Producer gas obtained from RDF gasification shall have better combustion properties in the calciner than small-size solid waste directly fed to the calciner. Thus, hard-to-burn fuel can be made easily combustible. Gaseous fuels are clean and easy to transport than solid fuels. Combustion efficiency is high and requires low excess air as compared to solid alternative fuels. It has been discussed in detail in the next section.

1.2 RDF gasification - an opportunity for the cement industry to enhance TSR

Gasification may be considered a suitable waste treatment technology for converting solid waste to clean gaseous fuel by impeding impurities entering the pyro-processing system. It offers unique advantages as the product is producer gas and may be directly burned in the calciner/kiln without gas cleaning. In addition, high moisture, which is problematic to the kiln system, will participate in gasification reactions to a certain extent and increase the heating value of producer gas by contributing to H_2 production through a water gas shift reaction. The heating value variations of the input fuel mix (coal and producer gas) are reduced substantially due to consistent producer gas composition. Moreover, it offers better clinker quality due to no additional ash.

Although gasification technology is not new, its application in the cement industry is still developing. The cement plant needs an entirely new set up of gasifiers to be integrated with its existing pyro-processing system. Some patents and articles reported in the literature ideated several gasifier-calciner integration configurations that may require cement plant retrofit. However, some modelling and experimental studies are required to establish RDF-based producer gas as an alternative fuel. Modelling and simulating process parameters in a calciner provide an accurate picture of the impact of fuel utilization in the system without rigorous full-scale trial runs. Researchers have used macroscopic, microscopic tools, soft models, kinetic models, mathematical models, machine learning, fuzzy logic, etc., to model the calciner [39-42]. The researchers have predicted calciner outlet temperature, gas composition and degree of calcination, etc., at varying TSR. Most of the models concentrate on solid alternative fuels. Impact assessment with a fuel mix of solid and gaseous fuels needs in-depth analysis. It has to be supported by accurate producer gas composition from the gasifier model. To decide the % TSR in a cement plant using producer gas, producer gas components, including minor components, LHV, gas yield and CGE of producer gas is of utmost importance.

Several equilibrium, phenomenological, multi-zone, and Aspen Plus-based models were reported in the literature for biomass gasification [43-45]. However, the researchers could not establish their suitability for complex materials like RDF. Later, some Aspen Plus and

Gibbs free energy-based RDF gasifier models were developed [46-48]. However, they have certain limitations. The Gibbs free energy-based model considered all reactions in equilibrium without any solid ash and tar. The Aspen Plus models reported so far also neglected tar formation. Tar is an important criterion when designing a downdraft gasifier, as a higher amount of tar can be a bottleneck during the gasifier operation. Hence, there is a need for models incorporating tar steam reforming in the reduction zone of RDF gasification. Moreover, the input RDF to gasifier models has been considered dry or dry ash free. Indian RDF has a high ash content of 30-40%; thus, an ash-free basis will enhance the elemental components, with a corresponding rise in LHV and the producer gas yield. It necessitates the inclusion of RDF ash content in the molecular weight of RDF to predict the realistic values of producer gas properties. The modelling studies also supplement experimental studies. For experimental studies, the researchers have used downdraft-type gasifiers for RDF gasification [49-56], except for one study each on an updraft gasifier [57] and a bench-scale rotary kiln reactor [58]. These studies are primarily focussed on power generation. A few studies have also taken up the co-gasification of RDF and biomass. The major limitation of these studies is input RDF properties where the maximum RDF ash content is 15% which is too low considering the Indian scenario. Hence, high ash RDF gasification and co-gasification with biomass trials must be explored further to design future gasifiers to take up high ash content without clinkering problems.

After successful integration, it is envisaged that cement plants facing bottlenecks to enhance TSR above 15-20% shall benefit from gasification technology. Even white cement plants can utilize RDF in their pyro-processing system without affecting the whiteness of clinker. As per IS 8042, the iron content in white cement should be less than 1%, and the degree of whiteness should be greater than 70%. As producer gas has no residual ash, the whiteness index and iron content can be easily maintained. However, its techno economics needs to be carried out.

The government of India has set a target of 100 million tonnes of coal gasification by the year 2030 with an investment of Rs 0.4 million crores [59, 60]. Once gasified coal usage is achieved in the cement industry, it will promote co-gasification of coal and waste, having the advantage of improved producer gas quality.

1.3 Objectives of the research

- To carry out the experimental study of RDF gasification and evaluate the performance of the process
- To develop the process models for system integration of RDF gasification and calciner of the cement plant
- To study the effects of co-processing of producer gas with conventional fuel on calciner performance
- To carry out the techno-economic analysis of RDF gasification for a cement plant with an overall target of 15% thermal substitution rate (TSR)

1.4 Organization of the Thesis

Considering the broad research objectives, the thesis consists of seven chapters.

Chapter-1 discusses the overview of the cement industry with the significance of alternative fuel utilization. RDF derived from MSW is projected as one of the key alternative fuels to replace the main fuel highlighting the challenges and issues cement plants face in achieving high TSR through RDF firing. A concept of RDF gasification and its integration into the cement industry has been proposed. Objectives and methodology have been discussed in detail in this chapter.

Chapter-2 reviews the prior research work on RDF gasification and the integration of RDF gasification in the cement manufacturing process. After the detailed review, the identified research gaps are discussed.

Chapter-3 describes the experimental setup for RDF characterization, RDF gasification, procedures and measuring instruments. The characterization techniques like pyrolysis-gas chromatography, mass spectrometry (Py-GC/MS), and thermogravimetric analyzer (TGA) used for RDF characterization have been elaborated in detail. The analytical instrument used for determining the producer gas composition is gas chromatography (GC)-thermal conductivity detector (TCD). The gasifier experiments were carried out in a downdraft gasifier installed at BITS Pilani setup. Four types of RDF, i.e., RDF C, D, E, and F, having LHV in the range of 12.07-14.36 MJ/kg, are used to carry out experiments. RDF C and F are fluffy types, while RDF D and E are in pellets form. Out of these, RDF D, E, and F are mixed with biomass to perform co-gasification.

Chapter-4 discusses the model development (one for RDF gasification and two for cement plant calciner), where producer gas derived from RDF gasification act as an input to the calciner. The downdraft gasifier simulation was carried out using MATLAB software, while the calciner model simulation was carried out in Aspen Plus and an excel spread sheet. The validation of models is also presented.

Chapter-5 provide elaborative discussions on gasifier and calciner modelling and experimental studies along with validation. A comparative analysis has been done for two calciner models. Experimental studies compared the performance of RDF gasification with RDF-biomass mix co-gasification in terms of heating value, producer gas yield, and cold gas efficiency.

Chapter-6 explains the white cement manufacturing process and the gasification potential for the white cement industry in India. The techno-economic feasibility of RDF gasification in a white cement plant calciner has been undertaken. The capital investment required, operating cost, and profitability have been discussed in detail. Several key economic indicators like IRR, NPV, and discounted payback are also presented. The sensitivity analysis for key financial indicators has been worked out by varying critical parameters viz RDF price, producer gas yield, capital cost, operating hours of the gasifier, and ash market by ± 10%.

Chapter-7 concludes the entire research work by showing the gaps in the literature, the scope of work, a summary of the results, recommendations, and the future scope of the work. The key takeaways of the study have been indicated in bullet points.

CHAPTER – 2

LITERATURE REVIEW

2.0 Literature review

This chapter presents a technical review of the prior research on alternate fuel utilization in the cement plant through direct firing or gasification. This review covers the study of experimental and modelling work carried out in the area of RDF gasification and their applicability in cement plant calciner, particularly in a white cement plant where there is no established alternative fuel. It also focuses on identifying the research gaps in the integration of the gasification process to the calcination process in cement plants.

2.1 Alternative fuel utilization in grey cement

The cement industry is energy intensive using coal, petcoke, oil, and gas as the primary fuel, and different types of waste as alternative fuels are used to replace conventional fuels.

2.1.1 Direct firing of RDF

Solid fuels like coal and petcoke are finely ground before firing in a kiln and calciner to meet the heat requirement for calcination and clinkerisation, respectively. Any other solid alternative fuel, like RDF with separate handling and firing system, can replace these fuels. The direct firing aspects of RDF in kiln and calciner have been discussed in the next section.

2.1.2 Direct firing of AF/RDF in the calciner

Limestone calcination is an endothermic reaction with the heat of reaction of 178 kJ/mole [61]. This process is critical for clinker production as raw meal calcination affects the clinker quality, plant operation, and environmental emissions [62]. A calciner is a preferred option for AF firing since it requires a low temperature (800-900°C) for calcination compared to clinkerisation (1400-1450°C) in the kiln. It can handle low heat value fuels with varying characteristics. Specific energy consumption reduction targets, enhanced waste utilization and pollutant emission mitigation have led to calciner systems modification. Low NOx calciner [63], staged combustion [64], a pre-combustion chamber for alternative fuels [65-67], calciner loop duct extension and controlled hot spot, etc., are some of the latest installations/ modifications for calciner in cement plants. The norm for retention time in a calciner for new plants has changed from 3-4 sec to 15-17 sec so that the cement plants can easily fire large quantities of multiple solid/liquid fuels of varying characteristics. The technologies such as calciner electrification [68], gasification, and carbon capture [69, 70] are not yet implemented. It requires extensive research, including the calciner's modelling. Several authors have tried to model calciner in the past and successfully validated calciner models and implemented them in cement plants. Section 2.4 covers an extensive review of calciner modelling.

a) Direct firing of AF/RDF in the kiln burner

RDF firing in the main burner is more challenging as compared to calciner. Stringent alternative fuel quality, like heat value, particle size (2D and 3D), moisture content, etc., are crucial to firing in the main burner to avoid coating problems and impact clinker quality. RDF size must be reduced to less than 25 mm for complete combustion in the kiln. At higher TSR, this size is further reduced to less than 3 mm [71]. Usage of different types of AF necessitates modern multi-channel burners, which offer better flame shape control, high flame momentum, and the flexibility to use different kinds of AFs [72]. For burners, primary air pressure, flow rate, flame momentum, coal velocity, and solid alternative fuel velocity are vital varying parameters to optimize fuel combustion. The rising trend is to have a satellite burner in addition to the main burner, which can enhance RDF feeding by up to 50% [73]. High-temperature zone and oxidizing conditions with sufficient residence time are some of the preconditions for achieving high TSR through a satellite burner. D'Hubert [74] compared kiln burners of reputed suppliers viz KHD Pyrojet, FCT Turbojet, Unitherm MAS, Polysius Polyflame, Dynamis D-Flame, FLSmidth Jetflex, Fives-Pillard Novaflam, ATEC-Greco Flexiflame, and Rockteq International for cement application. Richard Cunningham [75] presented a case study of Irish Cement Ltd (ICL), Limerick, Ireland, where the swirlax burner was modified to high thrust low primary air. Thus petcoke firing increases from 70 to 100% with increased sulphur intake from 4 to 4.5% without coating problems. Such solutions apply to all high-sulphur alternative fuels. According to Lockwood et al. [76], RDF usage in kiln burners requires no unique technology except an RDF handling system. Still, considering environmental impact, it limits the maximum utilization to 30%. One recent trial run has been conducted at Hanson cement's Ribbleesdale plant in Lancashire. Fuel mix of hydrogen, meat and bone meal, and glycerine byproducts were cofired in kiln burner, which showed promising results [77].

It is known that process measurements are difficult to carry out in a kiln; hence, it is always challenging to predict kiln inside conditions. Thus, kiln burner modelling is essential in determining fuel combustion behaviour concerning coating formation, emissions, etc. Several researchers have developed and validated kiln models, as discussed further. Liedmann et al. [78] modelled the co-firing of RDF in a kiln burner, focusing on RDF burnout behaviour and local heat release through CFD simulation. Out of the nine simulations performed, the base case showed a low RDF conversion rate of around 40%, with material falling onto the clinker bed. Separate introduction improved burnout by 8% with enhanced residence time by over 30%. Haas and Weber [79] developed a kiln combustion model for cofiring RDF having HHV below 20 MJ/kg. The model examined the sintering zone temperatures with RDF properties to achieve process optimisation. One of the CFD studies by Pieper et al. [80] assessed the impact of light and heavy coating layers in the kiln with RDF as AF. The study concluded that the thick coating in the sintering zone would change the kiln temperature profile and shift it towards the kiln inlet. It will decrease the RDF residence time in the gas phase leading to lower alite content with high-free lime in the clinker. Pieper et al. [81] also simulated a rotary kiln using a 1 D model in CFD, considering the coupling of the gas phase and solid bed. 50% RDF and 50% lignite is the fuel mix. The results indicated a narrow flame shape, lower gas temperature in the sintering zone, and lower alite and high free lime in the clinker. One paper reported that the plants operating at a high% TSR through RDF with petcoke as the primary fuel are facing coating problems in the kiln refractory lining. RDF ash with high chloride and alkalis gets combined with petcoke sulphur, resulting in coating formation [82].

AF feeding position is also critical for co-processing any alternative fuel as it impacts char burnout. Ariyaratne et al. [83] simulated the cofiring of meat and bone meal (MBM) and coal in the kiln. MBM annulus feeding was compared to central tube feeding. It was observed that annulus feeding provides better char burn out, facilitating larger particles spread across kiln cross-sections. Thus, fine grinding of fuel is significant to maintain product quality. Table 2.1 describes the critical parameters of different burners to achieve more than 25% TSR through RDF. This table has been compiled after consultation with different reputed suppliers and literature data.

Table 2.1 Comparison of kiln burners of different suppliers for 25% TSR and above through RDF

Parameter	**Dynamis [84]**	**Fives FCB**	**Thyssen Krupp Industries Ltd.**	**Unitherm [73]**	**KHD [85]**
25% TSR through kiln main burner	Challenging but achievable	Yes, with a satellite burner	Yes, beyond that, plants operate but the impact on the process is inevitable. Can be directly fed to kiln hood	Yes	Yes
2D (particle size)	20 X 20 X 0.1 mm Entrained	< 30 mm, (thickness < 1 mm)	< 30 mm (flyable)	20-30 mm	0-30 mm
3D (particle size)	10 X 10 X 5 mm Non-entrained by the gas phase	90% 2D		5 mm	0-4 mm
Moisture	15 to 20%	1 tph for 50 MW (max)	< 15%	15-20%	-
Flame momentum	8-9.5 (Upto 11 N/MW)	New PA blower with 500 mbar pressure	-	8-9 N/MW	-

Because of the above, it can be said that RDF coprocessing in kiln/calciner is feasible. However, some impacts are inevitable, which need some modification in the system. For calciner, several pre-combustors are available to achieve high TSR through calciner. FLS hot disc, Polysius step combustor, and KHD pyro rotor are some of them. Seven pyro rotors are installed in cement plants for AF co-processing, where the retrofit is done in calciners helping in production increase with reduced emissions [67]. Hot disc technology can be employed where a wide variety of coarse alternative fuels like RDF, whole tyres are fired in calciner [65]. The prepol step combustor has a static combustion grate with fuel retention time of 15-20 min for drying and igniting alternative fuel like RDF [66]. With all these technologies, cement plants can achieve high TSR in calciner; however, no such technology is still available for kiln burners. Hence TSR in the kiln burner is lagging. A breakthrough in pre-combustion technology is required to improvise AF firing through the kiln burner.

2.1.3 Issues and challenges related to direct combustion of AF/RDF

The Indian cement industry is gearing up fast to increase the uptake of waste for co-processing. Confederation of Indian Industry (CII) prepared a vision document that envisaged a TSR of 25% (15% from RDF only) by the year 2025, considering different types of waste and their availability [29] which is difficult to achieve in the current scenario until a game changer technology arises to maximize alternative fuel utilization. Several issues and challenges at high TSR need to be addressed. Table 2.2 summarises the problems/challenges of utilizing RDF directly as a fuel for the cement industry under different categories of process, environment, and system design associated with negative or positive impacts. A negative impact on the process means increased specific heat consumption or reduced clinker production due to AF utilization and vice versa. An increase in emissions indicates a negative environmental impact during AF usage. The clinker quality is deteriorating due to AF usage. Issues related to chute jamming are covered in system design aspects. Some case studies are available in the literature on trial runs of AF in cement plants. Mohapatra et al. [[86, 87] shared their experiences of RDF utilization, agro waste, and tyre chips as co-fuels for coal in the cement manufacturing process based on a trial run at M/s Vikram Cements Ltd. RDF was brought from Jaipur MSW processing plant. M/s Vikram Cement achieved around 3% TSR from RDF out of the total 5% TSR. Initially, the yield of RDF was around 12-13% with a calorific value (CV) of only 6.28 MJ/kg, which was increased to 7.95-9.20 MJ/kg after reprocessing and double refining. Mixing waste polythene and plastics with RDF increased CV to around 10.46-11.30 MJ/kg. The clinker mineralogy without using RDF and with RDF indicated normal clinker phases and free lime. In a nutshell, it was concluded that alternative fuel utilization does not negatively impact cement engineering properties [10,12,13]. However, white cement's whiteness is affected due to the presence of iron in high ash-content alternative fuels. Thus, ashless fuels are the need of the hour in white cement.

Table 2.2 Summary of the problems/challenges of utilizing RDF directly as a fuel for the cement industry

Reference	Significance of the article	Impact on system parameters						
		Process	Environment	System Design	Clinker Quality	Cement quality	Coating/ buildup problem	Solution proposed
[88]	Emphasized the change in the existing system. Discussion on AF firing location and adverse effects on clinker quality.	Negative	-	-	Negative	Negative	Negative	No
[89]	The addition of sulfated materials such as gypsum, etc., to the raw meal having a minimum sulfur quantity of 30% is studied for chlorine fixation in the clinker, to tackle the chloride problem of RDF.	Negative	-	-	Negative	Negative	Negative	Yes
[90]	A CFD simulation case study is presented on				-	-		

Reference	Significance of the article	Impact on system parameters						
		Process	Environment	System Design	Clinker Quality	Cement quality	Coating/ buildup problem	Solution proposed
	calciner optimization to achieve 100% TSR in the calciner of a German cement plant replacing fine RDF with a coarser one.	Negative	Negative	Negative			Negative	Yes
[91]	It covers the status of AF utilization in India, focusing on the RDF challenges, opportunities, and plant experiences	Negative	Negative	Negative	Negative	Negative	Negative	Yes
[92]	RDF replaced 15% of petcoke in the fuel mix, indicating that it would not pose any problem with clinker quality and environmental emissions.	-	No impact	-	No impact	-	-	-

Reference	Significance of the article	Impact on system parameters						
		Process	Environment	System Design	Clinker Quality	Cement quality	Coating/ buildup problem	Solution proposed
[87, 93]	A case study of M/s Vikram Cements Works, reporting the usage of different types of alternative fuels, including RDF at 9.28% TSR.	-	No impact	-	No impact	No impact	-	-
[94]	Aspen Plus simulation was conducted to co-process waste tyres, RDF, and Meat and Bone Meal (MBM) as AF for 25%, 15%, and 5% TSR respectively	No impact	No impact	-	-	-	-	-
[95]	Trial runs for co-processing of RDF at a pilot scale in a cement	-	No impact	-	No impact	No impact	-	-

Reference	Significance of the article	Impact on system parameters						
		Process	Environment	System Design	Clinker Quality	Cement quality	Coating/ buildup problem	Solution proposed
	plant in Turkey at 8, 12, and 15% TSR							
[96]	CFD study was conducted to assess the impact of coating layers on clinker properties in the kiln with RDF as AF	Negative	-	-	Negative	-	-	-
[97]	Trials run for RDF & rice husk mix up to 5% TSR at a cement plant	-	No impact	-	No impact	No impact	-	-

- *No reference available in the paper*

2.2 RDF characterization and kinetic models

Several researchers have done RDF characterization, including proximate, ultimate, DTA/TGA/DTG, and tried to analyze the constituents of RDF based on different decomposition temperatures. Several kinetic models have been proposed to fit the experimental data, which can be called a good fit. Tibor Szucs et al. [98] reported that three reaction groups, cellulosic materials (paper, textile, biomass), plastics and remaining char, are dominant in RDF with decomposition temperatures of around 300°C, 470°C and 600-700°C respectively. A genetic algorithm was applied to compare modelling values using different models (1, n, expanded n, Distribution Activated Energy Model) with experimental TGA results at three different heating rates 5, 10, and 15 °C /min. Ozge et al. [99] conducted TGA and DTG at heating rates of 5, 10, 20, and 50 °C /min on an RDF sample in an N_2 atmosphere and revealed that there are three exothermic peaks. The first peak represents moisture loss at 120°C, second and third peak represents cellulosic and plastic decomposition in the temperature range of 250-400°C and 450-550°C, respectively. FTIR and SEM also supported in detailed characterization. Model-free methods (FWO, KAS, Friedman) and model-fitting methods were applied to determine kinetic parameters for the best fit of experimental data. It is concluded that RDF pyrolysis can be modelled with four reaction steps (190-340, 350-460,470-680, 680-890°C) with a reaction order of 1.5 for the first three reactions and 1st for the fourth reaction. Milos Radojevic et al. [100] also used similar model-free methods (FWO, KAS, Friedman) for SRF kinetic analysis and compared them with experimental TGA data. Results indicated that Friedman's kinetic method showed higher values for kinetic parameters. Valerio Cozzani et al. [101] reported two distinct weight loss peaks during RDF pyrolysis by DSC/TG at heating rates of 10 and 20°C/min in the presence of N_2. One peak of cellulose degradation was noted at 250°C, and another of plastics degradation at 450-500°C without any interaction between RDF components. Another endothermic peak occurred at 650-750°C due to inorganic filler in the paper related to the decomposition of $CaCO_3$. The isothermal weight loss curve in pure N_2 also confirmed that plastic decomposition started above 400°C. A kinetic model was developed based on the pyrolysis rate of individual components and the global reaction rate obtained by the weighted sum method. A weighted average model with a single-step approach fitted well with the TGA experimental data.

N Miskolczi et al. [102] investigated Malaysian RDF kinetic parameters based on the TGA curve. RDF consists of 5.1% newspaper, 59.8% plastics (polyethylene 64.6%, polypropylene 17.5%, Polystyrene 10.1%, other 7-8%), cardboard 28.6% and others 6.5%. TGA at 20°C /min indicated paper degradation at 188-413°C (max at 340°C) and plastics degradation at 410-560°C (max at 470-495°C). The RDF weight loss curve was compared to individual components and was found to be aligned. First-order kinetics was used for the decomposition reaction. Temperature for weight loss was identified in ascending order: Cardboard> newspaper> polystyrene> polypropylene> polyethylene. The reaction kinetic parameters (activation energy and pre-exponential factor) of pyrolysis of RDF and its components (papers and plastics) were determined by an independent parallel first order reaction model based on the TG data. A four-step reaction model was developed where the first three steps belong to the decomposition of cellulose, hemi cellulose and lignin, while the fourth step was for plastics.

Danias and Liodakis [103] highlighted the importance of RDF characterization due to its heterogeneous nature and linked it to marketability. TGA analysis of plastics, lignocellulosic materials and RDF samples was carried out separately under a non-isothermal

N_2 atmosphere from 25 to 800°C. Ligno cellulose compounds major mass loss occurred in the range of 220-380°C while plastics (except PVC) decomposition at 420-490°C. PVC decomposed in two steps, first at 305°C related to the release of HCl and second at 470°C linked to the degradation of remaining hydrocarbon residue. Lignocellulosic content in RDF is determined using statistical techniques and TGA methods and corroborated with proximate and ultimate analysis. Bosmans et al. [104] investigated RDF pyrolysis of excavated waste, a combination of 59% MSW and 41% industrial waste. DTA and DTG curves were plotted, which indicated that temperature in the range of 250-380°C (<400°C) and > 400°C is associated with the devolatilization of lignocellulosic and plastic material, respectively. No separate peak for lignin was identified. The author also compared the cellulosic fraction of RDF considered with different wood and other RDFs available in the literature and explained the lower peak temperature for RDF is comparable to wood due to the catalytic effect of inorganic material in RDF. Modelling in MATLAB code was done assuming four independent parallel first-order reactions, and kinetic parameters obtained were compared with predicted and measured DTG curves. The results obtained are a good fit for the data. It was concluded that RDF from MSW is a better fit for data than exotic waste. Grammelis et al. [105] compared the thermal decomposition and behaviour of paper, plastic, and tetra pack with RDF samples. TGA and DSC were performed for the samples at a 20°C heating rate in the temperature range of 30-1000°C. Plastics and mostly paper have a single degradation step, while RDF has four. All paper decomposition takes place between 300-400°C, and plastic was found to be thermally more stable than paper resulting in less char yield. HCl released from PVC reacts with cellulose to accelerate its reactivity. Kinetic parameters were determined for the thermal degradation of RDF and other samples with the help of kinetic modelling using an independent parallel reaction model considering cellulose, hemicelluloses, lignin and plastics as a first, second, third, or fourth fraction. The calculated parameters provided a good prediction of experimental data.

Luo et al. [106] conducted experimental studies in a customized fixed-bed reactor with real-time weighing, which acts as a macro-thermal gravimetric analyzer and can take samples up to 4 grams. TGA experiments were conducted at different heating rates (10, 20, 30°C/min) for nine components (PE, PET, PVC, PS, cellulose, hemicellulose, lignin, pectin and starch) of MSW. The kinetics modelling was done based on Flynn–Wall–Ozawa method and the activation energies of the samples were calculated. Sharma and Sheth [107] also investigated large-size biomass particles using macro TGA in which Jatropha de-oiled cake is pyrolyzed from 350 to 700°C. An apparent kinetic model was developed using Logarithmic DE, and kinetic parameters fitted well within the experimental data values. Bio-oil, char and gas yields are predicted for different input particle sizes.

2.3 RDF gasification

Gasification transforms feedstock, like biomass, RDF, etc., into producer gas rich in hydrogen and carbon monoxide [108]. Gasification occurs in a reducing environment requiring heat, whereas combustion occurs in an oxidizing environment releasing heat [109]. Different gasifiers, like fixed beds, fluidized beds, and entrained flow gasifiers are applicable, depend upon gas-solid contacting patterns, each having merits and demerits [110-112]. There are several steps in RDF gasification, including drying, pyrolysis, combustion, and gasification. The combustion of fuel occurs in a sub-stoichiometric environment in the combustion zone.

The heat liberated during combustion derives from the drying, pyrolysis, and reduction zone endothermic reactions, as mentioned below in eq 1-7.

The first stage is heating and drying at about 160°C, where moisture is removed from the feedstock.

$$RDF_{wet} \longrightarrow RDF_{dry} + H_2O \quad (2.1)$$

The second stage is pyrolysis, around 400 - 700°C in the absence of oxygen. Thermal cracking reactions occur, and gases such as H_2, CO, CO_2, CH_4, H_2O and NH_3, tar (condensable vapours), and char as the residue is liberated. Vapours produced in this stage undergo thermal cracking to gas and char.

$$RDF_{dry} \longrightarrow char + tar + H_2O + CO + CO_2 + H_2 + CH_4 \quad (2.2)$$

The next step is gasification, a chemical process in which char reduction is predominant through various chemical reactions in the temperature range of 800-1000°C [113].

$$C + H_2O \longrightarrow CO + H_2 \text{ (Water gas reaction)} \quad (2.3)$$

$$C + CO_2 \longrightarrow 2CO \text{ (Boudouardreaction)} \quad (2.4)$$

$$CO_2 + H_2 \longrightarrow CO + H_2O \text{ (Shift reaction)} \quad (2.5)$$

$$C + 2H_2 \longrightarrow CH_4 \text{ (Methanation reaction)} \quad (2.6)$$

$$CH_4 + H_2O \longrightarrow CO + 3H_2 \text{ (steam reforming)} \quad (2.7)$$

The resulting syngas contains H_2, CO, CO_2, CH_4, C_xH_y [114]. The performance evaluation is based on higher heating value (MJ/Nm^3), cold gas efficiency, hot gas efficiency, carbon conversion efficiency, equivalence ratio, etc. The modelling and experimental studies related to RDF gasification have been discussed in subsequent sections.

2.3.1 Experimental studies

Very few experimental results have been reported on RDF gasification. Rao et al. [57] performed experimental runs for RDF pellets, wood chips, and charred soyabean straw (CSS) pellets in an updraft countercurrent fixed bed gasifier with a biomass feeding capacity of 15-25 kg. Syngas obtained for RDF pellets had a CV of 5.59 MJ/Nm^3 with a cold gas efficiency of 73%. A comprehensive mass and energy balance has been worked out. The results indicated that gas obtained from RDF gasification is low in tar content and at par with global energy content compared to wood chips gasification. The second law-based cold gas efficiency was found to be highest for RDF pellets, followed by charred soyabean straw pellets and wood chips, which establishes its usage as an alternative fuel through the gasification route.

Khosasaeng and Suntivarakorn [51] experimented with RDF gasification in a 30-kW single throat downdraft gasifier of 1.70 m height with a radius of 0.25 m and the single throat tilting at 45°. Several parameters like syngas composition, heat value, and cold gas efficiency were studied at varied ER from 0.15-0.5. The optimum syngas heat value is 5.87 MJ/Nm^{3,} and cold gas efficiency was 73% at ER value of 0.35 with air as the gasifying agent.

Dalai et al. [56] gasified 1 g RDF fluff and RDF pellet in a fixed bed reactor. The results reported that higher C and H content produce syngas with high H_2 and CO content. The researcher studied the effect of different steam-to-waste ratios, and the optimum value for syngas yield is 2. Heat value reduces with an increase in this ratio as more liquid products are obtained. However, the concern is the quantity of 1 g in powder form, which will not give a real picture of RDF gasification since RDF is heterogeneous.

Dussadee et al. [54] conducted experimental studies for RDF-5 (as per ASTM standards) in a downdraft gasifier to produce syngas for power generation. The maximum electric power produced was 9 kW with minimum specific fuel consumption of 1.53 kg/kWh at a load of 7.5 kW.

Ribeiro et al. [115] performed RDF experimental trial runs on a fixed bed gasifier using steam and air as gasifying agents. The effect of temperature and different molar ratios of gasifying agents in gas production, gas composition, and mass conversion of RDF was evaluated. They concluded that steam gasification is more efficient at 750°C than at 850°C and vice versa for air gasification. The optimal steam-to-fuel ratio and ER are 1.0 and 0.4, respectively. Comparatively, air gasification produced more syngas flow rate than steam gasification. However, air gasification results in gas with less calorific value over steam gasification. It is due to the nitrogen dilution effect and more oxidant reactions.

Galvagno et al. [58] conducted an experimental study of RDF gasification with steam conducted in a bench-scale rotary kiln reactor in a temp range of 850-1050 °C in the gasifier. RDF obtained from an Italian company was characterized using TGA and DTG, which shows that material gets completely decomposed at around 800 °C due to the decomposition of paper, plastic, wood, etc. Gas analysis was done using gas chromatography and FTIR for RDF at different temperatures.

Park et al. [50] performed gasification trial runs in an 8 tpd SRF gasification plant in Y City, Korea. The syngas was utilized further to produce power at the rate of 0.75 kW/kg SRF for 12 days. SRF of CV 3000-3500 kcal/kg was obtained to convert it to syngas having a heat value of 1162 kcal/Nm^3. The average gasification temperature was 825 °C with a syngas (CO, H_2) composition of 17.14%. Optimum operating conditions like charging rate: of 55-60%, ER:0.21-0.33 were determined, and CGE and CCE worked out to 68.8% and 90%, respectively. Detailed studies and measurements were done for pollutants at the gasifier outlet, including HCN, NH_3, HCl, H_2S, COS, dust, and tar. The typical measured values, in this case, are NH_3: 900 ppm, HCl: 4.5 ppm, HCN: 60 ppm, H_2S, and COS: 33 ppm.

Uthaikiattikul et al. [55] performed the gasification of RDF in a laboratory-scale downdraft gasifier of 10 kg/hr capacity. The downdraft gasifier height is 2000 mm with 600 m diameter. The experimental parameters include the variation of air flow rate from 12 to 24 Nm^3/hr. Syngas has a maximum heating value of 2.67 MJ/Nm^3 at 12 Nm^3/hr with a cold gas efficiency of 65.83%, which is insufficient for power generation. The measured parameters also included temperature distribution along the height of the reactor and syngas composition. A study has been conducted on a downdraft RDF gasifier in a pilot plant to burn RDF in an Otto cycle-based Internal Combustion Engine to produce electrical power [53]. A gasifier model was developed to compare experimental data with theoretical results using Aspen Plus software. The predicted results were used to conduct a techno-economic analysis for power generation. A compilation of literature highlighting key points related to RDF gasification experimental studies for better understanding is shown in Table 2.3.

Table 2.3 Review of RDF gasification experimental studies

Reference	Feed material	Feed flow rate	Gasifier type	Gasifying agent	Highlights
[49]	Commercial RDF, saw dust	10-15 kg/hr	Downdraft	Air	Co-gasification produced better LHV of 4.65 MJ/Nm^3 than 4.34 during RDF gasification
[50]	SRF	333 kg/hr	Downdraft	Air	The syngas (heat value of 1162 kcal/Nm^3) was utilized further to produce power at the rate of 0.75 kW/kg SRF for 12 days

Reference	Feed material	Feed flow rate	Gasifier type	Gasifying agent	Highlights
[51]	RDF	10 kg	Single throat downdraft	Air	ER=0.35, LHV 5.87 MJ/Nm^3
[115]	RDF	0.45 kg	Lab scale fixed bed	Air and steam	Steam gasification is more efficient at 750°C than at 850°C and vice versa for air gasification. Optimal S/F ratio (1.0) and ER (0.4)
[53]	RDF	-	Downdraft	Air	TEF for Otto cycle Internal Combustion Engine (ICE)
[54]	RDF 5	30 kg	Downdraft	Air	The maximum electric power produced was 9 kW with minimum SFC of 1.53 kg/kWh at a load of 7.5 kW.
[55]	RDF	10 kg	Downdraft	Air	Syngas has a maximum heating value of 2.67 MJ/Nm^3 at 12 Nm^3/hr with cold gas efficiency of 65.83%
[56]	RDF fluff and RDF pellet	0.001 kg	Fixed bed within electric furnace	N_2 with steam	Char, liquid and gaseous products as output. Optimum S/W is 2
[58]	RDF, poplar wood, scrap tyres	5 kg	Bench-scale rotary kiln reactor	Steam	All the materials show a comparable gas production

Reference	Feed material	Feed flow rate	Gasifier type	Gasifying agent	Highlights
[57]	RDF pellets, wood chips, charred soybean straw (CSS) pellets	10 kg	Updraft	Air	5.58 MJ/Nm^3, CGE with RDF and CSS pellets was over 8% higher than the CGE obtained with wood chips

2.3.2 Modelling studies

Over the years, several authors have used different approaches to model downdraft gasifiers. Zainal et al. [116] employed equilibrium modelling to predict the gasification process for a downdraft gasifier. They studied the effects of moisture content and gasification zone temperature on the heating value of the syngas [16]. Giltrap et al. [117] developed a phenomenological model of a downdraft gasifier by incorporating mass and energy balance around a differential length of the reduction zone [17]. Babu and Sheth [118] modified the model proposed by Giltrap and incorporated exponentially varying char reactivity factors to predict the temperature profile and syngas composition more accurately along the length of the gasifier. Ratnadhariya and Channiwala [43] adopted a kinetic-free, stoichiometric approach to model the downdraft gasifier. The model was validated using twenty-four different biomass feedstock. Sharma and Sheth [119] developed an equilibrium model for a downdraft gasifier and validated it with the experimental results for diverse air-to-biomass and air-to-steam ratios. Gao and Li [45] combined the pyrolysis and combustion zone, assuming that the volatiles and the gases from the pyrolysis zone were cracked into the equivalent amount of CO, CH_4 and H_2O. Diyoke et al. [44] modelled the pyrolysis and combustion zone separately based on the experimental data available in the literature. The pyrolysis and combustion zone output was fed as the input to the reduction zone. All these models are for biomass as fuel, and since RDF is a heterogeneous fuel with varying properties, these models require suitable modifications for RDF gasification in a downdraft gasifier. Very few articles are available on RDF gasification modelling. Barba et al. [46] developed an RDF gasification model based on Gibbs Free Energy Gradient Method (GMM), where chemical potential forms the basis. The two-step model includes producing a carbonaceous residue and a primary gas and modifying the primary gas composition made earlier using adjustable parameters resulting in final syngas. In another article [120], they conducted a lab-scale and pilot-scale run for RDF gasification in a rotary gasifier, and the results were modelled using GMM. The gas yield is about 1.5 Nm^3/kg RDF, and the syngas LHV spans the range of 6–6.5 MJ/Nm^3. In Aspen Plus, multizone gasifier models have been developed by several researchers and most of them have used RSTOIC for drying, RYIELD for pyrolysis and RGIBBS or REQUIL for combustion and gasification [47, 48, 53]. All these reactors have certain limitations. The equilibrium reactor (REQUIL) assumes a long enough residence time for the chemical reactions to reach equilibrium, which is not realistic. Vounatsos et al. [47] has reported that the methane is underestimated from the pyrolysis step since chemical equilibrium under atmospheric pressure does not predict the methane precisely, which plays a considerable role in the energy balance of the process. Moreover, the model has neglected tar formation, and the char (pure carbon) has been considered to not participate in the thermodynamic equilibrium calculations. Násner et al. [53] developed the RDF gasification model using Aspen Plus. The gasification temperature was calculated using MATLAB, which was treated as an input to the RGIBBS reactor. In general, the equilibrium model results overestimated the amount of CO and H_2, underestimated the yield of CO_2, and predicted an outlet stream free from CH_4, tars and char. The study reported the gasification temperature to be uniform in all the directions: axial and radial which is not realistic. An advanced Aspen Plus model was developed by Juma Haydary [48], which considered two-stage pyrolysis/gasification of RDF. The author reported that, although the model represented a parametric study for RDF gasification, it can be improved further in future through kinetic modelling of the reduction zone. Using Aspen Plus, Tavares et al. [4] modelled biomass gasification in a downdraft gasifier. The pyrolysis stage was modelled using the RYIELD reactor to release volatiles and solid char. The model has neglected the formation of tar, considering that downdraft gasification produces insignificant tar, which is a shortcoming of the model. It was assumed that the total yield of volatiles is equal to the volatile content of the biomass and the total yield of chars is equal to fixed carbon and ash contents. CH_4 predicted through Aspen Plus simulation showed major deviation from experimental literature values, and the author reported the reason for it is that an equilibrium model neglects significant gasification issues such as system kinetics and fluid dynamics. All the Aspen Plus models consider equilibrium in the reduction zone, which fails to predict the syngas composition precisely since it does not consider the effect of the residence time of the reactants inside the gasifier. Moreover, Aspen Plus based models have not considered the formation of tar and minor components such as S, Cl which affects syngas composition depending upon S, Cl content in RDF. Char reactivity factor (CRF) cannot be incorporated in Aspen Plus which is a valuable parameter while modelling a gasifier as it varies in accordance with certain feedstocks. The summation of different types of downdraft gasifier models with their limitations is given in Table 2.4.

Table 2.4 Review of downdraft gasifier models

Reference	Fuel	Model	Description	Limitation
[116]	Biomass	Equilibrium	Studied the effects of moisture content and gasification zone temperature on the HV of the syngas	Equilibrium reactor assumes a long enough residence time for the chemical reactions to reach equilibrium, which is not realistic
[117]	Biomass	Reduction zone based	Mass and energy balance around a differential length of the reduction zone	Accuracy is limited by the availability of data on the initial conditions at the top of the reduction zone
[118]	Biomass	Modified Giltrap	Incorporated exponentially varying CRF to predict the temperature profile and syngas composition more accurately along the length of the gasifier	Accuracy is limited by the availability of data on the initial conditions at the top of the reduction zone
[43]	Biomass	Kinetic-free, stoichiometric approach (3 Zones)	Prediction of maximum temperature in oxidation zone of gasifier	Pyrolysis zone product and temperature are obtained simply through mass and energy balance, No tar in pyrolysis
[121]	Biomass	Equilibrium	Air steam gasification experimentation, effects of MC, ER, and S/B on the composition are predicted	Over-prediction for methane
[45]	Biomass	3 zone model	Combined the pyrolysis and combustion zone, CO,	Inability to predict gas concentrations at the two zones and the omission of

Reference	Fuel	Model	Description	Limitation
			CH_4 and H_2O as pyrolysis products	H_2 and tar in the assumed pyrolysis gas
[44]	Wood	Matlab (3 zone model)	Tar considered	
[46]	RDF	Gibbs Free Energy Gradient Method	Two-step model includes producing a carbonaceous residue and a primary gas and modifying the primary gas composition	All reactions in equilibrium. No solid ash and tar
[120]	RDF	Gibbs Free Energy Gradient Method	Lab scale and pilot scale runs in rotary gasifier	All reactions in equilibrium. No solid ash and tar
[47]	RDF	Aspen Plus based	Optimum operational temperature: 850 and 900 °C. ER ranges from 0.27 to 0.42.	Methane is underestimated from the pyrolysis step, neglected tar formation
[53]	RDF	Aspen Plus based	Gasification temperature was calculated using MATLAB, which was treated as an input to the RGIBBS reactor	The study reported the gasification temperature to be uniform in all the directions: axial and radial which is not realistic
[48]	RDF	Aspen Plus based	Two-stage pyrolysis / gasification of RDF	It can be improved further in the future through kinetic modelling of the reduction zone

2.4 Cement plant calciner modeling

Calciner modelling has been divided into two categories: theoretical and empirical. Theoretical models cover Aspen Plus, CFD, material, and energy-based models, while empirical models include data-driven, fuzzy logic-based ones. Several works of literature are available on calciner models for different applications. Nhuchhen et al. [122] developed a thermal energy flow model from the energy and momentum balance equations to achieve 50% TSR for twenty-four alternative fuels with natural gas as a primary fuel in the kiln. The model is difficult to implement due to time constraints. However, the devised regression equation can be helpful in future predictions while utilizing AF. Wydrych et al. [123] proposed a mathematical shrinking core model based on a combination of gas-phase and particle motion description. Further, this data is utilized for CFD model development to determine the pre-calciner's particle residence time and the radiative heat exchange between gas and limestone. Similarly, several CFD models are there where emissions are also predicted. Mikulčić et al. [124] studied the efficiency of the calciner along with pollutant emissions with the help of a CFD model. The model predicted the decomposition rate of limestone particles, the burnout rate of coal particles, and the pollutant emissions of a newly designed cement calciner. The major advantage is the demonstration of calciner characteristics that cannot be measured. Wang et al. [125] modelled the co-firing of high-carbon-ash (HCA) inside the cement calciner. They conducted a drop tube test and collected the resulting fly ash to study the unburnt carbon content. It is reported that 30% TSR is feasible. However, the study did not cover the fuel aerodynamic characteristics and different particle heat-up rates to particle size. Nakhaei et al. [126] studied the NO emissions from a cement calciner where two cases, case A petcoke fired and case B coal-fired, were simulated using CFD. Using the Eulerian approach, they simulated the solid particles according to the Lagrangian formulation and the gas phase. The extent of the calcination reaction, the emissions, and the temperature variations of the calciner were predicted and validated. The study shall be useful in developing futuristic NO emissions models for fuel mix with AF. Cristea et al. [127] developed a CFD-based 3D simulation model of a four-stage industrial calciner, and the results predicted are close to plant operational data. ASPEN models focused on predicting pollutant emissions and energy consumption at different TSRs for different alternative fuels. The model supports staged combustion simulation helpful in controlling NOx emissions from the calciner by adjusting the input parameters. Machine learning and fuzzy logic models were data-driven, where calciner input data (raw meal, fuel, tertiary air, etc.) were used to model and optimize the calciner output. Different approaches like statistical, mathematical with grey correlation analysis, just in time Gaussian mixture regression, hybrid clustering algorithm, DCS based were used extensively to model the calciner as specified in Table 2.5. All these data driven models are mainly for conventional fuels and not validated for alternative fuel.

Table 2.5 Review of calciner/kiln burner models

Reference	Type of Model	Parameters Studied	Fuel	Input Data	Specifications of the model	Key findings
[128]	Theoretical	CO_2 emissions and heat requirements	Coal	Fuel composition, Inlet temperature.	CO_2 capture model, a thermodynamic model	Thermal fuel substitution was found to be more efficient than mass substitution. The conversions of $CaCO_3$ decreased with increased TSR.
[122]	Theoretical	Emissions and Thermal energy intensity	24 different types of AF	LHV, Oxygen Fraction in fuel	A numerical model for various fuels	The thermal energy intensity increased with an increase in the fuel's moisture content, and a similar trend was found with O_2 content in the exit of the pre-calciner.
[129]	Theoretical	Calcination at various temperatures	NF	Flow rates, reactor length, temperature	A numerical model to calculate the reaction rates and conversions	The rate of calcination increases and remains constant with the increase in temperature. And the calcination of $CaCO_3$ increased significantly with reduced particle size.

Reference	Type of Model	Parameters Studied	Fuel	Input Data	Specifications of the model	Key findings
[130]	Theoretical	Outlet temperature and emissions	Coal	Flowrate	Kinetic model coupled with CFD modelling	The flow characteristics and temperature in the calciner
[131]	Theoretical	Raw meal decomposition rate (RMDR)	Coal	Gas density, the heat of the pulverized combustion	Matlab Simulation	RMDR predicted within the acceptable limits for error.
[94]	Theoretical (Aspen Plus)	Outlet temperature, NOx, O_2, CO, CO_2	Coal, TDF, RDF, MBM	Raw material, Coal, Tertiary Air, Kiln Gas	Separate combustion and calcination models	RDF showed the least CO_2 emissions among the three fuels. An increase in the thermal substitution of alternate fuels decreased the conversion.
[132]	Theoretical (Aspen Plus)	Outlet temperature, NOx, O_2, CO, CO_2	RDF	Raw material, Coal, tertiary air, kiln gas	DD Calciner model with separate unit operations for fuel decomposition and combustion	Staging combustion could help control NOx emissions

Reference	Type of Model	Parameters Studied	Fuel	Input Data	Specifications of the model	Key findings
[133]	Theoretical (CFD)	NOx and CO emissions, residence time, Burnout	Coal (Main), Petcoke, and Oil	Inlet temperature, flow rates, tertiary air	Modelling the largest calciner in the world. It is an MI-CFD model	Increased usage of petcoke increased the NO_X and CO emissions while increased oil consumption reduced them.
[134]	Theoretical (CFD)	Temperature contour, velocity profile, calcination	Coal	Pulverized cement raw meal and coal flow rates, Air and flue gases flow rates, Coal Properties	The model has been prepared based on an IFRF Furnace	The turbulence caused by the swirling air increased the active length of the calciner. The role of the geometry of the calciner highlighted
[135]	Theoretical (CFD)	The hydrodynamic behaviour of a gas-solid flow in the precalciner	Coal	Continuity equations, Gas and solid-phase momentum conservation equations , Turbulent kinetic energy Equation of the solid phase	It is a numerical model that was later fed into the CFD Model	The velocity profiles showed that the bottom of the calciner had the highest turbulent flow field and particles scattered more effectively.

Reference	Type of Model	Parameters Studied	Fuel	Input Data	Specifications of the model	Key findings
[123]	Theoretical (CFD)	NOx and CO_2 emissions	Coal	User-defined function, reaction rate from the shrink core model	It is a shrink-core model integrated into the CFD model.	The shrink core model calculated the particle residence time more accurately.
[124]	Theoretical (CFD)	Emissions from the calciner outlet	Coal	Mass flow rates, temperatures, mass ratios	The model has a spiralling tertiary air inlet increasing the turbulence.	The swirled flow enhanced the mixing phenomena, and lower CO levels were observed
[40]	Theoretical (CFD)	NOx emissions, NH_3 slip, and the reducing agent consumption	NF	The geometry of the SNCR, data from the plant	It is a typical calciner model for high-efficiency SNCR.	The project had an end goal of limiting the NO_X/NH_3 levels and achieving the target.
[136]	Theoretical (CFD)	Emissions, Hot-Reburn Conditions	Coal, Petcoke, and other AFs	Mass flow rates, Temperatures	It is an MI-CFD model based on an initial mathematical model	CO emissions increase with increased AF substitution. NOx emissions increase when medium to high volatile coal is replaced with low volatile fuel.

Reference	Type of Model	Parameters Studied	Fuel	Input Data	Specifications of the model	Key findings
[137]	Theoretical (CFD)	Pressure drop in pyro-processing	Coal	Mass flow rates, Temperatures, Pressures	MI-CFD model of an inline calciner	The pressure losses of pyro-processing can be reduced, enabling either increased clinker production or reduced power consumption.
[42]	Theoretical (CFD)	Emissions from the calciner outlet	Coal, Petcoke, AF1, and AF2	Composition of the fuels, Flow rates, Temperature	MI-CFD model of a separate line calciner	Petcoke showed the highest NOx and SOx emissions, followed by AFs and coal.
[138]	Theoretical (CFD)	NOx emissions	Coal and Petcoke	Clinker production (tpd),% firing in kiln/calciner, Overall air-fuel equivalence ratio in calciner and riser.	A comparative study with two calciner conditions is presented. In calciner A, the raw material is fed to lower and upper calciner vessels from the 4th and 3rd cyclone stages, respectively.	The generation of NO from char-N oxidation and depletion of NO by char-C are the most significant contributors to NO formation and reduction

Reference	Type of Model	Parameters Studied	Fuel	Input Data	Specifications of the model	Key findings
					The raw meal is fed to only the lower calciner vessel from the 5th cyclone stage in calciner B.	
[125]	Theoretical (CFD)	Optimal TSR of High-carbon-ash	Coal, High-carbon-ash (HCA)	Inlet temperatures, Velocities, Mole fractions	The heat value of HCA was first determined using a drop test, and later a calciner model was developed where HCA was fired in the chamber.	TSR >30% didn’t give a satisfactory output.
[139]	Empirical (Soft Sensor/AI/ML)	Apparent degree of calcination	NF	Mass flow rate, Inlet and Outlet Temperature, Inlet and Outlet Pressure, and Tertiary air temperature	LS-SVM-based ANN Model	The model showed a favourable learning ability. It also showed satisfactory prediction accuracy.

Reference	Type of Model	Parameters Studied	Fuel	Input Data	Specifications of the model	Key findings
[140]	Empirical (Soft Sensor/AI/ML)	Calciner Outlet Temperature	Coal	Coal feeding and other field data from the plant.	Regression model	The sliding mode control improved the efficiency of the outlet temperature calculated using the regression model.
[141]	Empirical (Soft Sensor/AI/ML)	Calciner Outlet Temperature	Coal	Raw material feeding, Tertiary air temperature, Coal injection in the kiln inlet and main burner	Process control model	The accuracy in predicting the outlet temperature can be improved by utilizing the appropriate model.
[142]	Empirical (Soft Sensor/AI/ML)	Calciner outlet temperature and oxygen content of the exhaust	Coal	Raw materials, coal-fed for furnace, coal-fed for kiln, rotary speed of kiln, and negative pressure of C1 export.	Artificial neural network (Heuristic dynamic programming)	ADHDP improves the system operation stability more effectively than manual operation. For a large scope of changed data, the proposed method can perform well on control.

Reference	Type of Model	Parameters Studied	Fuel	Input Data	Specifications of the model	Key findings
[131]	Empirical (Soft Sensor/AI/ML)	Raw meal decomposition ratio	Coal	Calciner temperatures, calcium oxide content, ferric oxide, and silica content	A combination of the Fuzzy Model, KL Divergence, and S kernel functions	Prediction of the raw meal decomposition rate within acceptable error limits
[143]	Empirical (Soft Sensor/AI/ML)	Recognizing working conditions to optimize the control of calciner and cooler	Coal	Calciner exit temperature, outlet temperatures of the cyclone reactors, pressure beneath the grate cooler	Different DCS manufacturers design DCS systems. (VB 6.0 programming)	A list of operating conditions has been identified.
[144]	Empirical (Soft Sensor/AI/ML)	Calciner outlet temperature	Coal	Coal feeding, raw material feeding, quantity of tertiary air	Mathematical and Grey correlation analysis	The online switching model improved the efficiency of the mathematical model developed.
[145]	Empirical (Soft Sensor/AI/ML)	Abnormal condition detection	Coal	Calciner temperature, 1^{st}	Statistical	The model can reduce the chances of 5^{th} cyclone feed tube blockage.

Reference	Type of Model	Parameters Studied	Fuel	Input Data	Specifications of the model	Key findings
				cyclone cone pressure		
[146]	Empirical (Soft Sensor/AI/ML)	Calciner outlet temperature	Coal	Calciner coal feed, kiln head coal feed, raw material feed, and ID fan speed	Mathematical adaptive multi-dimensional Taylor network control (adaptive MTN)	Simulation results verify the effectiveness and feasibility of adaptive MTN.
[144]	Empirical (Soft Sensor/AI/ML)	Calciner outlet temperature	Coal	Raw material feeding and coal feeding, tertiary air temperature	Single-Input and Single Output (SISO) and Multiple-Input and Single-Output (MISO) Models based on regression models	Out of all the developed models, the three inputs model showed the highest accuracy.
[147]	Empirical (Soft Sensor/AI/ML)	NOx Emissions	Coal	Preheater fan speed, calciner outlet temperature, kiln tail temperature, kiln tail pressure,	Just-In-Time Gaussian (JIT) Mixture Regression	Integrating the JIT model improved the efficiency and accuracy with which the emissions were predicted.

Reference	Type of Model	Parameters Studied	Fuel	Input Data	Specifications of the model	Key findings
				kiln coal feeder, kiln head pressure, kiln head temperature, grate cooler pressure		
[148]	Empirical (Soft Sensor/AI/ML)	The efficiency of the hybrid model developed	Coal	Calcination outlet temperature, kiln speed	ANFIS model coupled with a hybrid clustering algorithm	A hybrid clustering algorithm is more efficient and accurate when compared to FCM and Subclust algorithms.

2.5 Process integration of gasification and cement plant kiln / calciner

The share of global syngas output is 61% from coal, 29% from petroleum, 7% from gas, 2% from petcoke, and only 1% from biomass, and almost negligible contribution from MSW or RDF [149]. Syngas applications include waste management, biofuel production (e.g., FT kerosene), hydrogen production, refinery integration, etc. Recent trends indicate interest in syngas production from RDF waste via gasification, which can be used as an alternative fuel in the cement industry. An onsite gasification plant is needed to use the syngas in the cement plant. Few researchers have reported the integration of the gasification process with cement plants.

Chatterjee et al. [150] studied three working models for the co-processing of MSW in China; a) the Sinoma model, which involves direct pre-treatment and co-processing; b) the Conch model considering gasification pre-treatment and co-processing c) the Huaxin model, which refers to fermentation pre-treatment and co-processing. Each model has its own merits and demerits. In the conch model of MSW gasification, gasification takes place in a fluidized bed furnace to obtain syngas as an alternative fuel, and ash discharged from the bottom is utilized as a raw material in cement. However, the Sinoma model is reported to perform better. A 450 tonnes per day MSW-based facility for a cement plant capacity of 5000 tonnes per day clinker based on the Sinoma model was set up in 2013 in China. Wang [151] studied the Jinyu model of RDF thermal treatment focused on RDF quality for co-processing in cement kilns. MSW is pretreated to produce low-quality and high-quality RDF. High-quality RDF having a CV of more than 2500 kcal/kg, moisture less than 30%, and particle size less than 50 mm is directly combusted in cement plants. However, low-quality RDF undergoes pyrolysis and gasification in a vertical rotary gasifier, and the syngas obtained is sent to the kiln system. Greil et al. [152] were the first group to report the integration of gasification integration in the cement plant of 5000 tpd capacity. A circulating fluidized bed gasifier is installed with shredded wood as feedstock, providing the syngas to the calciner. At the same time, the burnt-out ash is fed to the raw mill acting as a raw material component, thus no waste generation through the process. Several configurations utilizing the concept of waste heat recovery, air preheating, and oxy-fuel gasification lime as sorbent for hydrogen production compared to RDF combustion have been shown in Fig 2.1 and discussed in sections 3.1, 3.2, and 3.3 for syngas firing in kiln/calciner.

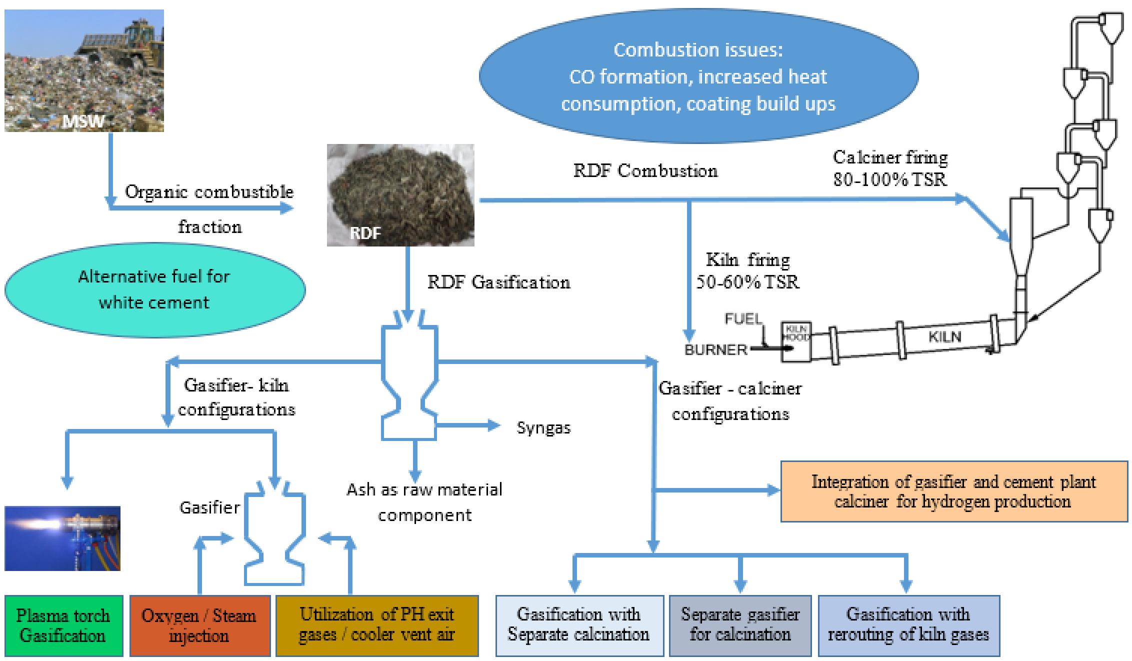

Fig. 2.1 RDF combustion vs gasification integration in the cement industry

2.5.1 Configurations for syngas firing in the calciner

Hjuler[153] reported two different configurations (A and B) for syngas firing in the calciner involving the recirculation of kiln exhaust gases and CO_2-based gasification with a waste heat recovery system. Wensan et al. [154] demonstrated separate waste gasification integrated into the calciner of the pyro-processing system as discussed in configuration C. Schuermann et al. [155] explored the utilization of kiln exhaust gases in gooseneck type gasifying reactor through configuration D. Gasifier is integrated further with calciner to utilize syngas as fuel in the calciner. Weil et al. [156] presented configuration E on enhancing hydrogen production through gasification. The calcium oxide produced during limestone calcination in cement plant calciner will be utilized in gasification without affecting calcination. These configurations, A to E, are discussed in detail in the next section.

i. Configuration A

Fig. 2.2 describes configuration A of the integrated system of calciner and gasifier [153]. This system discusses raw meal calcination, enhancing waste heat recovery for power generation, and gasification integration. In this system, calciner exhaust hot gases (around 900°C) is utilized for fuel gasification in a gasifier to obtain syngas. The syngas is sent to the calciner as an alternative fuel for calcination purposes. Initially, the raw meal gets heated in a preheater by utilizing hot gases and enters the calciner. Calcined material is split into two streams; one stream is fed to the kiln for further clinkering reactions. The other stream is sent to the riser duct, which receives kiln exhaust gases and is supplemented with secondary fuel and air for further combustion. The idea is to raise the calcined material's temperature further and send it back to the calciner, where it can transfer heat for raw meal calcination. It will eliminate the use of direct solid fuel combustion in the calciner. Exhaust gases from the riser duct are sent to the preheater for material preheating purposes. It is entirely different from the typical case where high-temperature kiln exhaust gases enter the calciner through the riser duct. Further calciner exhaust gases are sent to the preheater, which is used for preheating the raw meal. Different scenarios of calciner exhaust gas recirculation are explored for this purpose.

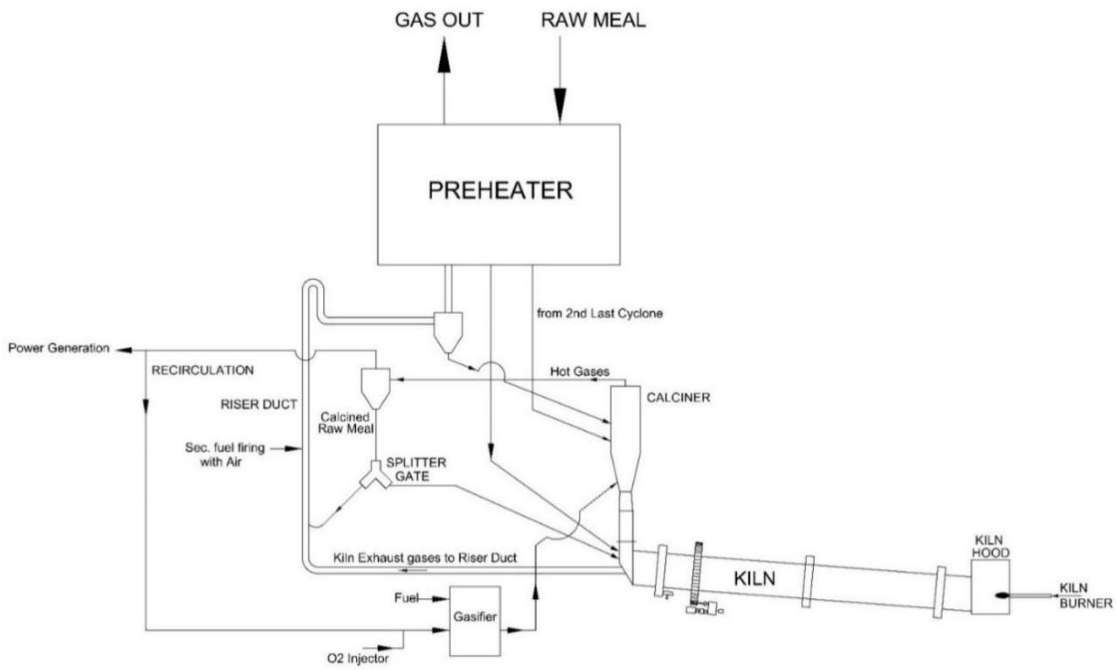

Fig. 2.2 Gasification with separate calcination- configuration A [153]

ii. Configuration B

Fig. 2.3 describes configuration B of the integrated system of calciner and gasifier [153]. Integration proposed in this configuration is based on the carbon capture for clinker production as CO_2 is circulated in the system with waste heat recovery. CO_2 is used as a gasifying agent in the gasifier, and produced syngas is fed to the calciner. It is combusted with pure O_2. Calciner exhaust gases containing CO_2 are utilized to generate power, and low-temperature turbine exhaust with CO_2-rich vapour is recirculated to a clinker cooler. It replaces ambient air for clinker cooling purposes. Water/water vapour is added to the cooler to adjust CO_2 concentration. The CO_2 takes up the recuperated heat from the clinker and enters the gasifier with solid/liquid tertiary fuel. Syngas thus obtained after gasification along with O2 are used for the calcination of raw meal. The rest of the process of the material split into kiln and riser duct and further recirculation of material to calciner is similar to configuration A.

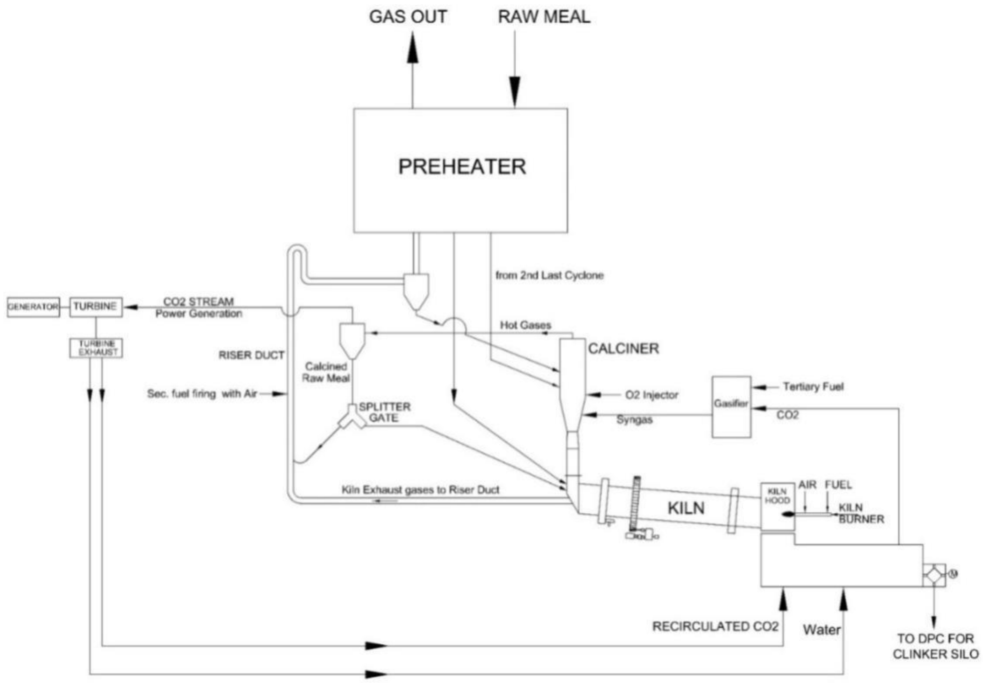

Fig. 2.3 Gasification with separate calcination- configuration B [153]

iii. Configuration C

Fig. 2.4 describes configuration C of the integrated system of calciner and gasifier [154]. This system proposes gasification for different calciner configurations like inline calciner, separate line calciner, and without calciner. Household waste, industrial waste, including waste plastics having a calorific value of 4.18 to 12.55 MJ/kg, is gasified in a fluidized bed gasifier to generate syngas as a fuel. The gasifier is also supplied with auxiliary fuel (scrap tires, charcoal, wood chips, etc.) to maintain the temperature inside around 500-600°C. Air is supplied from the blower to the gasifier for fluidization purposes. The incombustible material settles with fluidizing sand at the bottom of the gasifier, and a classifier separates it. Sand is transported back to the gasifier, while the ash containing metallic components is utilized as raw material for clinker manufacture. The temperature inside the calciner is more than 800°C with a residence time of more than two seconds which may be sufficient for the complete combustion of syngas. The negative pressure is maintained in the calciner, which helps draw syngas from the transport line. A bypass line from the kiln inlet has also been considered to control chloride and alkali concentration during gas circulation in the preheater. A detailed computational fluid dynamics (CFD) simulation was done for syngas as partial fuel replacement in the preheater with or without calciner. The ratio of the flow rate of syngas over the flow rate of kiln exhaust gas was established by simulation along with prediction of the amount of gas generated in the gasifier (Nm^3/hr), CO concentration in the calciner, the gas pressure in the calciner (kPa) & gasifier and flow rate ratio of syngas/kiln exhaust gas, etc.

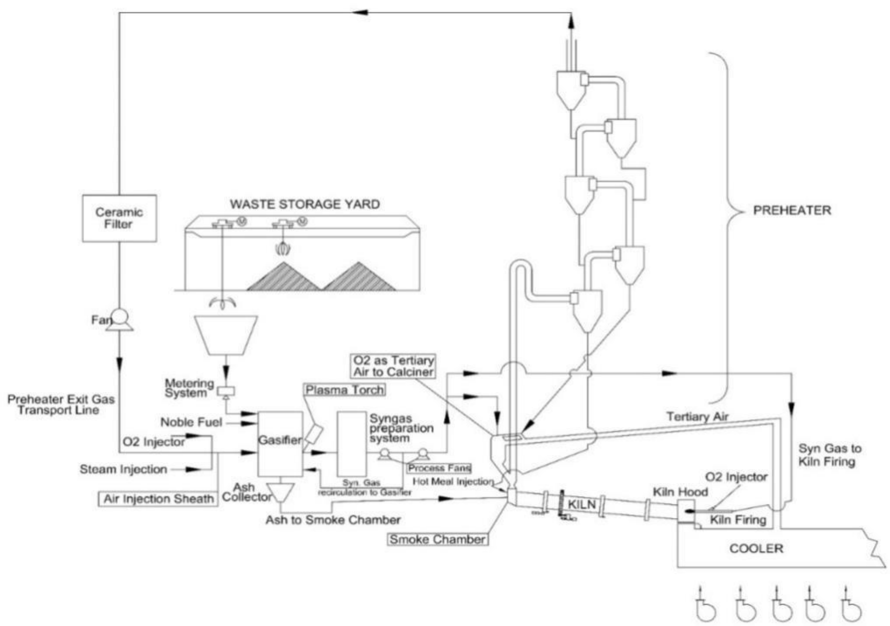

Fig. 2.4 Separate gasifier for calcination- configuration C [154]

iv. Configuration D

Fig. 2.5 describes configuration D of the integrated system of calciner and gasifier [155]. This configuration incorporates a new way of integrating gasifying furnaces in the clinker manufacturing process using process gases inside the kiln system. The two energy-intensive reactions in clinker manufacturing are calcination at 800-850°C and clinkering at around 1450°C.

An inverted U-shape gasifying furnace is employed to pyrolyze the fuels and is located between the calciner and kiln. The kiln exhaust gas stream and the gasifier outlet are connected above the tertiary air duct. Fuel gasification occurs in a gasifier in the presence of kiln exhaust gas at a high temperature, along with a portion of tertiary air from the cooler. The calciner receives fuel which gets burnt in the calciner in the presence of balanced tertiary air to provide heat for raw meal calcination. Tertiary air is split between the calciner and gasifier using an adjustable flap valve. The calciner has a swirl chamber for completely burning gasifier syngas and optional fuel injection into the calciner.

Streit and Feiss et al. [157] highlighted the particular type of calciner developed by KHD recently named Pyroredox. A gasifier is connected upstream to the calciner, and the gasification zone is separated from the oxidation zone. Gasifier best uses the Boudouard reaction, reducing NOx emissions without impacting production and specific heat consumption in cement plants.

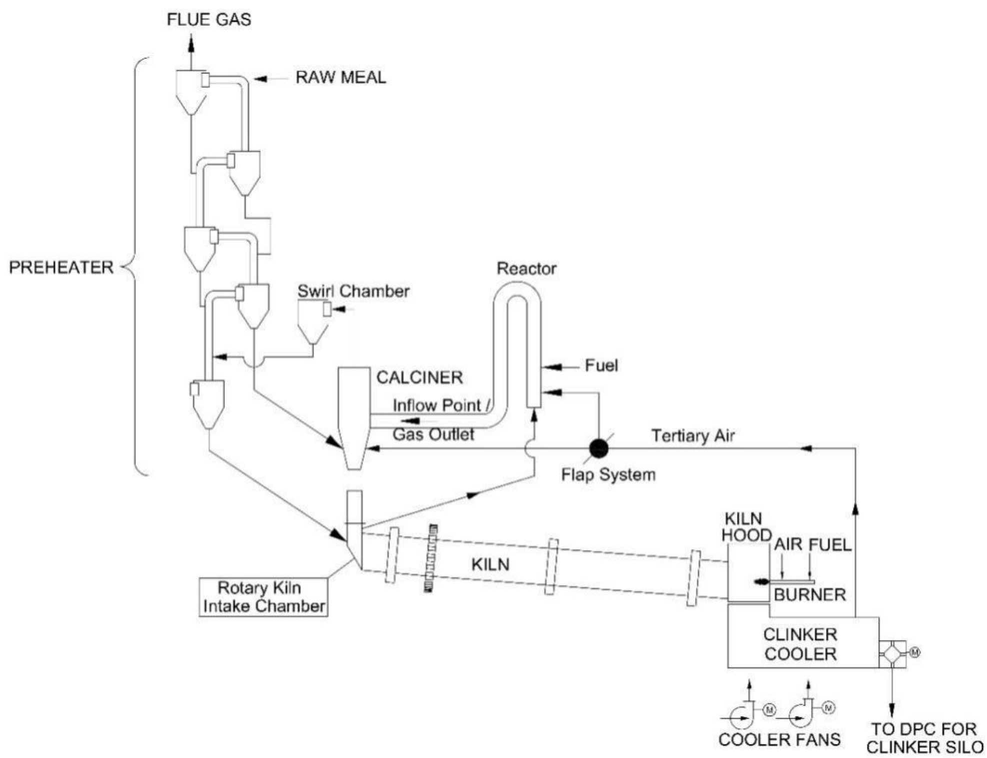

Fig. 2.5 Gasification reactor using kiln gases for gasification- configuration D [155]

v. Configuration E

Fig. 2.6 describes the configuration E of the integrated system of calciner and gasifier [156]. This configuration involves a unique concept focusing on enhanced separate hydrogen production, taking advantage of the cement manufacturing process. Hydrogen will be the future fuel; hence its production in different ways is an ongoing research process. Thermal gasification of waste to obtain hydrogen is one of them. The removal of nitrogen and carbon dioxide from syngas enhances hydrogen concentration. Some sorbents like CaO is helpful, leading to in-situ CO_2 capture by forming calcium carbonate after reacting with carbon dioxide. It is produced by dissociating calcium carbonate through the calcination process, which is energy intensive. This calcination is a crucial process in cement production, and here lies the opportunity for hydrogen production where this linkage can gainfully utilize lime from calcined material.

During clinker manufacturing, the raw meal enters the preheater at 40-50°C and then undergoes preheating to reach 750-850°C until the second lowermost cyclone before entering the calciner. The material gets 30-40% calcined in the preheater and achieves 85-90% calcination before entering the kiln for further reactions. A hot pre-calcined meal from the second lowermost cyclone is supplied as a heat source for the gasifier placed in parallel through a siphon where fluidization is done by superheated steam. Fuel fed to the gasifier undergoes drying and pyrolysis at a temperature of approximately 650°C after contacting pre-calciner raw meal. Tar cracking occurs in the presence of steam in an upper zone of the gasifier. The catalytic activity of CaO also enhances it. The gas composition changes with enriched hydrogen after the removal of CO_2. The unburnt char/ash/coke and carbonated meal obtained from the gasifier bottom at 600°C are recirculated back to the calciner. The carbonated meal is heated further to more than 850°C for calcination. Coke burnt in the presence of air is a source of heat. A calcined meal from the last cyclone enters the kiln. The downstream of the gasifier consists of a gas cleaning unit that removes the impurities like chlorine, sulfur, and mercury. Further, the gas is fed into a pressure swing adsorption (PSA) unit for hydrogen separation. The tail gas obtained can be used as a fuel substitute for the calciner for heat recovery.

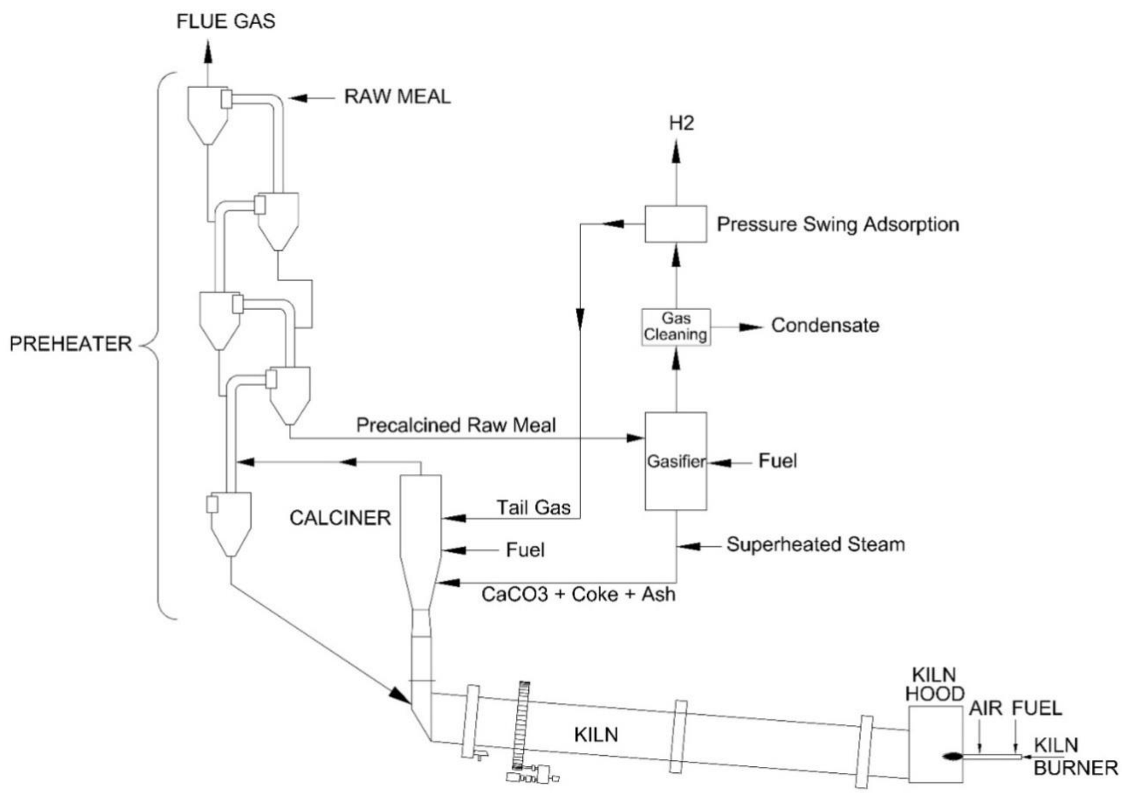

Fig. 2.6 Integration of gasifier and cement plant calciner to enhance hydrogen production - configuration E [156]

vi. SWOT analysis of various configurations

All five calciner configurations have some pros and cons. SWOT analysis has been done in Table 2.6 to illustrate the advantages, disadvantages, configuration improvement points, and relevant circumstances for each configuration.

Table 2.6 SWOT analysis of calciner configurations

Configuration	Strength	Weakness	Opportunities	Threats
A	Enhanced waste heat recovery for power generation due to the availability of calciner exhaust gases at high temperature Calciner exhaust gas utilization for gasification will reduce the fuel requirement of the gasifier. Reduction in carbon footprint	Calciner exhaust gases may contain SOx and NOx, which can impact gasifier operation Major retrofit required in the kiln system	Establishing syngas as an alternative fuel in the calciner	A split of calcined meal in the riser duct and kiln is critical and may result in operational issues. Lack of experience in gasifier operation
B	Decrease in fossil fuel consumption in the calciner	Water addition to the clinker cooler for CO_2 adjustment will lead to increased water consumption in pyro-processing.	Establishing syngas as an alternative fuel in the calciner CO_2 is circulated in the system for waste heat recovery, thus reducing CO_2 emissions by up to 50%. Establishment of Carbon capture technology	O_2 injection requires separation of O_2 from the air, which can be unviable The rest of the CO_2 is to be sent underground

Configuration	Strength	Weakness	Opportunities	Threats
C	No major retrofit is required as the gasifier is a separate unit to be integrated with the calciner Ash-containing metallic components can be utilized as raw material for clinker manufacture	Air at ambient temperature as a gasifying agent is to be heated, leading to high energy consumption	Establishing syngas as an alternative fuel in the calciner High heat value of syngas by O_2 injection, steam injection, or plasma torch gasification	Plasma torch gasification/O_2 injection is energy-intensive and thus may be unviable
D	Reducing conditions created in gasifiers due to kiln gases will help in controlling NOx emissions too, which is a major issue for the cement industry Minimal chance of bulky fuels falling down the calciner	Gasifier ash cannot be separated as it becomes an integral part of the kiln system due to kiln gases in the gasifier. The tertiary air split between the gasifier and calciner is critical Operational problems in calciner are expected due to the re-routing of kiln gases previously used for maintaining gas velocity to	Advantage of utilizing kiln gases with optimum O_2% in the gasifier	Fuel firing location and syngas velocity are critical, considering material lifting in the calciner

Configuration	Strength	Weakness	Opportunities	Threats
		prevent material from falling directly into the kiln.		
E	Both gasification technology and pyro-processing adopt benefits of each other Elimination of the sorbent regeneration step for gasification Elements like MgO or Fe show catalytic activity related to tar decomposition Fuel ash from gasifiers can be used as alternative raw material for cement production.	Hydrogen utilization as an alternative fuel in the cement industry is still at the research stage Storage, transport, safety, utilization, and scale-up issues for hydrogen utilization	Cement plants can become self-reliant for hydrogen production as a fuel Potential to reduce fuel combustion and CO_2 emissions since hydrogen is a clean fuel	Availability of superheated steam in cement plant The degree of calcination will reduce as pre-calcined material entering the gasifier from the second last cyclone gets converted to $CaCO_3$, which will also undergo calcination in the calciner

2.5.2 Configuration for syngas firing in the kiln only

The applicability of syngas as an alternative fuel in cement rotary kilns depends on its calorific value and the level of impurities. Syngas mainly contains hydrogen and carbon monoxide. As per the literature, hydrogen alone could not be used as an alternative fuel in cement rotary kilns due to its explosive properties combined with different combustion and radiation properties. But dilution with other gases like N_2 or steam can make it useable in the future [158]. A recent investigation showed that hydrogen can be used along with biomass in a kiln burner and will support overcoming the low calorific value limitation associated with high levels of biomass usage [159]. To the best of the authors' knowledge, no literature is available for syngas utilization as the primary fuel in cement rotary kilns where the temperature required in the burning zone is 1300-1450°C for clinkerisation reaction.

Researchers have reported syngas application in lime kiln plants where the temperature required is around 800-900°C for calcination purposes. Talebi and Goethem [160] investigated a plasma gasifier performance fed with RDF to generate syngas with a 0.82 mass ratio of plasma gas to feedstock. They applied syngas clean-up technologies before using them in the kiln. The desired calcination temperature is attainable with syngas as fuel. The adiabatic flame temperature of syngas is higher than that of coke oven gas which is a fuel for the lime kiln. However, the low heat value of syngas increases the fuel quantity requirement, which needs system modification.

2.5.3 Configuration for syngas firing in the kiln and calciner both

Fig. 2.7 shows the configuration of the integrated system for the kiln and calciner with gasifier [161]. The kiln and calciner must be fed with alternative fuels to achieve complete waste utilization in clinker production. As discussed in the previous section, the kiln fuel firing requirement is more specific, making 100% waste utilization quite challenging. Hue et al. [161] illustrated the gasification integration concept in cement plants considering 100% syngas as fuel for kilns and calciner. To achieve this, a high NCV with minimum impurities is the precondition. Some of the ideas presented in the patent for enhancing the NCV of syngas along with an increase in the energy efficiency of gasifiers are (a) the utilization of preheater exit gases available at more than 250°C in the gasifier, (b) quaternary (heated) air from clinker cooler at gasifier inlet, (c) injecting O_2 into the gasifier, reducing nitrogen impact, (d) steam injection into a gasifier, and (e) enrichment of C by addition of noble fuel (coal, petcoke) along with the waste. Syngas obtained from the gasifier is sent to the syngas purification unit to remove tar, chlorine, sulphur, etc. The purified syngas is fed as fuel to the calciner and kiln in a pre-defined ratio. Plasma torch gasification is proposed between the gasifier and the syngas purification unit. Due to high temperatures, tar is cracked into smaller condensable molecules. This system sends waste from the storage yard to the gasifier via the metering system. Some noble fuels (coal, petcoke) shall be fed along with waste to increase carbon content. Air is used as a gasification agent for the purpose. The preheater exit gases or cooler vent air can be provided instead of ambient air. Steam/O_2 also can be utilized to increase heat value. A calciner is supplied with two tertiary air ducts for O_2 and air. Oxygen injection is done at the kiln outlet to improve combustion inside the kiln. The raw meal gets preheated and undergoes calcination in the calciner. The temperature increases from 60°C to 800°C and enters the kiln for clinkering reactions. The gas will supply the heat for calcination at ~850°C and clinkerisation at ~1450°C. The rest of the system will not change. Ash from the gasifier is collected at the bottom and sent to the smoke chamber, where some unburnt carbon in ash gets burnt, and available heat can be used for combustion.

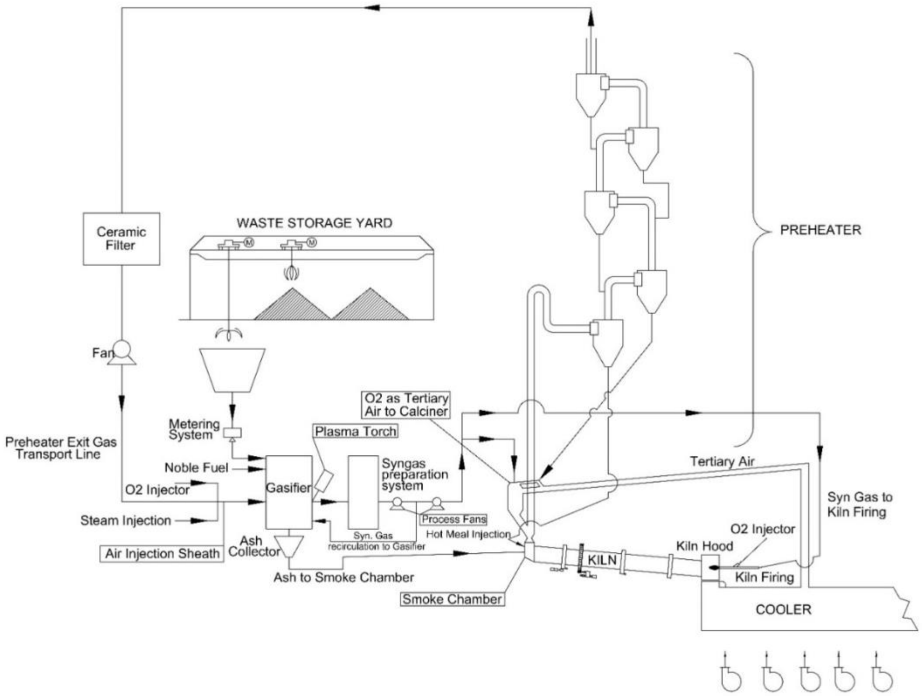

Fig. 2.7 High-quality syngas from waste gasification for pyro-processing [161]

Another way of ash utilization is an alternative raw material. Ash collected is ground with other raw materials and sent to the preheater as feedstock. It will help in utilizing mineral components present in ash as feedstock for clinker manufacture. Fig 2.8 shows the schematic diagram indicating ash utilization as cement raw material.

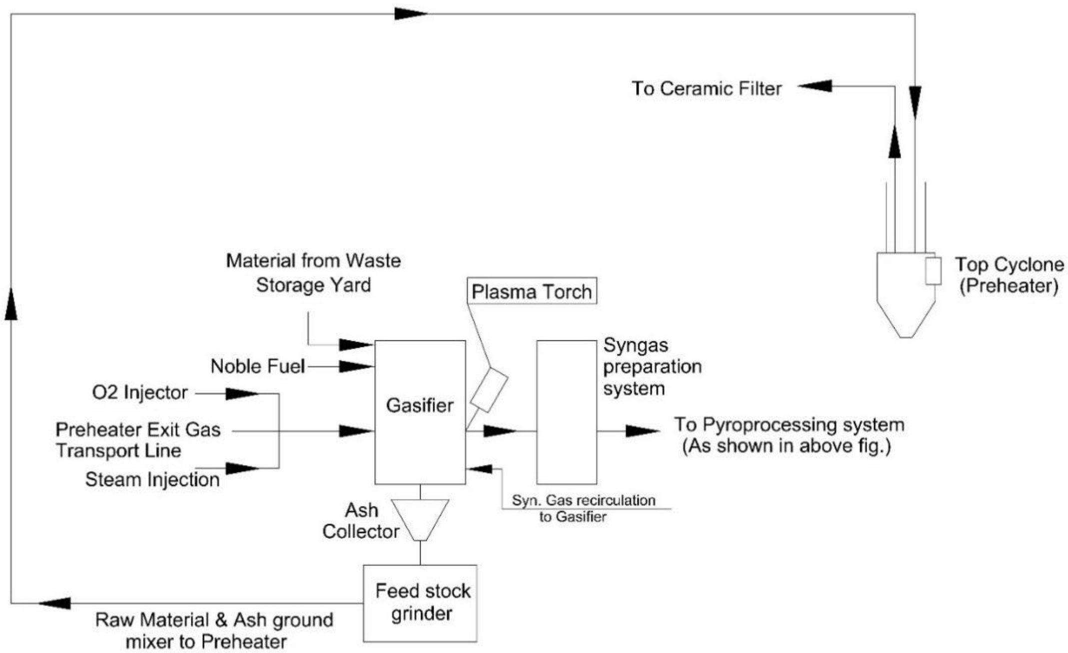

Fig. 2.8 Gasifier ash utilization as a raw material component for clinker manufacture [161]

2.5.4 Remarks on the configuration of syngas firing in the kiln

Oxygen use instead of the air shall be uneconomical due to energy-intensive air separation techniques employed, considering past experiences. Similarly, the plasma torch done at a very high temperature is highly energy intensive. Hence this technology does not look promising to be applied soon. It can become viable only when there is some economical option for an energy source for oxy gasification and plasma torch. H_2 as a part fuel has been explored but is still nascent. The design must be modified accordingly for 100% H_2 utilization in the kiln, which is a potential area of future research. Renewable H_2 will be an asset in this case.

2.6 Techno-economic feasibility studies for RDF gasification

Further moving from modelling to techno-economic feasibility, few studies are available covering alternative fuel aspects in cement plants. One study reported the application of reverse logistics networks for RDF production planning using topology optimization to maximize RDF utilization in Brazilian cement plants [162]. Some studies compared the techno-economic performance of RDF combustion and gasification for electricity generation [163, 164]. The reported electrical efficiencies of the system were 13-20% and 19-27%, respectively, for combustion and gasification. Some standalone studies are available for RDF-based power generation [53]. RDF gasification was performed in a pilot plant to burn RDF in an Otto cycle-based Internal Combustion Engine to produce electrical power. However, no literature covers the techno-economic aspects of integrating gasifiers into white cement plants to achieve high TSR for thermal application. In fact, regarding producer gas utilization in cement plants, only one cement plant-related study focuses on the life cycle assessment of plasma torch gasification (PTG) for cement plants [165].

Sabiron [165] investigated the life cycle assessment of plasma torch gasification (PTG) for cement plants. PTG is carried out using external electric energy sources, and the wastes are gasified in plasma flames at higher temperatures (as high as 2000°C or more) compared to conventional gasification processes. Technically, this performance reduces the gasification time and enhances the quality of the syngas since fewer oxidant compounds are required to complete reactions. Consequently, a richer gas in hydrogen (H_2) is obtained.

2.7 Site visits experiences

Some site visits were carried out to RDF preparation plant, material recovery facility, landfill site and cement plants using RDF to understand the ground situation of MSW processing, which have been discussed in detail in next section.

2.7.1 Visit to RDF plant of M/s UTCL, Jaipur

UTCL installed a 350 tpd MSW processing plant at Jaipur to cater to the MSW received from Municipalities in Jaipur. The processed MSW, i.e., RDF, is sent to nearby cement plants of UTCL to co-process as an alternative fuel. The Jaipur plant has a ballistic separator that separates the RDF based on size and density from heterogeneous MSW. Two-dimensional fractions like flexible cardboard, paper, and plastic film carry over the top to the front of the machine. Rigid and three-dimensional plastic and metal containers exit at the back of the machine. The third fraction, including fines sorted, will fall through the sieve mesh to ensure minimal loss of recyclables. The plant experiences frequent shutdown issues. Mixing expired chocolates with wrappers in the waste is done to improve the RDF calorific value. Fig. 2.9 highlights the processing steps from MSW feeding to RDF generation.

Fig. 2.9 Preparation of RDF at Jaipur RDF plant of UTCL

2.7.2 Visit to Kerala source segregation model

Kerala has a well-established decentralized Solid Waste Management (DSWM) system, which segregates and processes waste at the source to the maximum extent possible and then at the community level. Total Municipal Solid Waste generation in Kerala is ~3.7 million tonnes annually. The maximum waste is generated from households, followed by institutions. Out of the total 3.7 MTPA waste, about 18% is non-biodegradable, containing plastic, paper, cloths, metals, glass, rubber & leather, etc. Approximately 4-5% of material is recycled from this 18% waste.

A meeting was conducted with the Clean Kerala Company, which removes non-biodegradable waste and converts it into resources wherever possible. A visit was also carried out to the material collection facility (MCFs), established at the LSG level (Panchayats and Urban Local Bodies), for storing and segregating non-biodegradable waste. At MCF, municipal solid waste is segregated by a team of Saphai Sathis, where paper, plastic, leather, rubber, etc., is segregated. Resource Recovery Facilities (RRF) with shredding and baling facilities have also been established in the blocks, big Municipalities, and all corporations. As the current practice in Kerala, this non-biodegradable waste is collected by aggregators and sent to the recyclers and cement plants in bales form. Cement plants located in neighbouring states of Kerala receive these bales and further shredding and co-processing at their facilities in cement plants.

2.7.3 Visit to Ghazipur landfill

The MSW at the Ghazipur landfill contains food and garden waste, paper, plastic, glass, metals, garden trimmings, toiletries, rubber, ceramics, packaging box, textiles, batteries, wood waste, etc. Nearly 140 lakh tonnes of legacy waste are at the Ghazipur landfill, which is processed through biomining. Biomining refers to clearing the open dumpsites by segregating the prevailing waste into different constituents and converting the biodegradable portion into compost and the remaining non-recyclable plastic as refused-derived fuels, which can be used as an alternative fuel in industries. The compostable part of the waste is removed through sieving and sold for use as soil enrichers/fertilizers or landscaping. The trommel screens were installed at the Ghazipur landfill at different locations. The material was separated into three fractions: RDF, compostable matter, and inert fraction, as shown in Fig. 2.10. RDF was sent to nearby waste-to-energy plant, and some portion was sent to cement plants in Rajasthan.

Fig. 2.10 Waste processing through trommel screens at landfill site

2.7.4 Visit to RDF briquette manufacturing unit

A visit was undertaken to an RDF machinery manufacturing unit in Ghaziabad, India, to learn about the practical aspects of RDF briquetting. RDF is compressed to form briquettes in a briquette machine, which is easy to carry on conveyors and can be fed to the boiler. However, the cost is high compared to RDF. Fig. 2.11 shows the typical RDF and sawdust mixed briquette prepared by the manufacturer.

Fig. 2.11 Briquette of RDF and saw dust mix

2.7.5 *Visit to cement plants*

The site visits were carried out at some of the cement plants in Rajasthan, Chattisgarh, Andhra Pradesh, and Tamil Nadu, which utilize RDF and plastics as alternative fuels. The plants are facing operational issues like CO formation, specific heat consumption increase, shredder operation problems, and system jamming during RDF utilization. One cement plant has installed a kiln bypass system to avoid operational issues at a high TSR of 35%. The site visit pictures are shown in Fig. 2.12a and Fig. 2.12b.

Fig. 2.12a AF shredder operation in a cement plant

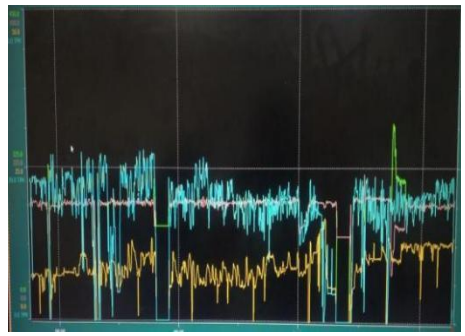

Fig. 2.12b CCR mimic showing AF feed of 25 tph in a high TSR cement plant

2.7.6 *Outcome of the visits / interactions*

It can be inferred from the above that there is no standard way of preparing RDF in India. Source segregation, briquetting, biomining, and MSW to RDF conversion plants are different models in India to prepare RDF. Moreover, cement plants using RDF via direct combustion face operational issues paving the way for technology like gasification to enhance TSR.

2.8 Research gaps

From the above literature reviews and site visits, the following research gaps are identified:

1. Limited experimental work has been carried out for the RDF gasification and co-gasification. Moreover, its application to the cement industry is scarce.
2. Only a few authors have worked on theoretical studies of RDF gasification. They reported Gibbs-free energy-based and Aspen-Plus-based models to predict producer gas quality. The models have limitations as they don't capture minor components like tar, H_2S, and HCl and consider RDF input ash-free. A realistic RDF gasifier model with ash and minor components needs to be developed, including separate modelling of drying, pyrolysis, combustion, and reduction zones of gasifier.
3. The literature survey highlighted that multiple cement plant calciner models are available; however, few models investigated the impact of different alternative fuels at varying TSR for grey or white cement. These models consider only solid alternative fuel. Hence co-processing of producer gas in a white cement plant is one area that is left unexplored. Such models are necessary to look into the aspects of process integration of gasifier and cement plant calciner using producer gas and achieve the perfect integration strategy. Further, it will support optimizing calciner design for coal/petcoke - producer gas co-firing calciner systems.
4. Techno-economic feasibility of producer gas (derived from RDF) has been explored mainly for power generation. The techno-economic analysis study for producer gas application as an alternative fuel for a grey or white cement plant is to be explored for industrial-scale application.

CHAPTER – 3

EXPERIMENTAL STUDIES

This chapter discusses the RDF characterization methodology followed by gasifier experimental work along with operating conditions in detail. RDF characterization techniques cover bomb calorimeter, CHNS analyzer, TGA and Py-GC/MS. The procedure for gasification includes downdraft gasifier details with feedstock of RDF or a mix of RDF and biomass. The details of the analytical equipment used and the methodology for analyzing producer gas components are also highlighted.

3.0 Experimental Studies

The description of the experimental work for the RDF gasification and producer gas analysis is reported in four parts:

1. Characterization of the RDF
2. Experimental setup description, along with analytical instruments used
3. Sample preparation using a palletizer
4. The methodology followed and the operating conditions used

3.1 Materials

Refuse-derived fuel (RDF): Six RDF samples named RDF A, B, C and F have been sourced from cement plants across India, while RDF D and E are taken from waste management companies. These are representative commercial RDF fluff/pellet samples having low heating value and high ash content, being utilized in Indian cement plants in 4 different zones of India or prepared in RDF plants. Zone wise representation includes RDF A, C and F (Southern Zone), RDF B (Central Zone), RDF D (Northern Zone) and RDF E (Western Zone). Samples are ground in a vibratory cup mill (Make: RETSCH) and passed through a 150-micron sieve. Proximate and ultimate analyses of RDF were performed as per BS EN and IS 1350: Part 2, respectively. The equipment used for ultimate analysis is the CHNS analyzer (Make: Variomacro Elementar, Germany). A bomb calorimeter (Make: IKA; Model: C5000) determines gross calorific value. The proximate, ultimate, LHV, and ash analysis results of six RDF samples conducted at NCCBM laboratories are tabulated in Table 3.1 and 3.2. Ash characterization was performed as per IS 1727:1967.

Table 3.1 Proximate and ultimate analysis of fuel

RDF	Proximate analysis (% air-dried basis)				Ultimate analysis (% air-dried basis)						LHV MJ/kg (air-dried basis)
	Total moisture	VM	Ash	FC	C	H	N	S	O	Cl	
A	1.02	52.90	40.23	5.80	36.59	5.56	0.40	0.60	15.21	0.50	16.08
B	2.02	38.17	53.86	5.90	37.31	5.82	0.40	0.30	0.32	0.50	10.52
C	2.61	55.34	35.26	6.80	37.45	4.78	1.30	0.30	17.68	0.60	14.09
D	2.58	43.92	51.00	2.50	30.20	4.92	0.70	0.30	9.89	0.50	12.07
E	3.57	58.54	31.86	6.03	38.57	5.66	0.70	0.30	18.97	0.40	14.36

RDF	Proximate analysis (% air-dried basis)				Ultimate analysis (% air-dried basis)						LHV MJ/kg (air-dried basis)
	Total moisture	VM	Ash	FC	C	H	N	S	O	Cl	
F	0.79	55.00	31.45	13.00	46.16	7.13	0.50	0.30	13.66	0.30	13.78

Table 3.2 RDF ash characterization

RDF	CaO %	SiO_2 %	Fe_2O_3 %	Al_2O_3 %	MgO %	Na_2O %	K_2O %	LOI %	SO_3 %
A	22.04	44.64	9.9	10.7	2.69	1.5	1.51	1.56	1.23
B	12.05	54.39	12.35	11.87	1.25	1.69	1.75	0.96	1.45
C	23.77	39.14	10.76	10.94	5.69	3.67	1.38	0.72	1.87
D	11.84	56.84	6.31	12.01	4.23	2.79	2.06	2.02	1.43
E	11.00	51.00	12.35	13.20	1.31	1.72	1.75	0.88	1.42
F	9.48	61.83	4.45	13.46	0.62	1.67	1.34	3.74	0.55

Note: For gasifier experimentation work, RDF C, D, E and F have been considered.

Biomass pellets: Biomass pellets have been sourced from M/s Favorite Suppliers, Jaipur, India. Pellets are cylindrical, 6–7 mm in diameter and 15–25 mm in length. The proximate, ultimate, and LHV analyses of biomass samples provided by the supplier are tabulated in Table 3.3.

Table 3.3 Proximate and ultimate analysis of biomass

Name of Sample	Proximate analysis (% dry basis)			Ultimate analysis (% air-dried basis)					LHV MJ/kg (air-dried basis)
	VM	Ash	FC	C	H	N	S	O	
Biomass	82	2	16	48.6	6.2	0.33	-	44.87	16.55

3.2 Experimental setup and analytical equipment

The gasification experimental study was carried out using the single-throat downdraft gasifier equipped with a producer gas cleaning system. A thermogravimetric analyzer (TGA) and pyrolysis-gas chromatography combined with mass spectrometry (Py-GC/MS) are used for RDF characterization. The analytical instrument for determining the producer gas composition is gas chromatography with a thermal conductivity detector (GC-TCD).

3.2.1 Gasifier experimental setup

The experimental setup mainly consists of six major pieces of equipment: downdraft biomass/RDF gasifier, venturi scrubber, sand bed filter, flare unit, air compressor, and data logger. The downdraft gasifier is divided into four reactive zones: drying, pyrolysis, combustion and reduction. The height of the gasifier reactor is 1100 mm, and the diameter of the pyrolysis and reduction zone is 310 mm and 150 mm, respectively. The reduction zone and oxidation zone heights are 100 mm and 53 mm, respectively. The schematic diagram and photograph of the downdraft gasifier experimental setup are shown in Fig. 3.1 and Fig. I.1 (Appendix I).

A grate is placed at the bottom of the gasifier to support charcoal burning during gasifier start-up. Moreover, the coarse residual ash during gasifier operation gets collected above the grate while the fine passes through the grate. Fine residue below the grate is contained in the water tray. A grate shaking mechanism is incorporated in the gasifier, which can be rotated along its axis from -30° to +30°. Gasifier clogging due to charcoal and material agglomeration is prevented by grate shaking. Two nozzles are provided in the oxidation zone of the gasifier (at 10 cm height above the grate), through which air is supplied continuously from an air compressor. A rotameter (Make: Fisher and Porter Co., Range: 0–11 scfm for the fluids having specific gravity 1.0 at 1 atm pressure) is provided to control the airflow rate entering the gasifier to maintain a constant equivalence ratio (ER). A water seal is provided at the top (circular lid) and bottom of the gasifier (open container) to have a downward flow and prevent gas leakage. The top seal is tightly connected to the gasifier body, providing safety against back pressure. The producer gas exits the gasifier from the bottom through a gas line and reaches the flaring unit. A flame gun is used to ignite the gas whenever required. The temperature of the oxidation and reduction zones of the gasifier are recorded in the data logger using thermocouples. It captures temperature readings after every minute, which helps analyze the combustion and gasification trend.

The producer gas cleaning system consists of a venturi scrubber and sand bed filter to prevent moisture and dust from escaping to the environment. The venturi scrubber consists of the converging section, diverging section, throat, and cyclonic chamber. Water and dust-laden gas enter the venturi scrubber from the top of the converging section and come in contact with the throat section. The clean gas gets released from the top of the cyclone, and water droplets with the absorbed dust get collected from the bottom. The gas from the venturi scrubber passes through the sand bed filter, two compartments based on a rectangular chamber supported on wire mesh. The gas stream moisture is removed after passing through wood shavings and a coarse and fine sand bed.

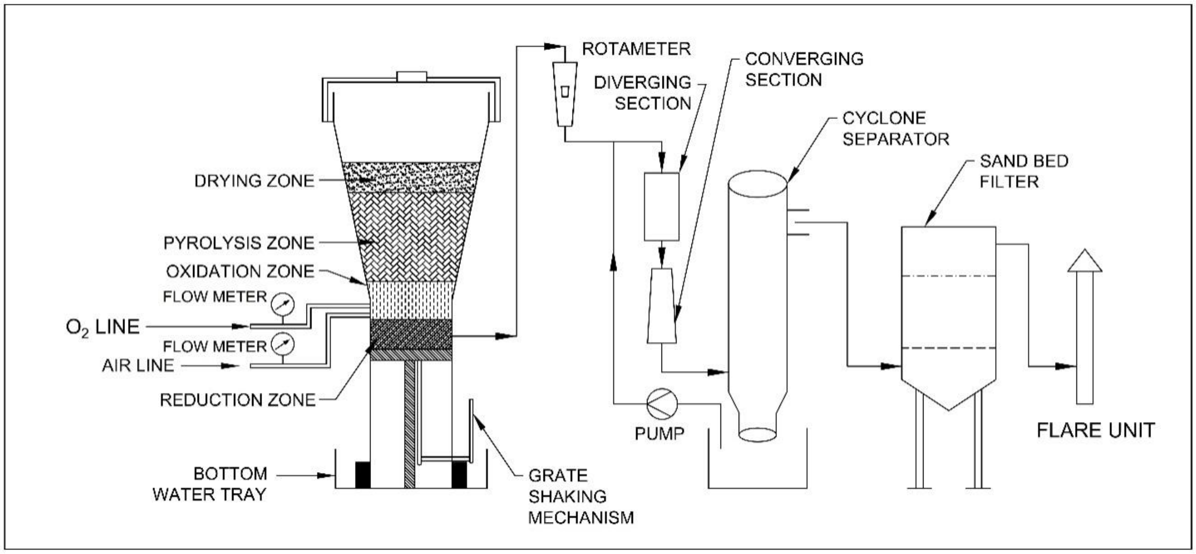

Fig. 3.1 Schematic of downdraft gasifier setup

3.2.2 Analytical instruments

3.2.2.1 Thermo-Gravimetric Analyzer (TGA)

The thermal degradation characteristic of RDF samples from different sources in inert and oxidizing conditions were studied using the TGA model TGA 4000; Perkin Elmer make (Fig. I.2 of Appendix I). TGA shows the change in weight with respect to temperature. The TGA of RDF samples A, B, C, D, E and F were conducted in a nitrogen environment with a 20 ml/min purge flow rate. A fixed quantity of RDF was placed in the reactor. Samples were heated up to 950°C in an inert environment at heating rate of 20°C/min with a hold for 3.0 min at 120°C and 950°C.

3.2.2.2 Gas chromatography

Producer gas composition (CO, H_2, CH_4, CO_2, and N_2) is determined using a gas chromatography model (Shimadzu GC-2014) along with a thermal conductivity detector (TCD) (Fig. I.3 of Appendix I). The GC analysis shows the composition of gases (CO, H_2,

CH_4, CO and CO_2) at different times and temperatures in the reactor. The column used is of carbosphere having a length of 1.8 m and inner diameter of 2 mm along with a maximum column temperature of 200˚C. Argon has been used as a carrier gas with a flow rate of 15 ml/min. The injection temperature and thermal conductivity detector temperature are maintained at 120˚C each. The gaseous samples were collected in the micro syringe every 5 minutes from the outlet of the gasifier burner, ensuring no leakage. It is then put into the GC column at every 30 min interval for analysis. The carrier gas moves through the column along with the sample molecules. The stationary phase inhibits the motion of the molecules. The difference in the boiling point of components leads to low boiling point components progressing faster toward the end of the column than high boiling point molecules. The outlet stream from the column reaches the detector at distinct times. The thermal conductivity detector (TCD), a non-destructive universal detector, is widely used in gas chromatography for its high reliability and ease of operation. The detector sends signals to the computer in the form of intensity vs retention time. This calibration curve determines the concentration of each component of the producer gas.

3.2.2.3 Pyrolysis-gas chromatography-mass spectrometry (Py-GC/MS)

Pyrolysis tests covering the characterization of the chemical composition and the structure of volatile and non-volatile compounds in RDF samples were carried out in a Py-GC/MS pyrolyzer (Shimadzu TQ 8040 NCI) equipped with a pyro probe (Fig. I.4 of Appendix I). The heat-induced cleavage of bonds within the chemical structures of the sample produces a train of low molecular weight species, which are indicative of specific types of macromolecules present in the sample (like lignin, PVC, cellulose, etc.). This mixture of compounds is then passed into the GC and MS analytical columns. About 0.45 mg of RDF sample was taken, and evolved gas analysis (EGA) was carried out to determine the different peaks associated with pyrolysis products. The heating ramp was 10°C/s. Moreover, a single-shot analysis for six samples was also done at 550°C. The characterization is performed under an inert (helium) atmosphere by analyzing the thermal degradation products of the compounds obtained after heating the sample to elevated temperatures.

3.3 Sample preparation using a palletizer

RDF F samples are obtained in fluff form. To reduce the heterogeneity of RDF and to maintain the heating value in the range of 3500-4000 kcal/kg fuel mix, RDF F is mixed with biomass pellets in 50:50 ratio to form RDF F-biomass mix pellets. Water and waste oil are added to the palletizer, which supports the preparation of pellets. Pellets are sun-dried later (Fig 3.2) to remove the added moisture before feeding to the gasifier. The palletization is performed in the palletizer model GET 2; make: M/s Gangotree Energy Projects Pvt Ltd, Pune. The photograph of the set up is shown in Fig. I.5 of Appendix I. The height and diameter of the RDF F-biomass mix pellet are in the range of 1.8-2 cm and 2-2.5 cm, respectively.

Fig. 3.2 Photograph of RDF-biomass mix pellets

3.4 Experimental procedure

In this section, the procedure followed for RDF gasification, RDF-biomass co-gasification, and RDF characterization is discussed in detail. Since RDF properties vary from location to location, RDF from different sources has been considered for experimentation work. The equivalence ratio is varied to study the effect on product yield and producer gas composition. The experimental procedure is divided into two parts: (1) gasification of RDF and (2) co-gasification of RDF and biomass. Both processes are discussed in sections 3.4.1 and 3.4.2, respectively. The experimental run details for gasification and co-gasification are given in Table 3.4.

Table 3.4 Downdraft gasifier experimental runs

Exp No	Feedstock	Airflow (Nm^3/hr)	O_2 flow (Nm^3/hr)	ER
1	RDF C fluff	6.00	-	0.58
2	RDF D pellet	6.00	-	0.36
3	RDF D pellet	5.00	-	0.38
4	RDF D pellet	5.00	1.10	0.45
5	RDF E pellet	6.00		0.44
6	50:50 mix of RDF E pellet and biomass pellet	6.00	-	0.35
7	50:50 mix of RDF E pellet and biomass pellet	8.00	-	0.46
8	30:70 mix of RDF E pellet and biomass pellet	7.50	-	0.36
9	RDF E pellet-biomass pellet mix (50:50)	7.00	-	0.45
10	RDF F fluff and biomass pellet mix (50:50)	7.00	-	0.47
11	RDF F fluff and biomass pellet mix (50:50)	5.80	1.20	0.68

3.4.1 RDF gasification in a downdraft gasifier

Experimental runs nos. 1, 2, 3, 4, and 5 are specific to RDF gasification only. 2-3 kg of RDF as feedstock is measured on a weighing balance. The compressor is switched on for air supply.

Water filled in the container is placed under the gasifier and in the circular trough at the top to prevent the gas from escaping from the gasifier, acting as a seal. About 500 g of charcoal is dumped as a heap into the reduction zone of the gasifier above the grate. 20-25 ml of diesel is added to aid charcoal combustion. The air is introduced in the biomass gasifier through nozzles, and its flow rate is maintained constant through a rotameter. The data logger is attached to monitor the temperature readings of the combustion and reduction zone. Once the combustion zone temperature reaches above 700°C and combustion is uniform across the combustion zone, around 2-3 kg RDF is fed into the oxidation zone of the gasifier. Once combustion starts properly and spreads across the oxidation zone, which generally takes about 3–5 min, the gasifier top cover is closed and considered as the start time of the experiment. After every minute, combustion and reduction zone temperatures are recorded at each thermocouple location. Producer gas samples are collected by syringes every 5 minutes for analysis using gas chromatography with a thermal conductivity detector.

Experimental runs are varied from 20-30 min depending upon the material and air flow rate. At the end of the experiment, any residual char, including leftover RDF, is removed from the gasifier and weighed. Fused clinker analysis has also been done on a case-to-case basis. The airflow rate is varied from 5 to 6 Nm^3/h in the present experimental runs. In one experimental run no 4 for RDF D, O_2 content is enriched to 35%, and the rest 65% is N_2 with an airflow rate of 5 Nm^3/hr and O_2 flow rate of 1.1 Nm^3/hr.

One of the experimental runs, no 3 for RDF D is carried out using spargers at two sides of the gasifier to distribute the air as gasifying agent circumferentially and prevent the cold spots formation, as shown in Fig 3.3. The air-sparger ring has an external diameter of 15 cm, equal to the diameter of the gasifier throat section. There are 14 holes in the air sparger, each having a diameter of 5 mm. The outer diameter of the air-sparger is the same as the inner diameter of the two nozzles. Hence it can be easily removed as and when required.

Fig. 3.3 Photograph of sparger

3.4.2 Co-gasification of RDF and biomass in a downdraft gasifier

Experimental runs nos. 6-11 are based on the co-gasification of RDF and biomass. Co-gasification of RDF and biomass in different ratios have been performed either by making pellets or by mixing pellets, and details of runs are given in Table 3.4. The procedure is the same as mentioned in section 3.4.1. In the RDF-biomass mix experimental runs, the airflow rate varies from 6 to 8 Nm^3/h. In experimental run no 11, O_2 content is enriched to 35%, and the rest 65% is N_2 with an airflow rate of 5.8 Nm^3/hr and O_2 rate of 1.20 Nm^3/hr.

CHAPTER – 4

MATHEMATICAL MODELLING AND SIMULATION

4.0 Mathematical Modelling and Simulation

This chapter describes the mathematical model development and simulation in two sections. The first section describes the model development for the downdraft gasifier and calciner, and the second incorporates the simulation of gasifier and calciner models. In section 4.1, model development is divided into three sections, i.e., section 4.1.1, multi-zone model development of downdraft gasifier, section 4.1.2, stoichiometric model development for calciner, and section 4.1.3, Aspen Plus model development for calciner**.** In section 4.2, the simulation methodology of all the models is discussed. The idea is to develop a model for the calciner using producer gas derived via the RDF gasifier model and study the integration of white cement plant calciner without full-scale trial runs.

4.1 Model development

4.1.1 Model development for downdraft gasifier

Fig. 4.1 represents the schematic of the downdraft gasifier model. The model consists of four zones, i.e., drying, pyrolysis, combustion, and reduction, where different thermochemical phenomena occur. The zone-wise model explanation is given in the next section.

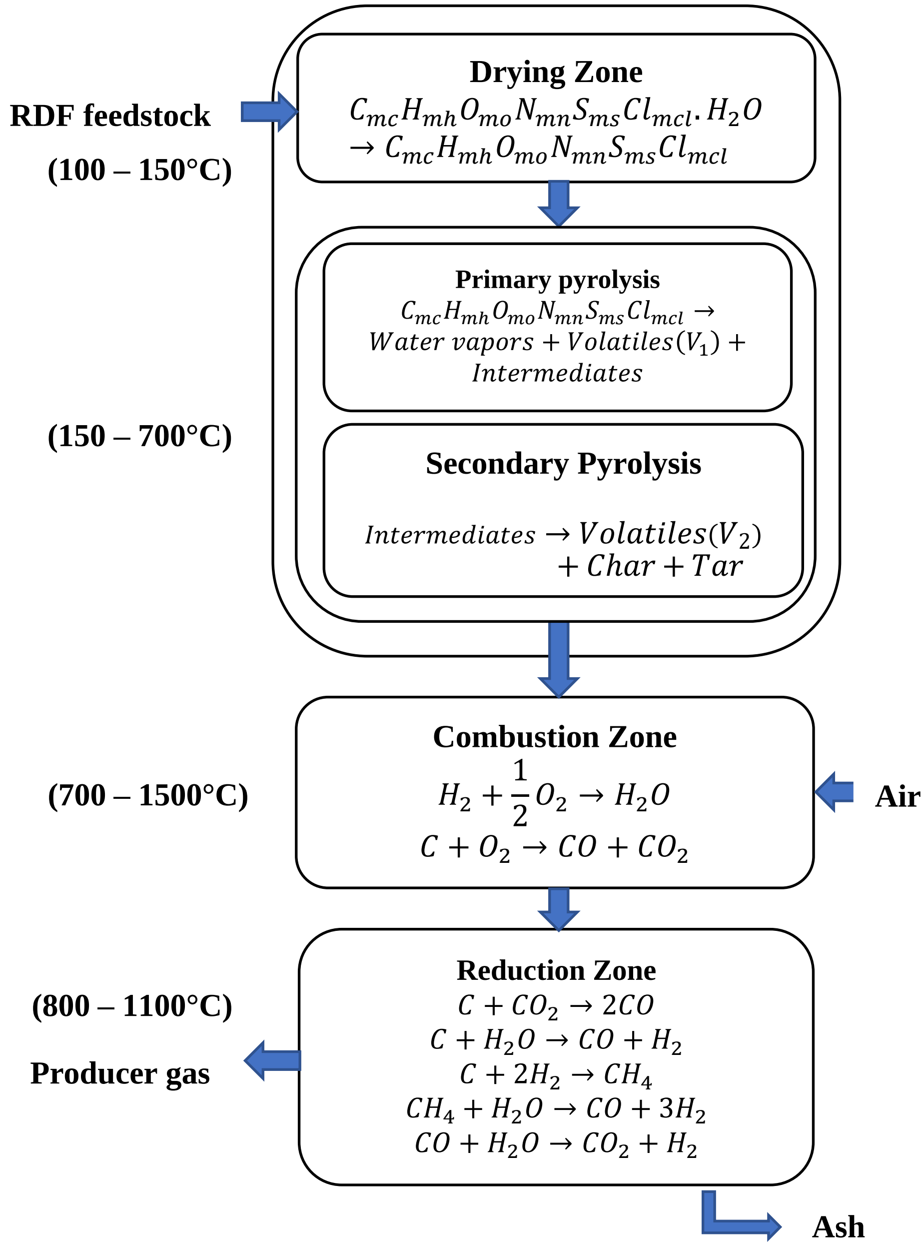

Fig. 4.1 Schematic diagram of downdraft gasifier model

4.1.1.1 Drying zone

The moisture content of RDF affects the temperature attained inside the gasifier. In the drying zone, the RDF moisture content is reduced by the heat generated due to the exothermic reactions of the oxidation zone. The temperature of the drying module increases from an initial temperature of 25°C to a temperature of 100°C until the vaporization of water molecules starts, and the temperature increases up to nearly 200°C; afterward, the pyrolysis process takes over [166]. A relatively simplified approach was adopted for modelling the drying zone [44]. It is assumed that all the moisture of the fuel vaporizes, and the corresponding energy required (Q_{dry}) is the sum of the sensible heat required for the moisture to reach the drying temperature (Q_s) and the latent heat required for the moisture to vaporize (Q_l).

$$Q_{dry} = w\left(C_{p,w}\Delta T + \Delta h_{v,w}\right) \tag{4.1}$$

Where w denotes the moisture content per mole of the fuel, $C_{p,w}$ is the specific heat of water, ΔT represents the temperature difference between the initial and final state of the moisture and $\Delta h_{v,w}$ is the latent heat of the vaporization of water. Eq. (4.2) calculates the moisture content in the RDF sample.

$$w = \frac{MW_{RDF} \cdot MC}{MW_{H_2O} \cdot (1 - MC)} \tag{4.2}$$

where MW_{RDF} represents the molecular weight of RDF, MC is the moisture content of the fuel and MW_{H_2O} is the molecular weight of water. Molecular weight of RDF is calculated using ultimate analysis of RDF and RDF ash composition. The weighted average of each RDF ash component with respect to molecular weight will provide the total molecular weight of the ash.

4.1.1.2 Pyrolysis zone

The heat generated due to the exothermic reactions in the oxidation zone mainly drives the pyrolysis zone reactions. The dried RDF gets thermally cracked into the water vapour, intermediates, and volatiles at a relatively lower temperature [167, 168], as shown by Eq. (4.3).

$$C_{mc}H_{mh}O_{mo}N_{mn}S_{ms}Cl_{mcl} \rightarrow Watervapor + Volatiles(V_1) + Intermediates \quad (4.3)$$

Further decomposition of intermediates at higher temperature ranges leads to the generation of volatiles (V_2), char, and tar [3,4] as per Eq. (4.4).

$$Intermediates \rightarrow Volatiles(V_2) + char + tar \quad (4.4)$$

The volatiles contains gases such as CO, CO_2, H_2, N_2, H_2O, CH_4, C_2H_4, and other hydrocarbons with components of sulphur and chlorine. The tar generated during the pyrolysis zone is assumed to remain constant throughout the gasifier. Thus, the overall reactions inside the pyrolysis zone are represented by the following reaction scheme:

$$C_{mc}H_{mh}O_{mo}N_{mn}S_{ms}Cl_{mcl}Ash_{mash} \rightarrow n_{char}Char + n_{CO}CO + n_{CO_2}CO_2 + n_{CH_4}CH_4 + n_{C_2H_4}C_2H_4 + n_{H_2}H_2 + n_{N_2}N_2 + n_{HCl}HCl + n_{H_2S}H_2S + n_{H_2O}H_2O + n_{tar}\left(C_{mc_{tar}}H_{mh_{tar}}O_{mo_{tar}}\right) + n_{Ash}Ash \quad (4.5)$$

Where the molecular weight of ash is to be determined using known ash composition

To determine the stoichiometric coefficients n_j of the product species evolved in the pyrolysis zone, the following assumptions were made:

The char is modelled as pure carbon. All the elemental hydrogen and oxygen are assumed to be released during the devolatilization process [43, 44, 119, 169].

All the pyrolysis zone's volatiles are modelled as an ideal gas [170].

Nitrogen (if any) inside the fuel is released as nitrogen gas. The nitrogen gas thus produced is assumed to remain inert throughout the gasifier, and the formation of NH_3 and HCN were neglected [44].

50% of the HCl formed from the elemental chlorine is assumed to be part of the producer gas [171, 172]

All of the sulphur content is assumed to form H_2S.

Temperature and heat distribution is assumed to be uniform at every point inside the pyrolysis zone.

The formation of higher molecular weight hydrocarbons, such as oils, phenolic compounds, and aromatic compounds, occurs in the gasifier's pyrolysis zone, as reported in the literature [53]. All such compounds are lumped into tar for a more realistic model approach.

The first six equations (4.6-4.11) obtained by doing elemental balances on carbon, hydrogen, oxygen, nitrogen, sulphur, and chlorine are as follows:

$$n_{char} + n_{CO} + n_{CO_2} + n_{CH_4} + 2n_{C_2H_4} + n_{tar} \cdot mc_{tar} = mc \quad (4.6)$$

$$4n_{CH_4} + 4n_{C_2H_4} + 2n_{H_2} + n_{HCl} + 2n_{H_2S} + 2n_{H_2O} + n_{tar} \cdot mh_{tar} = mh \quad (4.7)$$

$$n_{CO} + 2n_{CO_2} + n_{H_2O} + n_{tar} \cdot mo_{tar} = mo \quad (4.8)$$

$$2n_{N_2} = mn \quad (4.9)$$

$$n_{H_2S} = ms \quad (4.10)$$

$$n_{HCl} = mcl \quad (4.11)$$

In the case of biomass, the chemical composition of tar and the amount of tar generated depends upon the type of biomass and temperature. For the downdraft gasifier, the maximum tar yield is negligible and assumed to be independent of temperature. The tar molecular formula was represented by $CH_{1.03}O_{0.33}$ with the maximum inert tar yield of 4.5% by mass based on literature [44, 169, 173] has been considered. Also, the tar yield in producer gas generated from RDF is 45% lesser than that of woodchips [57, 173].

$$n_{tar} = \frac{4.5}{100} * (0.55) * (MW_{RDF}) \tag{4.12}$$

It is assumed that half of the available hydrogen inside the fuel, after the formation of water and tar, evolved as hydrogen gas. At the same time, 4/5th of the available oxygen inside the RDF is utilized in water formation [43, 44].

$$2n_{H_2} = \frac{1}{2}\left(mh - n_{Tar} \cdot mh_{tar} - 2n_{H_2O} - 2ms - mcl\right) \tag{4.13}$$

$$n_{H_2O} = 0.8 * (mo - n_{Tar} \cdot mo_{tar}) \tag{4.14}$$

Rest 1/5th of the oxygen was assumed to have evolved in the formation of CO and CO_2. The formation of CO and CO_2 in terms of the number of moles is assumed to occur according to the inverse of the ratio of their molecular weight [43, 44, 174], as shown in Eq. (4.15).

$$\frac{n_{CO}}{n_{CO_2}} = \frac{MW_{CO_2}}{MW_{CO}} \tag{4.15}$$

50% of the hydrogen after the formation of tar and water was assumed to have evolved in the formation of CH_4 and C_2H_4. Also, the formations of CH_4 and C_2H_4 in terms of the number of moles was assumed to occur according to the inverse of the ratio of their molecular weight [43, 44].

$$\frac{n_{CH_4}}{n_{C_2H_4}} = \frac{MW_{CH_4}}{MW_{C_2H_4}} \tag{4.16}$$

Finally, the eleven simultaneous equations are solved to obtain the yield of the product species n_j ($n_{char}, n_{CO}, n_{CO_2}, n_{CH_4}, n_{C_2H_4}, n_{H_2}, n_{N_2}, n_{HCl}, n_{H_2S}, n_{H_2O}$ and n_{tar}) inside the pyrolysis zone. It has been noted that the CH_4 and CO_2 composition is usually lower than the experimental results for lower ER. It is due to hydrogen generation, and water molecules in the pyrolysis zone that were associated with certain factors of the hydrogen and oxygen content of the fuel. As the hydrogen and water content increases, the methane and carbon dioxide content will decrease, respectively, as the hydrogen and oxygen content of the RDF is fixed. For this reason, two factors, a and b, are associated with the generation of H_2 and H_2O from the fuel hydrogen and oxygen content. Initially, both values were fixed at one and were progressively decreased by 0.05 to get a satisfactory result. A value of 0.85 for a and 0.75 for b was adopted in the present model. Similar assumptions for the pyrolysis zone are adopted by other authors [175-178].

4.1.1.3 Combustion Zone

The products of the pyrolysis zone enter the combustion zone, where char and some of the volatiles react with the limited supply of air. The combustion reactions are exothermic, and some of the heat generated during the combustion reactions is used to drive the drying/pyrolysis of the fuel. The temperature inside the combustion zone reaches up to 1000-1200°C. The actual amount of air supplied inside the combustion zone is calculated by the following formula:

$$y = \emptyset \cdot x \quad (4.17)$$

Where y is the actual amount of air supplied in the combustion zone, $\emptyset$ is the equivalence ratio which is defined as the ratio of actual air to stoichiometric air per unit quantity of fuel $(C_{mc}H_{mh}O_{mo})$.

$$Equivalence\ ratio(\emptyset) = \frac{(Air/Fuel)_{actual}}{(Air/Fuel)_{stoichiometric}} \quad (4.18)$$

x is the stoichiometric amount of air which is calculated by

$$x = (mc + 0.5mh - 0.25mo) \quad (4.19)$$

The following assumptions are made while modelling the combustion zone:

All the oxygen is reacted inside the oxidation zone, and no oxygen remains unreacted at the end of the combustion reactions.

Hydrogen has a higher affinity towards oxygen, and all the hydrogen will first react with the oxygen supplied and produce water vapour [43, 44, 166, 176].

$$n_{H_2}H_2 + \frac{n_{H_2}}{2}O_2 \rightarrow n_{H_2}H_2O \tag{4.20}$$

Balance oxygen, which is left after reacting with hydrogen, is consumed in the char oxidation reactions due to the large reaction area available for the adsorption of O_2 on highly active char [43, 44].

$$Char + O_2 \rightarrow CO_2\ ; \Delta H_R = -393.8\frac{kJ}{mole} \tag{4.21}$$

$$Char + \frac{1}{2}O_2 \rightarrow CO\ \ ; \Delta H_R = -110.6\frac{kJ}{mole} \tag{4.22}$$

The char oxidation reactions are assumed to proceed according to the inverse ratio of their heat of reactions in the form of $\frac{N_{CO}}{N_{CO_2}} = \frac{(\Delta H_R)_{CO_2}}{(\Delta H_R)_{CO}}$. The overall char oxidation reactions can be represented by Eq. (4.23).

$$n_{char}Char + (\emptyset - \frac{n_{H_2}}{2})O_2 \rightarrow N_{CO}CO + N_{CO_2}CO_2 \tag{4.23}$$

CH_4 and C_2H_4 have low burning velocities [43]. Due to this fact, the oxidation of C_2H_4 is assumed to occur next.

$$C_2H_4 + 3O_2 \rightarrow 2CO_2 + 2H_2O \tag{4.24}$$

The output of the combustion zone, in terms of the number of moles of constituents n_j, is found by performing mass balance and assuming that all the unreacted compounds of the pyrolysis zone contribute to the final product of the combustion zone.

4.1.1.4 Reduction Zone

The products of the combustion zone enter the reduction zone. The reduction zone is modelled as a cylindrical gasifier bed with a uniform cross-sectional area of A and negligible variation in gas and bed properties in the radial direction. The significant species considered in the reduction zone are $N_2, CO, CO_2, H_2O, CH_4$ and H_2 as reported in the literature [117]. The main set of reactions assumed to be occurring inside the reduction zone are illustrated in Table 4.1.

Table 4.1 Frequency factor and activation energy for reduction reactions [45, 116-118, 179]

i	Reaction	A_i (1/s)	E_i (kJ/mol)
1	Boudourd $C + CO_2 \leftrightarrow 2CO$	36.16	77.39
2	Water-gas $C + H_2O \leftrightarrow CO + H_2$	1.517×10^{4}	121.62
3	Methane formation $C + 2H_2 \leftrightarrow CH_4$	4.189×10^{-3}	19.21
4	Steam reforming $CH_4 + H_2O \leftrightarrow CO + 3H_2$	7.301×10^{-2}	36.15
5	Water-gas shift $CO + H_2O \leftrightarrow CO_2 + H_2$	2.824×10^{-2}	32.84
6	Tar steam reforming $CH_{1.03}O_{0.33} + 0.67H_2O \leftrightarrow CO + 1.18H_2$	70	16.74

The reactions were in the form of $n_A A + n_B B \leftrightarrow n_C C + n_D D$ and the rate expressions for the reactions were assumed to follow the Arrhenius-type temperature-dependent equation and are represented by Eq. (4.25).

$$r_i = nCRFA_i \exp\left(\frac{-E_i}{RT}\right).\left(P_C^{n_C} P_D^{n_D} - \frac{P_A^{n_A} P_B^{n_B}}{K_i}\right) \tag{4.25}$$

The corresponding rate expressions for the six reactions in Table 4.1 are reported in Table 4.2. CRF is the char reactivity factor determining the extent of reactions occurring in the reduction zone.

Table 4.2 Rate expressions for reduction reactions

i	r_i (mol m^{-3} s^{-1})
1	$r_1 = nCRF\,A_1\exp\left(\frac{-E_1}{RT}\right).\left(P_{CO_2} - \frac{P_{CO}^2}{K_1}\right)$
2	$r_2 = nCRF\,A_2 exp\left(\frac{-E_2}{RT}\right).\left(P_{H_2O} - \frac{P_{CO}.P_{H_2}}{K_2}\right)$
3	$r_3 = nCRFA_2\,exp\left(\frac{-E_3}{RT}\right).\left(P_{H_2}^2 - \frac{P_{CH_4}}{K_3}\right)$
4	$r_4 = nCRF\,A_3 exp\left(\frac{-E_4}{RT}\right).\left(P_{CH_4}.P_{H_2} - \frac{P_{CO}.P_{H_2}^3}{K_4}\right)$
5	$r_5 = nCRFA_5\,exp\left(\frac{-E_5}{RT}\right).\left(P_{CO_2}.P_{H_2} - \frac{P_{CO}.P_{H_2O}}{K_5}\right)$
6	$r_6 = nCRFA_6\,exp\left(\frac{-E_6}{RT}\right).\left(P_{CH_{1.03}O_{0.33}}^{1.25}.P_{H_2O}^{0.25}\right)$

The value of R_x for constituent species, N_2, CO_2, CO, CH_4, H_2O, H_2 and tar are illustrated in Table 4.3 [117]. Material balance for the constituents along differential bed length Δz yields Eq. (4.26).

$$\frac{dn_x}{dz} = \frac{1}{v}\left(R_x - n_x\frac{dv}{dz}\right) \tag{4.26}$$

Similarly, the temperature, pressure, and density variation along the length of the reduction zone is represented by [45, 117, 118]:

$$\frac{dT}{dz} = \frac{1}{v\sum_x n_x c_x}\left(-\sum_i r_i \Delta H_i - v\frac{dp}{dz} - p\frac{dv}{dz} - \sum_x R_x c_x T\right) \tag{4.27}$$

$$\frac{dv}{dz} = \frac{1}{\sum_x n_x c_x + nR}\left(\frac{\sum_x n_x c_x \sum_x R_x}{n} - \frac{\sum_i r_i \Delta H_i}{T} - \frac{dP}{dz}\left(\frac{v}{T} + \frac{v\sum_x n_x c_x}{P}\right) - \sum_x R_x c_x\right) \tag{4.28}$$

$$\frac{dP}{dz} = 1183\left(\rho_{gas}\frac{v^2}{\rho_{air}}\right) + 388.19v + 79.896 \tag{4.29}$$

Table 4.3 Overall rate of generation of the species

$Species$	$R_x (mol.m^{-3}.s^{-1})$
N_2	0
CO_2	$-r_1 + r_5$
CO	$2r_1 + r_2 + r_4 - r_5 + r_6$
CH_4	$r_3 - r_4$
H_2O	$-r_2 - r_4 - r_5 - 0.67 \cdot r_6$
H_2	$r_1 + r_2 - r_3 + 2r_4 - r_5 + 1.18 \cdot r_6$
$CH_{1.03}O_{0.33}$	$-r_6$

4.1.2 Stoichiometric model development for calciner

A stoichiometric model for the inline calciner of the white cement plant has been developed, which is applicable for solid and gaseous fuel mix firing. The model shall be able to simulate solid and gaseous fuel together by combining combustion and calcination governing equations. Mass and energy balances are carried out to establish the technical performance at 15% TSR. Producer gas quantity and temperature entering the calciner are derived from the gasifier model.

4.1.2.1 Model assumptions

- The calciner operates in a steady state such that the gas composition will be similar at any instant and any location within the calciner.
- Generally, fuel NOx formation occurs in calciner; however, N_2 is considered inert to avoid complexity, and NOx formation is not considered.
- Radiation loss in calciner ranges from 16-20 kJ/kg clinker. Accordingly, 0.4% of total heat input is considered calciner radiation loss.

- The impact of producer gas firing location in calciner has been ignored.
- All reactions in the calciner occur at the same temperature indicated by the calciner outlet temperature. Thus, a uniform degree of calcination is achieved.
- It is assumed that unburnt carbon leading to CO formation is negligible due to the complete combustion of fuel. With producer gas replacing petcoke, air-to-fuel mixing improves, facilitating better combustion.
- Petcoke ash is only 6.4%, which is non-reactive and shall be part of the hot meal (calciner outlet material in this case).
- The degree of calcination is constant at 88% for all the cases.
- 100% petcoke firing has been considered the baseline scenario, while co-firing of petcoke and producer gas in calciner in different ratios are alternate scenarios.
- The material to be calcined entering the calciner is 44059.9 kg/hr and is the same in all cases.
- The theoretical air requirement for complete combustion in the kiln is calculated considering the kiln: calciner firing ratio as 60:40 as per the actual firing. The actual air requirement is estimated considering the excess air based on the actual oxygen concentration (4.1%) at the kiln inlet.
- 12% calcination in the kiln is the basis to determine the kiln combustion products, which is an input to the calciner.
- Tar with molecular formula $CH_{1.03}O_{0.33}$ [44] gets generated from the gasifier as part of the producer gas and takes part in the combustion reaction in calciner liberating heat.

4.1.2.2 Model description

The cement production comprises three key steps: a calcination step which occurs in a reactor called pre-calciner; a second step, where the clinker is produced in a rotary kiln and the third and final step, where the cement is produced from the clinker by adding gypsum and other cementitious materials. Reinforced suspension preheater (RSP) calciner is one type of inline calciner (ILC) that incorporates a swirl calciner with a burner for fuel firing and a mixing chamber to increase clinker production and reduce heat consumption [180]. The present case incorporates an RSP calciner; its schematic is given in Fig.4.2.

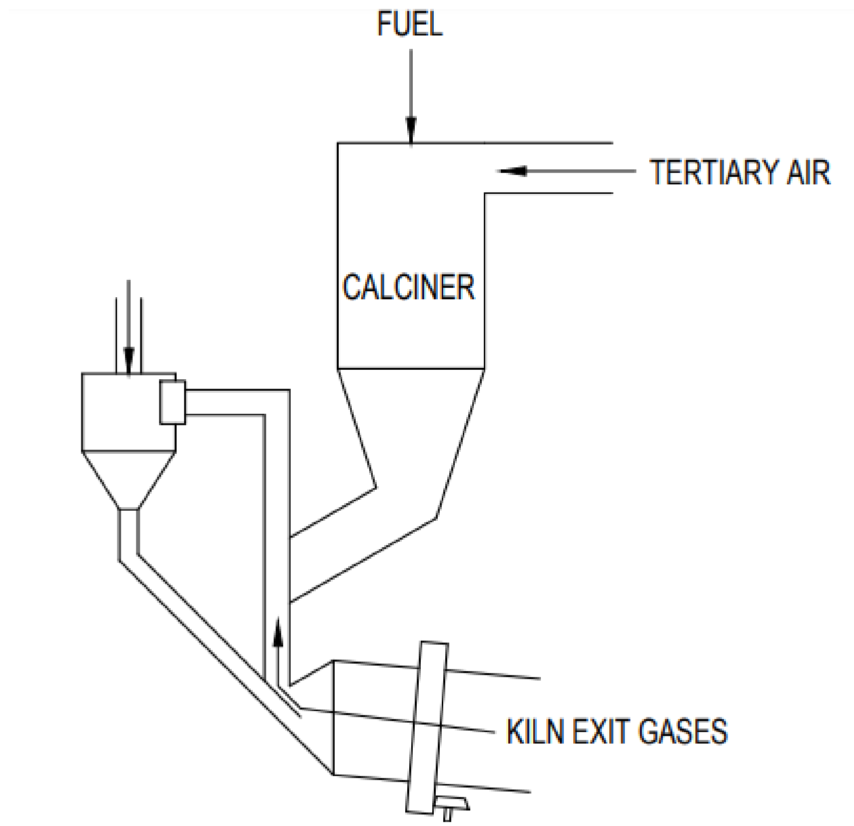

Fig. 4.2 Schematic diagram of the RSP calciner

All components of the input and output streams of the calciner are identified as shown in Fig. 4.3. Input and output stream components for all components are indicated in Table 4.4.

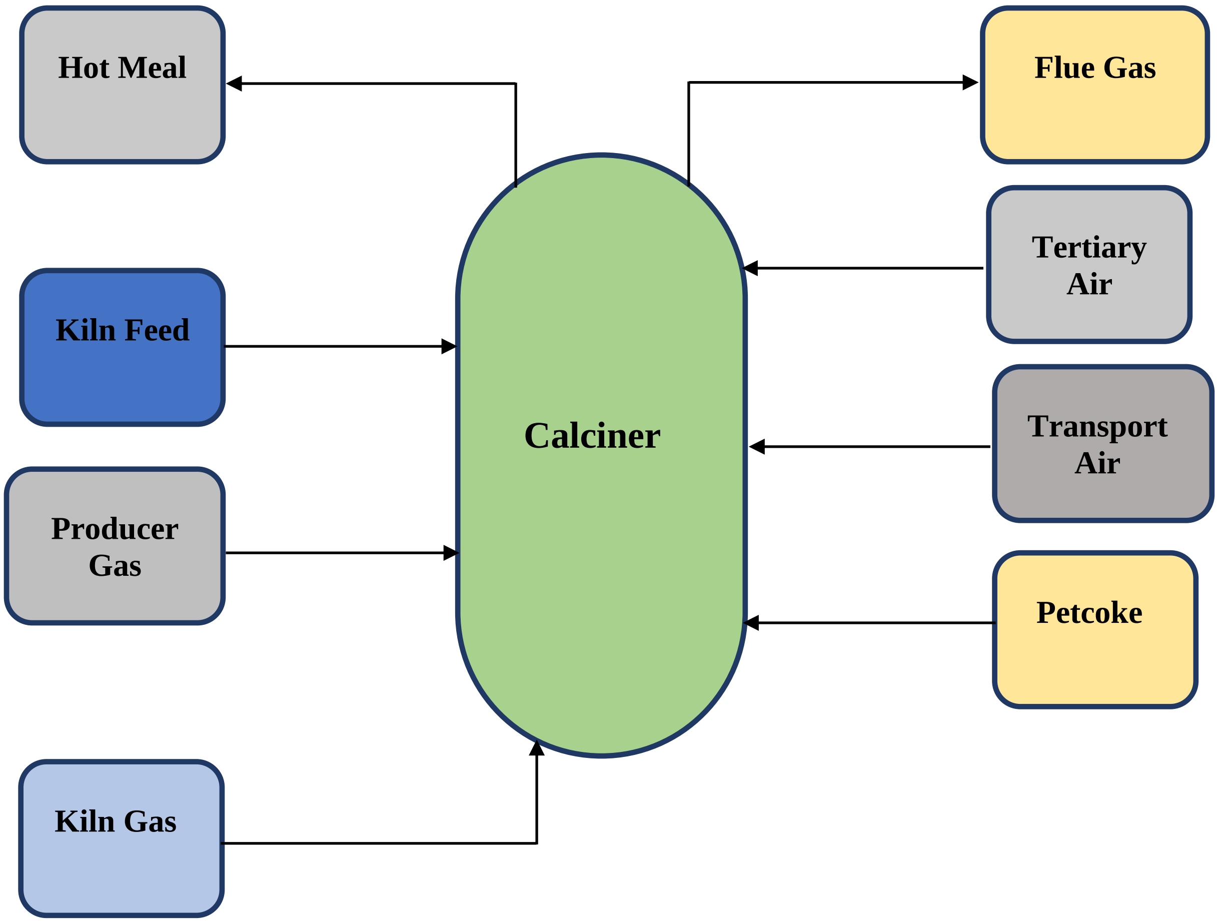

Fig. 4.3 Calciner inlet and outlet streams

Table 4.4 Inlet and outlet streams components [181]

Inlet Stream	Inlet stream components	Outlet Stream	Outlet stream components
Material Stream Kiln Feed (KF)	$CaCO_3$, $MgCO_3$, MgO, CaO, SiO_2, Al_2O_3, Fe_2O_3, K_2O, TiO_2	Hot meal (HM)	$CaCO_3$, $MgCO_3$, MgO, CaO, SiO_2, Al_2O_3, Fe_2O_3, K_2O, TiO_2, Fuel Ash
Petcoke (PF)	C, H, N, S, O	Flue gas (FG)	CO_2, O_2, N_2, H_2O, SO_2
Producer gas (AF):	CO, CO_2, N_2, CH_4, H_2		
Kiln Gas (FG-K):	CO_2, O_2, N_2, H_2O		
Tertiary Air (TA):	N_2, O_2		
Transport Air (TR):	N_2, O_2		

Combustion reactions

Eqns. (4.30-4.32) denotes the petcoke combustion and Eqns. (4.33-4.36) indicate the producer gas combustion and their heat of reaction [182]. Tar is part of producer gas with the tar molecular formula $CH_{1.03}O_{0.33}$ [44] and Eqn. (4.36) represents tar combustion. Stoichiometric analysis of the combined combustion equation for primary fuel with producer gas is shown in Eqn. (4.37).

$$C + O_2 \rightarrow CO_2 \qquad \Delta h = -393.5 \text{ kJ/mol} \tag{4.30}$$

$$H_2 + \frac{1}{2} O_2 \rightarrow H_2O \qquad \Delta h = -285.8 \text{ kJ/mol} \tag{4.31}$$

$$S + O_2 \rightarrow SO_2 \qquad \Delta h = -297.2 \text{ kJ/mol} \tag{4.32}$$

$$CO + \frac{1}{2} O_2 \rightarrow CO_2 \qquad \Delta h = -283.01 \text{ kJ/mol} \tag{4.33}$$

$$H_2 + \frac{1}{2} O_2 \rightarrow H_2O \qquad \Delta h = -285.8 \text{ kJ/mol} \tag{4.34}$$

$$CH_4 + \frac{1}{2} O_2 \rightarrow CO_2 + 2H_2O \ \Delta h = -1039.98 \text{ kJ/mol} \tag{4.35}$$

$$CH_{1.03}O_{0.33} + 1.09O_2 \rightarrow CO_2 + 0.515H_2O \ \ \Delta h = -22.65 \text{ kJ/mol} \tag{4.36}$$

$$W_{PF} \{W_{PF\text{-}1}C + W_{PF\text{-}2}H_2 + W_{PF\text{-}3}N_2 + W_{PF\text{-}4}S + W_{PF\text{-}5}O_2\} + W_{AF} \{W_{AF\text{-}1}CO + W_{AF\text{-}2}CO_2 + W_{AF\text{-}3} N_2 + W_{PF\text{-}4}CH_4 + W_{AF\text{-}5}H_2 + W_{AF\text{-}6} H_2O + CH_{1.03}O_{0.33}\} + \lambda_a(1+L_{lk})(O_2+\frac{aN_2}{aO_2}N_2) + N_{FG\text{-}K\text{-}CO2} CO_2 + N_{FG\text{-}K\text{-}O2} O_2 + N_{FG\text{-}K\text{-}N2} N_2 + N_{FG\text{-}K\text{-}H2O} H_2O = m_1CO_2 + m_2O_2 + m_3N_2 + m_4CO + m_5C + m_6H_2O + m_7SO_2 \tag{4.37}$$

where,

W_{PF}: Mass flow rate of the primary fuel petcoke (kg/unit time)

W_{AF}: Mass flow rate of the alternate fuel producer gas (kg/unit time)

$W_{PF\text{-}I}$: Weight fraction of the corresponding component in the primary fuel

$W_{AF\text{-}I}$: Weight fraction of the corresponding component in the alternative fuel

N_{FG-K}: Molar flow rate of flue gas constituents from the kiln

$\lambda_a(1 + L_{lk})$: Air demand

The total molar flow rate of flue gas is a sum of m_1, m_2, m_3, m_4, m_6, m_7, and $n_{cal-CO2}$.

$$m_{FG} = m_1 + m_2 + m_3 + m_4 + m_6 + m_7 + n_{cal-CO2} \quad (4.38)$$

where the m_5 is the mass flow rate of unburnt carbon C, which is negligible due to the complete combustion of fuel, $n_{cal-CO2}$ is calcined CO_2 obtained through calcination reactions (Section 3.3.2).

Calcination reactions

The calcination reactions occurring in the calciner are given in Eqn. (4.39) and Eqn. (4.40). CO_2 is evolved from preheater stages through calciner. CaO from the calciner moves to the bottom-most cyclone and enters the kiln.

$$CaCO_3 \rightarrow CaO + CO_2 \quad \Delta h = 179.17 \text{ kJ/mol at } 25°C \quad (4.39)$$

$$MgCO_3 \rightarrow MgO + CO_2 \quad \Delta h = 100.69 \text{ kJ/mol at } 25°C \quad (4.40)$$

The heat of the reaction at the calciner outlet temperature is to be calculated to establish heat balance [183].

4.1.2.3 Mass balance

The precalciner system is designed for at least 85-90% calcination before the material enters the kiln. However, kiln feed is already 30-40% calcined at the calciner inlet due to partial calcination in the top preheater stages. The material flow rate at the calciner inlet and outlet will be determined in this case. The degree of calcination at the calciner inlet is defined as

$$100 \,.\, [1 - \frac{LOI_{CI} \,.(100 - LOI_{kF})}{LOI_{kF} \,.(100 - LOI_{CI})}] \quad (4.41)$$

Where LOI is loss on ignition

As shown in Eqn (3.42) and Eqn. (3.43), the composition of kiln feed and partially calcined kiln feed at the calciner inlet is given as the sum of different components.

$$m_{kF} = m_{CaO} + m_{SiO2} + m_{Al2O3} + m_{Fe2O3} + m_{MgO} + m_{K2O} + m_{TiO2} + m_{LoI} + m_{others} \quad (4.42)$$

$$m_{CI} = m_{CaOCI} + m_{MgOCI} + m_{SiO2CI} + m_{Al2O3CI} + m_{Fe2O3CI} + m_{K2OCI} + m_{TiO2CI} + m_{othersCI} \quad (4.43)$$

where m_{kF} *and* m_{CI} are the total mass flow rate of kiln feed and partially calcined feed at the calciner inlet.

Once the degree of calcination is obtained using Eqn. (3.41), CaO and MgO at the calciner inlet are calculated using Eqn. (4.44) and Eqn. (4.45)

$$m_{CaOCI} = (m_{CaCO3}.\ DOC_{CI}) \cdot \frac{56}{100} \quad (4.44)$$

$$m_{MgOCI} = (m_{MgCO3}\ .\ DOC_{CI}) \cdot \frac{40.30}{84.31} \quad (4.45)$$

The mass flow rate of other components such as Al_2O_3, Fe_2O_3, MgO, K_2O and TiO_2 at calciner inlet will be the same as their mass flow rate in kiln feed, considering their inert nature.

Similarly, for calciner outlet (CO), CaO and MgO are calculated using Eqn. (4.46) and Eqn. (4.47)

$$m_{CaOCO} = m_{CaOCI} + ((m_{CaCO3CI}\ .\ DOC_{CO}) \cdot \frac{56}{100}) \quad (4.46)$$

$$m_{MgOCO} = m_{MgOCI} + ((m_{MgCO3CI}\ .\ DOC_{CO}) \cdot \frac{40.30}{84.31}) \quad (4.47)$$

where DOC_{CO} is the degree of calcination at the calciner outlet

$$m_M = m_{CaOCO} + m_{MgOCO} + m_{SiO2CI} + m_{Al2O3CI} + m_{Fe2O3CI} + m_{K2OCI} + m_{TiO2CI} + m_{othersCI} \quad (4.48)$$

where m_M is the calciner outlet flow rate or a hot meal.

Tertiary air (m_{TA}) and transport air (m_{TR}) is available from the plant data.

Thus, the overall mass balance as per Eqn. (4.49) is

$m_{CI} + m_{TA} + m_{TR} + m_{FG\text{-}K} + W_{PF} + W_{AF} = m_M + m_{FG} + m_{Ash}$ (4.49)

4.1.2.4 Energy balance

Sensible heat and heating value related to fuel, the sensible heat of partially calcined kiln feed, kiln exit gas, and air component are the input parameters. In contrast, the flue gas, hot meal enthalpy, the heat of reaction for calcination reactions, and radiation loss form the output parameters for energy balance. Eqn. (4.51) represents the energy balance equation and Eqn. (4.50) calculates the enthalpy.

$Q = m \cdot c_p \cdot dT$ (4.50)

The specific heat values (c_p) are taken from Nuchen et al. [39] and Perry's handbook [177].

$Q_{CI} + Q_{TA} + Q_{TR} + Q_{FG\text{-}K} + Q_{PF} + Q_{AF} = Q_M + Q_{FG} + Q_{Ash} + Q_{dH\text{-}All\ Reactions}$ (4.51)

Where Q_{CI}, Q_{TA}, Q_{TR}, $Q_{FG\text{-}K}$, Q_{PF}, Q_{AF}, Q_M, Q_{FG}, and Q_{Ash} represent the calciner inlet feed, tertiary air, transport air, kiln exit gas, petcoke, producer gas, hot meal, flue gas, and ash respectively. Q_{dH} denotes the heat of the reaction of $CaCO_3$ and $MgCO_3$ at a specific calciner outlet temperature.

4.1.3 Aspen Plus model development for calciner

An alternative calciner model has been developed using Aspen Plus software based on the previous models proposed by Zhang et al. [132] and Rahman et al. [94, 184]. The Aspen Plus model divides the combustion process into different unit operations (drying, pyrolysis, and combustion). A separate inbuilt reactor is assigned for each unit operation and executed. A combustion reaction is based on Gibbs free energy minimization principle, and the model has been augmented for producer gas firing along with petcoke at different TSRs. The simulation performs each unit operation block's material and energy balance, and results are obtained for each stream based on the raw material and fuel input. The model predicts the calciner outlet flow rate in tonnes per hour (tph), calciner outlet gas composition in terms of% O_2,% CO,% N_2,% CO_2, calciner outlet temperature (°C), hot meal flow rate (tph), including $CaCO_3$, CaO in the solid-phase stream.

4.1.3.1 Assumptions

- A calciner operates steadily, and turbulence, pressure losses and false air infiltration are ignored.
- The calcination process is divided into two separate processes: combustion and calcination. The combustion process is simulated using two reactors, RGIBBS reactor and RYIELD reactor, which are assumed to remain at a constant temperature.
- All reactions occur at the same temperature in the calciner, as indicated by the calciner outlet temperature.
- SiO_2, Al_2O_3, and Fe_2O_3 present in kiln feed are considered inert and do not participate in chemical reactions.
- Petcoke properties are considered on a dry basis, and its ash is considered non-reactive.
- N_2 is considered inert and shall not take part in chemical reactions.
- Heat loss from the calciner has also been considered.

4.1.3.2 Model description

Fig. 4.4 represents the proposed Aspen Plus model for the inline calciner and Table 4.5 indicates all ASPEN PLUS blocks and streams deployed in the simulation. The model incorporates five modules of different unit operations, one Fortran code, and fourteen streams.

Petcoke is a non-conventional component mentioned separately in Aspen Plus. For calculating the enthalpy and the density of non-conventional components like petcoke, the selected model is HCOALGEN and DCOALGEN [185, 186]. The heat value of the petcoke is fed to the model. The chosen thermodynamic methods are based on the Peng-Robinson equation of state since they suit high-temperature combustion. Since petcoke is not a conventional compound with a definite formula, modelling petcoke combustion requires its decomposition into elements based upon proximate and ultimate analysis, illustrated in the next paragraph.

The stream carrying existing fuel petcoke decomposes in an RYIELD reactor, which executes based on the calculator block (B2) with Fortran commands. The petcoke decomposition depends upon its proximate and ultimate analysis. The exiting stream from the RYIELD reactor, PET-Y, is transported to the PETCOMB reactor for the complete combustion of decomposed compounds in the presence of MIXGAS. MIXGAS (mixture of KILNGAS, TA, PA) from MIXER1 fulfills the air requirement for the PETCOMB reactor. The KILNGAS stream represents the rotary kiln exit gases entering the calciner through the kiln riser.

Contrary to the grey cement production plant, where tertiary air tapping is from the cooler, ambient air heated by preheater exit gas is termed tertiary air, which is to be utilized in kiln and calciner to reduce fuel consumption. PA is transport air for petcoke conveying in the calciner. The Q1 heat stream is required for petcoke decomposition and is a negative value entering the RGIBBS reactor. The PETCOMB is an RGIBBS reactor that works on Gibb's free energy minimization principle. All input parameters of the RGIBBS reactor are entered into the model. PRO1 is the output in the form of combustion products along with the heat of combustion Q2. PRO1 (combustion products), along with Q2, enters the calciner for the calcination reaction. The calcination is an endothermic reaction, and the Q2 heat will be utilized to calcinate the raw material ($CaCO_3$) in the RSTOIC reactor. The SSPLIT operator is applied to separate gases and solid materials from the product stream. This solid material (MATOUT) is the hot meal that enters the kiln. Calciner exit gases (GASOUT) pass through different preheater stages and leave through top-stage cyclones.

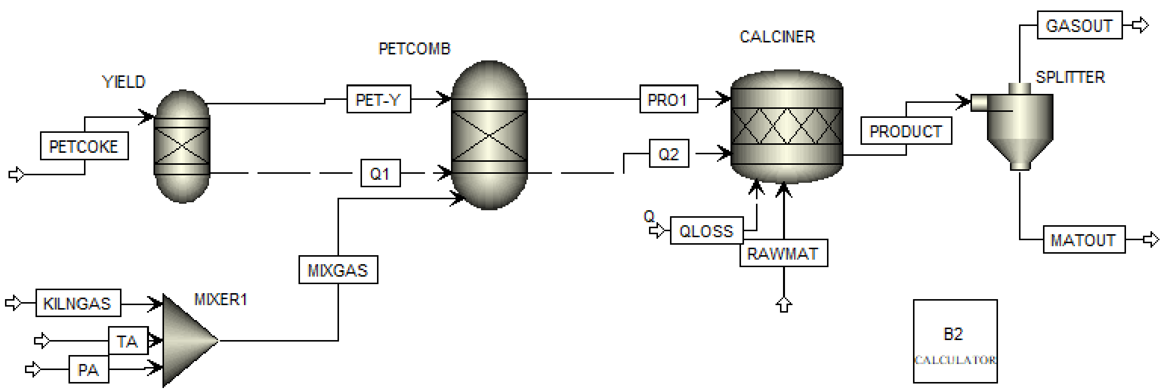

Fig. 4.4 Process model for calcination using ASPEN PLUS

Table 4.5 The description of the ASPEN blocks

ASPEN PLUS Block / Stream	**Block ID**	**Description**
RYIELD	Yield	RYield reactor decomposes petcoke into its conventional elemental components
RGIBBS	Petcomb	Conventional fuel components from RYIELD reactor undergoes combustion in RGIBBS reactor based on Gibbs free energy minimization
MIXER	Mixer1	The mixer is used to obtain a mix of kiln gas, tertiary airalong with transport air for petcoke
RSTOIC	Calciner	RSTOIC reactor is used for calcination using input heat from RGIBBS reactor
SSPLIT	Splitter	This block splits calciner outlet product into gaseous and solid streams, respectively
PETCOKE	Stream	Existing fuel to the system

ASPEN PLUS Block / Stream	Block ID	Description
KILNGAS	Stream	Kiln exit gases entering calciner
TA	Stream	Ambient air heated by preheater exit gas entering calciner as tertiary air
PA	Stream	Transport air for petcoke conveying to the calciner
PET-Y	Stream	Yield from RYIELD reactor to RGIBBS reactor
MIXGAS	Stream	The mixture of kiln gas, tertiary air, transport air
Q1	Stream	The heat required for petcoke decomposition
PRO1	Stream	Products of combustion
Q2	Stream	The heat released along with fuel combustion
QLOSS	Stream	External heat loss through calciner
RAWMAT	Stream	Material entering the calciner
PRODUCT	Stream	Combination of material and gas exiting the calciner
GASOUT	Stream	Calciner exit gases
MATOUT	Stream	Calciner exit material (hot meal entering kiln)

4.1.3.3 Model augmentation

Model augmentation is carried out to introduce the co-firing of producer gas and petcoke in the calciner. The Aspen Plus model of the RSP inline calciner has been modified accordingly, and its flowsheet is shown in Fig. 4.5. As petcoke is getting replaced by producer gas, the air requirement changes, and it can be determined by optimizing the split of the combustion gases stream into two different streams. A splitter is introduced for this purpose after MIXER1, which splits the gases into two streams named MG1 and MG2. The fraction MG1 is for petcoke, and another fraction MG2 is for producer gas combustion. Producer gas enters MIXER 2 along with MG2.For producer gas combustion, an RSTOIC reactor is used where chemical reactions for the combustion of producer gas components are added along with the heat of combustion. The PETPRO and SYNPRO are the combustion products from PETCOMB and SYNCOMB reactors, respectively. Combustion products and the respective combustion heat are introduced in a calciner for calcination. The remaining part of the model is the same as the base model (Fig. 4.4). Table 4.6 describes all model input parameters required for the simulation of the augmentation scenario in comparison to the base model.

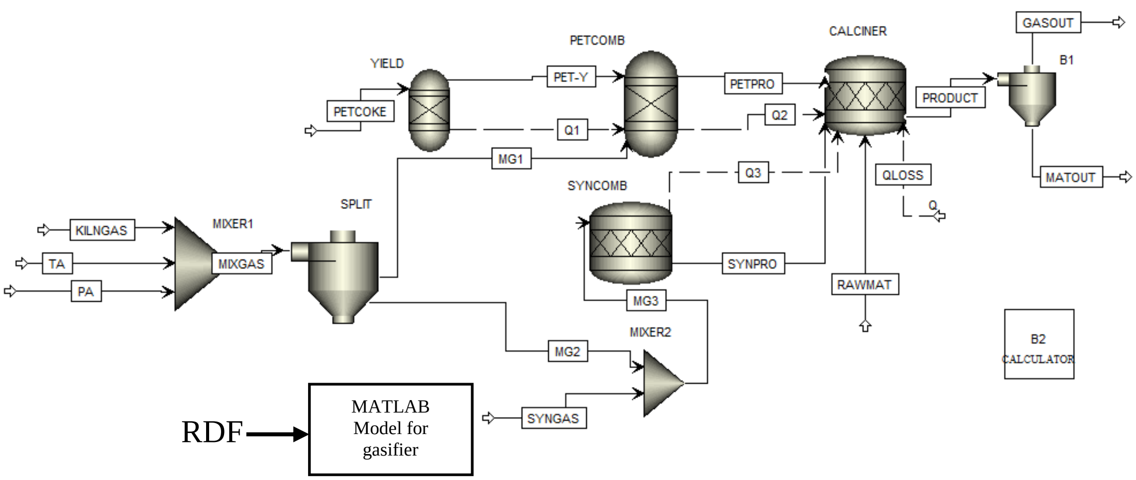

Fig. 4.5 Augmented process model for calcination using Aspen Plus

Producer gas combustion is accompanied by the following reactions 4.52, 4.53 and 4.54.

$$CO + 0.5\ O_2 \rightarrow CO_2 \quad (4.52)$$

$$CH_4 + 2\ O_2 \rightarrow CO_2 + 2H_2O \quad (4.53)$$

$$H_2 + 0.5\ O_2 \rightarrow H_2O \quad (4.54)$$

The heat of combustion for the above reactions is taken from the Aspen properties database. N_2 and CO_2 in producer gas are inert components and will not take part in chemical reactions. Producer gas requirement at 8 and 15% TSR is calculated and fed as input to the calciner with petcoke, as indicated in Table 4.6. Mix gas (kiln gas + tertiary air + primary air) distribution through the splitter is optimized, and the operating range is determined by sensitivity analysis at different ratios

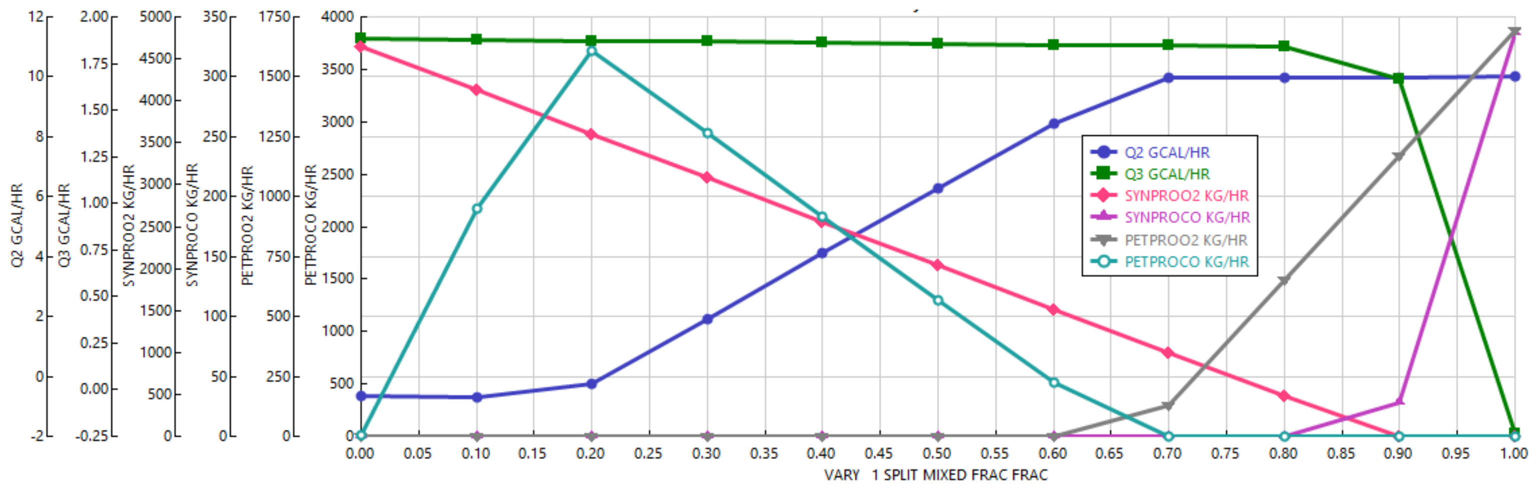

Fig. 4.6 Operating range for mix gas (MG1) for petcoke and producer gas combustion at 8% TSR

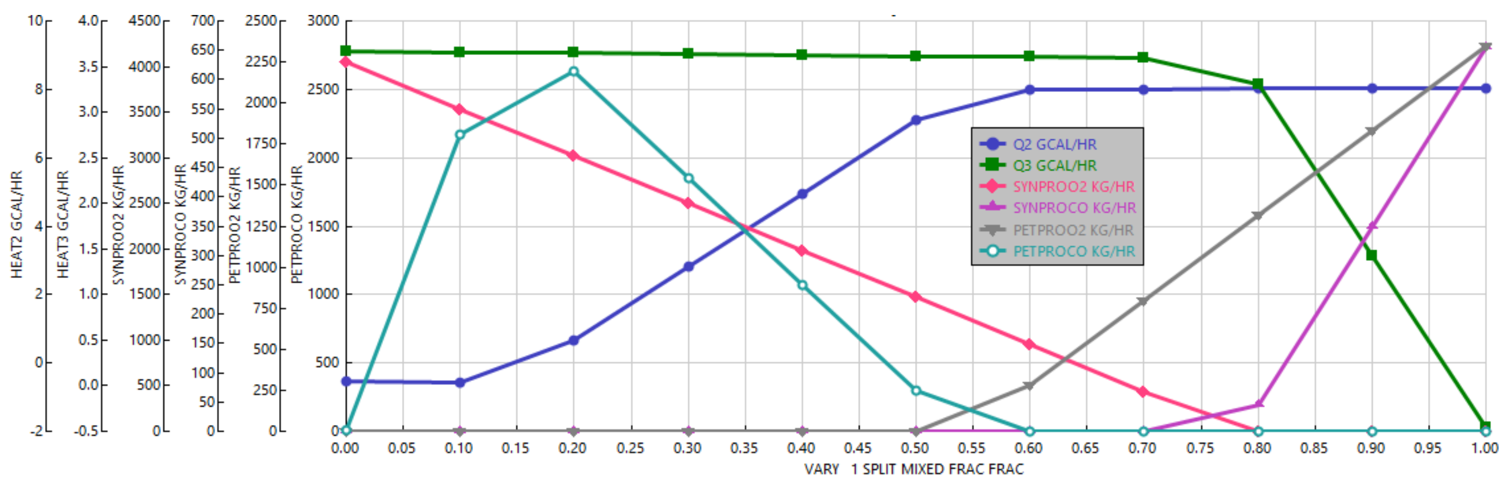

Fig. 4.7 Operating range for mix gas (MG1) for petcoke and producer gas combustion at 15% TSR

The optimum air-to-fuel ratio for petcoke and producer gas combustion at 8% and 15% TSR is shown in Fig. 4.6 and Fig. 4.7, respectively. The fraction of total mix gas (MG1) for petcoke combustion is plotted against petcoke and producer gas combustion products along with their respective heat requirement Q2 and Q3 using the sensitivity analysis tool of Aspen Plus. It can be inferred that no CO generation is observed for a certain range of MG1 (X-axis), indicating an optimum operating range. That range is 0.70-0.80 for 8% TSR and 0.60-0.70 for 15% TSR. Thus, 0.80 and 0.70 have been considered as operating point for 8% and 15% TSR respectively.

Model parameters of Aspen Plus reactors for the base model and the augmented base model

Table 4.6 shows the base model and augmented model input parameters used for simulation. The output of one reactor is input to another reactor as per the flowsheet.

Table 4.6 Base model and augmented model simulation parameters

Component	Parameter	0% TSR	8% TSR	15% TSR
Producer gas	Flow rate (kg/hr)	NA	2441.70	4735.32
	Temperature (°C)	NA	593	593
	Pressure (mmWG)	NA	10236	10236
	Composition (wt%), wet basis	NA		
	CO	NA	13.82	13.82
	H_2	NA	0.93	0.93
	CO_2	NA	9.34	9.34
	CH_4	NA	2.03	2.03
	N_2	NA	54.95	54.95
	H_2O	NA	18.93	18.93
Petcoke	Flow rate (kg/hr)	1720	1383.38	1085.50
	Temperature (°C)	50	50	50
	Pressure (mmWG)	11000	11000	11000
Kiln gas	Flow rate (kg/hr)	40557	40557	40557

Component	Parameter	0% TSR	8% TSR	15% TSR
	Temperature (°C)	1050	1050	1050
	Pressure (mmWG)	10316	10316	10316
Tertiary air	Flow rate (kg/hr)	14329	14329	14329
	Temperature (°C)	267	267	267
	Pressure (mmWG)	10296	10296	10296
Transport air	Flow rate (kg/hr)	714	500	450
	Temperature (°C)	60	60	60
	Pressure (mmWG)	11036	11036	11036
Calciner feed	Flow rate (kg/hr)	44060	44060	44060
	Temperature (°C)	775	775	775
	Pressure (mmWG)	10216	10216	10216
YIELD	Temperature (°C)	700	700	700
	Pressure (mmWG)	10416	10416	10416
PETCOMB	Temperature (°C)	850	850	850
	Pressure (mmWG)	10256	10256	10256
CALCINER	Pressure (mmWG)	10256	10256	10256
	Heat of reaction for $CaCO_3$ (kJ/mole)	169	169	169
	Heat of reaction for $MgCO_3$ (kJ/mole)	100.68	100.68	100.68
B1	Exit gas	1	1	1
SPLIT	Mix air ratio to PETCOMB	NA	0.8	0.7

4.2 Model simulation

4.2.1 Gasifier model

A set of simultaneous ordinary differential equations (4.26) to (4.29) are obtained employing mass and energy balance on a differential length of the reduction zone. The producer gas composition and temperature profile along the reduction zone length are found by solving the differential equations numerically using ODE45 in Matlab. Thus, molar density is derived after the reduction zone of all components (N_2, CO, CO_2, CH_4, H_2, H_2O, and tar). The total no of moles before the reduction zone along the N_2 mole fraction is also obtained from the model solving drying zone, pyrolysis zone, and combustion zone equations. Based on the N_2 balance, the final output's moles of each gaseous component are calculated.

4.2.2 Stoichiometric calciner model

Once the model equations are developed, baseline conditions are set where producer gas flow (W_{AF}) = 0 considering 100% petcoke firing for a fixed quantity of calciner inlet kiln feed. Then simulations are performed for baseline conditions. Further simulations are performed for varying TSR with petcoke and producer gas co-firing. RDF proximate, ultimate, and ash analysis is fitted into the gasifier model to determine producer gas properties and operational parameters. It will establish TSR to fix the producer gas and petcoke flow rates. Kiln feed flow rate with degree of calcination is used to establish calciner inlet and outlet flow rate using Eqns. (4.41-4.47). The kiln inlet flow rate is calculated based on the petcoke firing in the kiln and calculated combustion products and excess air at the kiln inlet. Other inputs are tertiary air and transport air obtained from the plant data. All inputs, temperatures, c_p values, and enthalpies are fed to the stoichiometric MS excel model. Then Eqn. (4.49) and Eqn. (4.51) are solved to perform material and energy balance. Further, the goal seek function of MS Excel performs iterations with calciner outlet temperature as an objective function till $\Delta h = 0$. The final values shall be the corresponding calciner outlet flow rate in tonnes per hour, calciner outlet gas composition in terms of% CO_2,% O_2,% N_2, and hot meal flow rate (tonnes per hour). The flowchart of the model simulation process is shown in Fig. 4.8 for a better explanation of the process.

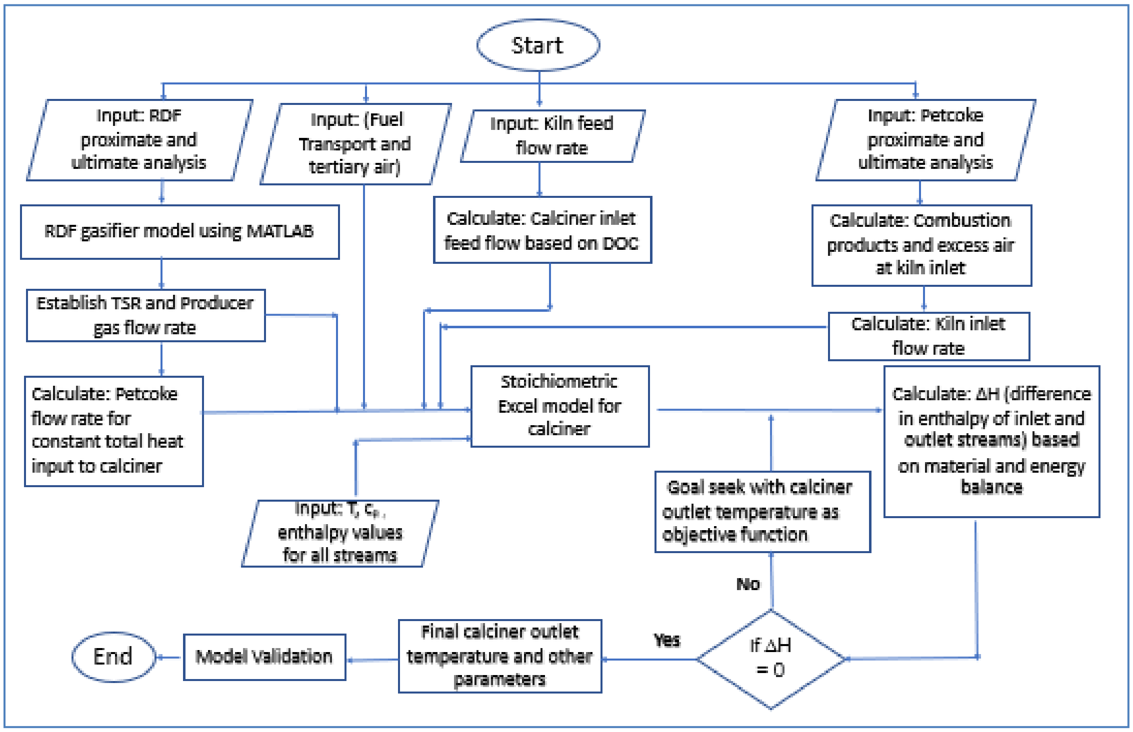

Fig. 4.8 Flowchart of the simulation process

4.2.3 Aspen model for calciner

The difference from the previous model is in the concept of the Aspen Plus simulation. Petcoke ultimate analysis is input to the Ryield reactor, where it gets decomposed and sent to RGibbs reactor along with a mixed air stream for combustion. Further calcination takes place in the Rstoic reactor using heat evolved during combustion. Material and energy balance is established at each stage by performing iterations. Final output parameters for the calciner are obtained. The flowchart of the simulation process of the Aspen Plus-based model is shown in Fig. 4.9.

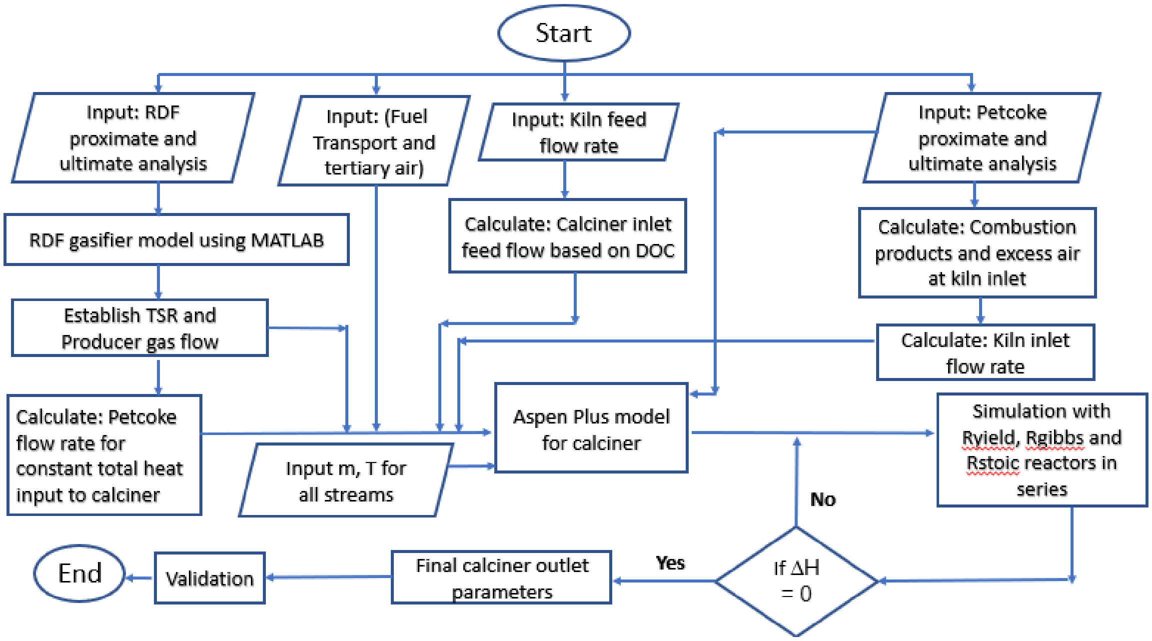

Fig. 4.9 Flowchart of the simulation process

CHAPTER – 5

RESULTS AND DISCUSSION

5.0 Results and discussion

This chapter presents the experimental and simulation results for the gasification of RDF and co-gasification of RDF & biomass mix using the downdraft type gasifier. This study develops a multi-zone RDF gasifier model (Chapter 4, section 4.1.1), and experiments are carried out to validate the model. Further, gasifier modelling results are used to simulate the developed calciner models (Chapter 4, section 4.1.2 and 4.1.3) to predict calciner outlet parameters for a white cement plant. The experimental study results are discussed in section 5.1 and 5.2, and the simulation results of the gasifier and calciner models are presented and discussed in section 5.3.

5.1 RDF characterization studies

5.1.1 Thermal analysis

The thermal analysis of six RDF samples A, B, C, D, E and F, was carried out using TGA showing the change in weight with respect to temperature. Fig. 5.1 a-f represents the results of experimental runs performed at a heating rate of 20°C/min. The first mass loss step observed at the beginning of experiment, from ambient temperature to about 220°C, is attributed to the loss of moisture and very light volatile matter content of the RDF. This temperature is high enough to ensure that the most tightly bound moisture was driven from the specimens. The presence of the shoulders in this region shows that there are different volatile matter fractions. The onset of the second zone is around 210°C, 230°C, 280°C, 250°C, 240°C and 250°C with its offset at about 500°C, 470°C, 500°C, 500°C, 460°C and 400°C for samples A, B, C, D, E, and F, respectively. This zone is attributed to the degradation of hemicellulose and cellulose components with a minor portion of volatiles from lignin at higher temperatures. Lower temperature volatiles in this region was due to hemicellulose decomposition, and at higher temperatures, cellulose decomposition was assumed as the decomposition temperatures of hemicellulose, cellulose, and lignin are in ascending order in line with the literature data [104]. The sources of these can be jute, hemp, cotton, wood, paper, etc. The boundary for the 3rd zone is set at 770°C, 790°C, 755°C, 720°C, 740°C and 780°C for RDF A, B, C, D, E, and F, respectively, and represents the devolatilization of lignin and plastic and remaining cellulose. The downward curve after the offset of the 3rd zone represents the slow decomposition of char material with the release of high-temperature volatiles. The reactions between char and volatiles, which were coming from previous phases of the process, might be another cause of this last peak. Sample A, B, C, D, and F encountered multiple shoulder peaks, while sample E saw no shoulder in the main decomposition range and had a consistent downward curve. When the degradation temperatures and decomposition rates of different types of volatile matter present in RDF samples are close to each other, fewer peaks are formed, which might be the case observed in E.

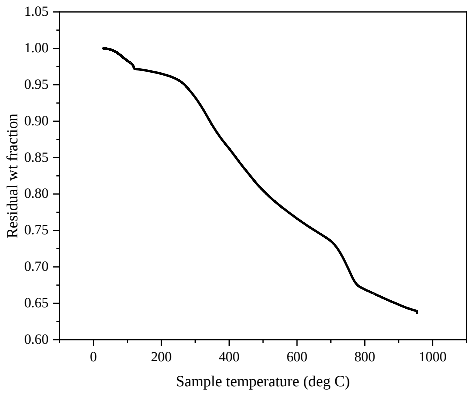

a) Sample A

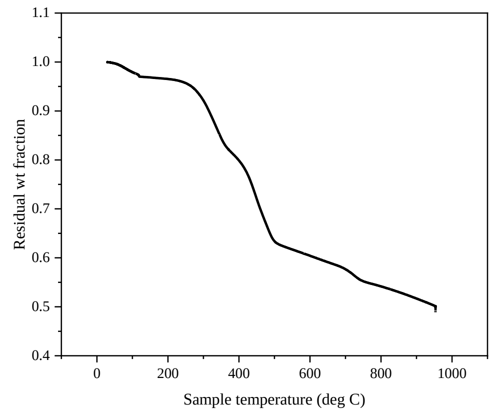

b) Sample B

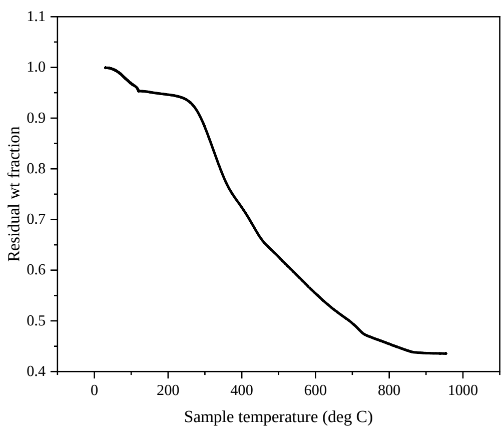

c) Sample C

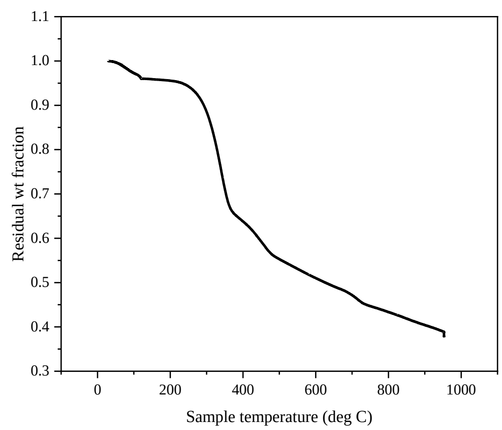

d) Sample D

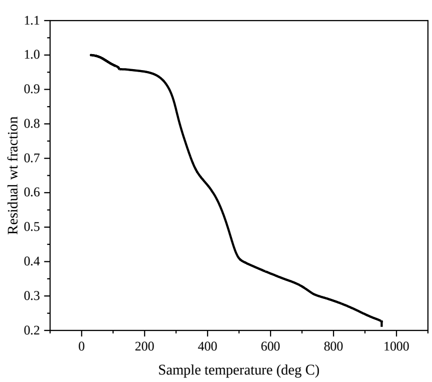

e) Sample E

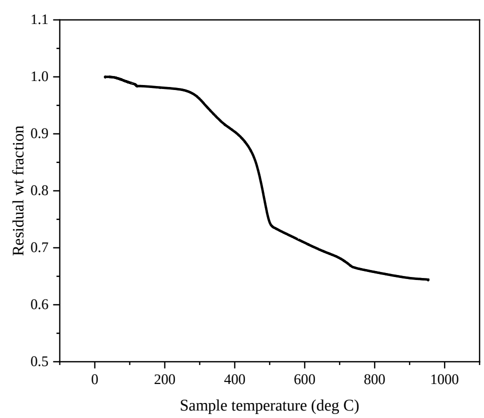

f) Sample F

Fig. 5.1 Thermogravimetric analysis of six RDF samples

5.1.2 Py-GC/MS analysis

Pyrolysis is one of the critical steps in RDF gasification. The pyrolytic compounds generated get reduced in the reduction zone contributing to final gasification products. Py-GC/MS is useful for identifying pyrolytic compounds and determining high molecular weight hydrocarbons, such as oils, tars, phenolic compounds, and aromatics compounds. It shall be corroborated further to identify the parent source material. The evolved gas analysis mass spectrometry (EGA MS) and single-shot analysis of six different RDF samples have been done to investigate thermal decomposition and to obtain qualitative and semi-quantitative data. EGA MS and single shot analysis results are discussed in section 5.1.2.1 and 5.1.2.2, respectively.

5.1.2.1 EGA MS

Fig. 5.2 represents the thermograms of all six RDF samples using the EGA MS method. Each sample shows a unique thermal degradation profile; however, some common traits can be drawn out in each thermogram. Thermogram has been divided into four sections for an easier understanding. All six samples of EGA results showed their first peak at a temperature below 200°C. It could be attributed to the desorption of low molecular weight volatile fraction. Another prominent peak was observed between 200 to 450°C and between 450-600°C. In the end, there is one peak between 600-700°C.

Table 5.1 represents the components obtained during EGA for six RDF samples where the pyrolytic products of all six samples except E resemble dcarboxy methyl cellulose and sodium alginate. CMC is a water-soluble derivative of cellulose that is highly hygroscopic [187]. It is used in oral, injectable, and pharmaceutical drugs [188]. Sodium alginate ($NaC_6H_7O_6$) is alginic acid's linear hydrophilic polysaccharide derivative. Sodium alginate is an edible protective coating to extend cheese and poultry's shelf-life [189]. The curves of samples B, C, D and E resembled chitin in various instances. Chitin is the second most abundant biopolymer after cellulose. Its chemical structure resembles cellulose, except the hydroxyl (OH) groups are replaced by the acetyl amine ($NHCOCH_3$) group. It finds its usage in textile, food, photography, medical, environmental applications, cosmetics, waste, and sewage treatment [190-195]. The fishing industry is one of the most significant contributors of chitin in waste, and seafood waste is also considered a potential source of chitin [196].

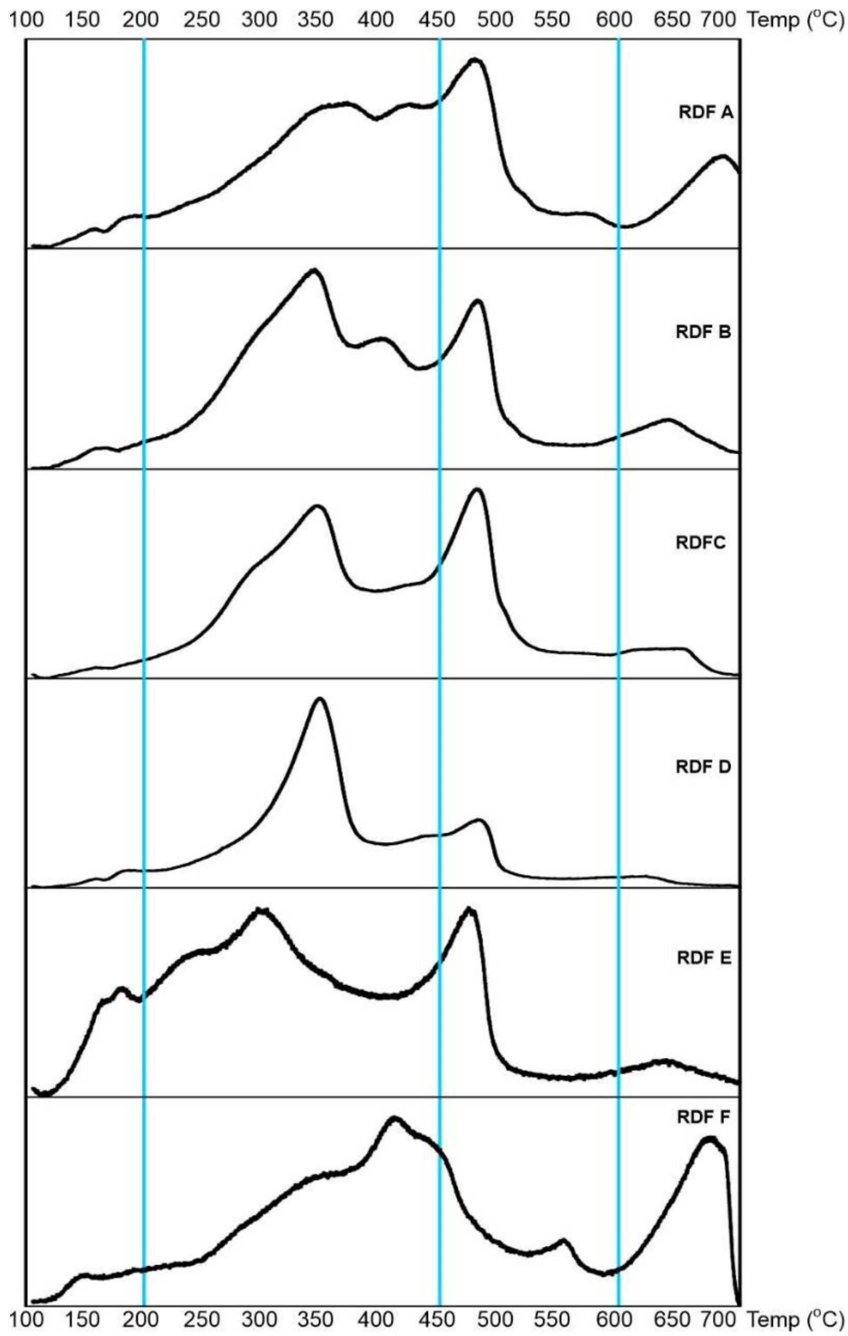

Fig. 5.2 Thermograms of RDF

Table 5.1 EGA analysis of RDF

Sr No.	Component	Samples					
		A	B	C	D	E	F
1	Carboxymethylcellulose (CMC)	✓	✓	✓	✓	X	✓
2	Sodium Alginate	✓	✓	✓	✓	X	✓
3	Chitin	X	X	✓	✓	✓	✓
4	Poly(Ethylene maleic anhydride)	✓	✓	✓	X	X	X
5	Cloth	✓	✓	✓	X	X	X
6	Raw cotton	X	X	X	✓	✓	X
7	Alpha olefin maleic anhydride copolymer	X	X	X	X	✓	X
8	Poly vinyl butyl	X	X	X	X	✓	X
9	Vinyl alcohol vinyl butyral-based copolymer	X	X	X	X	✓	X
10	Novon	X	X	X	X	✓	X
11	Poly(maleic anhydride)	✓	X	X	X	X	X
12	Polyacrylamide	X	X	X	X	X	✓

The EGA analysis of RDF samples A, B and C resembled cloth and polyethylene-maleic anhydrite (PEMAh). It is a bonding aid for polar to nonpolar substances as a compatibilizer for polymer blends. It can be found in recycled polymer, glass fibre, laminated films, laundry detergents, hard surface cleaners, textile finishing, cement setting, etc. [197, 198].

The EGA analysis of RDF sample E produced a chromatogram resembling chitin, raw cotton, novon, and polyvinyl butyral (PVB). PVB resin and PVB-based polymers are used in films & sheets, printing inks, adhesives, paints & coatings, varnishes, etc.[199]. Novon is the active ingredient in dental whitening gels and toothpaste and contains hydrogen peroxide, urea, and sodium tripolyphosphate [200]. RDF A and D resembled polymaleic-anhydrite and raw cotton, respectively. Poly maleic anhydrite is used as a thickener, dispersant, soil conditioner, detergent, medical drug, etc. Polyacrylamide, a polymer known for its water-absorbing properties commonly used as a flocculant, pulp processing and paper making, water treatment etc. finds its resemblance to sample F [201, 202]. The potential sources of the above-stated compounds can be found in MSW and thus can be present in the RDF samples used for this work.

5.1.2.2 Single shot analysis

EGA MS analysis only shows the peaks associated with pyrolytic compounds at a temperature range from 100 to 700°C, while single-shot analysis provides the names of the compounds associated with different peaks at a particular temperature. EGA peaks associated with the pyrolysis products of six RDF samples indicated that maximum pyrolysis occurs before 550°C. Thus, the same temperature has been used further for single-shot analysis. The pyrolytic products have been categorized into tabular form based on their functional groups in Tables 5.2-5.7, and a semi-quantitative analysis has been obtained using the peak area. The percentage of each compound in the tables is summed up to obtain the total area of every class, such as alkanes, alkenes etc. It will provide a better insight into the formation of main pyrolysis compounds. Figs. 5.3-5.8 represent the samples' chromatograms, with retention time on the abscissa and relative intensity on the ordinate.

a) RDF A

Table 5.2 indicates that the RDF A mostly comprises benzene-like aromatic rings (24.4%) followed by alkenes (9.49%), ketones (3.22%), alkanes (2.5%), N-containing (1.2%), phenolic (1.04%) and acid, aldehyde, alcohol and ester as minor compounds. Styrene (11.48%) and benzene (9.77%) were the most abundant compounds. It contains primary pyrolytic products of polystyrene, i.e., benzene (9.77%), toluene (1.12), styrene (11.48%), diphenylmethane (0.28%), and biphenyl (0.4%) [203].

The prominent identified peaks in the chromatogram in Fig. 5.3 were at 1.1, 4.29, and a duplet at 22.7 minutes, and these could be assigned to CO_2, styrene, 1-nonadecene (22.73 min) and heneicosane (22.76 min) respectively. The chromatogram matches that of styrene and polystyrene grafted with maleic anhydrite at several points. All this cumulatively confirms the presence of styrene in this sample.

Table 5.2 Single shot analysis of sample A

S. No.	Class	Compounds	Retention time / min	Area / %	Total area
1	Alkanes	2-nitropropane	2.325	0.23	2.5
		Nonane	4.37	0.22	
		Dodecane	8.863	0.2	
		Tetradecane	11.633	0.21	
			12909	0.5	
		Heptadecane	15.265	0.2	
			16.356	0.15	
			18.389	0.19	
		Heneicosane	17.395	0.12	
			19.333	0.1	
			21.116	0.12	
			22.756	0.11	
		Eicosane	20.224	0.15	
2	Alkene	2,4 dimethyl hept-1-ene	3.597	3.13	9.49
		1-Dodecene	8.745	1.26	
		(Z)-3-Hexadecene	10.174	0.33	
		1-pentdecene	11.531	1.13	
			12.816	0.39	

S. No.	Class	Compounds	Retention time / min	Area / %	Total area
			14.033	0.31	
		1-heptadecene	15.186	0.3	
			16.284	0.27	
		1-nonadecene	17.33	0.22	
			18.329	0.31	
			19.281	0.19	
			20.198	0.23	
			22.726	0.19	
		1-decene	5.723	1	
			21.073	0.23	
3	Alcohol	1-heneicosanol	21.917	0.23	0.51
		1-heptacosanol	23.507	0.28	
4	Ketone	1-hydroxy-2-propanone	1.845	0.9	3.22
		Acetophenone	6.931	0.89	
		Benzophenone	14.629	1.43	
5	Aldehyde	Benzaldehyde	5.308	0.56	0.56
6	Ester	Bis(2-ethylhexyl) phthalate	23.208	0.44	0.44
7	Acid	n-hexadecanoic acid	18.037	0.43	0.68
		Oleic acid	19.741	0.25	
8	Phenol	3-methyl phenol	7.025	0.45	1.04
		(Z)-2-methoxy-4-(1-propenyl) phenol	12.36	0.34	
		2,6-dimethoxy-4-(2-propenyl) phenol	15.358	0.25	
9	Benzenoid	Benzene	1.992	8.5	24.44
			3.305	1.27	
		Toluene	2.751	2.12	
		Styrene	4.285	11.48	

S. No.	Class	Compounds	Retention time / min	Area / %	Total area
		Biphenyl	11.49	0.4	
		Diphenylmethane	12.185	0.28	
		Diphenic anhydrite	15.925	0.39	
10	N containing	Benzonitrile	5.66	1.2	1.2
11	Inorganic	Carbon dioxide	1.062	13.2	13.2

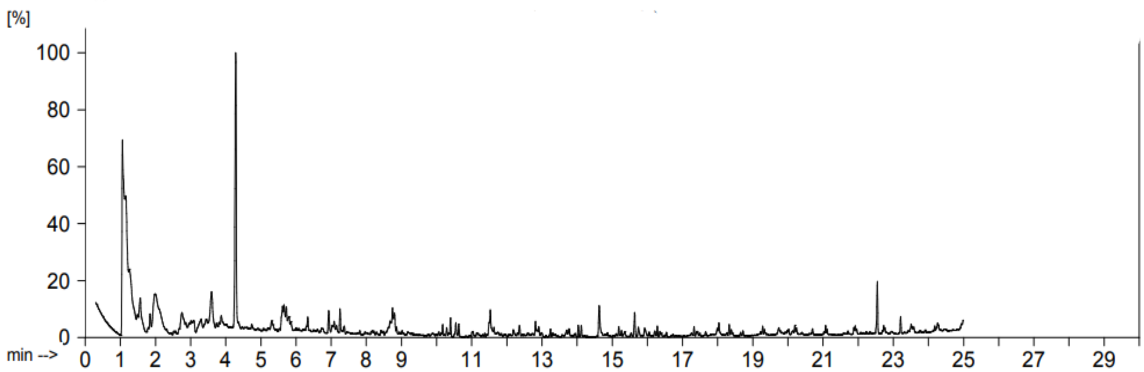

Fig. 5.3 Chromatogram of sample A

b) RDF B

RDF B pyrolytic products can be subdivided into alkene (44%), N-containing groups (6.27%), styrene (1.45%), and alcohol and ketones as minor categories. cis-1-chloro-9-octadecene was found to be 41.33%, followed by hydrazine carboxamide (6.27%) and molecular oxygen (29.66%), as shown in Table 5.3. The chromatogram shown in Fig. 5.4 had a cluster of peaks between 0.3-0.6 min with distinguishable peaks attributing to O_2 and cis-1-chloro-9-octadecene, respectively. Peaks at 1.2 and 1.4 min were due to 2-oxo-ethyl-ester-propanoic acid and 2,3-butanedione, respectively. A sharp peak of hydrazine carboxamide was observed at 1.5 min. Other major peaks at 3.57 and 4.26 min were attributed to 2,4 dimethylhept-1-ene and styrene, respectively.

Table 5.3 Single shot analysis of sample B

S. No.	Type	Compounds	Retention time/min	Area / %	Total area
1	Alkene	cis-1-chloro-9-octadecene	0.425	41.33	44
		Isoprene	1.291	0.49	
		2,4 dimethylhept-1-ene	3.571	1.24	
		1-methyl-4-(1-methylethenyl)-cyclohexene	6.339	0.27	
		(E)-3-tetradecene	7.250	0.25	
			8.744	0.15	
		7-methyl-1-undecene	10.635	0.27	
2	Alkanes	1-heptyl-2-methyl cyclopropane	5.714	0.18	0.18
3	Alcohol	11-methyldodecanol	10.398	0.25	0.64
		2-hexyl-1-octanol	11.526	0.39	
4	Ketone	2,3-butanedione	1.475	0.30	0.63
		1-hydroxy-2-propanone	1.840	0.33	
5	Acid	2-oxo-ethyl-ester-propanoic acid	1.243	0.62	0.62
6	Benzenoid	Styrene	4.262	1.45	1.45
7	N-containing	Hydrazinicarboxamide	1.539	3.45	6.27
			1.581	2.82	
8	Inorganic	Oxygen	0.338	9.04	29.66
			0.659	20.62	

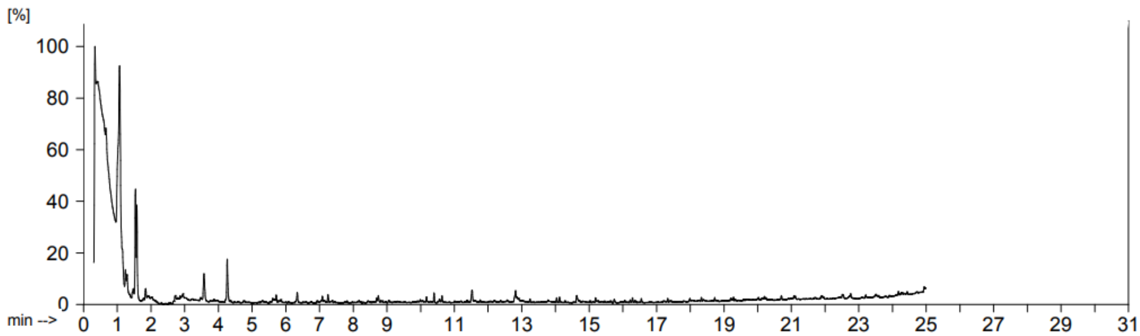

Fig. 5.4 Chromatogram of sample B

c) RDF C

Table 5.4 shows that the benzenoid compound (5% styrene) is the most abundant in sample C, followed by alkenes (4.68%), alcohol (3.00%), ketone (2.43%), ester (2.06%), alkane (1.51%), phenolic compounds (0.79%), and acid (0.56%). CO_2 and styrene were associated with two remarkable peaks in the chromatogram in Fig. 5.5 at 1.08 and 4.26 min, respectively. Other two major peaks were observed at 1.85 and 3.58 minutes, attributing to 1-hydroxy-2-propanone and 2,4 dimethylhept-1-ene.

Table 5.4 Single shot analysis of sample C

S. No.	Type	Compounds	Retention time/min	Area / %	Total area
1	Alkene	2,4 dimethylhept-1-ene	3.580	2.47	4.68
		1-Decene	5.71	0.72	
		1-Tridecene	10.127	0.16	
		(E)-3-octadecene	12.814	0.54	
		(E)-3-Eicosene	14.033	0.25	
		1-heptadecene	16.283	0.18	
		(Z)-9-tricosene	18.331	0.15	
		1-nonadecene	19.281	0.21	
2	Alkane	2-methyl hexacosane	20.885	1.51	1.51

S. No.	Type	Compounds	Retention time/min	Area / %	Total area
3	Alcohol	2-ethyl-1-hexanol	6.284	0.36	3.00
		1-hexacosanol	24.020	2.64	
4	Ketone	1-hydroxy-2-propanone	1.853	2.13	2.43
		Benzophenone	14.628	0.30	
5	Acid	Nonanoic acid	9.895	0.56	0.56
6	Ester	Heptacosyl heptafluorobutyrate	20.261	1.62	2.06
		Bis(2-ethylhexyl) phthalate	23.205	0.44	
7	Phenol	2-methoxy-4-vinyl phenol	10.557	0.50	0.79
		(Z)-2-methoxy-4-(1-propenyl) phenol	12.373	0.29	
8	Benzenoid	Styrene	4.267	5.00	5.00
9	Inorganic	Carbon dioxide	1.085	24.37	24.37

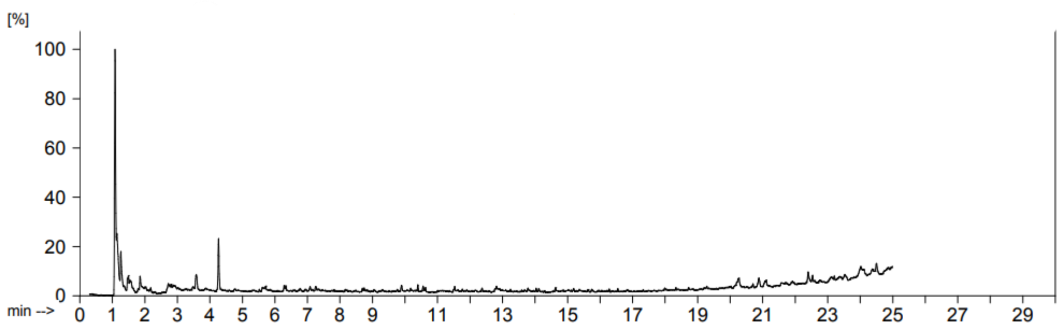

Fig. 5.5 Chromatogram of sample C

d) RDF D

Table 5.5 shows that RDF D can be categorized into ketones (12.04%), alkene (2,4 dimethyl hept-1-ene) (7.88%), benzenoid compound styrene (3.56%), 2-oxo-ethyl-ester-propanoic acid (2.78%), alcohol (1.35%) and ester, phenolic & N containing compounds as minor constituents. The hydrolysis and cracking of glucose/cellulose indicate the presence of 1,4:3,6-

dianhydro-alpha-d-glucopyranose, which has also been reported in the literature [204-206]. The source -of cellulose includes paper, textiles, plant fibres, etc. The chromatogram in Fig. 5.6 showed major peaks at 0.17, 0.97, 1.48, 3.01, 3.83, 10.56 and 14.65 minutes attributing to 1-hydroxy-2-propanone, 2,3-pentanedione, (E)-3-penten-2-one, 2,4 dimethyl hept-1-ene, styrene, 2-methoxy-4-vinyl phenol and benzophenone, respectively.

Table 5.5 Single shot analysis of sample D

S. No.	Type	Compounds	Retention time/min	Area / %	Total area
1	Alkene	2,4 dimethyl hept-1-ene	3.011	7.88	7.88
2	Ketone	1-hydroxy-2-propanone	0.170	8.03	12.04
		2,3-Pentanedione	0.972	0.74	
		(E)-3-penten-2-one	1.486	0.18	
		1-(acetyloxy)-2-propanone	3.385	0.77	
		2-methyl-2-cyclopenten-1-one	4.076	0.16	
		2-hydroxy-3-methyl-2-cyclopenten-1-one	6.198	1.76	
		Benzophenone	14.652	0.40	
3	Acid	2-oxo-ethyl-ester-propanoic acid	2.112	2.78	2.78
4	Alcohol	1-heptacosanol	22.265	1.35	1.35
5	Ester	Bis(2-ethylhexyl) phthalate	23.229	0.42	0.42
6	Phenol	2-methoxy-4-vinyl phenol	10.567	0.72	0.72
7	Benzenoid	Styrene	3.835	3.56	3.56
8	N-containing	Pyrrole	1.070	0.32	0.32
9	Carbohydrate	1,4:3,6-dianhydro-alpha-d-glucopyranose	9.063	0.42	0.42

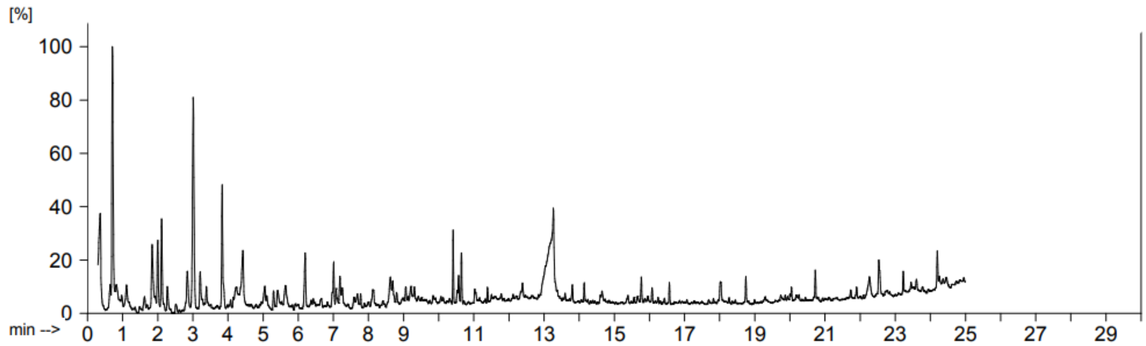

Fig. 5.6 Chromatogram of sample D

e) RDF E

The pyrolysis products of sample E can be divided based on their chemical structures into seven categories dominated by alkanes (8.65%), alkenes (6.82%), alcohol (6.78%) and ketones, nitrogenous compounds and benzenoids as minor constituents as shown in Table 5.6. The two major constituents in the pyrolysis products are 2-methylhexacosane (7.52%) and octacosanol (4.35%) . The first peak was observed at 1.1 min, as shown in the chromatogram in Fig. 5.7. It was due to the evolution of CO_2. Further, major peaks at 1.3, 2.7, 3.6, 4.3, 14.6, 19.6, 22.4, 24.2 and 24.9 minutes could be attributed to ethylidene cyclopropane, toluene, 2,4 dimethyl hept-1-ene, styrene benzophenone, 1-heptacosanol, octacosanol, 1,37-octatriacontadiene, 2-methylhexacosane and (Z)-octadecanamide, respectively.

Table 5.6 Single shot analysis of sample E

S. No.	Type	Compounds	Retention time/min	Area / %	Total Area
1	Alkanes	Tetratetracontane	19.884	1.13	8.65
		2-methylhexacosane	24.349	7.52	
2	Alkene	Ethylidinecyclopropane	1.375	3.33	6.82
		2,4 dimethyl hept-1-ene	3.616	1.03	

S. No.	Type	Compounds	Retention time/min	Area / %	Total Area
		1,37-octatriacontadiene	24.179	2.46	
3	Alcohol	1-heptacosanol	19.648	2.43	6.78
		Octacosanol	22.461	4.35	
4	Ketone	Benzophenone	14.630	1.62	
5	N containing	(Z)-9-octadecenamide	24.491	0.8	
6	Benzenoid	Toluene	2.774	0.85	2.45
		Styrene	4.293	1.60	
7	Inorganic	Carbon dioxide	1.163	28.63	

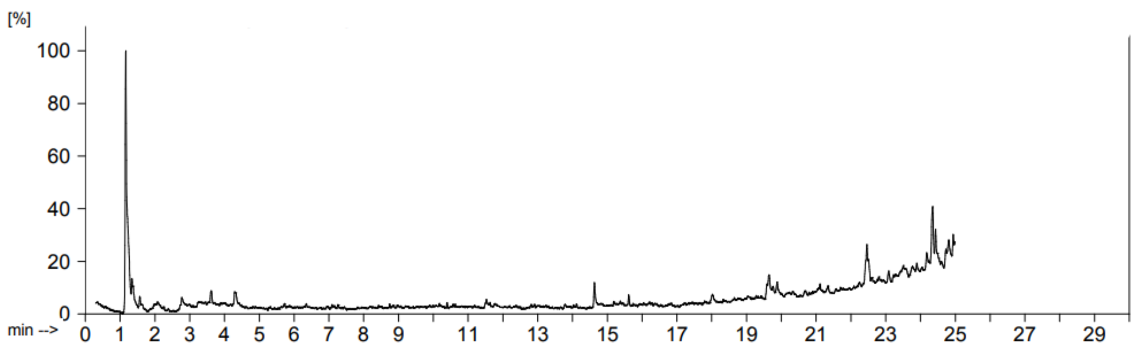

Fig. 5.7 Chromatogram of sample E

f) RDF F

Table 5.7 represents the single shot analysis of RDF F. Aromatic compounds (5.07%) were most abundant in RDF F, followed by alkenes (4.78%), acid (4.05%), ketone (2.37%), alcohol (1.74%) and alkane (0.19%). Styrene (3.70%), methyl methacrylate (4.05%), benzophenone (2.37%), 1-heptacosanol (1.74%) and 2,4 dimethyl hept-1-ene (1.67%) were relatively abundant. The chromatogram in Fig. 5.8 showed a remarkably sharp peak at 1.18, corresponding to CO_2. The other smaller prominent peaks at 2.25, 4.30, 5.54 and 14.63 were due to methyl methacrylate, styrene, n-butyl methacrylate and benzophenone, respectively.

Table 5.7 Single shot analysis of sample F

S. No.	Type	Compounds	Retention time / min	Area/%	Total area
1	Alkene	2,4 dimethyl hept-1-ene	3.632	1.67	4.78
		1-undecene	7.257	0.76	
		(Z)-3-Hexadecene	10.171	0.35	
		1-tridecene	12.812	0.36	
		1-heptadecene	14.028	0.50	
			16.280	0.34	
		1-nonadecene	17.325	0.42	
		Pentacos-1-ene	18.325	0.38	
2	Alkanes	Heptadecane	15.258	0.19	0.19
3	Alcohol	1-heptacosanol	22.247	1.74	1.74
4	Ketone	Benzophenone	14.631	2.37	2.37
5	Acid	Methyl methacrylate	2.258	1.65	4.05
		n-butyl methacrylate	5.546	2.40	
6	Benzenoid	Toluene	2.793	1.37	5.07
		Styrene	4.308	3.70	
7	Inorganic	Carbon dioxide	1.189	20.68	20.68

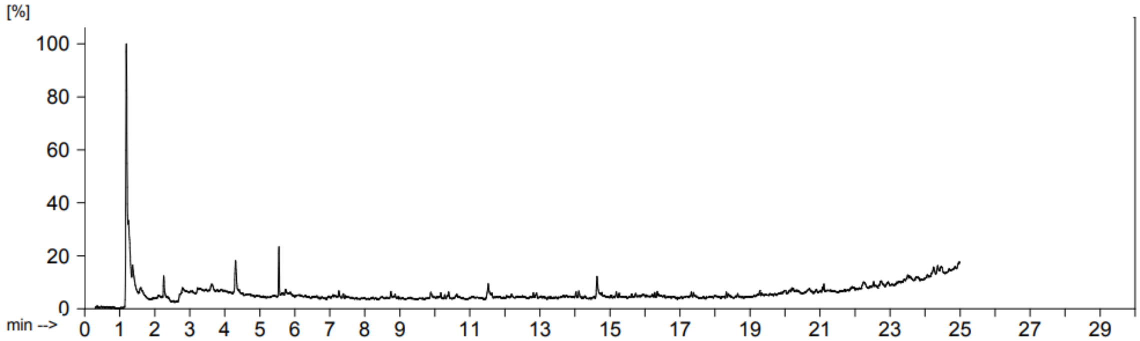

Fig. 5.8 Chromatogram of sample F

The literature review also found that the phenols and aldehydes were the prime pyrolytic products of lignin dissociation. It also indicates the presence of biomass like jute, cotton, wood chips, paper, textile etc., in RDF [207, 208]. Compounds like benzene, styrene, phenol, nonane, dodecane, toluene, octene and butene have been seen in the pyrolysis of uncoated printing and writing paper [209]. N-containing compounds (amides, nitriles, pyrrole etc.) could be due to human waste, plastics and polymers, plasticizers, certain soaps and detergents etc. Alkene was observed to be abundant in most of the samples. High-temperature dehydrogenation could be a possible justification for the presence of alkenes.

It can be inferred from single-shot Py-GC/MS analysis that apart from non-hydrocarbon gases (CO_2 and O_2), the long-chain alkenes were most abundant at 550°C and linked to high-temperature pyrolysis as available in the literature. Alkenes were followed by alkanes, aromatic compounds, and ketones as other major categories in the samples. Styrene was found in all the samples, and its peak was mostly seen between 3.7 to 4.3 min. The benzophenone compound was found in all the samples except sample B, and its peak was observed at 14.6 min in all the cases. 2,4-dimethyl hept-1-ene was seen in all the cases, with a peak between 3.0 to 3.6 min. The presence of pyrolytic compounds already seen in the pyrolysis of different plastics in previous literature confirmed the presence of a large amount of plastic in the RDF samples. The RDF A sample with the highest amount of polystyrene has higher LHV than others, indicating its contribution to LHV of RDF. Glucopyranose corresponds to the pyrolysis of cellulosic materials. Many compounds indicating the presence of biomass, like paper, jute, cotton, wood, textile, etc., were seen. Hence it can be concluded that plastic and biomass are one of the most significant constituents of RDF. The kind and contents of pyrolytic compounds differed in all the cases because of the complex composition of every kind of RDF.

5.2 Downdraft gasifier experimental runs

Several experiments are carried out with RDF and RDF-biomass mix as feedstock for gasification. Four types of RDF, i.e., RDF C, D, E, and F, having LHV in the range of 12.07-14.36 MJ/kg, are used to carry out experiments. RDF C and F are fluffy types, while RDF D and E are in pellets form. Out of these, RDF D, E, and F are mixed with biomass to perform co-gasification. RDF B was not considered due to its low LHV (11.64 MJ/kg). RDF A has similar properties to RDF C; hence RDF C is chosen. Table 5.8 shows downdraft gasifier experimental runs for different feedstock. Airflow rate is varied from 6 to 8 Nm^3/hr with fuel consumption ranging from 0.7 to 3.3 kg/hr for experimental runs of 30-40 minutes. An experiment on RDF gasification and RDF-biomass co-gasification, is carried out using air and pure O_2 mix as gasifying agents with O_2 concentration at 35%. Table 5.9 represents the mass balance established for all experiments with air flow rate and fuel consumption as inputs and producer gas and residual char as outputs. Mass balance closure is the ratio of the total output and input flow rates. It indicates the accuracy of the analysis of gasification. It also indicates the reliability of the results in terms of the fuel consumption rate and producer gas flow rate. The closure of mass balance for all is in the range of 85.49-105.53%. The mass balance closure values below or above 100% is due to the experimental errors.

Table 5.8 Results of downdraft gasifier experimental runs

Exp No	Feedstock	Airflow (Nm^3/hr)	O_2 flow (Nm^3/hr)	Fuel consumption (kg/hr)	ER	H_2	N_2	CO	CH_4	CO_2	LHV (MJ/Nm^3)	Gas yield (Nm^3/kg)	Cold gas efficiency (%)
1	RDF C fluff (dry)	6.00	-	1.51	0.51	4.07	75.00	9.75	0.57	10.61	1.87	3.65	48.56
2	RDF D pellet	6.00	-	1.97	0.36	5.93	68.86	9.78	0.69	14.75	2.12	3.44	60.44
3	RDF D pellet	5.00	-	2.32	0.26	6.22	69.51	9.94	0.79	13.53	2.21	2.43	44.08
4	RDF D pellet	5.00	1.10	2.74	0.45	8.73	56.02	19.41	1.40	14.44	3.89	2.54	81.88
5	RDF E pellet	6.00		1.95	0.44	6.43	71.99	9.41	1.00	11.18	2.24	3.34	52.09
6	50:50 mix of RDF E pellet and biomass pellet	6.00	-	2.94	0.35	9.11	62.88	14.01	2.04	11.96	3.48	2.53	56.93
7	50:50 mix of RDF E pellet and biomass pellet	8.00	-	3.02	0.46	8.08	62.94	18.41	1.32	9.66	3.67	3.27	77.65
8	30:70 mix of RDF E pellet and biomass pellet	7.50	-	4.00	0.36	8.22	60.27	19.01	1.65	10.59	3.88	2.42	59.12
9	RDF E pellet-biomass pellet mix (50:50)	7.00	-	2.69	0.45	6.12	68.98	11.40	1.01	12.48	2.46	2.94	46.83
10	RDF F fluff - biomass mix pellet (50:50)	7.00	-	2.80	0.47	5.73	68.36	13.00	1.15	11.76	2.67	2.84	50.13
11	RDF F fluff - biomass mix pellet (50:50)	5.80	1.20	3.21	0.68	9.99	57.37	15.55	1.60	15.30	3.62	2.45	58.48

Table 5.9 Mass balance closure

Exp Run	Input (kg/hr)		Output (kg/hr)		Mass Balance Closure
	Airflow	Fuel consumption	Producer gas	Char	
1	6.00	1.70	7.93	0.20	105.53
2	7.56	1.97	8.69	0.73	98.84
3	6.3	2.32	7.14	1.65	101.98
4	7.85	2.74	8.64	0.92	90.31
5	7.56	1.95	8.12	0.51	90.80
6	7.56	2.94	9.04	0.24	88.43
7	10.08	3.03	12.09	0.20	93.79
8	9.45	4.00	11.79	0.70	92.84
9	8.82	2.80	9.96	0.36	88.77
10	8.82	2.80	10.04	0.55	91.17
11	9.00	3.21	9.69	0.74	85.49

5.2.1 Effect on gasifier temperature zones

Combustion and reduction zones of the gasifier are critical to achieving combustion and reduction reactions, respectively, leading to equilibrium and product formation. The effect on gasifier combustion and reduction zones for varying fuel mix of RDF or RDF-biomass mix as feedstock is explained below.

i. RDFs

It is indicated from Fig. 5.9 that the maximum combustion zone temperature achieved is ~600°C, 860°C and 700°C in the case of RDF C fluff (dry basis), RDF D pellet and RDF E pellet, respectively. However, RDF C fluff having high moisture of 45%, could reach only 500°C. None of the cases with RDF fluff or pellet has consistent combustion zone temperature throughout the gasifier operation. It may be due to the high RDF ash content (31-51%), which disturbs the combustion phenomenon. Comparing RDF D pellet at different air flow rates of 5 and 6 Nm^3/hr, the temperature profile at 5 Nm^3/hr is much better. The temperature is around 730°C even after 40 minutes of gasifier operation. The sparger placed in the combustion zone distributes the air circumferentially throughout the combustion zone. In other cases, the temperature drops sharply at the end, which indicates RDF consumption. The other reason could be bridging inside the gasifier. Thus, only the central portion of material takes part in chemical reactions, which are less in quantity and gets exhausted early. It is further corroborated by gasifier pictures taken after the completion of the experiments (Fig. 5.25). It can be said that combustion zone temperature was not sustainable throughout, which is identified as one of the major issues during high ash RDF gasification. However, RDF E is able to achieve 700°C even after 30 minutes of operation. It is observed that even at air and O_2 mix at 35% O_2, the combustion zone peaked only up to 830°C, which is slightly lower compared to air gasification due to the increase in biomass consumption rate with oxygen enrichment in the gasifying agent. Similar trends have been reported for biomass gasification [210].

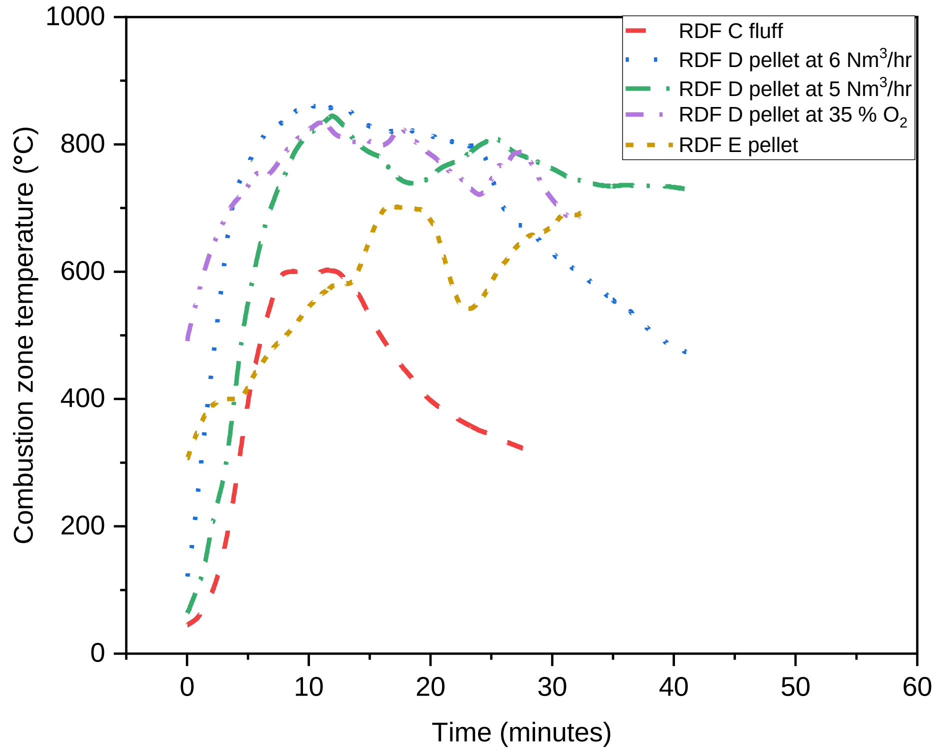

Fig. 5.9 Combustion zone temperature profile for RDFs

The reduction zone temperature fluctuates for all the cases, as shown in Fig. 5.10. This unsustainable behaviour is attributed to the heterogeneity of the fuel. The continuous rising trend of reduction zone temperature, particularly for RDF C fluff from 50 to 750°C and RDF D pellet at 5 Nm^3/hr to more than 750°C is indicative of part combustion taking place in the reduction zone, which is undesirable. RDF E achieved consistent reduction zone temperature range of 500-600°C even at 32 minutes of operation. In other cases, after 20-30 min of gasifier operation, the reduction zone temperature goes beyond the combustion zone temperature. It may be due to the burning of leftover charcoal present on the grate as per the trends in Fig. 5.10. On the contrary, during oxy gasification, a high reduction zone temperature achieved will shift the methanation reaction and steam reforming reaction to the reactants side leading to more conversion to H_2 and CH_4. It will increase the LHV significantly along with RDF consumption.

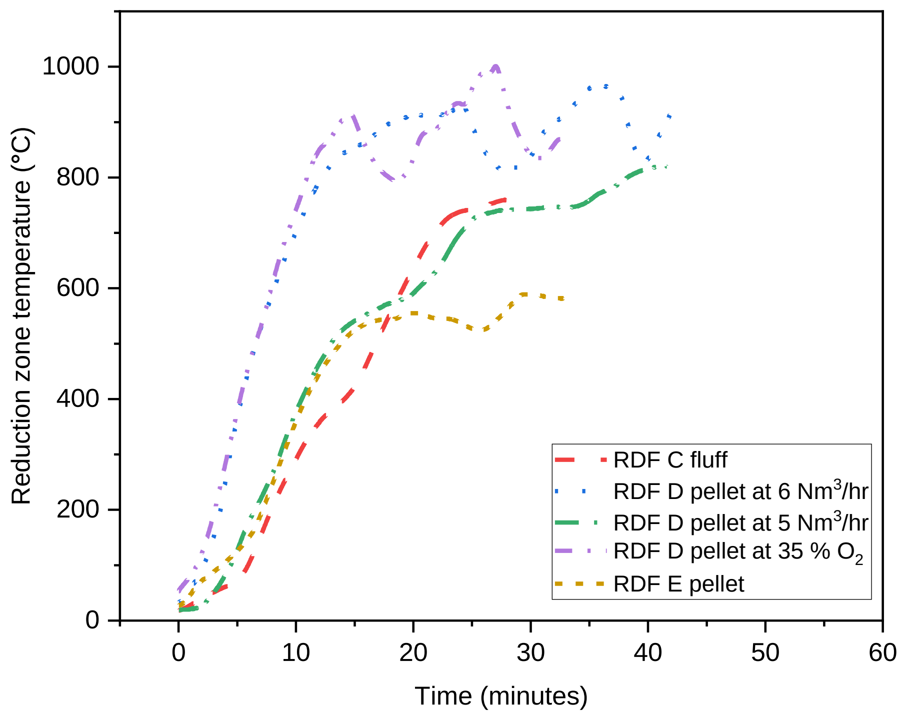

Fig. 5.10 Reduction zone temperature profile for RDFs

ii. RDFs and biomass mix

The combustion zone temperature profile of RDF and biomass mix is better than RDFs, as shown in Fig. 5.11. It is well supported by the maximum achieved combustion zone temperature above 800°C in all the cases except RDF E and biomass mix pellet (50:50) at 7 Nm^3/hr airflow. Moreover, sudden rise and drop in temperature, which was prominent in the RDFs case, are less in co-gasification, and temperature is consistent for a certain time, showing stable combustion. RDF E pellet and biomass pellet mix (50:50) at 8 Nm^3/hr air flow showed combustion zone temperature peaked at 1070°C. The feed was added to the gasifier when the combustion zone temperature reached around 550°C during start-up with charcoal. Thus, within 5 minutes of operation with a high airflow rate of 8 Nm^3/hr, the temperature reached more than 900°C easing out the burning of RDF in the mix. At the 30:70 ratio, the combustion zone temperature peaked at more than 800°C within 3 minutes of operation and remained consistent for the first 20 minutes. For RDF F and biomass mix pellet (50:50), temperature decreases after the initial 10 minutes of sustainable operation. It can be inferred that consistent quality biomass pellets are easy to burn, and mixing them with RDF pellets facilitated the burning of RDF pellets. It will result in complete combustion with the consistent producer gas flame throughout the operation except for two cases. Only RDF E and biomass mix pellet (50:50) and RDF F and biomass mix pellet (50:50) are not able to produce a sustainable flame. At oxygen enrichment (35% O_2), after an initial 20 min, the temperature stabilized to 820-890°C, while in all other cases, there is a downward temperature trend after 20 minutes. Oxy-gasification reduces air's N_2 content, which is a significant reason for the increase in temperature.

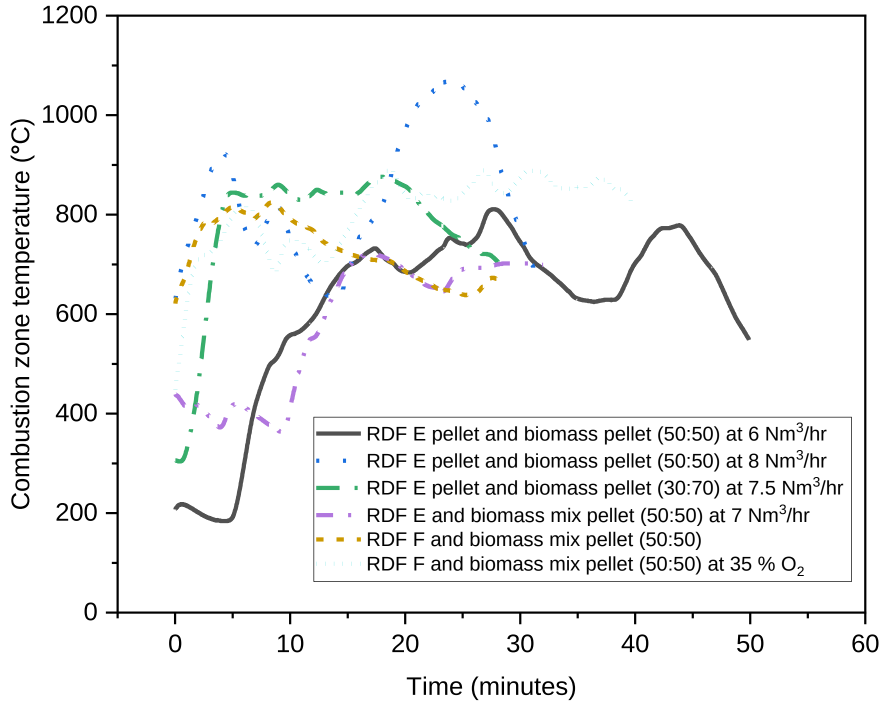

Fig. 5.11 Combustion zone temperature profile for RDFs and biomass mix

Reactions occurring in the reduction zone directly influence the producer gas properties, with reduction zone temperature as one of the significant parameters. In most cases mentioned in Fig. 5.12, the reduction zone temperature stabilizes after around 20 min of gasifier operation. It might be happening due to RDF heterogenous effect at the start. However, it gets further delayed by 10 min for feed with RDF E pellet and biomass pellet (50:50) at 6 Nm^3/hr. In the case of a higher air flow rate of 8 Nm^3/hr, the reduction zone temperature profile is higher than that for 6 Nm^3/hr. Similar behaviour is observed for the combustion zone temperature as well. However, as the biomass ratio is enhanced from 50 to 70% in a mix of RDF pellet and biomass pellet, the temperature rises steadily from start to end. It is to be noted that fuel consumption is 4 kg/hr, which is the highest among all cases, and no residue was left at the bottom of the gasifier after the completion of the experiment.

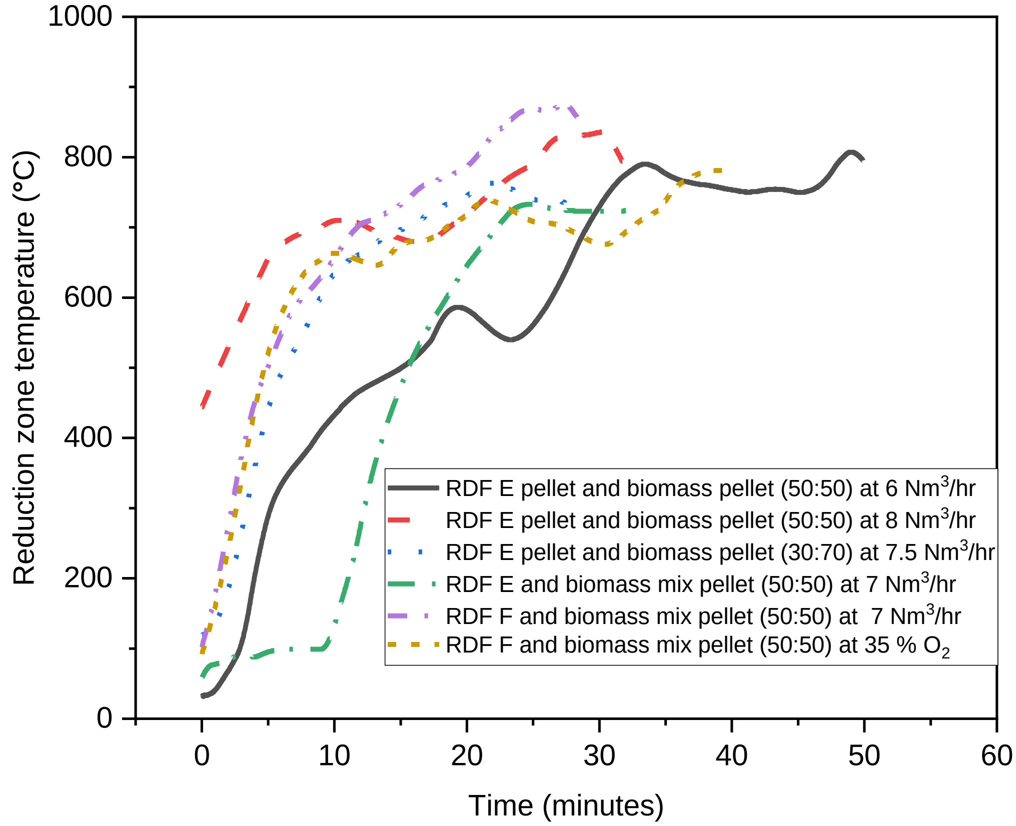

Fig. 5.12 Reduction zone temperature profile for RDFs and biomass mix

5.2.2 Producer gas composition variation with time

The producer gas composition has been determined using the gas chromatography technique, as discussed in section 3.2.2.2. Fig 5.13-5.23 show the variation of producer gas composition (N_2 free basis) over time for 11 experimental runs. The amount of N_2, an inert air component, remains constant with time in all runs; however, its vol (%) changes due to the other components' vol (%). The average concentration (over eleven experimental runs) of gas components H_2, CO, CO_2, and CH_4 is 20.60%, 39.07%, 36.92%, and 3.41%, respectively, on N_2 free basis. In most cases, H_2 increases initially and then decreases later. CO and CO_2 have opposing trends, i.e., when CO increases, CO_2 decreases, and vice versa. Experimental run no 7 and 8 show a high CO concentration of 48-49%. It is due to high reduction zone temperature above 600°C. The Boudouard reaction rate increases at high temperatures, resulting in more CO_2. The results of producer gas composition with air as a gasifying agent are compared with oxygen-enriched gasification. For all combustible components (CO, H_2 and CH_4), the concentration enhanced by 1.3%, 1.42% and 0.08% on average, with a significant decrease of 2.80% in CO_2 concentration. Exp no 2 and 3 have the same feedstock with a minor difference of 1 Nm^3/hr in air flow rate. In experiment run no 3, the combustion zone temperature remains above 700°C even at a later stage (after 25 min). At the same time, it keeps decreasing for experiment run no 2, as shown in Fig. 5.9. After 20 min, the effect is visible in the form of gas composition where CO_2 decreased from 53.97 to 31.59% in experiment run no 3 with a corresponding rise in CO and H_2.

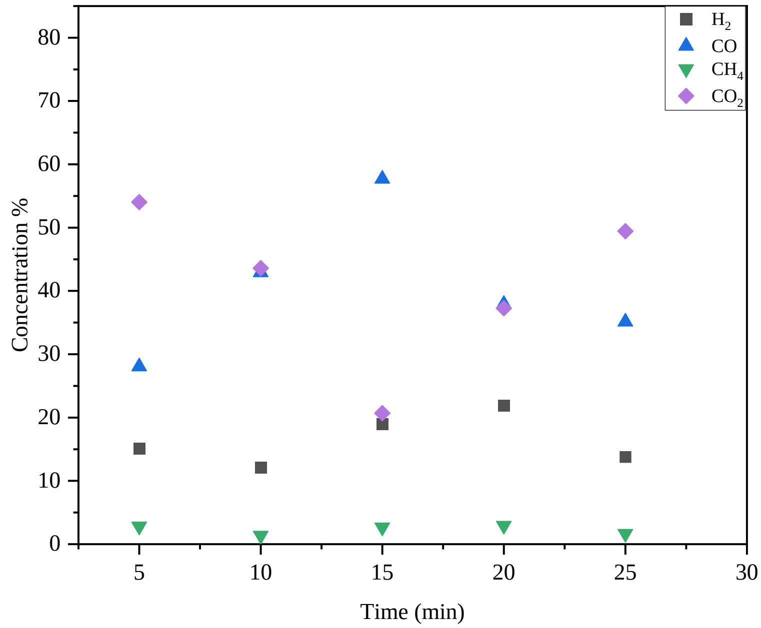

Fig. 5.13 Variation of producer gas composition with time for exp no 1 (RDF C Fluff)

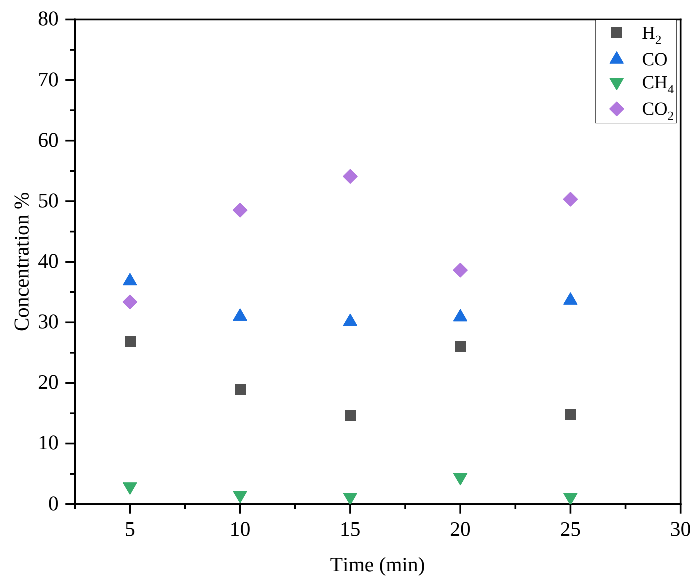

Fig. 5.14 Variation of producer gas composition with time for exp no 2 (RDF D pellet at 6 Nm^3/hr of air flowrate)

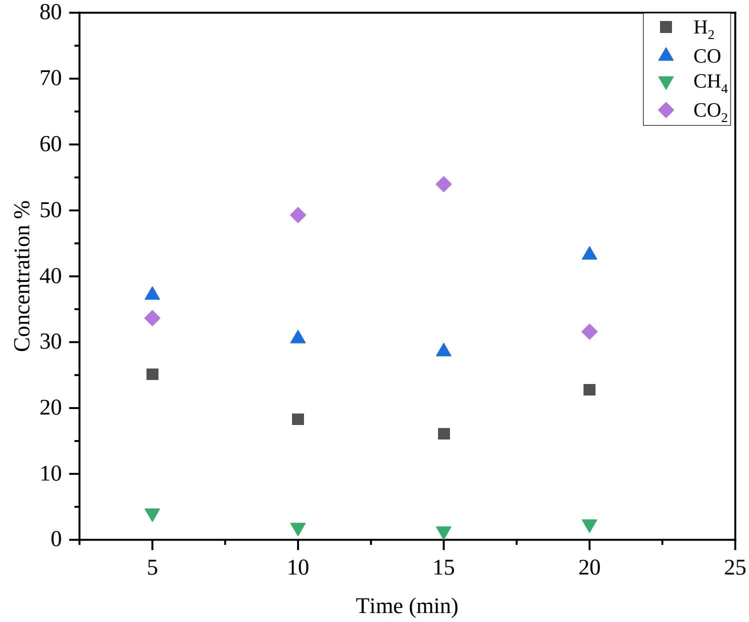

Fig. 5.15 Variation of producer gas composition with time for an exp no 3 (RDF D pellet at 5 Nm^3/hr of air flowrate)

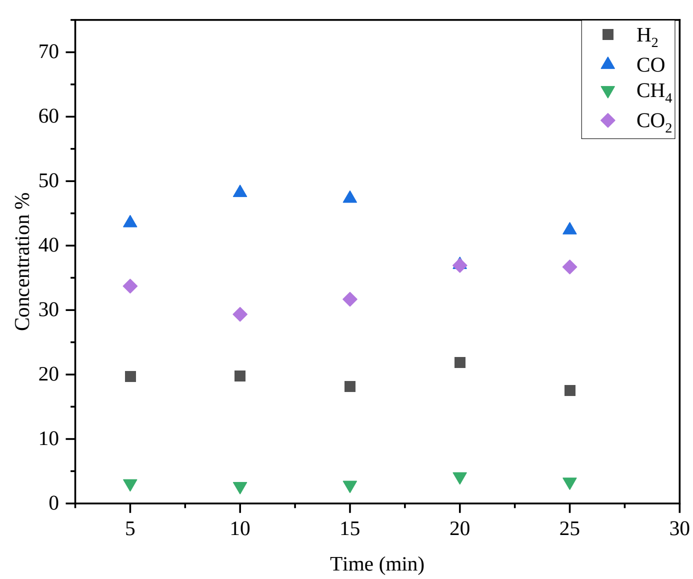

Fig. 5.16 Variation of producer gas composition with time for exp no 4 (RDF D pellet with air-O_2 mix as gasifying agent)

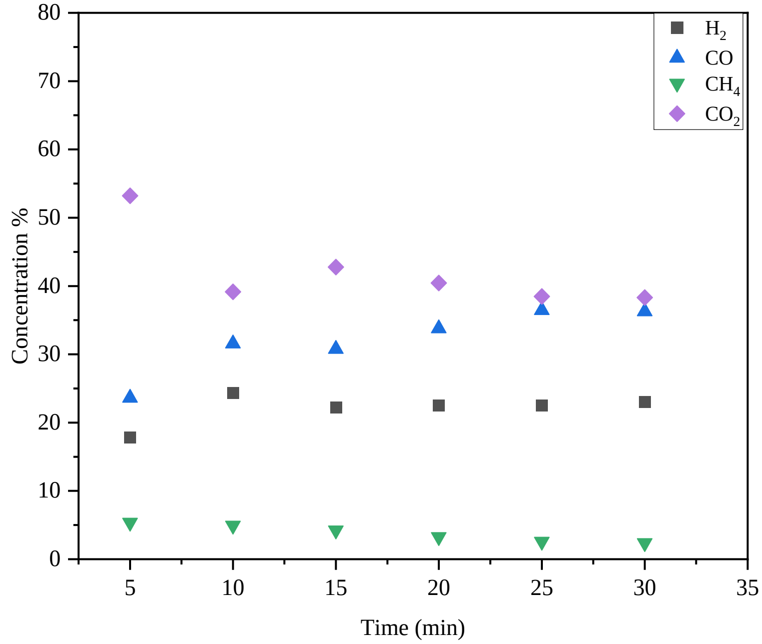

Fig. 5.17 Variation of producer gas composition with time for exp no 5 (RDF E pellet)

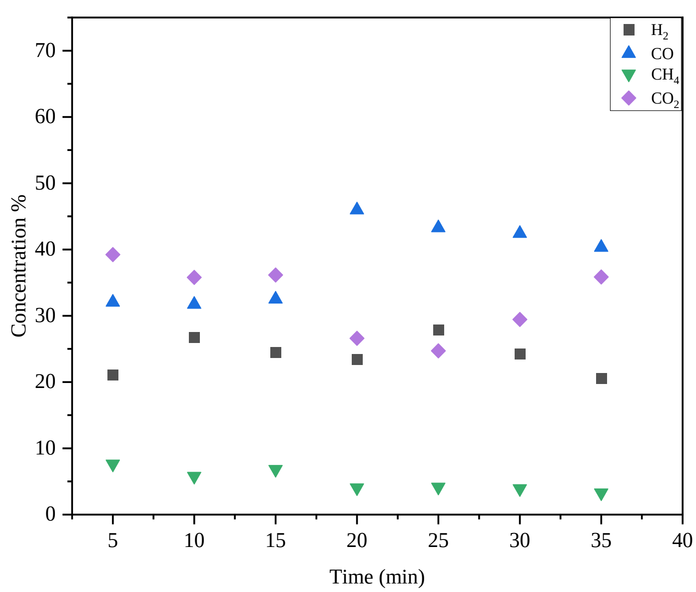

Fig. 5.18 Variation of producer gas composition with time for exp no 6 (RDF E pellet and biomass pellet (50:50) at 6 Nm^3/hr of air flowrate

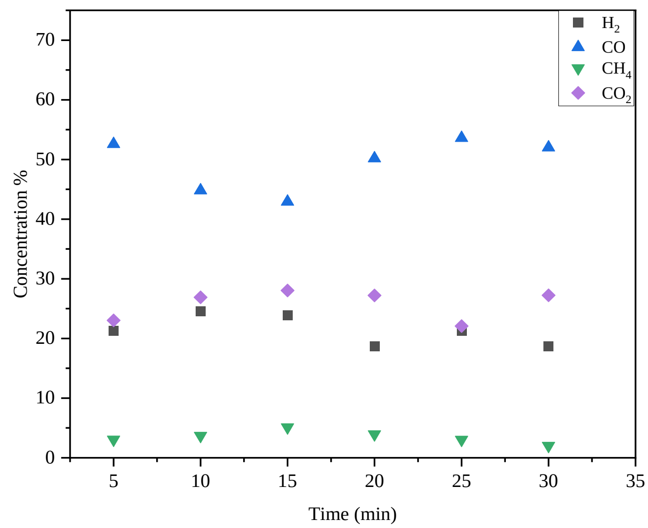

Fig. 5.19 Variation of producer gas composition with time for exp no 7 (RDF E pellet and biomass pellet (50:50) at 8 Nm^3/hr of air flowrate

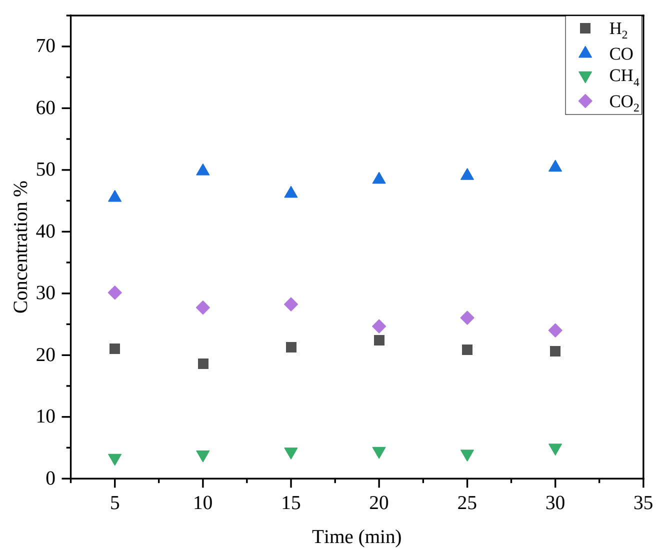

Fig. 5.20 Variation of producer gas composition with time for exp no 8 (RDF E pellet and biomass pellet (30:70) at 7.5 Nm^3/hr of air flowrate

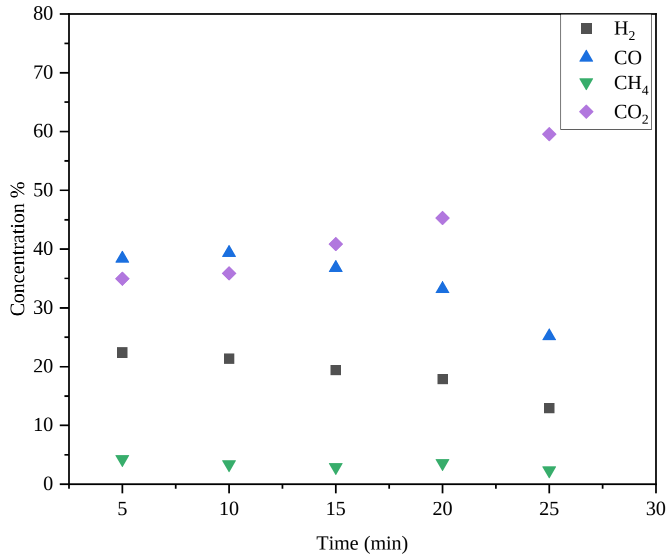

Fig. 5.21 Variation of producer gas composition with time for exp no 9 (RDF E pellet and biomass mix pellet (50:50) at 7 Nm^3/hr of air flowrate

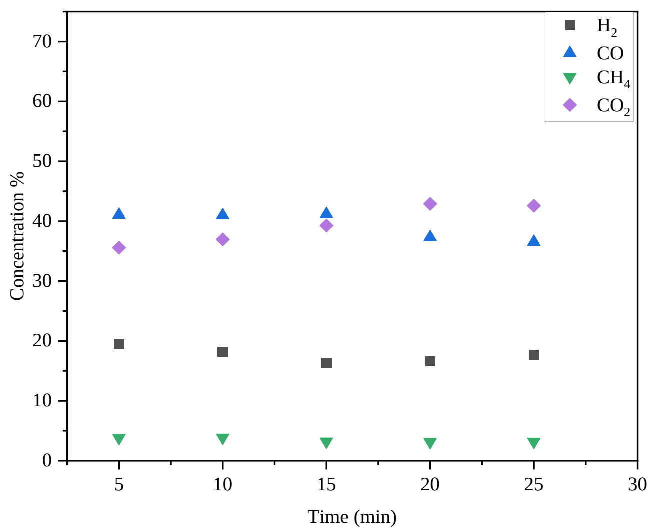

Fig. 5.22 Variation of producer gas composition with time for exp no 10 (RDF F and biomass mix pellet (50:50) at 7 Nm^3/hr of air flowrate

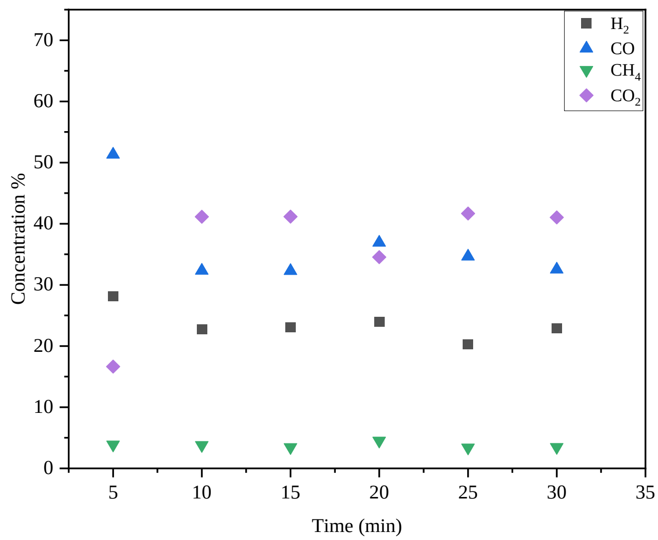

Fig. 5.23 Variation of producer gas composition with time for exp no 11 (RDF F and biomass mix pellet (50:50) with air-O_2 mix as gasifying agent

5.2.3 Effect of varying feedstock composition and gasifier operating conditions on producer gas properties

The average gas composition during stable conditions with consistent producer gas flame has been obtained from the dynamic variation results presented in section 5.2.2 to calculate the LHV of producer gas for all eleven experimental runs. The lower heating values of CO, H_2 and CH_4 are taken from the literature as 12.63, 12.63 and 35.88 MJ/Nm^3, respectively [109]. Since most of the cement plants in India use RDF fluff, the experimental run started with RDF fluff only. The moisture content in the RDF C fluff was around 45% which is too high for the gasifier. Hence, the preliminary experiment failed as no producer gas was obtained due to heat being taken up for drying. Thus, RDF fluff is sun-dried and used for the first experimental run. Further, all experiments were carried out on RDF pellets and a mix of RDF pellets and biomass.

Fig. 5.29 represents producer gas components concentration for different experiments. Experiment run no 1 has the highest N_2 content of 75%, and LHV is 1.87 MJ/Nm^3, the minimum among 11 runs. Bridging occurs as material forms a layer inside the gasifier near the combustion zone, and material in the central portion of the gasifier only takes part in reactions. The gasifier was opened once it got cooled, and the inside picture is shown in Fig. 5.24.

Fig. 5.24 Picture of the inside of the gasifier for the RDF fluff gasification

The experiment runs nos 2, 3, and 4 are conducted with RDF D pellets as feedstock. Run 2 and 3 use only air as a gasifying agent, while during run 4, the ambient air O_2 content is enriched from 21% to 35%. Exp 4 results are compared to the average values of exp 2 and 3 as the air flow rate does not vary much for 2 and 3. Run 4 is much better than runs 2 and 3, as fuel consumption increased by ~28% compared to the average of runs 2 and 3. Moreover, there is an appreciable rise in H_2 and CO content by 2.66% and 9.55%, respectively, with a drastic reduction of N_2 content by 13.16%. CH_4 quantity is doubled from 0.74 to 1.48% during oxy enrichment contributing to high LHV. It can be corroborated by the producer gas composition trend with time, as shown in Figs. 5.14-5.16. In run 3, the sparger is placed in the combustion zone to distribute ambient air better. Thus, the change in the airflow rate from 6 to 5 Nm^3/hr with a corresponding ER reduction from 0.36 to 0.26 resulted in improved fuel consumption. However, CGE reduced by 16% due to decreased gas yield.

The bridging effect for RDF pellet is comparatively less than RDF fluff with little material on the sides of the gasifier, as shown in Fig. 5.25. Some material is left at the bottom during oxy gasification (part of char in mass balance closure), as shown in Fig 5.26.

Fig. 5.25 Picture of the inside of the gasifier for the RDF pellets gasification

Fig 5.26 Picture of the inside of the gasifier for the oxy gasification of RDF pellets

Run no 5 was carried out with feed as RDF E pellets, while run nos 6 and 7 were conducted with RDF E-biomass pellets (50:50) at ER 0.36 and ER 0.46, respectively. Run no 8 is carried out on higher biomass composition with RDF E-biomass pellets (30:70). Run no 9 takes up the mix of RDF E and biomass pellets. Comparing the run no 6 and 7 average values with run no 5, it is observed that 50% RDF replacement by biomass increased H_2, and CO content by 2.17% and 6.80%, respectively, with a reduction in N_2 content of 9.08%. It also leads to an improvement of LHV by 1.41 MJ/Nm^3 and CGE by 15%. During gasifier inspection after exp no 6 and 7, it is observed that the gasifier is clean with very little biomass at the bottom (Fig. 5.27). It indicates effective gasification, verified by a consistent flame of burnt producer gas. Further, increasing the biomass content to 70% (run no 8) reduced the N_2 content by 9.08 to 11.72% with an appreciable rise in CO content by 9.6% with corresponding LHV and CGE increase by 1.7 MJ/Nm^3 and 6.6% respectively as compared to RDF E pellet scenario. In this case, the gasifier is also clean, with very little biomass at the bottom (Fig. 5.28). N_2 content is highest for a run no 5 as the reduction zone temperature is less than 600°C leading to low conversion to CO and H_2. Moreover, RDF consumption is also low (1.95 kg/hr) since the entire RDF fed to the gasifier does not participate in chemical reactions due to bridging, leading to low conversion. The lower fuel consumption increases the gas yield to 3.34 Nm^3/kg RDF, the maximum out of run nos 5-9. Run no 9 showed no significant improvement in producer gas composition compared to run no 5.

Fig. 5.27 Picture of the inside of the gasifier for the RDF pellet-biomass pellet mix (50:50) gasification

Fig. 5.28 Picture of the inside of the gasifier for the RDF pellet-biomass pellet mix (30:70) gasification

Exp no 10 and 11 are carried out for RDF F and biomass mix with different gasifying agents. Run no 11 compared to run no 10 showed significant improvement as all three combustible components of producer gas, i.e., H_2, CO and CH_4, increased by 4.26%, 2.56% and 0.45%, respectively, with reduced N_2 content by 10.98%. It occurs mainly due to O_2-enriched air as gasifying agent facilitating better combustion.

RDF fluff, RDF pellets, the mix of RDF pellets & biomass pellets and RDF-biomass mix pellets are different feedstock combinations tried for gasification, as discussed above. RDF E pellets produced better results than RDF D pellets considering LHV, combustion and reduction zone temperature profiles, less residual char (Table 5.9), and flame consistency. Further, it is noted that the densification of RDF in pellet form followed by co-gasification with biomass led to better burning behaviour with good consistent flame and minimum residue at the gasifier bottom.

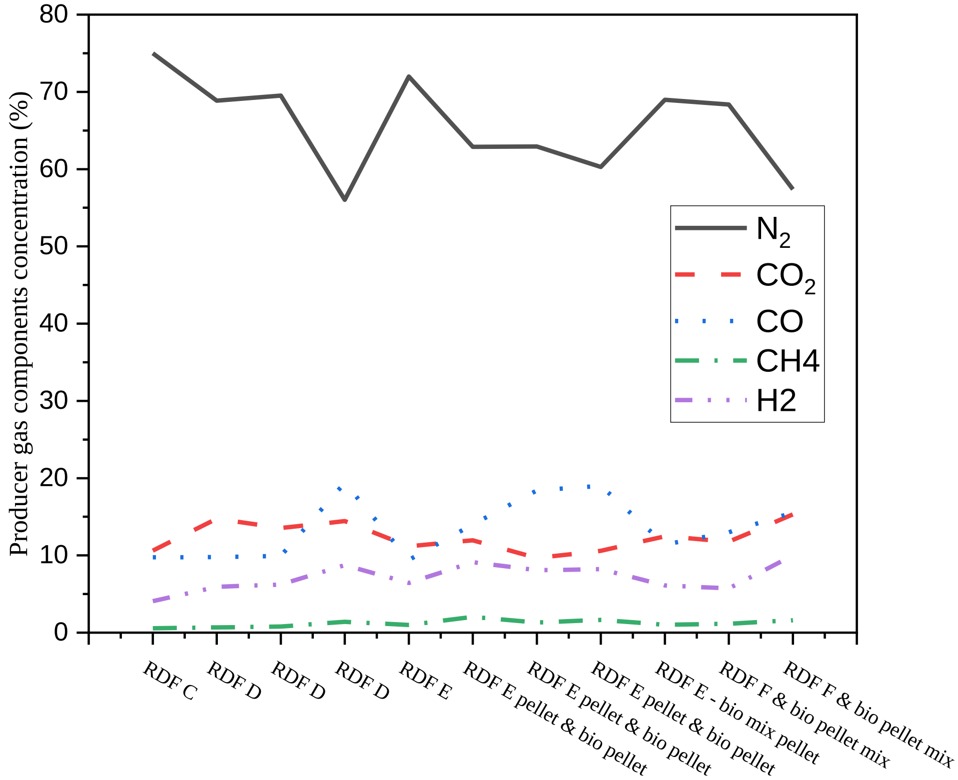

Fig. 5.29 Effect of varying feedstock and gasifier operation conditions on producer gas composition

5.2.4 Performance evaluation of RDF and RDF-biomass mix gasification

The lower heating value of producer gas (MJ/Nm^3), gas yield (Nm^3/kg fuel), and cold gas efficiency (%) are the most critical parameters to be considered for the co-processing of producer gas as an alternative fuel for clinker production. The higher the heating value, the more will be the replacement of conventional fuels in the calciner of cement plants. All three parameters in relation are discussed in sections 5.2.4.1 and 5.2.4.2.

5.2.4.1 Calorific value and yield of producer gas

Considering all runs, run no 1 has an exceptionally high peak indicating a gas yield of 3.65 Nm^3/kg RDF since the RDF consumption is low due to the fluffy nature of the material. N_2 content in producer gas is 75% and extinguishes the flame whenever trying to burn the producer gas. Thus, the heating value is low at 1.87 MJ/Nm^3. As the ER for RDF D (run no 2 and 3) decreased from 0.36 to 0.26 with a sparger in place for better air distribution, LHV rose from 2.12 to 2.21 MJ/Nm^3 along with a decrease in yield from 3.44 to 2.43 Nm^3/kg RDF. However, air with enriched O_2 (run no 4) increases the LHV and gas yield to 3.89 MJ/Nm^3 and 2.54 Nm^3/kg RDF, respectively, which is encouraging.

Similarly, for runs 6 and 7 having RDF E pellet and biomass pellet mix (50:50) as feedstock, LHV increased from 3.48 to 3.67 MJ/Nm^3 and gas yield from 2.53 to 3.27 Nm^3/kg fuel with an increase in ER from 0.35 to 0.46. This increase in heating value is attributed to a significant CO rise of 4.40%, as depicted in Fig. 5.13 of producer gas composition. Further enhancing the biomass content in the fuel mix to 70% (run no 8) improved the LHV to 3.88 MJ/Nm^3. It is close to the LHV obtained during oxy gasification of RDF D. However, the gas yield is lowered to 2.42 Nm^3/kg fuel since the fuel consumption increased by 34% owing to the ease of biomass burning and high heating value compared to RDF. Run no 9 utilized the pellet prepared by mixing the RDF and biomass in 50:50 ratio as the feedstock. In this case, LHV got reduced to 2.46 MJ/Nm^3. It could be possible due to the pellets being non-uniform in composition, and varying plastic content of RDF changes the pellets LHV frequently.

Another mix with RDF F fluff and biomass pellet (run no 10) was prepared for gasification. At ER value of 0.47, the LHV and gas yield was reasonably good at 2.67 MJ/Nm^3 and 2.84 Nm^3/kg fuel, respectively. The same feed is also gasified in the air with enriched O_2 content (run no 11) at a high ER of 0.68, and the results are encouraging. LHV got increased by 37%. However, the gas yield was reduced by 14% due to increased fuel consumption. It is noted that enhanced fuel consumption should be translated to higher producer gas flow generation theoretically; however, in practical situations, improved fuel consumption reduces the yield due to less N_2 in the gasifying agent.

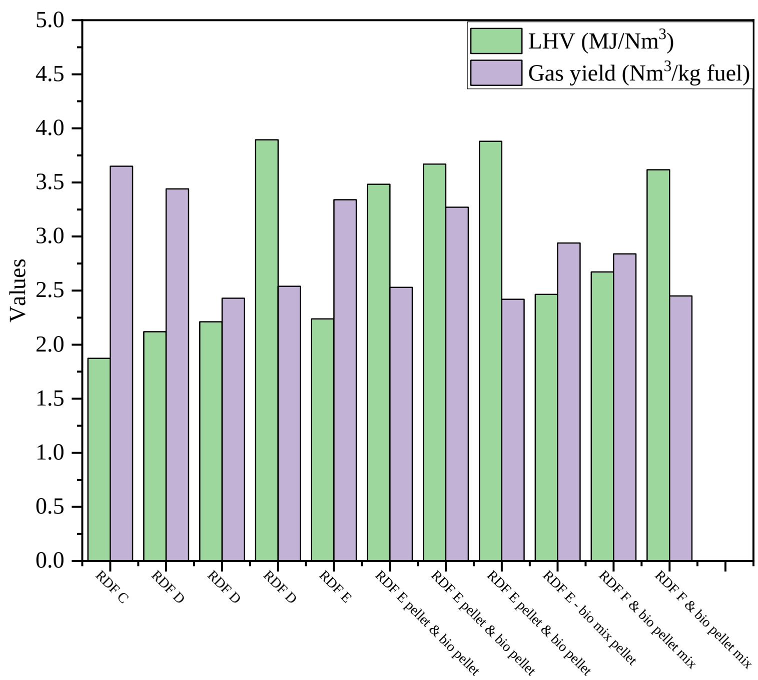

Fig. 5.30 LHV and gas yield for different experimental runs

5.2.4.2 Cold gas efficiency

The ratio of producer gas's heating value to feedstock's heating value is termed cold gas efficiency (CGE). It depends upon the LHV of biomass or RDF and the amount of producer gas per unit feedstock. Fig. 5.31 represents the CGE for different experimental runs. In RDF gasification only, CGE varied from 44.08 to 60.44%, with air as the gasifying agent. However, for run no 4 with oxy gasification for RDF D, CGE reached 81.88%, which is good. CGE varied from 50.13 to 77.65% for co-gasification cases, which is reasonably high compared to standalone RDF gasification. Run no 7 with RDF pellet and biomass pellet (50:50) mix shows maximum CGE due to high LHV and gas yield. Run no 11 also showed improved CGE compared to run no 10 with the same fuel mix. The reason is the change in the gasifying agent. In run no 11, air and O_2 mix as gasifying agents facilitated the combustion, thereby gasification and increasing the CGE.

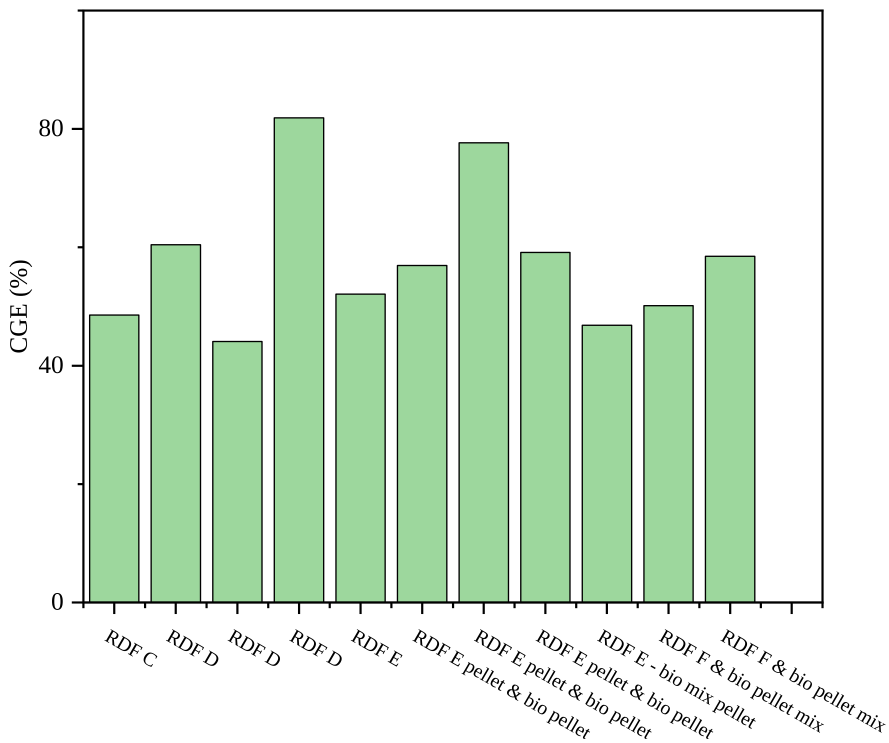

Fig. 5.31 CGE for different experimental runs

5.2.5 Comparison of results with literature data

In this section, the results of experimental runs are compared to values reported in the literature for similar studies. Khosasaeng et al. [51] investigated the RDF pellets gasification producing combustible gases (CO, CH_4, and H_2) for ER varying from 0.15 to 0.50 in a downdraft gasifier. They found the most optimum operating point to be at ER 0.35, with the heating value of producer gas at 5.87 MJ/Nm^3 and cold gas efficiency of 73.04%. Uthaikiattikul et al. [55] performed RDF gasification in a 10 kg/hr laboratory scale downdraft gasifier. It captured temperature distribution and predicted producer gas composition and LHV at 12, 18, and 24 Nm^3/hr, corresponding to ER 0.17, 0.26, and 0.35, respectively. Another study also performed gasification and co-gasification of RDF pellets having a high ash content of 16% with saw dust [49]. The maximum LHV reported for RDF gasification is 4.34 MJ/Nm^3 at an ER of 0.34, corresponding CGE of 59.24%. LHV increased to 4.65 MJ/Nm^3 during co-gasification.

Table 5.10a shows the LHV, gas yield, and CGE comparison of the present study for RDF fluff gasification with experimental studies reported in the literature [55]. Table 5.10b represents experimental results compared to the literature study [51] and [49] for RDF pellets. The deviations are majorly attributed to the high ash content of RDF (30-51%) in the RDF considered for the present study leading to high ER.

Table 5.10a Comparison of experimental study results with those reported in the literature for RDF fluff

Research Group	Feedstock	ER	LHV (MJ/Nm^3)	Gas yield (Nm^3/kg feed)	CGE
[55]	RDF fluff	0.35	2.12	4.81	49.05
Present study	RDF C fluff	0.58	1.87	3.65	48.56

Table 5.10b Comparison of experimental study results with those reported in the literature for RDF pellet

Research Group	Feedstock	ER	LHV (MJ/Nm^3)	CGE
[51]	RDF pellet	0.45	4.50	62.00
[49]	RDF pellet	0.30	3.90	42.84
Present study	RDF E pellet	0.44	2.24	52.09

5.2.6 Operational issues during the gasifier experimentation

Since the RDF is of commercial type with high ash content of 30-51%, it has been observed that the downdraft gasifier faced operational issues in processing high ash RDF due to the softening, agglomeration, and fusion of ash, leading to the formation of clinker. The extent of clinker formation is a function of temperature, the residence time of the feed in different zones of the gasifier, and the nature of the ash as reported in the literature [49]. Fused clinker samples were collected during gasifier inspection after each experiment. The samples were ground and characterized for C, H, N, S, and GCV. The results indicated no carbon content and heat value in the samples; hence it is concluded to be fused ash formed from the RDF ash content. This fused ash is further characterized to determine major oxides, and results indicated four major components, i.e., SiO_2: 47%, Fe_2O_3: 7.25%, Al_2O_3: 11.70% and CaO: 21.32%. The photograph of the fused sample is shown in Fig 5.32.

Fig. 5.32 Photograph of the fused clinker formation

5.3 Modelling and simulation

This section begins with the gasifier model, where validation has been taken up based on literature and current experimental study. It is followed by the parametric studies for RDF E. The parameters changed are ER, reduction zone inlet temperature, reduction zone length and moisture content of RDF.

Further, stoichiometric and Aspen Plus-based calciner models have been validated with white cement plant operational data for the base case scenario. The gasifier model predicted results for RDF E are a close fit to its experimental study with an RMSE of 2.27, as discussed in sections 5.2.3 and 5.3.1.1. Thus, the technical evaluation of the calciner has been conducted with RDF E-based producer gas as input to the calciner models to achieve 8% and 15% TSR.

The calciner model with higher accuracy has been considered further for the economic feasibility of producer gas utilization in a white cement plant in next Chapter-6.

5.3.1 Gasifier model

RDF gasification is gaining importance due to the operational issues (mainly due to high ash content) of RDF combustion. A multi-zone RDF gasification model is developed to predict the producer gas composition in the present study. It consists of drying, pyrolysis, combustion, and reduction zones where different thermochemical phenomena occur. The gasifier model is validated using the current study's experimental data and the data reported in the literature as discussed in the next section.

5.3.1.1 Model Validation

The model is validated using the experimental results furnished in the literature [51]. The experimental data reported RDF utilization as a fuel in a 30-kW single-throat downdraft gasifier of 1.70 m height with a radius of 0.25 m and the single throat tilting at 45°. The characteristics of the RDF used in the experimental study are summarized in Table 5.11 [51]. The model-predicted results are validated with the experimental data at different equivalence ratio.

Table 5.11 RDF characteristics used for model validation

Proximate analysis (as received basis)	**(% wt)**	**Ultimate analysis (as received basis)**	**(% wt)**
Volatile Matter	84.86	C	53.04
Fixed Carbon	10.14	H	8.94
Ash	4.80	N	0.67

Proximate analysis (as received basis)	**(% wt)**	**Ultimate analysis (as received basis)**	**(% wt)**
Moisture	4.00	O	28.56
High heating value (MJ/kg as received basis)		26.82	
Density (kg/m^3)		930	

Fig. 5.33 compares the composition of CO_2, H_2, CO, and CH_4. The estimated RMSE for the four components is 1.34. The model prediction matches closely with the experimental values of the molar concentration of CO_2, CO, and H_2. For ER range of 0.25 to 0.4, CO experimental values show variation from 12.9 to 14.4% with an average value of 13.98%, slightly higher than the model value of 12.02%. The model underpredicts the CH_4 concentration as indicated by the continuous downward trend. The models reported in the literature have not correctly predicted the CH_4 concentration in producer gas [47, 211]. It may be because many reactions occur in the downdraft gasifier in the reduction zone, which leads to the formation of CH_4. Higher temperatures may convert higher molecular weight hydrocarbons such as tar, oil, paraffin, and olefins into methane due to molecular reforming, rearrangement, and cracking. The widespread phenomenon of CH_4 formation cannot be adequately captured; hence, it remains underpredicted due to the unavailability of the kinetics of such reactions. In the present study, the methanation reaction is considered for methane formation.

Fig. 5.34 indicates the LHV and CGE comparison at different ERs, which shows that LHV and CGE, as per the model, are lower than experimental values. It is due to reduced H_2 and CH_4 concentration in producer gas.

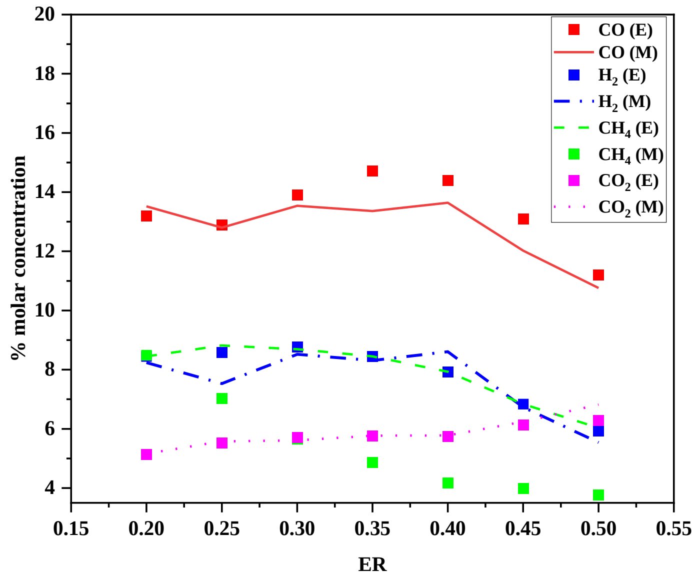

Fig. 5.33 Molar concentration of producer gas: model (M) vs experimental (E)

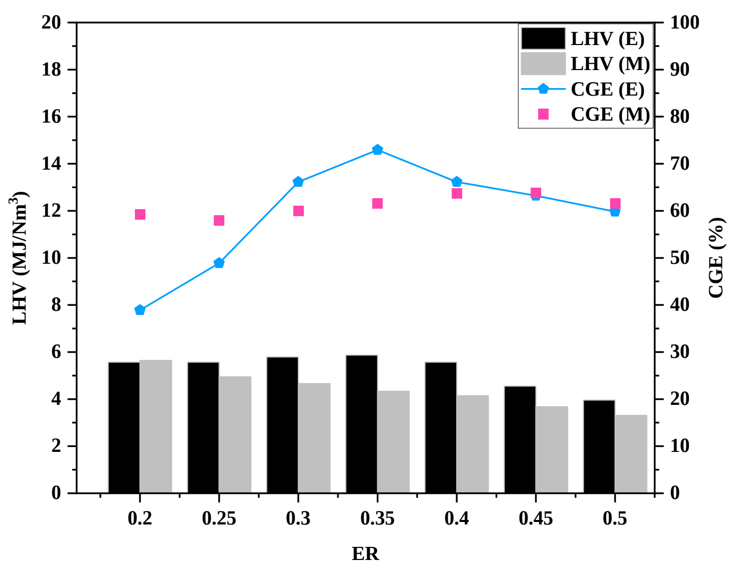

Fig. 5.34 LHV and CGE validation results: model (M) vs experimental (E)

Fig. 5.35 and 5.36 shows the validation of the model with the present study for the seven good experimental runs i.e., exp 2, 3, 5, 6, 7, 8 and 9. The model is simulated for the same ERs at which experiments have been performed, and the RMSE is calculated for producer gas components, LHV, and CGE. The reduction zone temperature for RDF gasification is considered to be 200°C lower than RDF and biomass co-gasification for modelling. The mean RMSE for producer gas components, LHV, and gas yield is 3.37, 1.30, and 1.03, respectively which is acceptable. The literature suggests the RMSE value for most of the downdraft gasifier models in the range of 3.0 to 4.5 [212]. It is noted that all parameters are better fit for co-gasification as compared to RDF gasification. It is evident from the RMSE for RDF E pellet gas composition, which is 2.27, much better than that for RDF D value of 4.70.

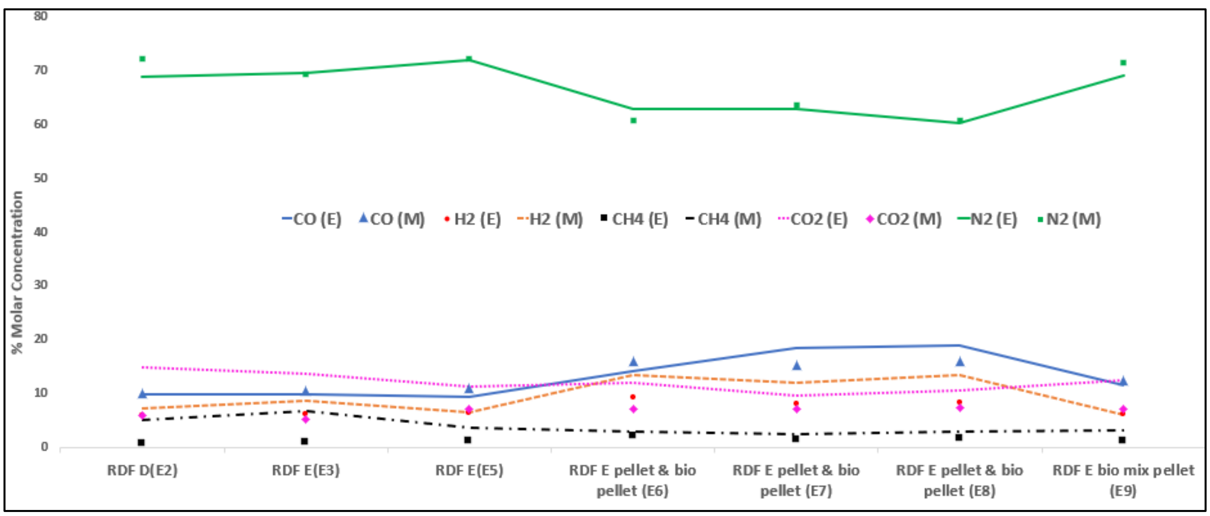

Fig. 5.35 LHV and CGE validation results: model predicted (M) vs present study (E)

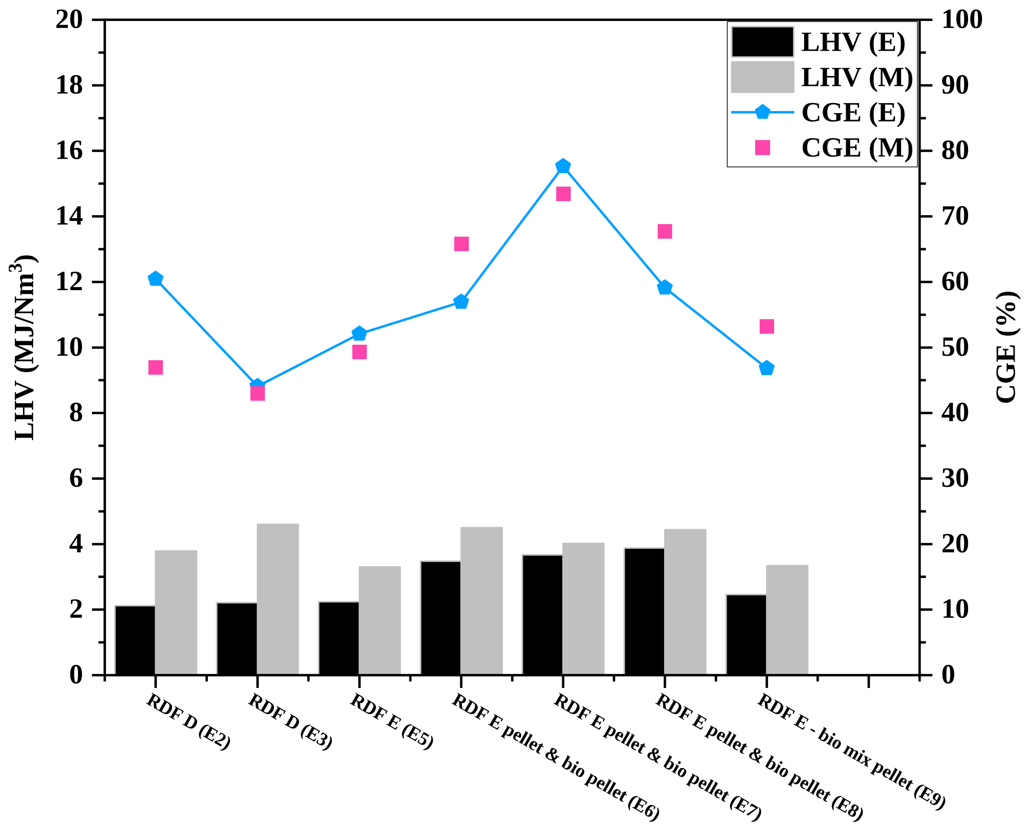

Fig. 5.36 LHV and CGE validation results: model predicted (M) vs present study (E)

5.3.1.2 Parametric studies

RDF composition varies depending on the type of MSW. RDF E has been considered to study the influence of process parameters. GCV,% C,% O,% N, and ash content of chosen RDF E are indicated in Tables 3.1 and 3.2. The parameters changed are ER, reduction zone inlet temperature, reduction zone length, and moisture content of RDF.

1) Effect of equivalence ratio

The equivalence ratio is one of the most important parameters determining the gasifier's producer gas quality and performance. The higher the equivalence ratio, the more air is available for the combustion of the char and hydrocarbons formed during the pyrolysis of RDF.

The combustion reactions are exothermic, and due to the higher combustion rate, more heat is available to increase the temperature of the pyrolysis zone and the reduction zone. Also, the heat generated in the combustion zone drives the endothermic reactions (char + H_2O and char + CO_2) inside the reduction zone. The equilibrium constants are temperature dependent, and their value depends upon the temperature or, ultimately, the equivalence ratio. Increasing the equivalence ratio will increase the char and gas oxidation reactions, enhancing the generation of CO and CO_2 in the combustion zone. Fig. 5.35 represents producer gas components concentration for RDF E at different ERs. The amount of nitrogen increases with increasing the ER, which leads to higher nitrogen concentration in producer gas from 31.52 to 54.52%, as shown in Fig. 5.36. Moreover, the CO concentration increases slowly from 10.74 to 11.81%, while the H_2 concentration decreases from 12.19 to 9.38% with increasing ER. All the reactions occurring in the reduction zone are endothermic except reactions 3 and 4 (Table 4.1 of Chapter-4).

As the equivalence ratio increases, the temperature inside the reduction zone increases, which shifts reactions 3 and 4 to the reactant side. Similarly, with an increase in equivalence ratio, reactions 1, 2, and 5 shift towards the product side. Also, the volatiles formed during the pyrolysis zone gets converted to more CO and CO_2 as the ER increases. Overall, the total number of moles of CO and H_2 increases with increasing the ER, but the mole fraction of H_2 decreases as the increase of N_2 concentration is much more dominant. For similar reasons, the CH4 concentration was reduced from 4.20% to 2.02% for RDF E. The CO_2 concentration for RDF E increases from 3.93 to 5.35% with an increase in ER since the enhanced air results in more CO_2 formation. If reducing conditions are favourable, more and more CO_2 will be reduced to CO, and the concentration of CO_2 will decrease.

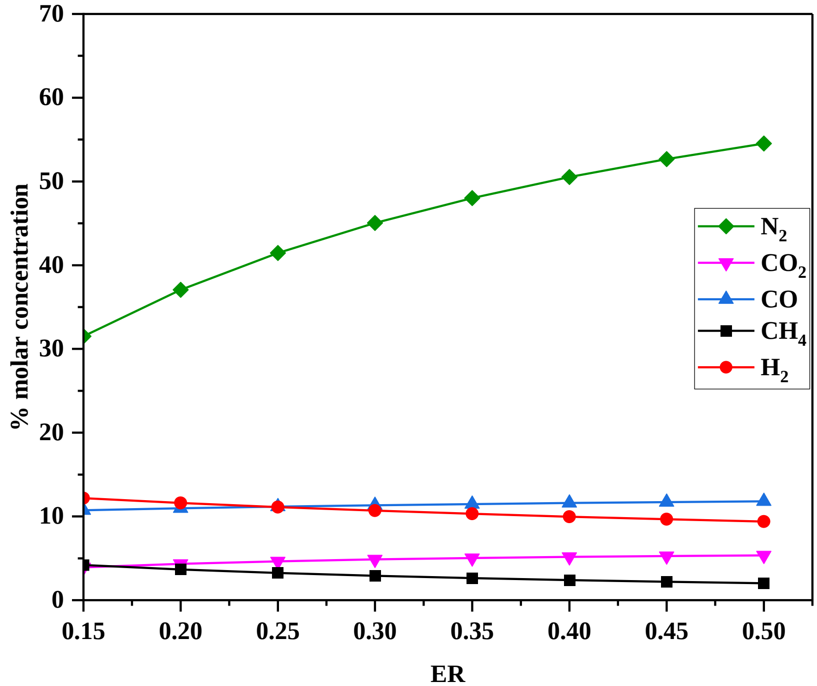

Fig. 5.37 Producer gas components concentration at different ER (RDF E)

Fig. 5.36 indicates heat value, yield, CGE and CCE at different equivalence ratios for RDF E. Cold gas efficiency (CGE) is defined as the ratio of LHV of producer gas produced to the LHV of the feedstock. Carbon conversion efficiency (CCE) is the ratio between the amount of carbon in the gas produced and the amount of carbon consumed in the RDF. The gas yield increases because of the char combustion reactions as the ER increases. Also, due to the char reduction reactions, the carbon conversion efficiency increases tremendously from 44.45% to 86.45% with varying ER. At higher ER, more amount of char gets converted to CO and CO_2, leading to the presence of less amount of char in the reduction zone. During the model's development, charcoal is considered readily available in the reduction zone for the solid-gas phase reactions. Moreover, as the CO, H_2, and CH_4 mole fraction summation decreases, the

LHV of the gas decreases significantly from 4.18 MJ/Nm^3 to 3.23 MJ/Nm^3 for RDF E over the range of ER from 0.15 to 0.50. The cold gas efficiency trend increases continuously with ER. The optimum ER range for RDF E is 0.35-0.40, considering the gas yield, LHV, CGE, and CCE trend. The decreasing LHV trend with an increasing CCE trend corroborates Ribeiro et al.'s RDF gasification experimental results [115].

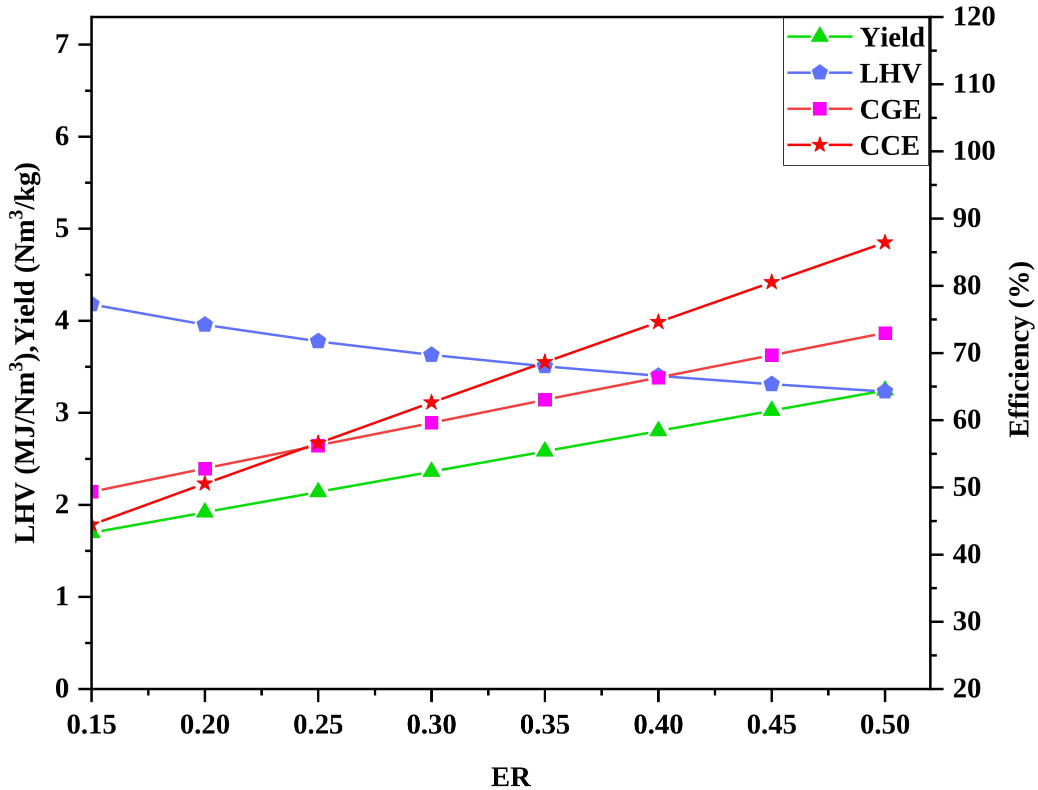

Fig. 5.38 LHV, yield, CGE and CCE at different ER for RDF E

2) Effect of RDF moisture content

The RDF moisture content affects the producer gas quality, including the gasifier's performance parameters, as shown in Fig. 5.37 and Fig. 5.38. Generally, fuel with low moisture content is desirable as it has a higher gross calorific value. The moisture content varies from

5% to 20%. The moisture content affects the operation of the gasifier in two different ways. Firstly, increasing moisture content will reduce the temperature in the reduction zone due to the energy required for drying. Secondly, increasing the moisture content will increase the amount of water vapour in the reduction zone, directly enhancing the water gas, water gas shift, and steam reforming reaction. Reactions 1 and 2 will shift towards the reactant side at a lower reduction zone temperature due to their exothermic nature. Also, reactions 3 and 4 will move more towards the right-hand side as they are endothermic. Overall, the mole% of CO and H_2 will decrease from 11.08% to 9.79% and 10.32% to 8.97%, respectively, as reactions 1 and 2 dominate more (refer Table 4.1 of Chapter-4). The mole% of N_2 also decreases from 45.32 to 42.10%; however, the number of moles remains constant. Accordingly, the CH_4 mole% decreased from 2.97% to 2.88%, and CO_2 mole% decreased from 4.87% to 4.58%.

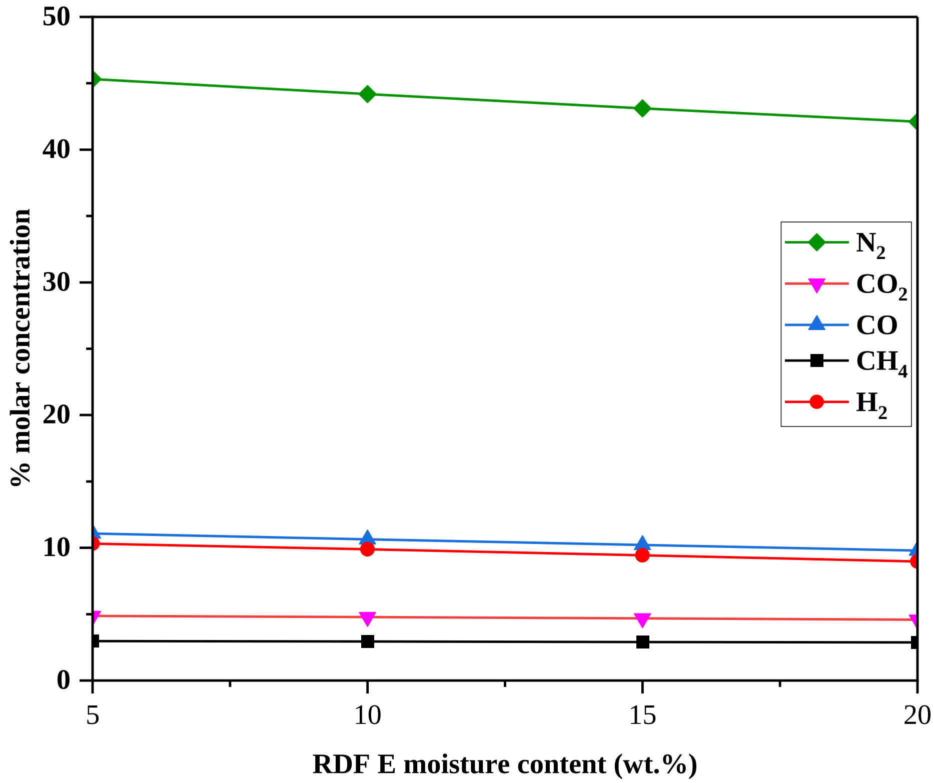

Fig. 5.39 Producer gas concentration variation with varying RDF E moisture

The trend of LHV and CGE, as shown in Fig. 5.38, indicates that it decreases consistently with increasing moisture content while the gas yield rises. The LHV decreases from 3.58 to 3.24 MJ/Nm^3 with a 5 to 20% moisture content. Accordingly, the CGE and CCE were reduced by 8.66% and 4.64%, respectively. It shows that high moisture content is not desirable for the performance of a downdraft gasifier. The gasifier can also utilize the waste heat available from different chemical unit operations to dry the moisture content of the RDF before feeding into the gasifier.

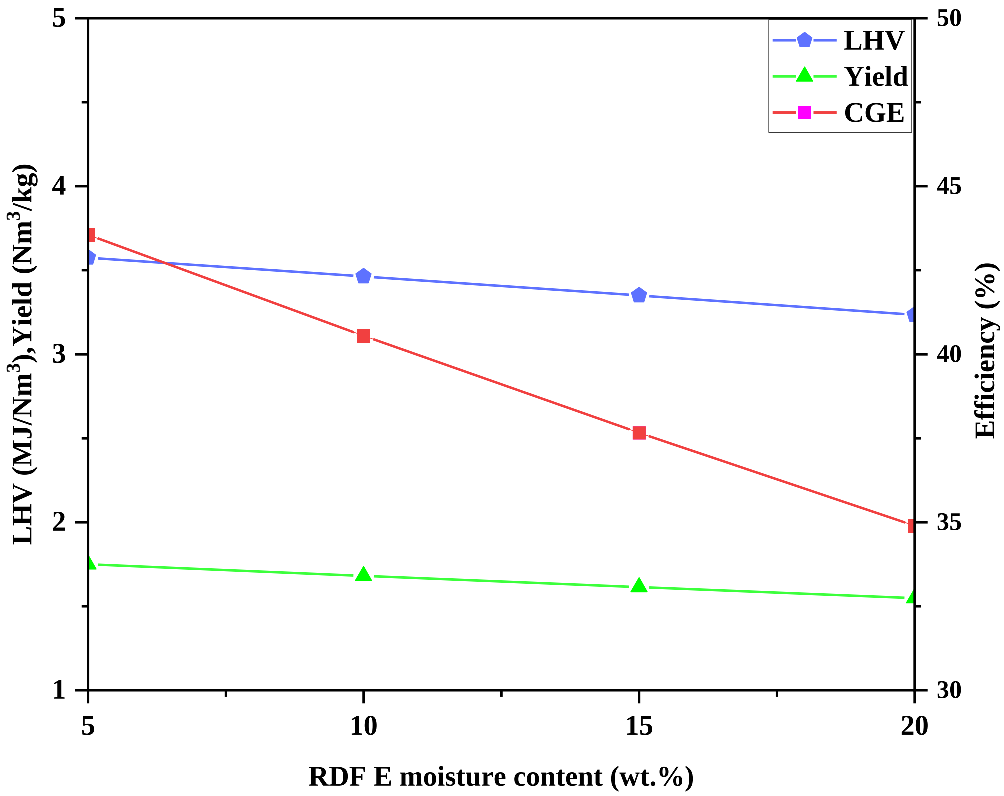

Fig. 5.40 Producer gas LHV, gas yield and CGE variation with RDF E moisture

3) Effect of reduction zone inlet temperature

Fig. 5.39 represents the variation in producer gas LHV & efficiency with an increase in temperature from 627 to 1127°C (900 to 1400 K), while Fig. 5.41 indicates producer gas concentration with temperature for RDF E. As the temperature increases, the Boudouard reaction rate, water gas and steam reforming reactions are enhanced, and reactions shift towards the right side, producing more CO and H_2. Due to this phenomenon, the overall gas yield and heat value increase since the H_2O component entering the combustion zone is reduced to H_2. As the heterogeneous char reactions occur more rigorously, more char gets reduced to volatiles. Thus, carbon conversion efficiency also increases.

As the temperature inside the reduction zone increases, the endothermic reactions shift towards the right, thus producing a more significant number of moles of CO and H_2. As the reduction zone temperature increases, the rate of an endothermic reaction, which generates CH_4 (reaction 4), increases and shifts towards the right. However, due to the exothermic nature of the methanation reaction, it moves towards the left. Hence, the overall rate at which CH_4 gets produced decreases. Moreover, the overall gas yield increases at a higher inlet temperature of the reduction zone, thus decreasing the mole fraction of CH_4. Although the number of moles of N_2 is independent of temperature rise, its mole fraction decreases due to the increase in the number of moles of other components of producer gas.

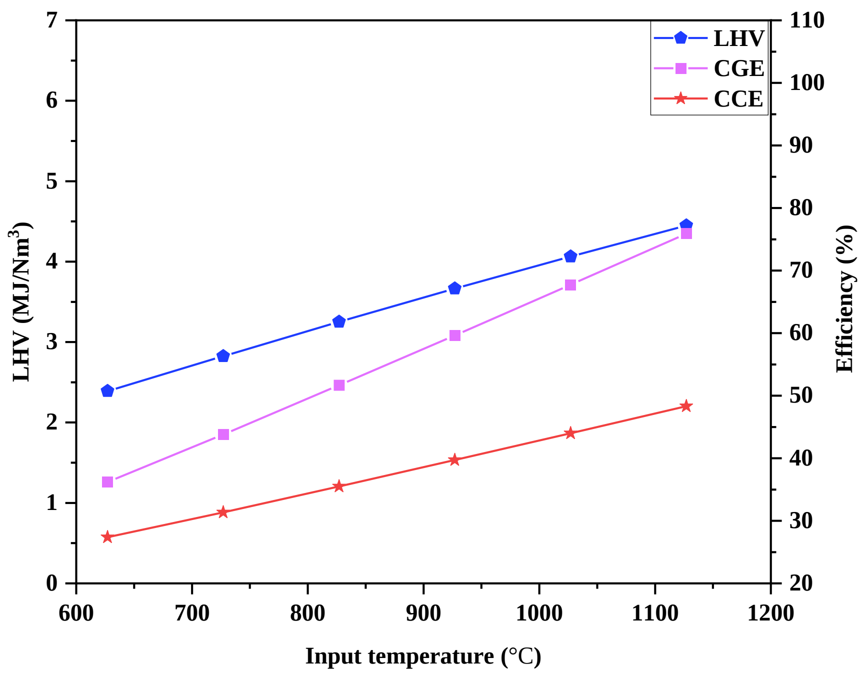

Fig. 5.41 Producer gas LHV and efficiency variation with temperature for RDF E

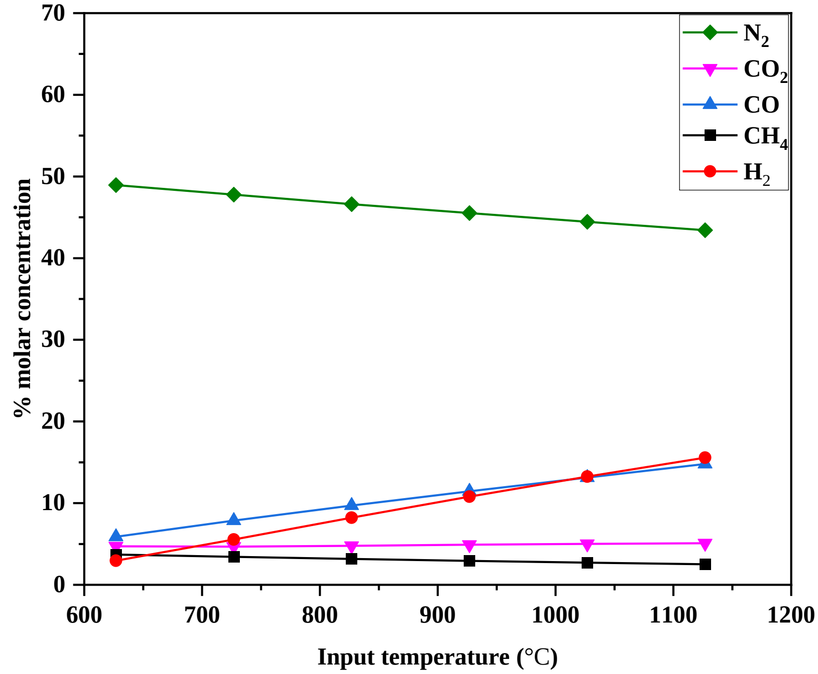

Fig. 5.42 Producer gas concentration variation with temperature for RDF E

4) Variation along the length of the reduction zone

The reduction zone of the gasifier is the zone where char reduction reactions take place. The length of the zone is critical since sufficient residence time is required to achieve equilibrium and attain the final producer gas composition. Table 5.12 describes the simulation parameters for the RDF E gasification reduction zone.

Table 5.12 Model simulation parameters

Parameters	Values
Bed length	0.25 m
Reduction zone inlet temperature	927°C
Moisture content	3.57%

Bed length is assumed to be 0.25 m with a reduction zone inlet temperature of 927 °C and CRF of 500 [118]. It is observed that with ER ranging from 0.15 to 0.50, equilibrium was achieved within 60% length (0.15 m) of the gasifier for RDF E. After that, the composition did not vary much with the change in length (0.15 to 0.25 m). Fig. 5.43 represents varying molar concentrations of different producer gas components along the length of the reduction zone for RDF E at ER 0.30. The reduction zone temperature got reduced from 927 to 636°C due to the heat required by the endothermic reaction occurring along the length of the reduction zone. Temperature change is more prominent up to the 60% length of the reduction zone as 90% conversion is achieved.

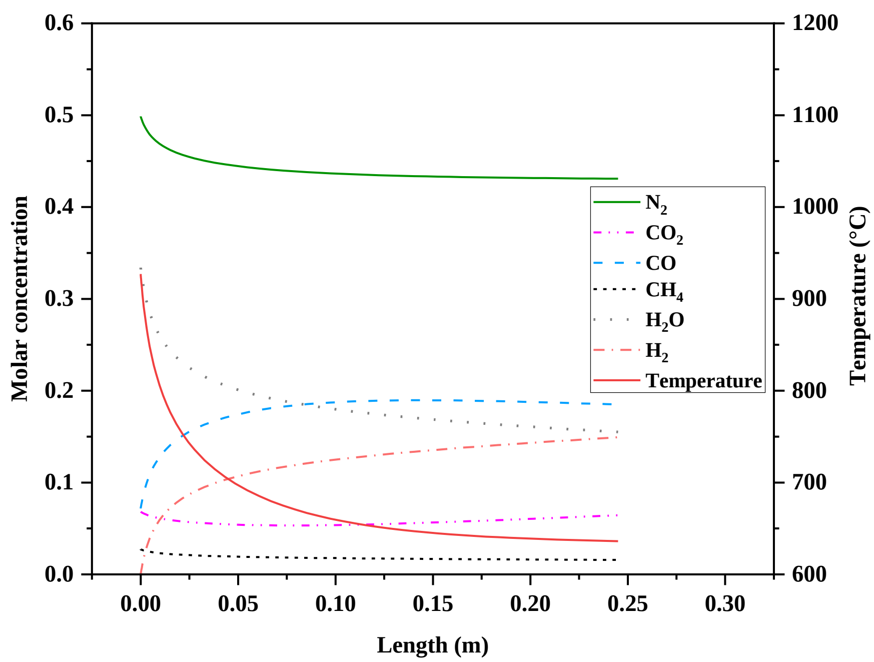

Fig. 5.43 Producer gas concentration and temperature variation with reduction zone length (RDF E)

5) Minor components variation with ER

HCl and H_2S formation directly correlate to RDF's Cl and S content. The minor components of producer gas HCl, H_2S, and tar variation are plotted with varying ER for RDF E in Fig. 5.44. HCl, H_2S, and tar concentration decreased from 0.079 to 0.041%, 0.115 to 0.060%, and 1.115 to 0.598%, respectively, with an increase in ER. As temperature increases with an increase in ER, tar reforming reactions occur, leading to more CO and H_2 formation and reduction in tar. Juma Haydary [213] modelled the RDF gasification using experimental results and predicted the tar & H_2S composition, which corroborates with the present model values.

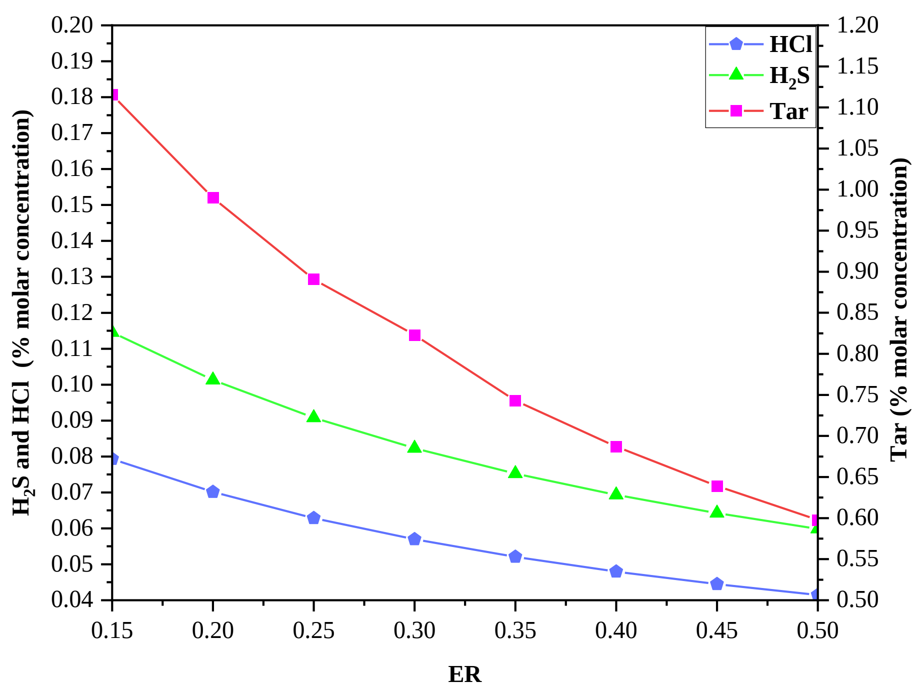

Fig. 5.44 Variation in composition of minor components with ER for RDF E

5.3.2 Calciner models

Calciner modelling effectively observes the calciner outlet parameters on changing the fuel mix without full-scale trial runs. In this regard, two calciner models, one stoichiometric and another Aspen Plus based, are developed and simulated with the same producer gas composition and temperature to compare the results.

5.3.2.1 Model parameters common to both models

The plant currently uses 100% petcoke as fuel. Model parameters include petcoke, proposed RDF E and producer gas properties. Petcoke properties have been obtained from the plant data. Petcoke, RDF E, and RDF E ash characterization results are shown in Table 5.13a, 5.13b, and 5.13c, respectively. RDF E composition, as shown in Fig. 5.13b is obtained through manual sorting and weighment. The theoretical air requirement for kiln fuel firing is calculated based on the ultimate fuel analysis [214]. The actual air requirement includes the excess air based on the measured oxygen concentration at the kiln inlet.

Table 5.13a Fuel characterization results (% w/w, air dried basis)

Fuel	C	H	O	N	S	Cl	Ash	Moisture	LHV (MJ/kg)
Petcoke	81.74	3.74	0.63	1.39	5.50	-	6.40	0.60	31.90
RDF E	38.57	5.66	18.97	0.69	0.27	0.41	31.86	3.57	14.36

Table 5.13b RDF E composition

RDF E	Plastic	Cloth	Rubber	Metal	Wood	Paper	Glass
% by wt	47.23	19.28	7.71	5.06	7.23	6.99	6.51

Table 5.13c RDF E ash composition (air-dried basis)

RDF	CaO	SiO_2	Fe_2O_3	Al_2O_3	MgO	Na_2O	K_2O	SO_3
% by wt	11.00	51.00	12.35	13.2	1.31	1.72	1.75	1.42

The RDF E properties in Tables 5.13a and 5.13c are input to the gasifier model. The producer gas properties and operational parameters for RDF E gasification are given in Table 5.14. Further, the producer gas properties (yield, LHV) obtained forms the basis of producer gas requirement per hour in calciner at 8% and 15% TSR, as shown in Table 5.15, to achieve the desired clinker production.

Table 5.14 Producer gas properties and operational parameters for RDF E gasification

Gasifier input and operational data	**Unit**	**Value**
Type of gasifier	Downdraft fixed bed	
Gasifying agent	Air	
ER	ER	0.30
Air-to-fuel ratio		1.75
Max size of RDF	mm	40
CCE	%	62.64
CGE	%	59.62
Characteristics and composition of producer gas		
Producer gas exit temperature	°C	593
Producer gas specific yield	Nm^3/kg RDF	2.36
Producer gas density	kg/Nm^3	1.03
CO	% vol	11.35
H_2	% vol	10.71
CH_4	% vol	2.92
CO_2	% vol	4.88
N_2	% vol	45.13
H_2O	% vol	24.18
Tar	% vol	0.82
Residual char	kg/kg RDF	0.39
Producer gas LHV	MJ/Nm^3	3.63
Producer gas LHV	MJ/kg RDF	8.56

Table 5.15 Input parameters for calciner models at 0%, 8% and 15% TSR

Parameter	0% TSR (Base case)	8% TSR	15% TSR
RDF used (kg RDF/hr)	Not Applicable	1000	1939
Yield (Nm^3/kg RDF)		2.36	2.36
Producer gas (Nm^3/hr)		2360	4577
Producer gas density (kg/Nm^3)		1.034	1.034
Producer gas mass (kg/hr)		2441.70	4735
Producer gas LHV (MJ/kg SG)		3.51	3.51
Available heat from producer gas on LHV basis (MJ/hr)		8562.67	16606.03
Producer gas sensible heat (MJ/hr)		2177.86	3639.08
Total producer gas heat available (MJ/hr)		10740.53	20245.11
Total heat requirement in kiln (MJ/hr)	80087	80087	80087
Total heat requirement in calciner (MJ/hr)	54880.36	54880.36	54880.36
% TSR through LHV	0	6.34	12.30
% TSR in calciner	0	19.5	36.9
Heat from petcoke firing in calciner (MJ/hr)	54880.36	44139.82	34365.25
Petcoke quantity (kg/hr)	1720	1383.38	1085.50

5.3.2.2 Calciner stoichiometric model

5.3.2.2.1Model validation

Fig. 5.45 and Fig. 5.46 represent model validation of calciner operating outlet parameters like calciner outlet gas flow, calciner outlet gas composition, and hot meal flow rate. Calciner outlet temperature and gas composition are measured values, while hot meal flow rate and calciner outlet gas flow are obtained through mass balance using plant data**. %** error for calciner outlet temperature, hot meal flow rate, and calciner outlet gas flow is 3.12, 0.85, and 5.09%, respectively. The predicted temperature is 892°C which is 29°C higher than the operating temperature. RMSE for calciner outlet gas composition (dry basis) is 3.56. All C has been assumed to be converted to $CO_{2;}$ hence CO is not part of the simulation.

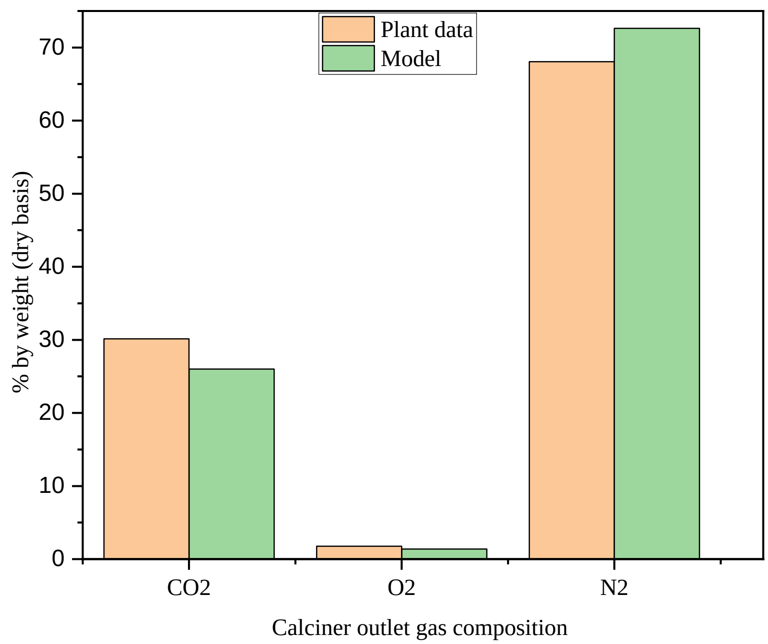

Fig. 5.45 Validation of stoichiometric calciner model gas composition

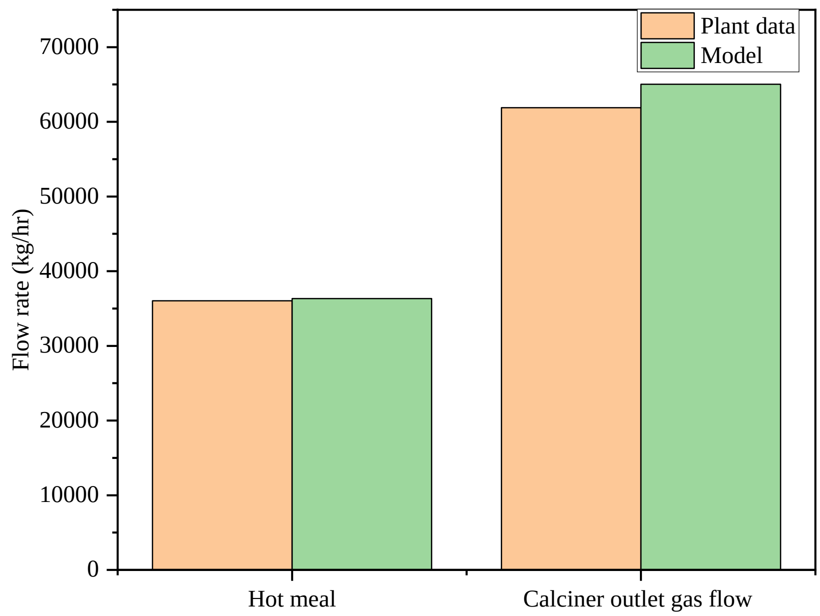

Fig. 5.46 Schematic of mass & energy balance for calciner

5.3.2.3 Material and energy balance of calciner

The material and energy balance (Table 3.11) for the calciner baseline scenario (100% petcoke firing) is carried out using a Microsoft Excel sheet. One kg clinker output is the basis. The kiln exit gas quantity was calculated based on the stoichiometric method's theoretical assessment. A similar approach is adopted by Kumar et al. [215] to report the energy balance of a cement plant's complete pyro-processing section.

The sensible heat of fuel, material entering the calciner, and combustion gases, including tertiary air, kiln exit gas, and fuel transport air, are inputs to the system. Heat loss through calciner exit gases, a hot meal including calcined and uncalcined material, moisture evaporation, ash absorption, and radiation are considered as output. The heat of the reaction is the energy required for calcination, calculated by thermochemistry principles. Calciner exit volume is 1.515 Nm^3/kg clinker corresponding to 2.19 kg/kg clinker, which is high compared to standard operating norms of 1.2-1.3 Nm^3/kg clinker considering 1.4-1.5 Nm^3/kg clinker at preheater exit [11]. It corroborates to kiln calciner firing ratio of 60:40, which reverses from the regular operation. The coefficients of specific heat values have been derived from the literature [48,49] and shown in Table 5.17.

Table 5.16 Calciner material and energy balance for the baseline scenario

Input parameters	**Mass Flow Rate (kg/hr)**	**Molar Flow Rate (Kmol/hr)**	**T in °C**	**C_p (kcal/kg°C)**	**C_p (cal/mol°C)**	**Heat flow (kcal/kg clinker)**
Petcoke sensible heat	1720.0		50	0.28		0.5
Petcoke combustion	1720.0					463.8
Tertiary Air	14329.0		267	0.24		30.4
Transport Air	715.0		60	0.24		0.2
Kiln Gas	40557.0		1050			418.7
CO_2	9539.0		1050	0.27		94.7
O_2	1756.1		1050	0.25		16.0
N_2	28430.5		1050	0.27		276.6
H_2O	831.4		1050	0.51		31.5
Kiln Feed	44059.9		775			428.3
$CaCO_3$	22807.0	228.07	775		31.78	193.5
CaO	8858.1	157.96	775		14.97	63.1
SiO_2	7807.4	129.95	775		38.20	132.5
Al_2O_3	1555.3	15.25	775		30.08	12.2
Fe_2O_3	105.1	0.66	775		33.56	0.6
$MgCO_3$	1329.5	15.77	775		31.92	13.4
MgO	440.8	10.94	775		12.29	3.6
K_20	262.7	2.79	775		27.59	2.1
TiO_2	65.4	0.82	775		18.08	0.4
Rest	828.6	9.84	775		27.39	6.8
Total	101380.9					1342

Output parameters	**Mass Flow Rate (kg/hr)**	**Molar Flow Rate (Kmol/hr)**	**T in °C**	**Cp (kcal/Kg°C)**	**Cp (cal/mol°C)**	**Heat flow (kcal/kg clinker)**
Hot meal (excluding coal ash)	36229.3		892			427.1
$CaCO_3$	6161.4	61.61	892		33.33	63.0
CaO	18179.6	324.19	892		15.60	155.3
$MgCO_3$	359.2	4.26	892		32.83	4.3
MgO	904.7	22.45	892		12.46	8.6
SiO_2	7807.4	129.95	892		42.83	169.9
Al_2O_3	1555.3	15.25	892		30.47	14.3
Fe_2O_3	105.1	0.66	892		33.77	0.7
K_20	262.7	2.79	892		28.81	2.5
TiO_2	65.4	0.82	892		18.21	0.5
Rest	828.6	9.84	892		26.87	8.1
Ash	110.1		892	0.2		1.2
dH $CaCO_3$						326.3
dH $MgCO_3$						13.6
Water Evap						50.1
Flue Gas						563.2
CO_2	22524.5		900	0.267		185.3
O_2	868.7		900	0.245		6.5
N_2	40038.2		900	0.264		325.1
SO_2	189.2		900	13.30		1.2
Radiation						5.4
Total	101381					1342

The thermal energy requirement from petcoke combustion and its sensible heat is 463.80 + 0.50 = 464.30 kcal/kg clinker as given in Table 5.16. Similarly, material and energy balances have been established for 8% and 15% TSR cases keeping the total thermal energy input requirement fixed at 464.30 kcal/kg clinker. The schematic diagram of material and energy balance for different TSRs are shown in Fig 5.47, Fig 5.48, and Fig. 5.49, respectively.

Table 5.17 Coefficients of specific heat values for the empirical equation

Species	**a**	**b**	**c**	**Temp (°C)**	**Ref**
$CaCO_3$	19.68	0.01189	307600	775	[177]
CaO	10	0.00484	108000	775	[177]
Petcoke	0.262	390	-	50	[216]
Tertiary air	0.237	23	-	267	[216]
Kiln exit gas	0.196	0.000118	-43	1050	[216]
Fuel conveying air	0.237	23	-	60	[216]

5.3.2.3.1 The technical performance of the system

The system's technical performance has been evaluated for an overall TSR of a maximum of 15-20%, which is satisfactory for a white cement plant at the initial stage of operation. Figs. 5.48 and 5.49 show the mass and energy balance for the system at 8% and 15% TSR using producer gas with 100% petcoke firing as a baseline scenario (Fig. 5.47). The results demonstrate the advantages of producer gas utilization in the white cement plant calciner. In the gasifier, the RDF with LHV of 14.36 MJ/kg gets converted to producer gas with an LHV of 3.63 MJ/Nm^3 with a cold gas efficiency of 59.62% and gas yield of 2.36 Nm^3/kg RDF. The producer gas temperature entering the calciner is 593°C. The higher ash in RDF reduces the gas yield and cold gas efficiency.

In the pyro-processing system, since there is no change in kiln firing and the degree of calcination is kept constant for all the cases, it is envisaged that kiln gas and tertiary air quantity entering the calciner remains consistent. However, there will be a reduction in transport air for petcoke by 37% as petcoke amount reduces at high TSR, which correspondingly decreases its sensible heat input. The petcoke quantity entering the calciner at 50°C reduces from 1383.38 kg/hr to 1085.5 kg/hr while producer gas quantity increases from 2441.7 kg/hr to 4735.32 kg/hr at 593°C as TSR increased from 8 to 15%. Thus, it can be inferred that at 15% TSR, 2.7% TSR contribution is from sensible heat, and the rest is from the heating value of producer gas. It brings a new dimension to the TSR term, where earlier, only the heating value of fuel is considered for combustion.

Cement production is never associated with solid waste generation, as ash forms part of the clinker matrix. However, gasifier operation generates solid residual ash. The ash generated is calculated to be 0.39 kg /kg RDF. However, the ash quantity increased by ~94% at 15% TSR. For that purpose, a proper ash management system must be installed, which has been discussed in the next chapter in section 6.4. The residual ash obtained from the gasifier bottom can be utilized as an alternative raw material for grey cement [217].

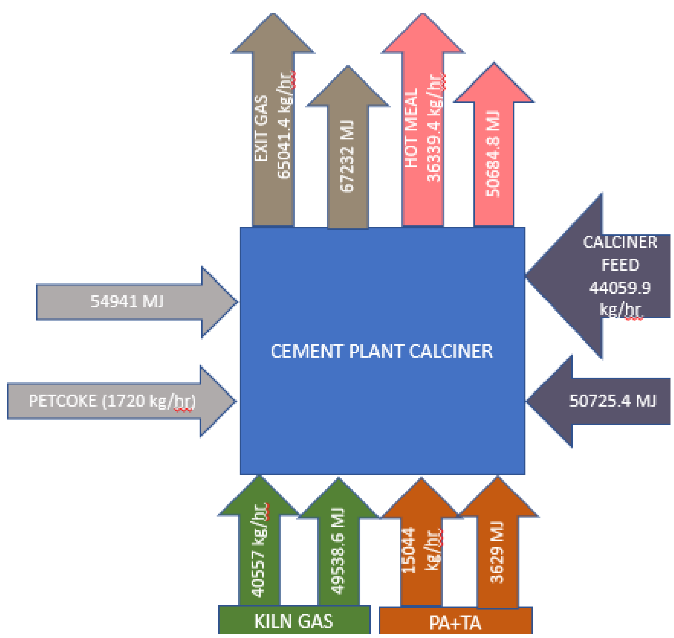

Fig. 5.47 Schematic of mass & energy balance for calciner at baseline scenario (100% petcoke)

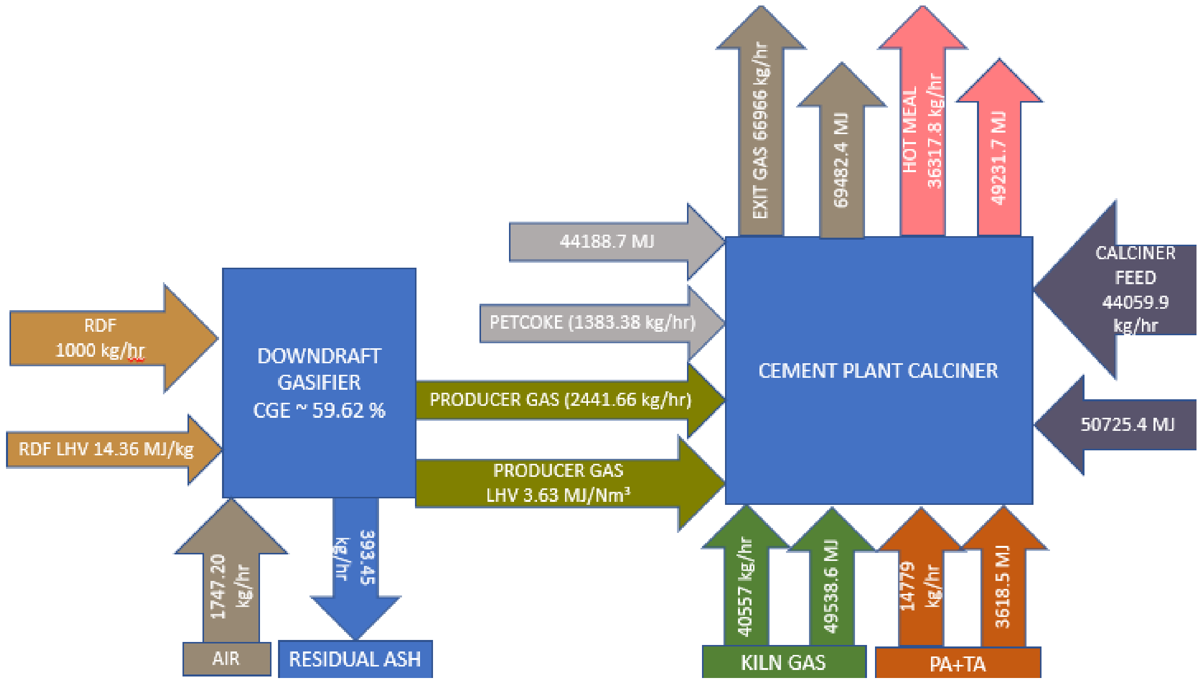

Fig. 5.48 Schematic of mass and energy balance for calciner at 8% TSR

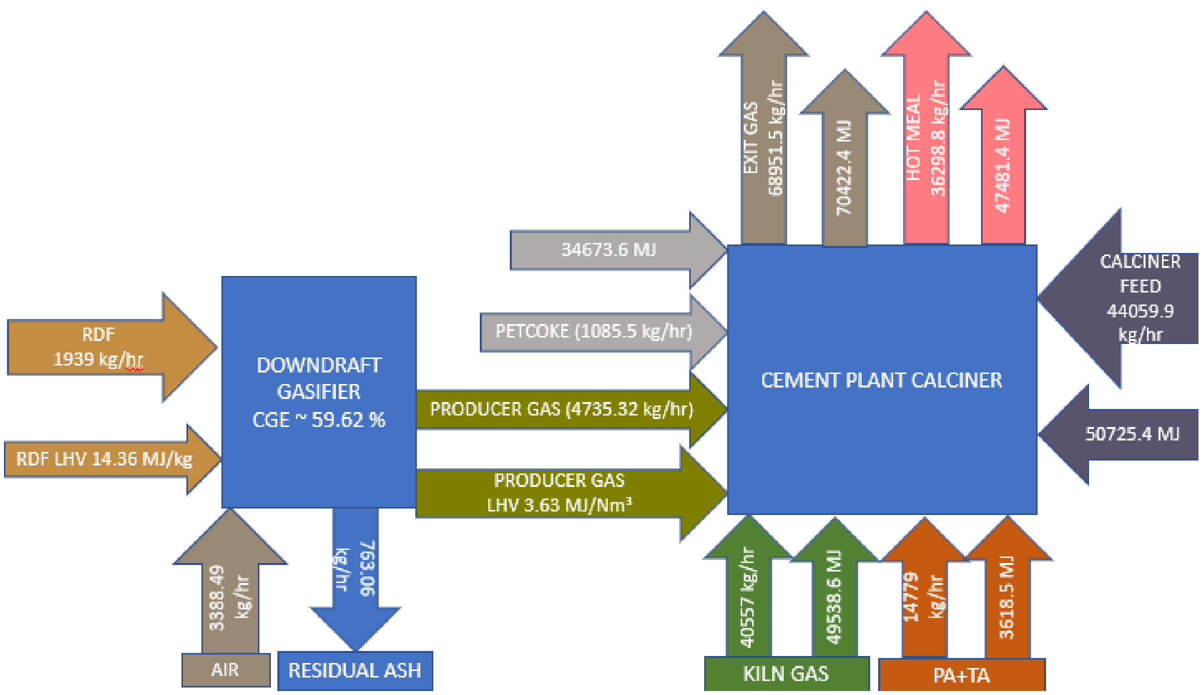

Fig. 5.49 Schematic of mass and energy balance for calciner at 15% TSR

The thermal performance comparison of the calcination system for TSR of 8.5 and 15% with baseline scenario (100% petcoke) have been illustrated in Table 5.19. It is indicative that the calciner outlet temperature decreased from 892 to 866°C at 15% TSR using producer gas. The decrease in temperature is primarily due to the rise of %N_2 in the calciner as producer gas entering the calciner has 60% N_2 by volume. The calciner outlet gas volume increases by 8.0% at 15% TSR due to the contribution of 0.02 Nm^3/kg clinker volume from the producer gas stream. It will lead to enhanced volume at the preheater exit, manageable by impeller tipping. However, the preheater fan power will increase by 26% for a corresponding increase in gas volume as per the fan law (for every 1% increase in fan flow, there is cubic times increase in fan power). The producer gas sensible heat is 18 to 30 times (corresponding to 8-15% TSR) more than the petcoke as it enters the calciner at 593°C, contributing to TSR.

Calciner outlet CO_2

The major benefit of producer gas is the reduction in carbon footprint due to the replacement of petcoke. Primarily the CO_2 emissions are due to limestone calcination and fuel combustion. The CO_2 generation due to the calcination does not change with TSR, as the degree of calcination is constant in the calciner model. The CO_2 obtained at the calciner outlet reduced from 796 to 791 kg/t clinker with an increase in TSR from 0 to 15%. The heat supplied by the producer gas hydrogen content leads to reduced CO_2. However, the producer gas contains 4% CO_2, negating the overall CO_2. The CO_2 mitigation potential is attributed to ~22% of the biogenic content (paper, wood and rubber) in RDF E. It accounts for 10.5% of the baseline scenario at 15% TSR, which is significant.

Calciner outlet SO_2

Considering the environmental impact, introducing producer gas as an alternative fuel will not impact SO_2 emissions since fuel sulphur does not contribute to SO_2 emissions and becomes part of clinker in sulphates form. High sulphur content in petcoke leads to dusty clinker formation and circulation of volatiles in the system. However, producer gas co-processing will decrease SO_2 from 6.69 to 4.22 g/kg clinker and support maintaining the alkali-to-sulphur ratio of 0.8 to 1.2, which is significant for smooth kiln operation.

A detailed analysis of the proposed TSR percentage has been done. The reasons for limiting the overall TSR up to 15% are: a) Generally, in a cement plant, the kiln-to-calciner firing ratio is maintained at around 40:60, while in this plant, it is vice versa. Thus, to achieve an overall TSR of 15%, TSR in calciner is estimated to be around 37% which is a reasonably high TSR considering white cement. Beyond that in, white cement calciner might be challenging. Hence the study limits the TSR to 15%; b) At 15% TSR, the calciner outlet gas volume increases by 8.0%, increasing the volume to be handled by the preheater fan. The preheater fan can handle that excess volume by impeller tipping. However, if the overall TSR is further raised to 20% with a corresponding ~50% TSR in the calciner, the preheater fan volume increases by 14.5%, which needs fan replacement leading to additional investment. Moreover, further TSR enhancement significantly drops calciner outlet temperature, affecting the degree of calcination and clinker manufacturing process.

Table 5.18 Calciner performance at different TSR

Fuel (% of thermal energy)	Calciner outlet temp (°C)	SO_2 at calciner outlet (g/kg clinker)	CO_2 at calciner outlet (kg/t clinker)	Calciner outlet gas volume (Nm^3/kg clinker)
100% Petcoke	892	6.69	796	1.62
92% Petcoke and 8% producer gas	886	5.40	793	1.69
85% Petcoke and 15% producer gas	866	4.25	791	1.75

5.3.2.4 Calciner Aspen Plus model

As explained in section 4.1.3 of Chapter 4, Aspen plus-based calciner model was developed to predict calciner outlet parameters using producer gas as an alternative fuel for a white cement plant. The model validation is shown in the below section.

5.3.2.4.1 Model validation

The plant data used for the validation of both models is the same. Fig. 5.50 and Fig. 5.51 represent the validation of the Aspen Plus model predicted gas composition and flow rates with plant operating data. Regarding calciner outlet gas composition, the modelled CO_2 and O_2 values are 3.67% and 0.56% lower than plant data, while the N_2 values are comparatively higher than 4.24%. The hot meal flow rate fits close to plant data with an error of 0.72%. As per the model, the calciner outlet gas flow is higher than plant data, with an error percentage of 5.16%. RMS error for calciner outlet gas composition (dry basis) is 2.82. The predicted calciner outlet temperature is 32°C higher than the actual plant data. All C has been assumed to be converted to $CO_{2;}$ hence CO is not part of the simulation.

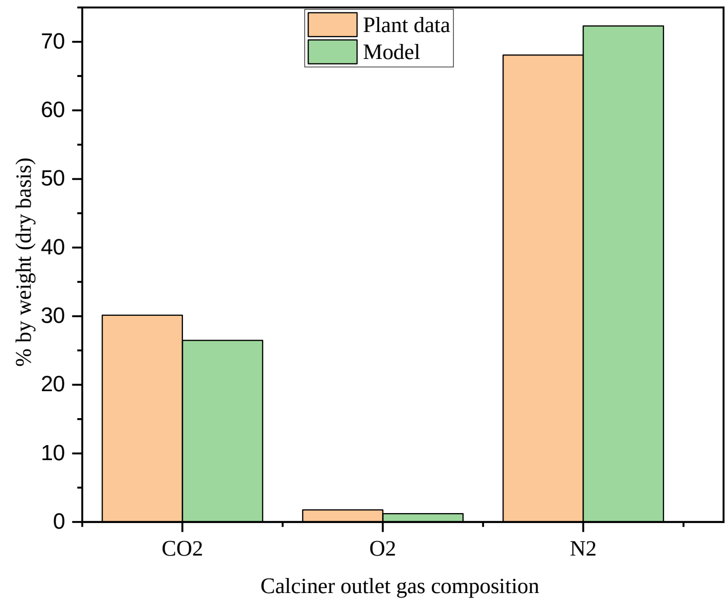

Fig. 5.50 Validation of Aspen Plus model predicted calciner outlet gas composition

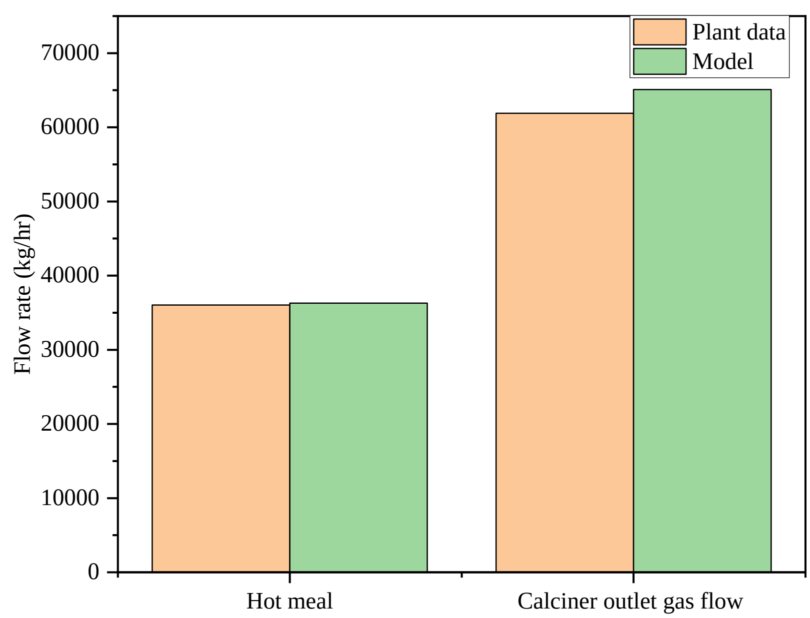

Fig. 5.51 Validation of Aspen Plus model predicted calciner outlet flow rates

5.3.2.4.2 Simulation results and discussions

Calciner operational performance at different TSRs is evaluated in terms of calciner outlet temperature, CO_2, SO_2 and calciner outlet gas volume, as mentioned in Table 5.19.

Table 5.19 Results of the simulation

Fuel (% of thermal energy)	**Calciner outlet temp (°C)**	**SO_2 at calciner outlet (g/kg clinker)**	**CO_2 at calciner outlet (kg/t clinker)**	**Calciner outlet gas volume (Nm^3/kg clinker)**
100% Petcoke	897	3.68	814	1.61
92% Petcoke and 8% producer gas	876	2.96	807	1.68
85% Petcoke and 15% producer gas	863	2.32	802	1.75

Calciner outlet temperature

Calciner outlet temperature reduces from 897 to 863°C at 15% TSR due to increased N_2 content in producer gas.

CO_2 emission

It can be inferred from Table 5.19 that CO_2 at the calciner outlet reduced from 814 to meagre 802 kg/t clinker with an increase in TSR from 0 to 15%. However, considering biogenic content, CO_2 mitigation potential accounts for 10.5% of the baseline scenario at 15% TSR, similar to the other calciner model since all parameters are the same.

Calciner exit gas volume

Table 5.19 shows the effect of increasing TSR from 8 to 15% on calciner exit gas volume, impacting preheater exit gas volume. Calciner exit gas volume rises by 4% and 7%, respectively, at 8 and 15% TSR compared to the baseline scenario. The significant contribution to gas volume rise is H_2O and O_2. H_2O content increases with TSR due to the rise in producer gas content having H_2O component and conversion of H_2 present in the producer gas to H_2O. Excess O_2 content increases with TSR since producer gas requires less O_2 than petcoke combustion.

In white cement production, preheater exit gases are used to preheat ambient air, which becomes part of combustion air later in the calciner and kiln. Thus, an increase in preheater exit gas volume by 7% (due to a change in calciner exit gas volume) and a reduction in preheater exit gas temperature by 2.38% at 15% TSR will not affect combustion performance in calciner and kiln considering waste heat recovery from preheater exit gases in operation.

Further, an impact assessment study for calciner is conducted for varying RDF moisture on gasifier and producer gas temperature.

Impact of moisture content

High RDF moisture is a major issue the cement industry faces during direct RDF combustion. Fig. 5.52 represents the change in heat value and producer gas temperature concerning the increase in RDF moisture. RDF moisture as part of producer gas will directly influence the combustion in the calciner. Hence, the first step is determining the impact of varying RDF moisture from 5 to 20% on producer gas heat value (MJ/Nm^3) and reduction zone temperature (°C). It can be seen that LHV decreases from 3.58 to 3.24 $MJ/Nm^{3,}$ and producer gas temperature decreases from 590 to 578 °C with the increase in RDF moisture content from 5 to 20%.

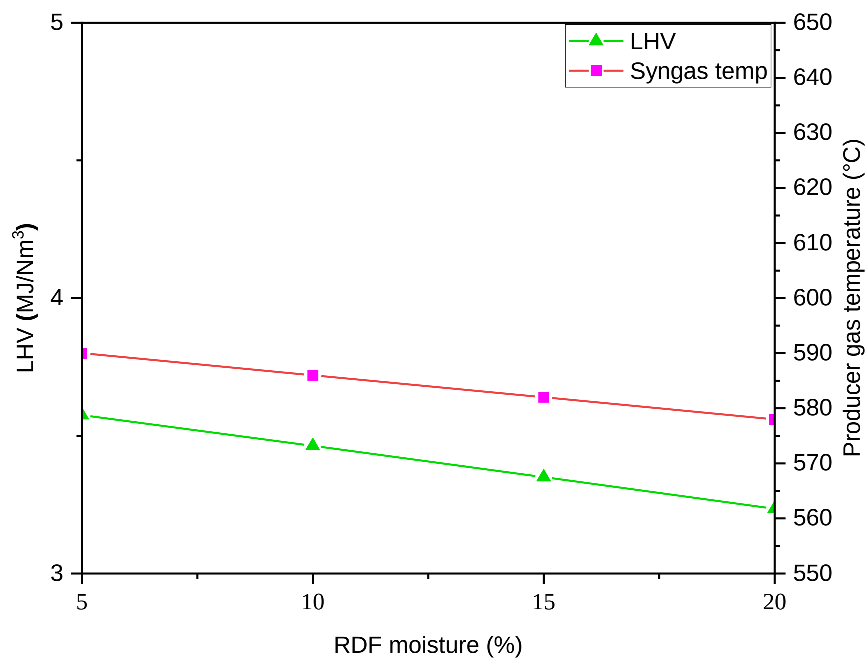

Fig. 5.52 Variation in LHV and producer gas temperature with% RDF moisture

At 8% TSR with 5% and 20% producer gas moisture, there is minimal impact on calciner outlet temperature and heat released for combustion. However, at 15% TSR, calciner outlet temperature drops by 3.5°C and 16.5°C with 5% and 20% producer gas moisture, respectively. Further, the heat released during combustion (Q3) decreases by 3.24% and 16.98%, respectively, for 5% and 20% producer gas moisture at 15% TSR. It indicates the negative impact of high moisture at high TSR.

Impact of producer gas temperature sensib

The producer gas temperature at the calciner inlet is 593°C as per the gasifier model. It may vary depending on the input conditions of the gasifier, reduction zone length and equivalence ratio. Fig. 5.53 depicts the calciner outlet temperature and Q3 for varying producer gas temperatures of 500-700°C at 8% and 15% TSR.

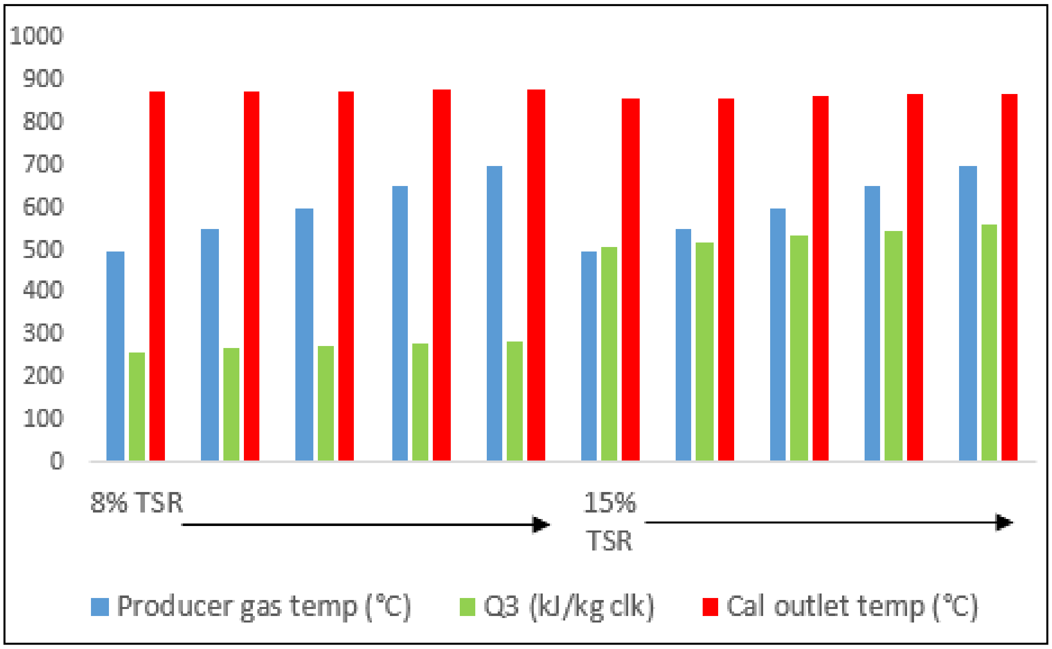

Fig. 5.53 Prediction of calciner outlet temperature and Q3 at varying producer gas temperature for 8% and 15% TSR

The results indicated a marginal increase in calciner outlet temperature by 6°C at 8% TSR if the producer gas temperature raised from 500 to 700°C. However, in the 15% TSR case, the calciner outlet temperature increased by 11°C. For the producer gas temperature range of 500-700°C, the heat released during producer gas combustion (Q3) increased by 9.90% and 10.10% for 8% TSR and 15% TSR, respectively. The producer gas temperature at the calciner inlet can be improved further if air input at ambient temperature to the gasifier is heated by waste heat available in the cement plant, which can be considered as direct fuel savings. One of the unutilized heat sources is kiln radiation, which can be tapped to raise the producer gas temperature, particularly in a white cement plant where kiln radiation losses are 4 to 5 times higher than grey cement. Mittal and Rakshit [218] highlighted the usage of kiln radiation heat for solar thermal calcination of phosphogypsum in a cement plant. White cement plants generally have kiln bypass systems. Cleaned kiln bypass gases (if available) at around 1000°C can also be utilized for process heating in the future.

5.3.3 Comparison of calciner models

The two calciner models have different approaches to predict calciner outlet parameters. The stoichiometric model uses combustion equations and calcination reactions to perform material and energy balance. Combustion and calcination are combined in a single reactor. However, Aspen Plus model splits the combustion and calcination into two different processes having dedicated reactors in Aspen Plus. Gibbs free energy minimisation is the driving force for combustion reactor. Fig. 5.54 represents the comparison of calciner models for % change in key parameters like calciner outlet temperature, specific gas volume, CO_2 and SO_2 with respect to the baseline scenario. It can be seen that predictions for all key parameters by both models at 15% TSR are matching. The calciner outlet gas volume is estimated to increase by 8% by both models compared to the baseline scenario. The percentage change in CO_2 estimated at 15% TSR by the stoichiometric model is 0.63% and 1.58% by the Aspen Plus model, which is comparable. SO_2 prediction is also quite similar in both models. However, the calciner outlet temperature predicted by the stoichiometric model for baseline scenario validation is 892°C, closer to the actual 865°C than the Aspen Plus model value of 897°C. ***Thus, the stoichiometric model has been considered further for economic analysis of RDF gasification in a white cement plant.***

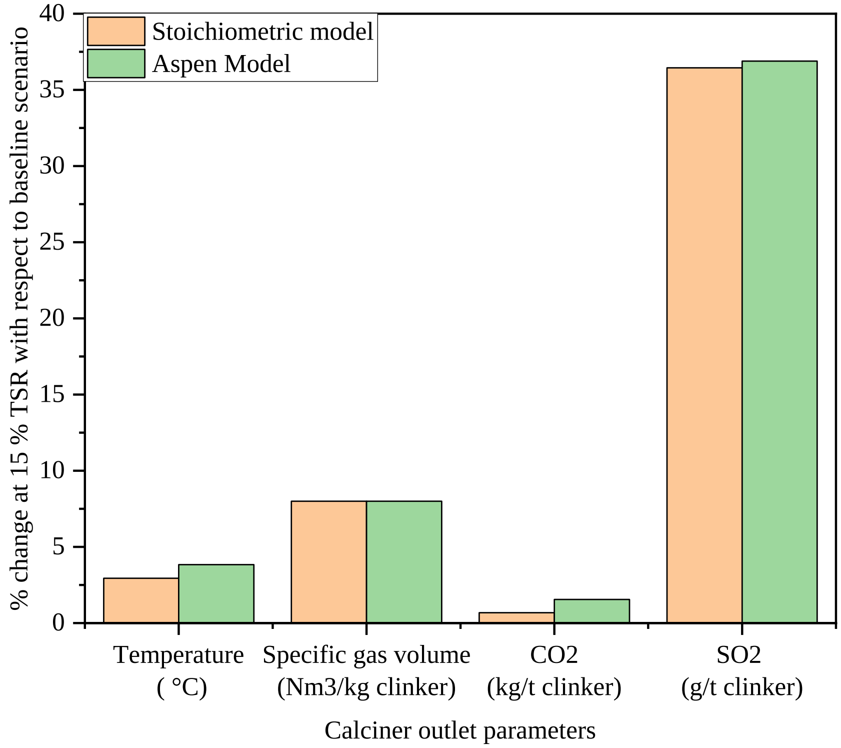

Fig. 5.54 Comparison of stoichiometric and Aspen Plus models

CHAPTER – 6

ECONOMIC FEASIBILITY OF RDF GASIFICATION FOR A WHITE CEMENT PLANT

This chapter covers the gasification potential and economic feasibility of RDF gasification in a white cement plant in India. Producer gas obtained from gasification has been considered an alternative fuel in cement plant calciner and co-processed with petcoke to achieve 15% TSR. The indicators used in economic feasibility analysis are discounted payback period, cash flow analysis, net present value (NPV), and internal rate of return (IRR).

6.0 Economic feasibility Study of RDF gasification for a white cement plant

The feasibility study for the RDF gasification is reported in four parts:

1) White cement manufacturing process
2) Energy scenario in white cement and the importance of RDF gasification as an alternative fuel
3) Gasification potential in the white cement industry in India
4) Economic analysis for RDF gasification

6.1 White cement manufacturing process

Biomass, RDF, plastics, sludges, liquid waste, hazardous waste, tyre chips etc., are some of the wastes utilized by cement plants globally. It is easily possible to achieve high TSR in grey cement as multiple options of alternative fuels are available [219]. In calciner, 100% TSR is well achievable with some operational issues. However, there is no established alternative fuel in white cement, so far as there are certain limitations in alternative fuel usage. To understand the limitations, a brief idea of the manufacturing process of white cement in comparison to grey cement is explained.

The basic requirement of white cement is whiteness. The raw materials for producing white cement should be pure and the colouring oxides should be the least. Generally, limestone having low iron content (<0.1%) and other colouring oxides such as Cr_2O_3, TiO_2 are the primary raw materials for white cement production [220]. There is no such constraint for grey cement. The raw meal having limestone and correctives are sent to the pyro-processing section, which undergoes preheating, calcination, clinkerisation, and cooling. The process of preheating and calcination of white cement is similar to grey cement production. However, the clinkerisation and cooling process technology is different. The sintering of the hot meal is difficult in the kiln due to the low flux percentage and some fluxes like fluorspar are added. Hence, the kiln burner creates a short and intense flame, leading to high shell radiation losses, high refractory and fuel consumption. Coal ash can tarnish whiteness; hence the fuel-fired in white cement kiln/calciner is usually fuel oil or gas or low ash solid fuels like petcoke. A heat exchanger is used to preheat the atmospheric air using the kiln preheater exhaust gases. This preheated air is used for combustion in the calciner as tertiary air and in the kiln as secondary air. Cooling the white cement clinker is a specialized process entirely different from grey cement. The cooling of white clinker takes place by water spray jet while air quenching is done for grey clinker. Due to the absence of air, the complete oxidation of colouring elements like Fe, Cr, Mn, Ti, Co, etc., is prevented. Further, the cooled white cement clinker is interground with gypsum and other additives to prepare white cement. Fig 6.1 represents the schematic diagram of the pyro-processing section of a white cement plant.

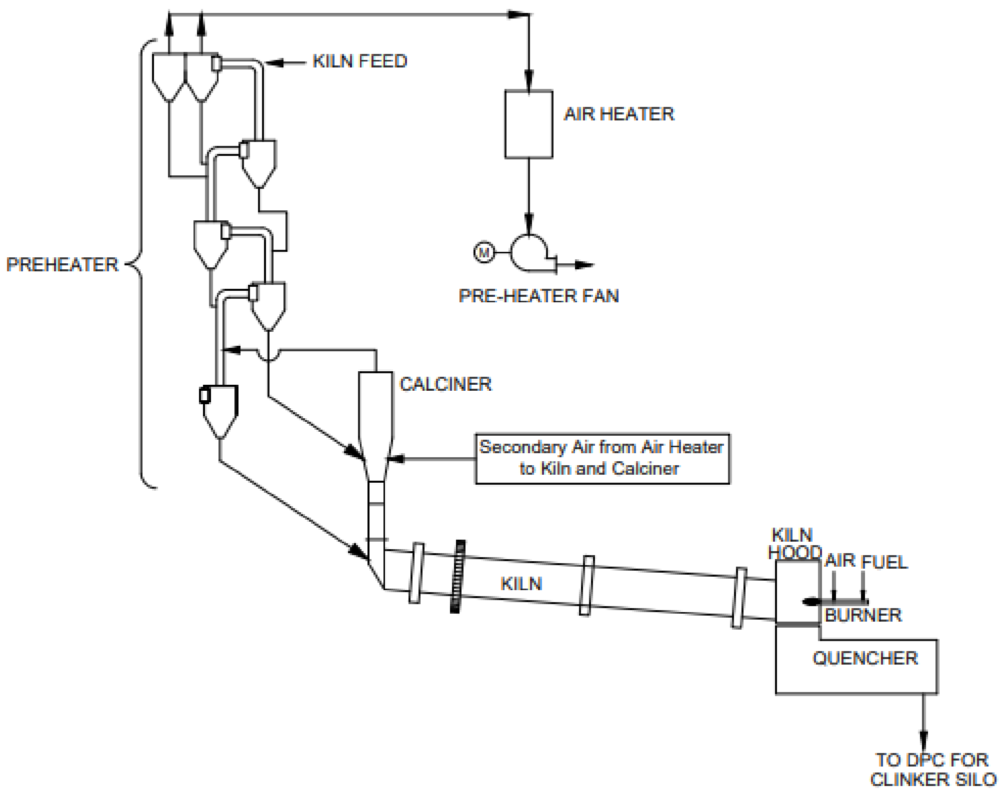

Fig. 6.1 Schematic of pyro processing section for white cement

6.2 Energy scenario in white cement and the importance of alternative fuel

White cement production globally is less than 1% of the total installed capacity [1, 221], but its specific heat consumption is 40-50% higher than grey cement. M/s JK White Cement in India has a specific energy consumption of 4 MJ/kg clinker with a mixture of 90% petcoke and

10% lignite. It is substantially higher than the normal operating range of 2.93-3.14 MJ/kg clinker for a grey cement plant [222]. Hence, white cement production corresponds to more fuel savings for the same% TSR for a grey cement plant having the same capacity [222]. Cementir Holding group, one of the leading white cement producers globally, has replaced only 3% of fossil fuel by AF in white cement in 2020 due to consistent cement colour demand and has set a target of 6% by 2030. Few alternative fuels are used in white cement: meat, bone meal, and TDI (toluene di-isocyanate) tar. Meat and bone meal have high phosphate content, improving white cement's reflectance [223]. In India, meat and bone meal are mainly used as poultry feed and fertilizer. Thus, its availability as fuel is uncertain. Moreover, there is a social stigma to utilizing MBM as an alternative fuel for cement production. Any other solid alternative fuel like RDF, rice husk, and tyre chips having high ash content is detrimental to the clinker quality due to the presence of clinker phase C_4AF which imparts colour to the cement [224]. Limestone and fuel ash are sources of iron in the clinker. Iron content in limestone is controlled by selecting the type of limestone, but ash-free conventional/alternative fuel ash remains a challenge. The problem is aggravated by a shortage of petcoke, leading to its import at higher prices. The petcoke, which was earlier available to white cement plants, is being utilized to produce value-added products via the gasification route by one of the leading refineries [225]. Thus, an alternative fuel for white cement is the need of the hour, which drives a novel idea of integrating gasification of high ash fuel like RDF resulting in minimal ash in clinker, which impacts the clinker quality.

6.3 Gasification potential in the white cement industry in India

Petcoke prices have risen steeply recently, and the white cement industry is looking for alternative fuel options to substitute it. One novel solution proposed is the gasification of RDF, which provides a consistent fuel in terms of producer gas without ash contamination. The availability of RDF in the vicinity of white cement plants will be the key to determining the potential of producer gas utilization in the Indian white cement industry. Two white cement plants in India are located in the state of Rajasthan. Table 6.1 shows the RDF gasification potential for the white cement industry in India. It is indicative that RDF availability in the state will not be an issue for gasification purposes to achieve 15% TSR.

Table 6.1 RDF gasification potential for the white cement industry [16, 226]

Parameter	**Value**	**Unit**
MSW generation expected by 2031	165	MTPA
RDF generation	24.75	MTPA
Availability of RDF for the cement industry	12.38	MTPA
White cement production	1.07	MTPA
RDF requirement for 15% TSR using producer gas from RDF gasification	0.08	MTPA
RDF availability in Rajasthan	0.66	MTPA

6.4 Economic analysis

The key objective is to look out for the economic feasibility of co-processing producer gas derived from RDF gasification. The indicators used in economic feasibility analysis are discounted payback period, cash flow analysis, net present value (NPV), and internal rate of return (IRR). NPV and IRR are standardized financial tools to assess the economic viability of projects. High IRR and an NPV greater than zero lead to an economically attractive option. The net present value method quantifies the impact of time on any particular future cash flow.

Each future cash flow is equated to its current value today, which means determining the present value of any future cash flow. An interest rate known as the discount rate determines the present value (PV). Thus, the current value of money at any specified time in the future is determined by the following Eq. (6.1).

$$PV = A \cdot \left(1 + \frac{DR}{100}\right)^{-n} \tag{6.1}$$

PV is the present value of A in n years, DR is the discount rate, and A is the cash flow (difference between revenue and expenditure) in n years. The net present value is the summation of the current value of all yearly cash flows. The IRR is calculated as the discount rate that equals the NPV to Rs 0.00 [227].

6.4.1 General assumptions

Considering the vintage of the plant, ten years of operation have been considered for savings calculation. A cement plant operates 24 hours per day continuously with 330 days per annum due to the shutdown period of 35 days for maintenance [228], and the same has been considered. It is assumed that the gasifier system shall be installed close to the pyro-processing system, where petcoke fuel can be substituted easily. It is presumed that RDF will be consistently available around the year to feed the gasifier and generate producer gas. The fuel price escalation of 5% yearly has been considered based on year-on-year (YoY) escalation in the recent past [229]. Two years moratorium period can be availed for loan repayment as prescribed by the Ministry of Power, Government of India which has been considered for financial analysis. The interest rate for loan repayment has been considered as 10% based on the economic model proposed by the Ministry of housing and urban affairs, Government of India, for such projects [16]. The debt to equity ratio is taken 50% as means of finance.

Depreciation is calculated using the straight-line method [230]. The Consumer Price Index (CPI) inflation is taken as 6% on average, considering the consumer price index (CPI) of 2021 and 2022 for the Indian cement industry [229]. The initial capital investment has been considered for 8% TSR in Phase I; after two years, additional capital shall be infused in Phase II to achieve 15% TSR. An MS excel model has been developed to evaluate the economic performance.

6.4.2 Capital costs

In this work, the total capital investment for downdraft gasifier installation has been discussed in detail. Tables 6.2a and 6.2b represent capital cost estimates. Table 6.2b indicates the capital cost as a factor of fixed capital investment. The costs and budgets were obtained from the machinery suppliers. The capital cost for a 150 kg/hr downdraft gasification unit has been obtained from the leading gasifier supplier in India. The cost has been scaled up for 1000 kg/hr gasification unit using the relationship between cost and scale as per Eq. (6.2).

$$\frac{C}{Ca} = \left(\frac{S}{Sa}\right)^{n} \tag{6.2}$$

where C is the cost of 1000 kg/hr proposed plant after scale-up, C_a is the cost of the reference plant at scale S_a (150 kg/hr), and n is the scale-up exponent [230]. The scale-up exponent, n, is usually in the range of 0.6–0.8 and is 0.6, which is the standard proportionality coefficient for scale economies used in manufacturing processes.

The total capital infusion of Rs 71.6 million is split into parts; Rs 51.6 million initially in Phase I and Rs 20 million in Phase II after two years. The investment costs include laboratory facilities, utility installation (compressed air), civil construction, automation and control, engineering projects, and other services. No land cost has been considered since the land will be available within the existing plant premises.

The total capital investment reported in the study is fixed capital investment only, which is the sum of direct and indirect plant costs. Direct plant cost covers equipment, piping, electrical, instrumentation and control, civil work, and service facilities installed at the site. Civil work includes a storage shed for RDF pellets, gasifiers foundation, hoppers foundation, and support to pipe connection to calciner. Indirect plant costs include engineering and supervision, construction expenses, legal expenses, contractor fees, and contingency. Equipment cost covers gasifier setup cost and mechanical auxiliary equipment, including hoppers, flexible belt conveyors, needle gates, and steel for duct. Ducting/chute and conveyors cost is based upon the complete ducting length installation at the site as per the general arrangement drawing.

Table 6.2a Capital cost estimates

S. No.	Description	Total Cost (Rs million)
1	Land and site development	2.5
2	Civil works and structures	13.6
3	Plant and machinery	32.9
4	Engineering & know-how along with expenses on training	4.0
5	Miscellaneous Fixed Assets (MFA)	14.0
6	Contingency	4.6
	Total Project Cost	71.6

Table 6.2b Capital cost estimates as% of fixed capital investment (FCI)

Component cost	**% of FCI**
Direct plant costs (DPC)	
Equipment cost	34.81
Piping	2.79
Electrical	3.49
Instrumentation and control	4.89
Civil work	18.96
Service facilities (installed)	13.97
Total DPC	78.91
Indirect plant cost (IPC)	
Engineering and supervision	5.59
Construction expenses	3.49
Legal expenses	2.79
Contingency	6.43
Contractor fee	2.79
Total IPC	21.09
Total direct and indirect cost	100

6.4.3 Operating costs

Fuel, electricity, maintenance, and manpower are part of the operating costs involved in co-processing the cement plant's producer gas, which is discussed below.

6.4.3.1 Fuel

Co-processing of RDF-based producer gas and petcoke is required for smooth plant operation. After discussion with the local RDF suppliers and considering the current market scenario, a lumpsum landed cost of Rs 0.00053/kJ for RDF pellet is envisaged for costing purposes. The present landed cost of petcoke is Rs 0.00069/kJ, as reported by the cement plant.

6.4.3.2 Utility

Utility costs include electricity and compressed air usage in the plant. This work requires electricity to meet compressed air requirements for gasifier operation, RDF handling, ash conveying system, and office/laboratory usage. The cement plant's existing power distribution system shall meet the electricity requirement. RDF gasification requires additional power of 10 kWh/tonne RDF for compressed air, RDF conveying, and ash disposal systems.

6.4.3.3 Manpower

A control room operator will be required to operate the gasifier on a shift basis, and one person shall be deputed at the site to manage RDF pellet handling. The initial salary has been considered Rs 19765 per month per person [231], according to the wages notification issued by the Ministry of Labour& Employment, Government of India. The annual increment of 5% in salary is considered.

6.4.3.4 Plant maintenance

The annual maintenance cost, including insurance, taxes, etc., is 5% of the total capital investment in line with previous comparable work [163].

6.4.4 Projected revenues

The income generated from petcoke usage savings, operating power cost reduction due to less petcoke grinding, BEE PAT scheme savings, and revenue from ash sales will be part of the annual cash flow.

6.4.4.1 Fuel savings

The difference in fuel cost leads to significant fuel savings, i.e., 2.8 times within ten years considering producer gas yield of 2.36 Nm^3/kg RDF and RDF cost of Rs 4500/tonne [232] considering the current market scenario.

6.4.4.2 Power savings

At 8% and 15% TSR, petcoke consumption shall be 1.38 tonnes/hr and 1.09 tonnes/hr, respectively. The corresponding grinding power consumed shall be 55.3 kW and 43.4 kW at 40 kWh/tonne petcoke of specific power. It leads to power savings of 3.5 kW and 6.0 kW at 8% and 15% TSR, respectively, compared to the baseline scenario.

6.4.4.3 Savings under the Bureau of Energy Efficiency-Perform Achieve and Trade (BEE-PAT) scheme

BEE under Govt. of India started a PAT program that was key in promoting energy efficiency in the cement industry. The cement sector was given energy targets under different PAT cycles for three years. The Indian cement industry achieved 82% and 48% higher than the target figure compared to the baseline year for PAT cycle one and PAT cycle two, respectively, which is commendable [233]. According to the BEE-PAT scheme, thermal energy from alternative fuel replacing conventional fuel for clinker production will not be considered for specific fuel consumption. Thus, if a cement plant overachieved fuel savings than the target given, it can be traded in terms of an Energy Saving Certificate (ESCert) after every three years. ESCert is a certificate issued by the Bureau of Energy Efficiency (BEE) for every metric ton of oil equivalent energy saving achieved by the cement plant over and above the targets set in PAT Cycle. The value of ESCert considered for calculation purposes is Rs 1840/tonne, the base price for ESCerts bidding in PAT Cycle II in 2023 [234, 235].

6.4.4.4 Revenue from ash sales

Ash obtained from the bottom of the gasifier shall be collected through a screw conveyor arrangement and sent to nearby grey cement plants to utilize as alternative raw material. The ash selling cost comparable to CPP bottom ash, excluding transportation, has been considered Rs 200/tonne [236].

6.5 Process design

The simulation results form the basis for developing the proposed calciner and gasifier system integration process design. In the present study, it is suggested to achieve 15% TSR through producer gas utilization capacity in two phases. It is due to the uncertainty of the alternate fuel supply and the inexperience in operating the cement plant with gaseous fuel. It is decided to consider 8% TSR during phase I (three years). The operational experience of phase I will help the designer to moderate the gasification system design if required. It is envisaged to achieve 15% TSR during the next seven years of plant operation (phase II).

Calciner outlet parameters, producer gas quantity, heating value, producer gas composition, ash quantity generated, and RDF requirement are established for 8% and 15% TSR, respectively, as discussed in Chapter 5. Two gasifiers of 1 tonne per hour RDF feeding capacity each are envisaged to operate at 15% TSR. Further, all main machinery and storage capacities are determined for the RDF gasification system. It is envisaged that the RDF pellets shall be procured by the cement plant from an RDF preparation facility through trucks. RDF shall be stored in a storage shed of 500 m^3 capacity considering three days of storage. RDF from the storage shed shall be transported to two nos. respective hoppers of 5 m^3 capacity each. Further, RDF from the hopper is sent to the respective gasifier through a flexible conveying system. The flexible conveying system has to feed the gasifier at the rate of 1 tonnes/hr. Thus, 1.2 tonnes/hr conveying capacity is chosen, considering a 20% design margin. The gasifiers shall be connected to the calciner through pipes. Residual ash from the gasifier bottom is collected in an underground pit through a screw conveying system. Each pit has a capacity of 125 m^3 and can store 70 tonnes ash. The flowsheet for the proposed plan with equipment design specifications for 15% TSR is shown in Fig. 6.2. Gasifier dimensions have been calculated by using Eqs. (6.3-6.5) [237-239].

$$SGR = FCR/Ar \quad (6.3)$$

$$Dr = 1130Gm/q \quad (6.4)$$

$$H = Dr + 1.5Dr \quad (6.5)$$

SGR and FCR are specific gasification and fuel consumption rates, respectively. SGR for RDF pellets is taken as 200 kg/m^2.hr, and FCR is 1 tonne per hour.

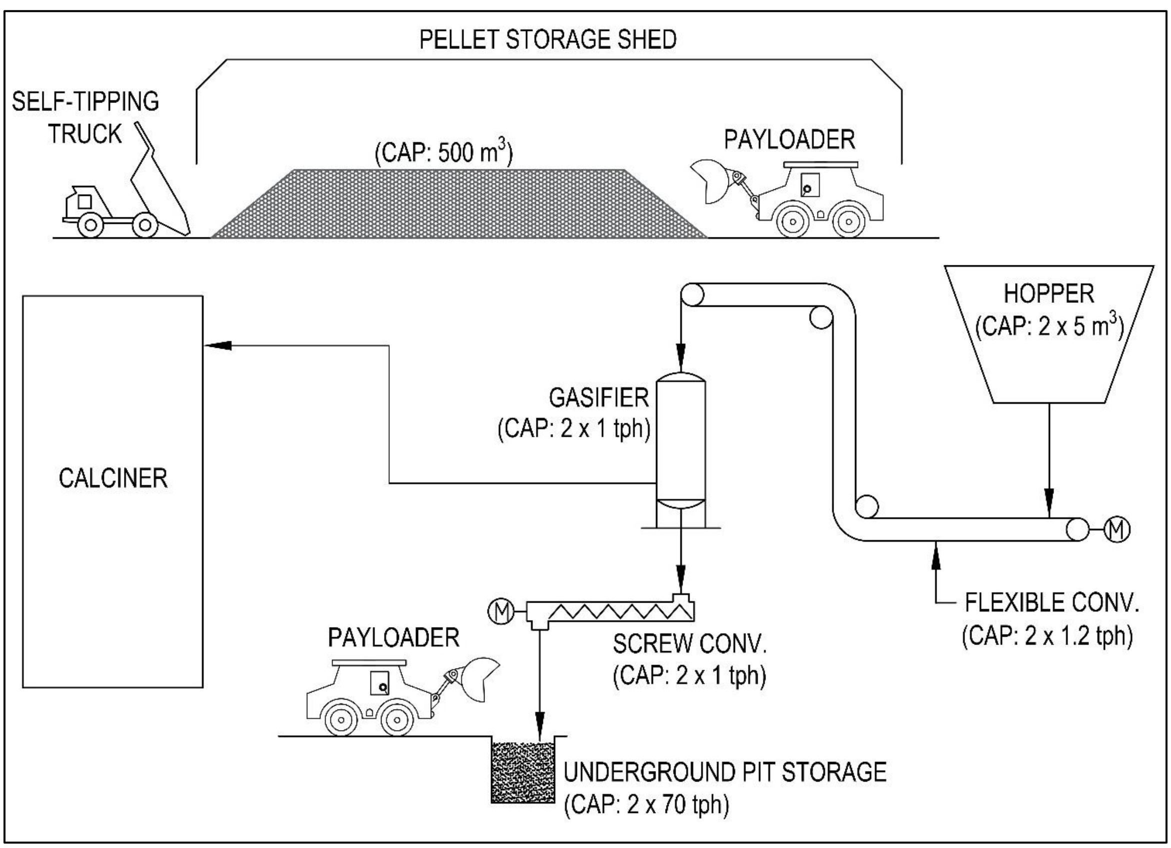

Fig. 6.2 Flowsheet for integration of RDF gasifier to calciner at 15% TSR

6.6 Economic performance of the system

The system's economic performance at 8% and 15% TSR is summarized in Table 6.3. As TSR increased from 8 to 15%, producer gas volume requirement increased manifold from 18.69 million Nm^3/year to 36.25 million Nm^3/year. The total net savings every year is the sum of savings due to the difference in the landed cost of petcoke and producer gas (in terms of Rs/kJ), BEE-PAT benefits, residual ash sales, and savings in grinding power. With the increase in TSR and no of years, net savings increased significantly by 2.9 times from Rs 12.43 million to Rs 36.59 million. Further, net profit is calculated by subtracting fixed costs from net savings. The fixed cost covers salaries, maintenance, depreciation, insurance, and interest on the term loan. It will decrease progressively from 12.94 to 9.85 million in ten years due to a reduction in the interest on the term loan. Earnings before interest, taxes, depreciation, and amortization (EBITDA), calculated by adding depreciation and interest back to net profit predicted to rise by four times in 10 years, is encouraging. For the first three years, EBITDA is Rs 7.65-8.76 million since the TSR is low, which increased to Rs 31.33 million in the next seven years at 15% TSR. It is mainly due to fuel savings attributed to prolonged high conventional fuel prices in the current scenario. 4^{th} and 8^{th} year shows a significant rise in EBITDA due to the revenue generated through the BEE PAT scheme benefits. The discounted payback period is five years and seven months, which is acceptable. It means the cement plant will recover that amount invested in the project in the specific period. It will be followed by the monetary benefits for the next four years and three months, as reflected in EBITDA and IRR. Since all the key financial indicators are within the range of acceptability, the model seems economically viable and can be implemented in the cement plant. The savings will further increase if good quality RDF at reasonable prices is supplied to the cement plant through a long-term agreement.

Table 6.3 Financials Summary Sheet

Parameter	Unit	Years									
		1	**2**	**3**	**4**	**5**	**6**	**7**	**8**	**9**	**10**
TSR	%	8	8	8	15	15	15	15	15	15	15
Producer gas volume (a)	(million Nm^3/yr)	18.69	18.69	18.69	36.25	36.25	36.25	36.25	36.25	36.25	36.25
Producer gas landed cost (b)	Rs/Nm^3	2.00	2.10	2.21	2.32	2.43	2.55	2.68	2.82	2.96	3.11
Producer gas cost, c= (a)·(b)	Rs million	37.42	39.29	41.26	84.01	88.21	92.63	97.26	102.12	107.23	112.59
Savings in petcoke (d)	Rs million	49	52	54	110	116	122	128	134	141	148
BEE-PAT benefits (e)	Rs million	-	-	-	5	-	-	-	9.7	-	-
Residual ash sales (f)	Rs million	0.62	0.62	0.62	1.21	1.21	1.21	1.21	1.21	1.21	1.21
Savings in power (g)	Rs million	0.13	0.13	0.13	0.26	0.26	0.26	0.26	0.26	0.26	0.26
Net savings (d-c+e+f+g)	Rs million	12.43	13.01	13.63	32.68	28.99	30.36	31.81	43.03	34.92	36.59
Salaries & Wages	Rs million	0.48	0.50	0.53	0.56	0.58	0.61	0.64	0.68	0.71	0.74
Repairs & Maintenance	Rs million	3.58	3.58	3.58	3.58	3.58	3.58	3.58	3.58	3.58	3.58
Depreciation	Rs million	4.59	4.59	4.59	4.59	4.59	4.59	4.59	4.59	4.59	4.59
Insurance	Rs million	0.72	0.74	0.76	0.78	0.81	0.83	0.85	0.88	0.91	0.93
Interest on the term loan	Rs million	3.58	3.58	3.28	2.68	2.09	1.49	0.89	0.30	0.00	0.00
Total Fixed Cost	Rs million	12.94	12.99	12.74	12.19	11.64	11.10	10.56	10.02	9.78	9.85

Parameter	**Unit**	**Years**									
		1	**2**	**3**	**4**	**5**	**6**	**7**	**8**	**9**	**10**
Net Profit	Rs million	-0.51	0.03	0.89	20.49	17.34	19.26	21.25	33.00	25.14	26.75
Dep. & Interest	Rs million	8.17	8.17	7.87	7.27	6.68	6.08	5.48	4.89	4.59	4.59
EBITDA	Rs million	7.65	8.19	8.76	27.76	24.02	25.34	26.73	37.89	29.72	31.33
IRR	%	18.30									
Discounted payback	Years	5 years 7 months									

6.6.1 *Cash flow, NPV, and IRR*

A cash flow diagram (Fig. 6.3) is a graphic representation of economic value with time. The benefits are represented as upward arrows, and investment or other costs as downward arrows. Cash flows are of two types, i.e., conventional and unconventional. In the conventional type, the initial cash outflow is followed by a series of cash inflows with only one change in sign-in cash flows. However, the present study follows the unconventional type where there are regular cash inflows and more than one cash outflow with more than one change in sign of cash flows. Zero years on the time coordinate is the beginning point where investment is made and time is taken for construction. The plant operation is envisaged to be started in 1st year and continued to the 10th year. The total investment at zero years and three years is based on cost estimates as tabulated in Table 6.2a and Table 6.2b. The cash position is negative at zero years, and the value is the total capital investment. The initial investment is Rs 51.6 million for one gasifier in Phase I, followed by investment in Phase II for another gasifier after achieving consistent 1st gasifier operation. From 1st year onwards, positive cash flow or revenue is Rs 7.7 million, which increased to Rs 18.6 million in the 10th year of operation. However, only in the 3rd year of operation is the net cash flow negative (Rs 12.2 million) due to the additional investment incurred. Fig. 6.4 shows the relationship between the NPV and IRR for discount rate variation between 10-20%, where lower discount rates offer higher economic performance. The highest NPV is Rs 27 million (point A) at an 10% discount rate. As the rate increases from 10 to 18.3%, NPV decreases to 0 at point B, which corresponds to 18.3% i.e., the IRR of the project by definition. Further increase in the discount rate from 18.3 to 20% will lead to negative values of NPV. The rate of return (interest rate) is 10% which is 8.3% less than IRR. Thus, the project is acceptable under both NPV and IRR evaluation criteria. A 8.3% margin is enough to tackle any uncertainties, including inflation, fuel price rises, etc. IRR variation with several factors has been discussed in the sensitivity analysis section.

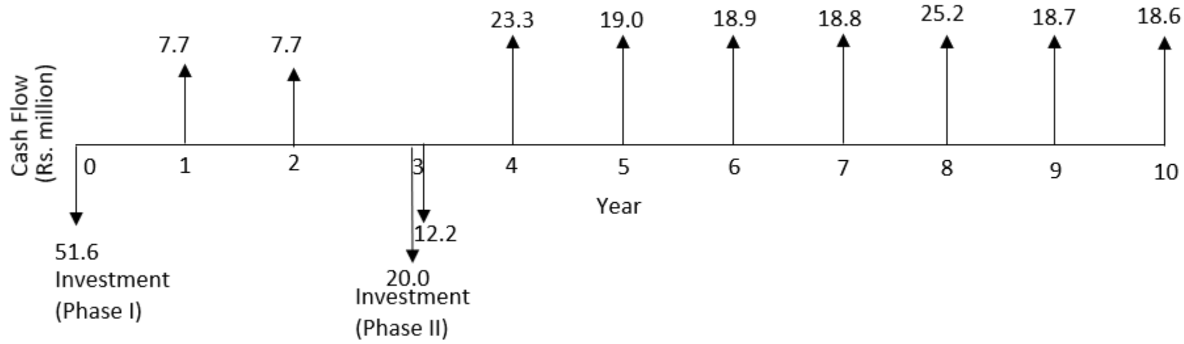

Fig. 6.3 Cash Flow Diagram

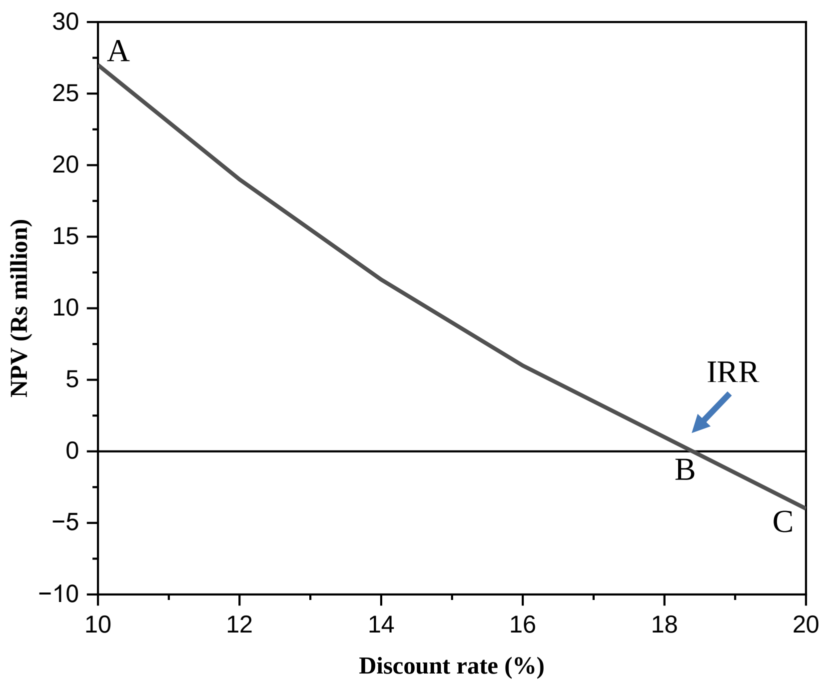

Fig. 6.4 NPV and IRR

6.6.2 Debt-Service Coverage Ratio (DSCR)

DSCR is a measure of the cash flow available to pay current debt. DSCR > 1 means the organization has sufficient income to pay its current debt obligations. In this case, DSCR works out to 4.24, which is attractive.

6.6.3 Sensitivity analysis

The sensitivity analysis is a valuable means of evaluating the model parameters and assumptions by accounting for the uncertainties in the model input parameters. It helps identify the most influential parameters and test the validity of the assumptions taken. The sensitivity analysis for key financial indicators has been discussed below by varying critical parameters by ± 10%. Fig. 6.5a and 6.5b represent the sensitivity analysis for key financial indicators by varying critical parameters by ± 10%. Five different parameters are chosen for sensitivity analysis viz RDF price, producer gas yield, capital cost, operating hours of the gasifier, and ash market.

i. RDF price

Different models of RDF preparation are flourishing in India, and prices vary from state to state. Thus, RDF price is one of the most critical parameters to be analyzed. Changes in waste policies, waste management, and implementation of Swachh Bharat Mission 2.0 are on the cards, which will impact the RDF cost in the future. The RDF price taken in the present study is an average of the prices in different regions. A ±10% variation in RDF price results in ~31% variation in net savings and 9.12 to 10.61% variation in IRR, which will significantly affect the project viability. Hence a long-term contract with the RDF supplier should be the basis of the project.

ii. Producer gas yield

Producer gas yield, evaluated in terms of Nm^3/kg RDF, depends upon RDF quality. An increase in yield will increase the gasifier's cold gas efficiency, adding monetary benefits by enhancing TSR in the calciner. A change in yield of ± 10% will result in an IRR variation range of 8.33-11.94%, which is noteworthy. The decrease in yield will increase the producer gas price (Rs/Nm^3).

iii. Capital cost

The capital cost reported in this study are indicative costs and may vary from supplier to supplier, technology, and feedstock. The capital cost variation may also occur depending upon the plant configuration and retrofit requirements, requiring sensitivity analysis. Presently, there is no RDF gasifier installation in a cement plant in India. Hence, capital cost variation must be considered for sensitivity analysis. A 2.66-3.24% variation in IRR is anticipated considering ± 10% variation in capital cost.

iv. Operating hours of gasifier

In the study, 330 days of gasifier operation with 24 working hours per day have been considered. 10% variation up and down is possible considering RDF quality, ER, maintenance, and gasifier clogging issues resulting in IRR variation up to 3%.

v. Residual ash selling cost

The market for gasifier ash is dynamic depending upon its quality and logistics for utilization in grey cement which demands sensitivity analysis. However, IRR variation is negligible considering ± 10% variation in residual ash selling cost.

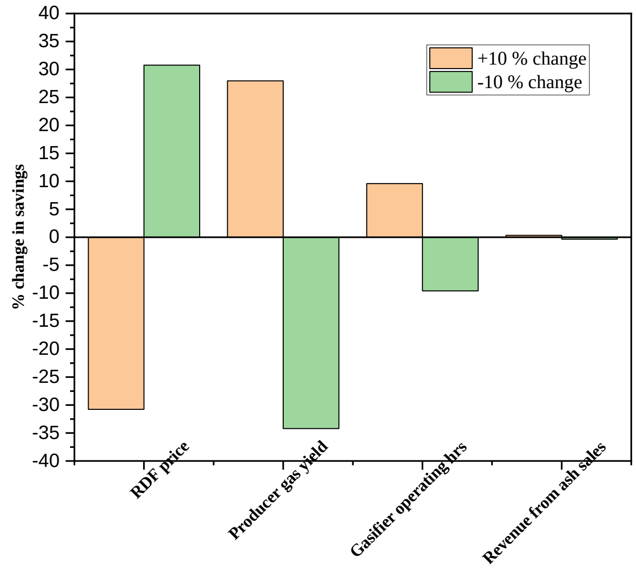

Fig. 6.5a Effect on changes on financial input parameters on savings for 15% TSR through producer gas

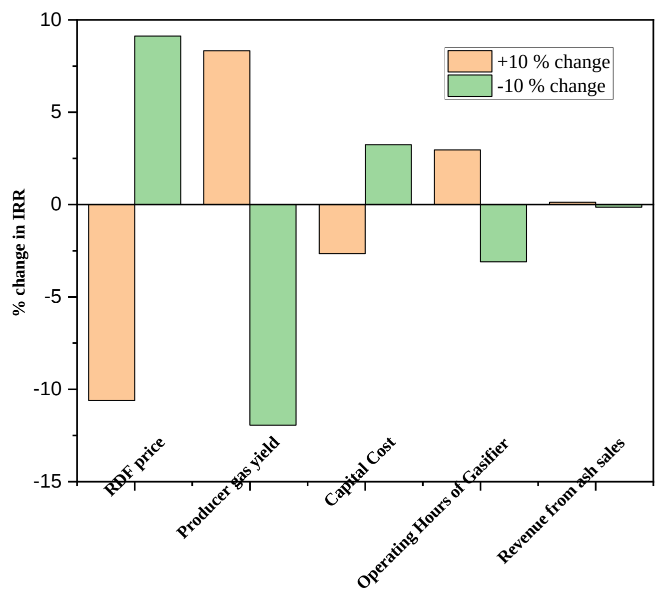

Fig. 6.5b Effect on changes on financial input parameters on IRR for 15% TSR through producer gas

CHAPTER – 7

CONCLUDING REMARKS

The research is focused on utilization of producer gas obtained from RDF gasification or co-gasification as an alternative fuel in the calciner of a cement plant. Gasification technology can be a game changer for white cement, as no established alternative fuel exists in that context, so far. To establish TSR using RDF gasification in cement industry, the performance of a downdraft gasifier in terms of gas flow rate, heating value and gas yield is to be determined. In this regard, several experimental studies have been conducted on a downdraft gasifier for RDF gasification and RDF-biomass mix co-gasification.

A multi-zone RDF downdraft gasifier model has been developed where each of the four zones, i.e., drying, pyrolysis, oxidation/combustion, and reduction, have been modelled separately. The results have been validated using experimental results available in the literature. Stoichiometric and Aspen Plus-based models were developed for calciner considering solid and gaseous fuel mix and compared. High ash RDF is taken as input to the gasifier model. The resulting producer gas and petcoke are considered for the calciner model to study the calciner performance parameters at varying TSR of 8% and 15%.

Further, techno-economic feasibility has been performed for RDF gasification in a white cement plant. This chapter summarises the present work, followed by conclusions, significant contributions and future scope of research in this area.

7.0 Summary

7.1 Introduction

Cement production is energy intensive and heavily relies on conventional fuels worldwide. The percentage of fossil fuel utilization in global cement production is around 94%. The rising conventional fuel cost and focus on environmental sustainability further gives impetus to waste utilization in cement production. In this regard, the cement industry constantly looks for waste-derived alternative fuels to replace conventional ones. The industry has tried different types of wastes as alternative fuels under hazardous and non-hazardous categories. ETP Sludge, TDI tar, paint sludge, process waste, waste residue, chemical sludge, process sludge, phosphate sludge, spent solvent, benzofuran, and waste lubricant oil are being used under hazardous waste category while non-hazardous wastes includes agro waste, tyre chips, RDF, plastic waste, biomass, wood chips, etc. The world average thermal substitution rate (TSR) for alternative fuel utilization is 18%. The Indian cement industry stands at 6%, which is low compared to the European nations, with approximately 46%. It aims to achieve a total TSR of around 30% by 2030 [28], which is daunting. RDF is the most potential waste to achieve this figure in the Indian cement industry. One of the major Indian cement company, Dalmia Cement (Bharat) Limited achieved 12.45% TSR for FY 2021-22, with a significant share from RDF [10]. RDF is a combustible fraction obtained from Municipal solid waste (MSW). MSW is defined as household waste, commercial and market area waste, institutional waste (e.g., from schools and community halls), horticultural waste, waste from road sweeping, and silt from drainage. It is to be noted that the top ten cement-producing nations are also top solid waste-producing countries; thereby, the tremendous potential lies in the cement sector of these nations to utilize this waste.

Due to heterogeneity, high moisture, and ash content in RDF, cement plants face operational issues during the direct combustion of RDF. It has been observed that there is an increase in CO formation at preheater outlet, which indicates incomplete the combustion. Operators resort to increasing air input to the system with an optimized fuel ratio to optimize combustion. It increases preheater fan power consumption, which handles more gas volume. Most of the cement plants consist of screw weigh feeding systems for continuous feeding of RDF, which often face jamming issues due to their heterogeneous and sticky nature leading to operational disturbances. Shredders, part of the pre-processing systems for RDF preparation in cement plants, also have jamming issues. Some plants with high% TSR due to RDF are facing coating issues on the refractory lining inside the kiln system. RDF has a high chlorine and alkalis content, which combines with petcoke sulphur, resulting in coating formation. RDF utilization leads to the circulation of volatile salts and clogging in lower preheater cyclones and riser pipe. Hence, it is the need of the hour that the cement industry, particularly in India, looks for other options for thermochemical treatment. RDF gasification is a technology to process waste to overcome the abovementioned challenges and use producer gas as an alternative fuel for co-processing. Gasification transforms feedstock like biomass, RDF, etc., into producer gas rich in hydrogen and carbon monoxide, which is combustible. It occurs in a reducing environment requiring heat, whereas combustion occurs in an oxidizing environment releasing heat. The performance evaluation of gasification is based on heating value (MJ/Nm^3), cold gas efficiency, carbon conversion efficiency, equivalence ratio, etc. The key advantages of gasification are better combustion properties in the calciner and good clinker quality due to no additional ash in the clinker. Heating value variations of the input fuel mix (coal and producer gas) are reduced substantially due to consistent producer gas composition. Both grey and white cement plants will be benefitted from this technology. There is not much literature available on RDF gasification for cement industry applications. In this context, the integration of RDF gasifier to calciner of cement plants is to be explored through modelling, experimental, and techno-economic feasibility studies.

7.2 Gaps in literature

Very few experimental results have been reported on RDF gasification and co-gasification. The problem of bridging and clinker formation was identified, and solutions were proposed to tackle this issue. The researchers have used mostly downdraft-type gasifiers for RDF gasification, except for one study each on an updraft gasifier and a bench-scale rotary kiln reactor. A few studies have also taken up the co-gasification of RDF and biomass to improve producer gas properties. The major limitation of all these studies is input RDF properties where the maximum RDF ash content is 15% which is too low considering the Indian scenario. Hence, high ash RDF gasification and co-gasification with biomass need to be explored further to design future gasifiers to take up high ash content without clinkering problems. The present study has taken up high ash RDF gasification in Indian conditions.

Over the years, several authors have used different approaches to model downdraft gasifiers for biomass gasification. Equilibrium modelling, kinetic free, stoichiometric approach, and phenomenological modelling by incorporating mass and energy balance around a differential length of the reduction zone are some of these. Some approaches incorporated varying char reactivity factors to predict the temperature profile and producer gas composition more accurately along the length of the gasifier. Another approach was modelling the pyrolysis and combustion zone separately based on the experimental data available in the literature. The pyrolysis and combustion zone output was fed as the input to the reduction zone. All these models are for biomass as fuel, and since RDF is a heterogeneous fuel with varying properties, these models require suitable modifications for RDF gasification in a downdraft gasifier. Very few articles are available on RDF gasification modelling including model based on Gibbs Free Energy Gradient Method (GMM), Aspen Plus, stoichiometric and non-stoichiometric models. All the Aspen Plus models consider equilibrium in the reduction zone, which fails to predict the syngas composition precisely since it does not consider the effect of the residence time of the reactants inside the gasifier. Moreover, Aspen Plus-based models have not considered the formation of tar and minor components such as S, and Cl which affect syngas composition. The equilibrium reactor (REQUIL) in Aspen Plus assumes a long enough residence time for the chemical reactions to reach equilibrium, which is unrealistic. The model also neglects the tar formation, and the char (pure carbon) is not considered to participate in the thermodynamic equilibrium calculations. Further, the drawback of the equilibrium models is that they overestimate the amount of CO and H_2, underestimating the yield of CO_2, and predicting an outlet stream free from CH_4, tars, and char. Some studies reported the gasification temperature to be uniform in all directions: axial and radial, which is unrealistic. Hence, an RDF gasifier model needs to be developed considering above mentioned limitations.

To study the producer gas from RDF gasification as alternative fuel in cement plant calciner, various calciner models using Aspen Plus, fuzzy logic, MATLAB, machine learning, CFD were proposed. The researchers have predicted calciner outlet temperature, gas composition and degree of calcination, etc., at varying TSR using these models. Most of the models concentrated on solid alternative fuels. Impact assessment with fuel mix of solid and gaseous fuels needs in-depth analysis. Moreover, models focusing on process integration aspects of gasifier and cement plant calciner are scarce. It needs to be explored to achieve the perfect integration strategy. A few patents and articles on gasifier integration to kiln and calciner have been reported in the literature. SWOT analysis has been done for calciner-gasifier integration configurations A, B, C, D and E.

Techno-economic feasibility of syngas (derived from RDF) has been explored mainly for power generation. The present study takes up all aspects related to the RDF gasifier model, calciner model and techno-economic feasibility for RDF gasification for producer gas application as an alternative fuel in a white cement plant.

7.2.1 Scope of work

The aim of this research is to explore producer gas obtained from RDF gasification or co-gasification as an alternative fuel in the calciner of a cement plant, mainly white cement. To establish TSR using RDF gasification in cement industry, the performance of a downdraft gasifier in terms of gas flow rate, heating value and gas yield is to be determined. In this regard, RDF characterization, gasification experimental studies, gasifier and calciner modelling and techno-economic feasibility study for RDF gasification in a cement plant has been undertaken. For experimental studies, RDF gasification and RDF-biomass mix co-gasification has been taken up with air or air-O_2 mix as gasifying agent. It will lead to establishing TSR considering the RDF quality, plant operation, and calciner limitations.

7.2.2 *Experimental studies*

RDF characterization and RDF/RDF-biomass mix gasification experiments are part of experimental studies. TGA and Py/GC-MS techniques have been used for six different types of RDF characterization. The thermal degradation characteristic of RDF samples A, B, C, D, E, and F from various sources in inert conditions was studied using the TGA, showing the change in weight with temperature.

Pyrolysis tests covering the characterization of the chemical composition and the structure of volatile and non-volatile compounds in RDF samples were carried out in a Py-GC/MS pyrolyzer equipped with a pyro probe. EGA was carried out to determine the different peaks associated with pyrolysis products. The heating ramp was 10°C/s. Moreover, a single-shot analysis for six samples was also done at 550°C. The characterization is performed under an inert (helium) atmosphere by analyzing the thermal degradation products of the compounds obtained after heating the sample to elevated temperatures.

Five nos. experimental runs in a downdraft gasifier with feedstock of RDF and six nos. with a mix of RDF and biomass have been conducted to generate producer gas. An experiment on RDF gasification and RDF-biomass mix as a feed, i.e., co-gasification, is carried out using air and pure O_2 mix as gasifying agents. Rest all were carried out with air as the gasifying agent.

The experimental setup mainly consists of six major pieces of equipment: downdraft biomass/RDF gasifier, venturi scrubber, sand bed filter, flare unit, air compressor, and data logger. The downdraft gasifier is divided into four reactive zones: drying, pyrolysis, combustion and reduction. A grate is placed at the bottom of the gasifier to support charcoal burning during gasifier start-up. Moreover, the coarse residual ash during gasifier operation gets collected above the grate while the fine passes through the grate. Fine residue below the grate is collected in the water tray. Two nozzles are provided in the oxidation zone of the gasifier (at 10 cm height above the grate), through which air is supplied continuously from an air compressor. The producer gas cleaning system consists of a venturi scrubber and sand bed filter to prevent moisture and dust from escaping to the environment. The temperature of the oxidation and reduction zones of the gasifier are recorded in the data logger using thermocouples.

7.2.3 Mathematical modelling and simulation

The modelling and simulation of the gasifier and calciner are briefly discussed in the below section.

7.2.3.1 Gasifier model

Most of the gasifier models are either Aspen Plus-based or equilibrium-based models. The present model incorporates a multi-zone approach for modelling the downdraft gasifier where the reduction zone has been modelled using a kinetic semi-equilibrium approach which is more realistic. The model consists of four zones where different thermochemical phenomena occur: drying, pyrolysis, oxidation/combustion and reduction/gasification. RDF gets dried in the drying zone, and the moisture gets released. Inside the pyrolysis zone, thermochemical conversion of the dried RDF takes place in an oxygen deficit environment to produce water vapours, volatiles (V_1) and intermediates. Further cracking of the intermediates occurs, and finally, char, volatiles (V_2), and gases ($CO, CO_2, CH_4, C_2H_4, H_2$ and H_2O) are obtained. The generation of primary tar is unavoidable in the pyrolysis zone, and the primary tar undergoes further cracking to produce volatiles and secondary tar. It is challenging to capture the complete tar cracking phenomena into the model; thus, tar is considered an input variable. All the higher-chain aliphatic compounds formed during pyrolysis were lumped into methane. The products of the pyrolysis zone thus formed enter the high-temperature combustion zone where the highly exothermic reaction occurs. The heat generated from the exothermic reactions provides the heat required to sustain the gasification reactions. Finally, the products of the combustion zone enter the reduction zone. A set of simultaneous ordinary differential equations is obtained employing mass and energy balance on a differential length of the reduction zone. The temperature profile and syngas composition along the reduction zone length are found numerically by solving the differential equations.

Tar is an important criterion when designing a downdraft gasifier, as a higher tar can be a bottleneck during the gasifier operation. The tar yield is a strong function of gasification temperature. The tar has been modelled as an input to the reduction zone based on the combustion zone temperature. The tar's molecular formula has been considered $CH_{1.03}O_{0.33}$ and the amount of tar supplied to the reduction zone has been modelled according to the values reported in the previous studies. Also, tar steam reforming reaction has been included in the current research and the kinetic data for the same is adopted from the literature. The variation in the syngas composition along the reduction zone's length has also been included.

7.2.3.2 Calciner stoichiometric model

A stoichiometric model for the inline calciner of the white cement plant has been developed, which is applicable for solid and gaseous fuel mix firing. The model shall be able to simulate solid and gaseous fuel together by combining combustion and calcination governing equations. Mass and energy balances are established for different TSRs to establish technical performance. Sensible heat and heating value related to fuel, the sensible heat of partially calcined kiln feed, kiln exit gas and air component are the input parameters, while the flue gas, hot meal enthalpy, the heat of reaction for calcination reactions, and radiation loss form the output parameters. The model is validated using plant operating data.

Producer gas quantity and temperature entering the calciner are derived from the gasifier model. Further, the base model developed is modified by augmenting the fuel parameters as per the producer gas requirement for 8.5 and 15% TSR, and simulations were performed. The model takes producer gas as part input with a specific yield of 2.36 Nm^3/kg RDF and HHV of 3.95 MJ/Nm^3at ER 0.30.

Once the model equations are developed, baseline conditions are set where producer gas flow is taken as 0 considering 100% petcoke firing for a fixed quantity of calciner inlet kiln feed. Then simulations are performed for baseline conditions. Other simulations are performed for varying TSR for petcoke, and producer gas co-firing based on RDF input to the gasifier model output. RDF proximate, ultimate, and ash analysis is fitted into the gasifier model to determine producer gas properties and operational parameters. It will establish TSR to fix the producer gas flow rate and petcoke flow rate. Kiln feed flow rate with DOC is used to establish calciner inlet and outlet flow rate. The kiln inlet flow rate is calculated based on the petcoke firing in the kiln and calculated combustion products and excess air at the kiln inlet. Other inputs are tertiary air and transport air obtained from the plant data. All inputs, along with their temperatures, c_p values, and enthalpies, are fed to the stoichiometric MS excel model. The material and energy balance is applied. Further, the goal seek function of MS Excel performs iterations with calciner outlet temperature as an objective function at the determined calciner outlet temperature. The final values shall be the corresponding calciner outlet flow rate in tonnes per hour, calciner outlet gas composition in terms of% CO_2,% O_2,% N_2 and hot meal flow rate (tonnes per hour).

7.2.3.3 Calciner Aspen Plus model

Aspen Plus model is an alternate to stoichiometric model for calciner. The model incorporates five modules of different unit operations, one FORTRAN code, and fourteen streams. Petcoke and clay are the non-conventional components that are defined separately in Aspen Plus. For calculating the enthalpy and the density of non-conventional features like petcoke, the selected model is HCOALGEN and DCOALGEN. For clay, ENTHGEN AND DNSTYGEN are specified. The heat value of the petcoke is fed to the model. The chosen thermodynamic methods are based on the Peng-Robinson equation of state since they suit high-temperature combustion. Since petcoke is not a conventional compound with a definite formula, modelling petcoke combustion requires its decomposition into elements based on proximate and ultimate analysis. The petcoke stream carrying existing fuel petcoke gets decomposed in a reactor, which executes based on the calculator block with FORTRAN commands. The petcoke decomposition depends upon its proximate and ultimate analysis. The decomposed products are transported to the combustion reactor for complete combustion in the presence of tertiary air, transport air, primary air, and kiln gas. These kiln exit gases enter the calciner through the kiln riser. The combustion reactor works on Gibbs free energy minimization. All input parameters of the combustion reactor are entered into the model, and output is in the form of combustion products. The calcination is an endothermic reaction, and the heat of combustion will be utilized to calcine the raw material in the stoichiometric reactor. The split operator is applied to separate gases and solid materials from the product stream. The solid material is considered the hot meal entering the kiln. Calciner exit gases pass out through different preheater stages and leave through top-stage cyclones.

Model augmentation is carried out to introduce the co-firing of syngas and petcoke in the calciner. A splitter is introduced, which splits the mix of air and kiln gases into two streams: petcoke and producer gas combustion. For producer gas combustion, a stoichiometric reactor is used where chemical reactions for the combustion of producer gas components are added along with the heat of combustion. Combustion products from petcoke combustion and producer gas combustion and their respective heat of combustion are introduced in calciner reactor for calcination. The remaining part of the model is the same as the base model.

The difference from the previous stoichiometric model is in the working of the Aspen Plus simulation. Petcoke decomposition products are obtained using a calculator function and sent to the combustion reactor along with a mixed air stream for combustion. Further, calcination occurs in the stoichiometric reactor using heat evolved during combustion. Material and energy balance is established at each stage by performing iterations. Final output parameters for the calciner are obtained.

7.2.4 Results and discussion

This section summarises the experimental results, modelling and simulation results and economic feasibility accomplished in the present study. The section also presents the validation of the proposed gasifier and calciner model using the experimental data.

7.2.4.1 Experimental studies

Six RDF samples listed as A, B, C, D, E and F from different locations across the country were studied using TGA and Py-GC/MS. In TGA, the first mass loss step from ambient temperature to about 220°C, is attributed to loss of moisture and very light volatile matter content of the RDF. This temperature was high enough to ensure that the most tightly bound moisture was driven from the specimens. Further, degradation of mainly hemi cellulose and cellulose component of the sample occurs with a minor portion of lignin volatiles at higher temperatures. It is followed by the devolatilization of cellulosic, plastic and lignin content. The reactions between char and volatiles, which were coming from previous phases of the process, might be cause of the last peak. The major decomposition for all the samples happened from around 230 to 790 indicating the much lower ignition and burnout temperatures when compared to TGA analysis of petcoke and coal.

Qualitative and semi-quantitative results were obtained by interpreting pyrolysis products from Py-GC/MS of RDF samples using EGA and single shot analysis method. EGA was used to derive qualitative results of pyrolytic products with peaks correlating with temperatures which could be attributed to the desorption of volatile fractions. It was found during single-shot analysis that apart from non-hydrocarbon gases (CO_2 and O_2), the long-chain alkenes were most abundant, followed by alkanes, aromatic compounds and ketones. The qualitative and semi-quantitative data could be used to improve the compositional studies of RDF along with its pyrolytic behaviour in gasifier, which could further strengthen future gasifier models where pyrolysis is one of the key steps.

Several experiments are carried out with RDF and RDF-biomass mix as feedstock for gasification. The closure of mass balance for all is in the range of 85.49-105.53%. The gasifier's performance, the effect on gasifier temperature zones, producer gas composition, and the effect of form of RDF and RDF-biomass mix for varying feedstock has been contemplated. The maximum combustion zone temperature achieved is ~600°C, 860°C, and 700°C in the case of

RDF C fluff, RDF D pellet, and RDF E pellet, respectively. However, the maximum achieved combustion zone temperature is above 800°C for different RDF and biomass mix with one feedstock combustion zone temperature peaked at 1070°C. The sudden rise and drop in temperature prominent in the RDFs case is less in co-gasification, and temperature is consistent, showing stable combustion. At oxygen enrichment (35% O_2), after an initial 20 min, the combustion zone temperature stabilized to 820-890°C, while in all other cases, there is a downward temperature trend after 20 minutes.

For reduction zone temperature, it has been observed that as the biomass ratio is enhanced from 50 to 70% in a mix of RDF pellet and biomass pellet, the temperature rise is steadier from start to end. Fuel consumption is 4 kg/hr, which is the highest among all cases, and no residue was left at the bottom of the gasifier after the completion of the experiment. Run no 1 using RDF fluff has the highest N_2 content of 75%, and LHV is 1.87 MJ/Nm^3, which is the minimum of all 11 runs. Moreover, there is severe bridging in the gasifier. Run 4 is much better than runs 2 and 3, as fuel consumption increased by ~28% compared to the average of runs 2 and 3 due to enriched O_2 content. There is an appreciable rise in H_2 and CO content by 2.65% and 9.55%, respectively, with a drastic reduction of N_2 content by 13.16%. It can be inferred from all experimental runs using RDF-biomass mix with air as a gasifying agent that run no 7 having RDF-biomass mix in 50:50 ratio shows best results with producer gas LHV of 3.88 MJ/Nm^3 and CGE of 77.65%.

Based upon the internal inspection of the gasifier after experimental runs, it can be said that the densification of RDF in the form of pellet followed by co-gasification with biomass led to better-burning behaviour with good consistent flame and minimum residue at the gasifier bottom.

7.2.4.2 Mathematical modelling and simulation

7.2.4.2.1Gasifier modelling

The multi-zone model developed for RDF downdraft gasification is applied to predict producer gas quality for RDF E. Further, parametric study is conducted for varying parameters such as ER, reduction zone inlet temperature, reduction zone length and moisture content of RDF. All five major gas components (CO, H_2, CH_4, CO_2 and N_2) are plotted with ER. Increasing the equivalence ratio will increase the char and gas oxidation reactions, increasing the generation of CO and CO_2 in the combustion zone. It is seen that the overall total number of moles of CO and H_2 increases with increasing the ER, but the mole fraction of H_2 decreases as the increase of N_2 concentration is much more dominant. The CH_4 concentration was reduced from 4.20% to 2.02% for RDF E due to similar reasons. The CO_2 concentration for RDF E increases from 3.93 to 5.35% with an increase in ER since the enhanced air results in more CO_2 formation.Moreover, as the CO, H_2 and CH_4 mole fraction summation decreases, the LHV of the gas decreases significantly from 4.18 MJ/Nm^3 to 3.23 MJ/Nm^3 for RDF E over the range of ER from 0.15 to 0.50. The effect of varying RDF moisture from 5 to 20% on producer gas concentration, LHV, gas yield, and CGE has been done. The LHV decreases from 3.58 to 3.24 MJ/Nm^3 with a 5% to 20% moisture content. Accordingly, the CGE and CCE were reduced by 8.66% and 4.64%, respectively.

Similarly, the effect of reduction zone inlet temperature from 900 to 1400 K on producer gas LHV & efficiency has been estimated. As the temperature increases, the Boudouard reaction rate, water gas and steam reforming reactions are enhanced, and reactions shift towards the right side, producing more CO and H_2. Due to this phenomenon, the overall gas yield and heat value increase since the H_2O component entering the combustion zone is reduced to H_2. Producer gas concentration and temperature variation along the length of the reduction zone has been investigated. Bed length is assumed to be 0.25 m with reduction zone inlet temperature as 1200 K. It is observed that with ER ranging from 0.15 to 0.50, equilibrium was achieved within 60% length (0.15 m) of the gasifier for RDF E. After that, the composition did not vary much with the change in length (0.15 to 0.25 m). Moreover, all three minor component concentrations, HCl, H_2S, and tar decreased from 0.079 to 0.041%, 0.115 to 0.060%, and 1.115 to 0.598%, respectively, with an increase in ER.

7.2.4.2.2 Calciner modelling

Calciner modelling has been done to establish the technical performance of the calciner system for an overall TSR of a maximum 15-20% which is satisfactory for a white cement plant at the initial stage of operation. Mass and energy balance for the system at 8 and 15% TSR using producer gas with 100% petcoke firing as a baseline scenario has been carried out. Accordingly, two calciner models, one stoichiometric and the other Aspen Plus based were modelled and simulated. The RDF having LHV of 14.63 MJ/kg gets converted to producer gas with an LHV of 3.63 MJ/Nm^3 with a cold gas efficiency of 59.62% and gas yield of 2.36 Nm^3/kg RDF and acts as input to the calciner models. The calciner models predicted calciner outlet temperature, specific gas volume, CO_2, and SO_2 with respect to the baseline scenario and are compared for output values. It can be seen that predictions for all critical parameters by both models at 15% TSR are almost similar. However, the calciner outlet temperature predicted by stoichiometric model for baseline scenario validation is 892 °C, closer to the actual value of 865 °C than the Aspen Plus model value of 897°C. Thus, the stoichiometric model has been considered further for economic analysis of RDF gasification in a white cement plant.

7.3 Conclusions

Based on the results obtained in the present study, the following conclusions are drawn:

1) RDF containing high ash content in the range of ~31-51% is quite challenging to gasify in a downdraft-type gasifier.
2) The major challenges faced during gasifier operation are unsustainable and low combustion zone temperature, inconsistent flame, and gasifier operational issues like fused clinker due to high ash and material bridging.
3) The feedstock-wise gasification performance with air as gasifying agent is found to be in the following order: RDF pellet-biomass pellet mix > RDF-biomass mix pellets > RDF pellets > RDF fluff considering LHV, CGE, consistent flame, fuel consumption rate and residual ash content which indicates RDF pellet-biomass pellet mix is the most suitable composition.
4) RDF gasification yield ranges from 2.43-3.65 Nm^3/kg RDF with LHV of 1.87-2.24 MJ/Nm^3 RDF and CGE of 44-60%.
5) Co-gasification results indicated the gas yield in the range of 2.42-3.27 Nm^3/kg RDF with LHV of 2.46-3.88 MJ/Nm^3 RDF and CGE of 46.83-77.65%. Upon adding O_2 to air as a gasifying agent for 50:50 RDF-biomass mix, LHV, and CGE increased by 35.5% and 8.35%, respectively.
6) RDF gasification performance can be improved by
    a. 50 to 70% replacement of RDF by biomass

b. Air-O_2 mix as gasifying agent (LHV and CGE increased by 78% and 30%, respectively)

7) Py/GC-MS results indicated that plastic and biomass are the most significant constituents of RDF. The long-chain alkenes were most abundant, followed by alkanes, aromatic compounds, and ketones in all RDF samples.
8) A multi-zone gasifier model developed for RDF gasification comprising four zones (drying, pyrolysis, oxidation/combustion and reduction). The model also covers minor components like tar, HCl and H_2S and incorporates RDF ash which is ignored in previous models.
9) The model-predicted composition of producer gas, gas yield and heating value is validated with the experimental data reported in the literature and those obtained in the present study.
10) Stoichiometric and Aspen Plus models were developed and validated with plant data to determine calciner performance at different TSR levels.
11) At 15% TSR, the calciner outlet temperature will get reduced by around 3%, with the increase in calciner exit gas volume by 8% (rise in Ph fan power) which is manageable.
12) CO_2 mitigation potential at 15% TSR is estimated to 10.5% of the baseline scenario
13) High sulphur content in petcoke leads to dusty clinker formation and circulation of volatiles in the system. Co-processing will decrease SO_2 from 6.69 to 4.22 g/t clinker and will support in smooth kiln operation.
14) Techno-economic feasibility for co-processing of producer gas with petcoke in a white cement plant has been carried out based on gasifier and calciner modelling results. IRR of 18.30% and discounted payback period of 5 years and 7 months for a 10-year gasifier

operation is acceptable. RDF price appears to be the most influential parameter affecting IRR and savings.

7.4 Future scope of research

The future scope of this work is highlighted below:

1) Development of chloride treatment techniques present in producer gas which is one of the major issues during RDF co-processing in cement plants
2) CFD modelling study can be taken up for calciner to study the producer gas behaviour and to decide its firing location.
3) Residual ash of gasifier bottom with high silica content (47%) can be used as an alternative raw material in grey cement by optimizing raw mix design and needs further investigation.
4) The study of heavy metals behaviour during RDF gasification can be taken up
5) Decarbonization has emerged as a significant challenge the cement industry faces in today's scenario. Carbon capture and utilization have been identified as one key lever to decarbonize the cement sector. Gasification technology can lead to the development of pre-combustion capture technology by separating CO_2 from producer gas leading to enriched H_2 production. H_2 as clean fuel has the potential to replace fossil fuels in cement plants. There is a vast potential for research in this area.

References

1. U.S. Geological Survey, *Mineral commodity summaries* (2020): Reston, VA. pp. 204-205.https://doi.org/10.3133/mcs2020.
2. Sada Sahu, Vahit AtakanKalbfleisch, B. *Low-CO2 synthesis SCMs*. Internationcal cement review,(2021). 9, 1-3, DOI. https://assets.ctfassets.net/jv4d7wct8mc0/4Mixl1YBEqDwa0UbDVVbjv/3ba7c868b430867fa6be191a5a9d7e65/ICR_REPRINT_2021-09_Solidia_Technologies_LR.pdf.
3. Chaturvedi, S.K., Ojha, P.N., Panda, D.K., Trivedi, A., Naidu, G.J., Mittal, A., Kukreja, K., Singh, B., Pandey, P., Shaw, S.K., Bohra, A., Liju, V., Vanghuri, S., Ahamed, G., Nath, K.R.P., Nagakumar, V., Reddy, K.P.K., Sharma, P., Mazumdar, R., Bhatnagar, S., Kaura, P.Venkatesh, V.: The Cement Industry India 2022. 1-2 (2022).
4. Pales, A.F. Leung, Y.: Technology Roadmap Low-Carbon Transition in the cement industry. IEA(2018). pp. 5,29.https://www.wbcsd.org/Sector-Projects/Cement-Sustainability-Initiative/Resources/Technology-Roadmap-Low-Carbon-Transition-in-the-Cement-Industry.
5. Miller, S.A., Habert, G., Myers, R.J.Harvey, J.T.: Achieving net zero greenhouse gas emissions in the cement industry via value chain mitigation strategies. One Earth, 4**,** 1398-1411 (2021).https://doi.org/10.1016/j.oneear.2021.09.011.
6. Sonebi, M., Ammar, Y.Diederich, P., Sustainability of cement, concrete and cement replacement materials in construction. Sustainability of Construction Materials pp. 371-396. Woodhead Publishing(2016).https://doi.org/10.1016/B978-0-08-100370-1.00015-9.
7. CII: Case study manual on alternate fuels & raw material utilization in Indian cement industry.(2011). pp. 1-90.https://shaktifoundation.in/wp-content/uploads/2017/06/afr-utilisation-in-cement-industry-final-10-jan-2012.pdf.
8. Brannvoll, F. Vasyutenko, M. *World markets, Energy and Freight update*. in *International Cement Conference Cemtech*. (2020).
9. B.N. Mohapatra, *Utilisation of alternative fuels and raw materials in Indian Cement Industry: The Current Scenario and Future Prospects*, in *Indian cement review*. (2022). pp. 58-61
10. Chetan Shrivastav, Arbind Singh, Satish Mishra, Vikas Mangal, Alok ChoubeyAniket Chaki. *Dalmia RGP carbon footprint roadmap*. in *17th NCB International Conference on Cement, Concrete and Building Materials*. (2022). New Delhi
11. Ananth, P.V.K.: Energy benchmarking for Indian cement industry. Author(2019). pp. 1-69.
12. Mukesh Sinha, M NemaniRao, N. *Quest of green fuel at Kadapa cement works*. in *17th NCB Interntional Conference on Cement, Concrete and Building Materials*. (2022). New Delhi
13. Murumkar, M., *Challenges while utilising hazardous industrial waste*, in *Indian cement review*. (2020). pp. 24-27
14. MoEFCC: List of processes generating hazardous wastes (2016). pp. 1-68.http://www.iwma.in/HWM%20Rules.pdf.

15. Deolalkar, S.P., Chapter 1 - General Introduction. in S.P. Deolalkar, Designing Green Cement Plants. pp. 63-69. Butterworth-Heinemann(2016).https://doi.org/10.1016/B978-0-12-803420-0.00008-1.
16. MoHUA, G.: Guidelines on usage of refuse derived fuel in various industries.(2018). pp. 13-14.http://cpheeo.gov.in/upload/5bda791e5afb3SBMRDFBook.pdf.
17. MNRE, G.:Bio energy. https://mnre.gov.in/bio-energy/current-status. Accessed 17 September 2021
18. Central pollution control board, M.o.E., Forest and Climate Change, Govt. of India: Interim Report of Monitoring Committee on Management of Hazardous Waste.(2019). pp. 41-42.http://www.indiaenvironmentportal.org.in/content/461822/interim-report-of-monitoring-committee-on-management-of-hazardous-waste/.
19. CPCB, M., GoI: Annual report 2019-20 on implementation of Plastic Waste Management Rules, 2016.(2019-20).https://cpcb.nic.in/uploads/plasticwaste/Annual_Report_2019-20_PWM.pdf.
20. Pasalkar, A.A., Bajaj, Y.M., Wagh, A.A.Dalvi, J.D.: Comprehensive Literature Review on use of Waste Tyres Rubber in Flexible Road Pavement. International journal of engineering research & technology (IJERT), 04**,** (2015).https://doi.org/10.17577/IJERTV4IS020596.
21. Bharati Chaturvedi Rajat Rai Handa: Circulating Tyres in the Economy. Chintan Environmental Research and Action Group(2017). pp. 16-17.https://cupdf.com/document/circulating-tyres-in-the-economy-reportfinalpdf-6-7-manufacturers-like-balaji.html.
22. CLE, s.b.M., GOI.Footwear Industry : Best Foot Forward. https://leatherindia.org/footwear-industry-best-foot-forward/. Accessed 12 April 2022
23. United nations industrial development organization: Wastes generated in the leather products industry.(2003). pp. 22-23.https://open.unido.org/api/documents/4788516/download/WASTES%20GENERATED%20IN%20THE%20LEATHER%20PRODUCTS%20INDUSTRY%20(23438.en).
24. Verisk Maplecroft: Waste Generation and Recycling Indices 2019 Overview and findings.(2019). pp. 5-6.https://www.maplecroft.com/insights/analysis/us-tops-list-of-countries-fuelling-the-mounting-waste-crisis/.
25. Cembureau The ECA: Activity report. Cembureau(2019). pp. 1-37.
26. Kosajan, V., Wen, Z., Zheng, K., Fei, F., Wang, Z.Tian, H.: Municipal solid waste (MSW) co-processing in cement kiln to relieve China's Msw treatment capacity pressure. Resources, Conservation and Recycling, 167**,** (2021).https://doi.org/10.1016/j.resconrec.2020.105384.
27. Central pollution control board, *Guidelines for Pre-Processing and Co-Processing of Hazardous and Other Wastes in Cement Plant as per H&OW(M & TBM) Rules, 2016* (2017). pp. 1-34
28. Global cement and concrete association.GCCA India Launches. https://gccassociation.org/news/gcca-india-launches/. Accessed April 2023
29. Ananth, P.V.k.: Approach paper for achieving 25% thermal substitution rate in Indian cement industry by 2025.(2016). pp. 1-8.http://www.ciiwasteexchange.org/doc/annexure_6.pdf.

30. Kukreja, K., Sharma, P., Mohapatra, B.Saxena, A. *Indian Cement Industry: A Key Player in the Circular Economy of India*. in *Enhancing Future Skills and Entrepreneurship*. (2020). Cham: Springer International Publishing
31. Sharma, P., Sheth, P.Mohapatra, B.N., Waste to energy: Issues, opportunities and challenges for RDF utilization in Indian cement industry. Proceedings of the 7th International Conference on Advances in Energy Research. pp. 891-900. Springer, Mumbai (2019).https://doi.org/10.1007/978-981-15-5955-6_84.
32. Kukreja, K., Anupam, Sharma, P.Bhatnagar, S., *Handling of Multi type Alternative Fuels : A Challenge and Opportunity for Cement Plant* in *16th NCB International Seminar on Cement, Concrete and Building Materials*. (2019): New Delhi
33. Kukreja, K., Mohapatra, B.N.Saxena, A. *Transfer chute design for solid alternative fuels*. Indian cement review,May ed. (2019). 52-53, DOI.
34. Rajamohan, R., Vinayagamurthi, K.Kumar, R.A.K., *Alternative Fuel & Raw Material: Our Journey with In-House Systems - A Glimpse*, in *15th NCB International Seminar on Cement, Concrete and Building Materials*. (2017): New Delhi
35. Abbas, T. Michalis Akritopoulos, *Calciner challenges*, in *World cement*. (2018)
36. Karstensen, K.H., Saha, P.K., Vigerust, E., Paulsen, A.A., Engelsen, C.J.Ahmadi, M. *Asia's plastic potential*. International Cement Review,March ed. (2021). DOI. https://www.cemnet.com/Articles/story/168461/asia-s-plastic-potential.html.
37. CPCB, M., GoI: National Inventory on Generation and Management of Hazardous and Other Wastes (2021).https://cpcb.nic.in/uploads/hwmd/Annual_Inventory2020-21.pdf.
38. Saxena, A., Chaturvedi, S., Ojha, P., Agarwal, S., Mittal, A., Sharma, P., Ahamad, G., Mazumdar, R., Arora, V., Kalyani, K., Anupam, Singh, B., Kukreja, K., Ahmed, R., Bohra, A.Kaura, P., *Compendium The Cement Industry India* (2019), National council for cement and building materials, India. pp. 251-260
39. Nhuchhen, D.R., Sit, S.P.Layzell, D.B.: Alternative fuels co-fired with natural gas in the pre-calciner of a cement plant: Energy and material flows. Fuel, 295**,** 1-16 (2021).https://doi.org/10.1016/j.fuel.2021.120544.
40. Speer, U. Keiser, A. *High efficiency SNCR control system with online — CFD and NOx prediction for the cement industry*. in *IAS/PCA Cement Industry Technical Conference*. (2017). Calgary, AB, Canada: IEEE.https://doi.org/10.1109/CITCON.2017.7951853.
41. Nance, G., Abbas, T., Lowes, T.Bretz, J. *Calciner design for lower CO and NOx using MI-CFD analysis to optimize "Hot-Reburn" Conditions*. in *2011 IEEE-IAS/PCA 53rd Cement Industry Technical Conference*. (2011).https://doi.org/10.1109/CITCON.2011.5934552.
42. Abbas, T., Bretz, J., Garcia, F.Fu, J. *SO_2, CO and NO analysis of a SL calciner using a MI-CFD model*. in *IAS/PCA Cement Industry Conference (IAS/PCA CIC)*. (2015). Toronto, ON, Canada: IEEE.https://doi.org/10.1109/CITCON.2015.7122597.
43. Ratnadhariya, J.K. Channiwala, S.A.: Three zone equilibrium and kinetic free modeling of biomass gasifier – a novel approach. Renewable Energy, 34**,** 1050-1058 (2009).https://doi.org/10.1016/j.renene.2008.08.001.
44. Diyoke, C., Gao, N., Aneke, M., Wang, M.Wu, C.: Modelling of down-draft gasification of biomass – An integrated pyrolysis, combustion and reduction process. Applied Thermal Engineering, 142**,** 444-456 (2018).https://doi.org/10.1016/j.applthermaleng.2018.06.079.

45. Gao, N. Li, A.: Modeling and simulation of combined pyrolysis and reduction zone for a downdraft biomass gasifier. Energy Conversion and Management, 49**,** 3483-3490 (2008).https://doi.org/10.1016/j.enconman.2008.08.002.
46. Barba, D., Prisciandaro, M., Salladini, A.Mazziotti di Celso, G.: The Gibbs Free Energy Gradient Method for RDF gasification modelling. Fuel, 90**,** 1402-1407 (2011).https://doi.org/10.1016/j.fuel.2010.12.022.
47. Vounatsos, P., Atsonios, K., Itskos, G., Agraniotis, M., Panagiotis, G.Kakaras, E.: Classification of Refuse Derived Fuel (RDF) and Model Development of a Novel Thermal Utilization Concept Through Air-Gasification. Waste and Biomass Valorization, 7**,** (2016).10.1007/s12649-016-9520-6.
48. Haydary, J.: Aspen simulation of two-stage pyrolysis/gasification of carbon based solid waste. Chemical engineering transactions, 70**,** 1033-1038 (2018).
49. Fazil, A., Kumar, S.Mahajani, S.M.: Gasification and Co-gasification of paper-rich, high-ash refuse-derived fuel in downdraft gasifier. Energy, 263**,** 125659 (2023).https://doi.org/10.1016/j.energy.2022.125659.
50. Park, S.-W., Seo, Y.-C., Lee, S.-Y., Yang, W.-S., Oh, J.-H.Gu, J.-H.: Development of 8 ton/day gasification process to generate electricity using a gas engine for solid refuse fuel. Waste Management, 113**,** 186-196 (2020).https://doi.org/10.1016/j.wasman.2020.06.004.
51. Khosasaeng, T. Suntivarakorn, R.: Effect of Equivalence Ratio on an Efficiency of Single Throat Downdraft Gasifier Using RDF from Municipal solid waste. Energy Procedia, 138**,** 784-788 (2017).https://doi.org/10.1016/j.egypro.2017.10.066.
52. Ribeiro, A., Vilarinho, C., Araújo, J.Carvalho, J., *Refuse Derived Fuel (RDF) Gasification Using Different Gasifying Agents*, in *ASME 2017 International Mechanical Engineering Congress and Exposition*. (2017).10.1115/IMECE2017-71268.
53. Násner, A.M.L., Lora, E.E.S., Palacio, J.C.E., Rocha, M.H., Restrepo, J.C., Venturini, O.J.Ratner, A.: Refuse Derived Fuel (RDF) production and gasification in a pilot plant integrated with an Otto cycle ICE through Aspen plus™ modelling: Thermodynamic and economic viability. Waste Management, 69**,** 187-201 (2017).https://doi.org/10.1016/j.wasman.2017.08.006.
54. Dussadee, N., Homdoung, N., Ramaraj, R., Santisouk, K.Inthavideth, S.: Performance Analysis of Power Generation by Producer Gas from Refuse Derived Fuel-5 (RDF-5). International Journal of Sustainable and Green Energy, 4**,** 44-49 (2015).10.11648/j.ijrse.s.2015040101.17.
55. Uthaikiattikul, T., Cherdpong, S., Laohalidanond, K.Kerdsuwan, S. *Experimental Study of RDF-Gasification for Power Generation : University ' s RDF Model*. (2011).
56. Dalai, A., Batta, N.Schoenau, G.: Gasification of refuse derived fuel in a fixed bed reactor for syngas production. Waste management (New York, N.Y.), 29**,** 252-8 (2008).10.1016/j.wasman.2008.02.009.
57. Rao, M.S., Singh, S.P., Sodha, M.S., Dubey, A.K.Shyam, M.: Stoichiometric, mass, energy and exergy balance analysis of countercurrent fixed-bed gasification of post-consumer residues. Biomass and Bioenergy, 27**,** 155-171 (2004).https://doi.org/101016/jbiombioe200311003.
58. Galvagno, S., Casu, S., Casciaro, G., Martino, M., Russo, A.Portofino, S.: Steam Gasification of Refuse-Derived Fuel (RDF): Influence of Process Temperature on

Yield and Product Composition. Energy & Fuels, 20**,** 2284-2288 (2006).https://doi.org/10.1021/ef060239m.
59. IEA.100 MT Coal Gasification Target by 2030 – Policies. https://www.iea.org/policies/12931-100-mt-coal-gasification-target-by-2030. Accessed 27 Aug 2021
60. India, G.o.: Five Year Vision Document 2019-2024 Group III - Resources.
61. Lin, S., Kiga, T., Wang, Y.Nakayama, K.: Energy analysis of CaCO3 calcination with CO2 capture. Energy Procedia, 4**,** 356-361 (2011).https://doi.org/10.1016/j.egypro.2011.01.062.
62. Qiao, J. Chai, T.: Soft measurement model and its application in raw meal calcination process. Journal of Process Control, 22**,** 344-351 (2012).https://doi.org/10.1016/j.jprocont.2011.08.005.
63. A/S, F.L.:Low NOx calciner. https://search.ebscohost.com/login.aspx?direct=true&db=edspgr&AN=edspgr.10974992&site=eds-live&scope=site. Accessed 25 September 2021
64. Keefe, B.P. Shenk, R.E., *Staged combustion for low-NOx calciners*, in *Cement Industry Technical Conference*. (2002), IEEE: Jacksonville, FL, USA. pp. 255-264. https://doi.org/10.1109/.2002.1006511.
65. FLSmidth.Efficient alternative fuel combustion device. https://www.flsmidth.com/en-gb/products/pyro/hotdisc-combustion-device. Accessed 15 Sep 2021
66. das, A., *Prepol® Step Combustor - A Flexible Solution for Low Quality Alternative Fuels*. (2020), Thyssenkrupp
67. Mersmann, M. Schmitgen, S. *Versatile AF burning*. International cement review,May ed. (2021). DOI. https://www.cemnet.com/Articles/story/170758/versatile-af-burning.html.
68. Tokheim, L.-A., Mathisen, A., Øi, L., Jayarathna, C., Eldrup, N.Gautestad, T.: Combined calcination and CO2 capture in cement clinker production by use of electrical energy. 4**,** 101-109 (2019).
69. Mathisen, A., Skinnemoen, M.Nord, L. *Evaluating CO_2 Capture Technologies for Retrofit in Cement Plant*. in *12th International Conference on Greenhouse Gas Control Technologies, GHGT-12*. (2014). Austin, Texas.https://doi.org/10.1016/j.egypro.2014.11.684.
70. Gerbelová, H., van der Spek, M.Schakel, W.: Feasibility Assessment of CO2 Capture Retrofitted to an Existing Cement Plant: Post-combustion vs. Oxy-fuel Combustion Technology. Energy Procedia, 114**,** 6141-6149 (2017).https://doi.org/10.1016/j.egypro.2017.03.1751.
71. Baier, H. Menzel, K. *Potentials of AFR co-processing*. in *2011 IEEE-IAS/PCA 53rd Cement Industry Technical Conference*. (2011). St. Louis, MO, USA: IEEE.https://doi.org/10.1109/CITCON.2011.5934550.
72. Bapat, J.: Advanced fuel burning technologies in cement production. Indian Cement Review, 30, No 6**,** 44-46 (2016).
73. Unitherm Cemcon. M.A.S Kiln Burner,. https://www.unitherm.at/en/products/mas-kiln-burner. Accessed 26 Aug 2021
74. D'Hubert, X. *Latest burner profiles*. Global cement magazine,(2017). 10-18, DOI. https://www.globalcement.com/magazine/articles/1018-latest-burner-profiles.

75. Cunningham, R., *Swirlax burner conversion leads to 100% petroleum coke firing*, in *World cement*. (1998)
76. Lockwood, F.C. Ou, J.J. *Review: Burning refuse derived fuel in a rotary cement kiln*. in *Proceedings of the Institution of Mechanical Engineers, Part A: Journal of Power and Energy*. (1993). IMECHE.https://doi.org/10.1243/PIME_PROC_1993_207_008_02.
77. Concrete, M.U.:World first UK hydrogen trials demonstrate pathway to net zero cement. https://mineralproducts.org/News-CEO-Blog/2021/release31.aspx. Accessed 8 Oct 2021
78. Liedmann, B., Wirtz, S., Scherer, V.Krüger, B.: Numerical Study on the Influence of Operational Settings on Refuse Derived Fuel Co-firing in Cement Rotary Kilns. Energy Procedia, 120**,** 254-261 (2017).https://doi.org/10.1016/j.egypro.2017.07.176.
79. Haas, J. Weber, R.: Co-firing of refuse derived fuels with coals in cement kilns: combustion conditions for stable sintering. Journal of the Energy Institute, 83**,** 225-234 (2010).https://doi.org/10.1179/014426010X12839334040898.
80. Pieper, C., Wirtz, S., Schaefer, S.Scherer, V.: Numerical investigation of the impact of coating layers on RDF combustion and clinker properties in rotary cement kilns. Fuel, 283**,** 1-14 (2021).https://doi.org/10.1016/j.fuel.2020.118951.
81. Pieper, C., Liedmann, B., Wirtz, S., Scherer, V., Bodendiek, N.Schaefer, S.: Interaction of the combustion of refuse derived fuel with the clinker bed in rotary cement kilns: A numerical study. Fuel, 266**,** 138-144 (2020).https://doi.org/10.1016/j.fuel.2020.117048.
82. *Alternate fuels and raw materials in cement industry*, in *3rd International Conference on Alternate Fuels and Raw materials in the cement industry*. (2017). pp. 24-25
83. Ariyaratne, W.K., Malagalage, A., Melaaen, M.Tokheim, L.-A.: CFD Modeling of Meat and Bone Meal Combustion in a Rotary Cement Kiln. International Journal of Modeling and Optimization, 4**,** 263-272 (2014).10.7763/IJMO.2014.V4.384.
84. Dynamis, *D-FLAME Burners and Combustion Systems – Reference List*.
85. Dembla, A.K., Varshney, D., Singh, B.Singh, V., *Technological aspects of alternative fuels & raw material utilization in cement industry*, in *Conserve green & sustainable resources*. (2019): New Delhi
86. Mohapatra, B., Vyas, S.Shekhar, C., *Indian experience of using AFR in cement kiln*, in *13th NCB international seminar on cement and building materials*. (2013): New Delhi
87. Gautam, S., Jain, R., Mohapatra, B., Joshi, S.Gupta, R., *Energy Recovery from Solid Waste in Cement Rotary Kiln and its Environmental Impact*, in *24th International Conference on Solid Waste Technology & Management* (2009): Philadelphia
88. Clark, M. *Impacts of alternative fuels*. International Cement Review,August ed. (2019). 58-59, DOI.
89. Mora, N., Martinez, J.Ayala, C., *Clinker production with high chlorine alternative fuels*, in *15th International Congress on the Chemistry of Cement* (2019): Prague, Czech Republic
90. Schmidt, D., Abbas, T.Akritopoulos, M. *Modelling 100% AF TSR*. International Cement Review,September ed. (2019). DOI.
91. Mohapatra, B., Chaturvedi, S., Saxena, A., Sharma, P., Bohra, A.Naidu, G., *Use of alternative fuels and raw materials in cement industry in India - Prospects & challenges* in *Conserve green & sustainable resources*. (2019): New Delhi

92. Kara, M., Günay, E., Tabak, Y., Durgut, U., Yıldız, Ş.Enç, V.: Development of Refuse Derived Fuel for Cement Factories in Turkey. Combustion Science and Technology, 183**,** 203-219 (2010).https://doi.org/10.1080/00102202.2010.512580.
93. Mohapatra, B.N., Vyas S.K., Shekhar, C., *Indian experience of using AFR in cement kiln*, in *Industrial Angels*. (2014). pp. 5-13
94. Rahman, A., Rasul, M.G., Khan, M.M.K.Sharma, S.: Aspen Plus Based Simulation for Energy Recovery from Waste to Utilize in Cement Plant Preheater Tower. Energy Procedia, 61**,** 922-927 (2014).https://doi.org/10.1016/j.egypro.2014.11.996.
95. Kara, M.: Environmental and economic advantages associated with the use of RDF in cement kilns. Resources, Conservation and Recycling, 68**,** 21-28 (2012).https://doi.org/10.1016/j.resconrec.2012.06.011.
96. Pieper, C., Wirtz, S., Schaefer, S.Scherer, V.: Numerical investigation of the impact of coating layers on RDF combustion and clinker properties in rotary cement kilns. Fuel, 283**,** 1-13 (2021).https://doi.org/10.1016/j.fuel.2020.118951.
97. El-Salamony, A.-H.R., Mahmoud, H.M.Shehata, N.: Enhancing the efficiency of a cement plant kiln using modified alternative fuel. Environmental Nanotechnology, Monitoring & Management, 14**,** 100310 (2020).https://doi.org/10.1016/j.enmm.2020.100310.
98. Szűcs, T., Szentannai, P., Szilágyi, I.M.Bakos, L.P.: Comparing different reaction models for combustion kinetics of solid recovered fuel. Journal of Thermal Analysis and Calorimetry, 139**,** 555-565 (2020).10.1007/s10973-019-08438-8.
99. Çepelioğullar, Ö., Haykırı-Açma, H.Yaman, S.: Kinetic modelling of RDF pyrolysis: Model-fitting and model-free approaches. Waste Management, 48**,** 275-284 (2016).https://doi.org/10.1016/j.wasman.2015.11.027.
100. Balac, M., Radojevic, M., Jovanovic, V., Stojiljkovic, D.Manic, N.: THERMOGRAVIMETRIC KINETIC STUDY OF SOLID RECOVERED FUELS PYROLYSIS.(2017).
101. Cozzani, V., Petarca, L.Tognotti, L.: Devolatilization and pyrolysis of refuse derived fuels: characterization and kinetic modelling by a thermogravimetric and calorimetric approach. Fuel, 74**,** 903-912 (1995).https://doi.org/10.1016/0016-2361(94)00018-M.
102. Miskolczi, N., Buyong, F.Williams, P.T.: Thermogravimetric analysis and pyrolysis kinetic study of Malaysian refuse derived fuels. Journal of the Energy Institute, 83**,** 125-132 (2010).10.1179/014426010X12759937396632.
103. Danias, P. Liodakis, S.: Characterization of Refuse Derived Fuel Using Thermogravimetric Analysis and Chemometric Techniques. Journal of Analytical Chemistry, 73**,** 351-357 (2018).10.1134/S106193481804010X.
104. Bosmans, A., De Dobbelaere, C.Helsen, L.: Pyrolysis characteristics of excavated waste material processed into refuse derived fuel. Fuel, 122**,** 198-205 (2014).https://doi.org/10.1016/j.fuel.2014.01.019.
105. Grammelis, P., Basinas, P., Malliopoulou, A.Sakellaropoulos, G.: Pyrolysis kinetics and combustion characteristics of waste recovered fuels. Fuel, 88**,** 195-205 (2009).https://doi.org/10.1016/j.fuel.2008.02.002.
106. Luo, J., Li, Q., Meng, A., Long, Y.Zhang, Y.: Combustion characteristics of typical model components in solid waste on a macro-TGA. Journal of Thermal Analysis and Calorimetry, 132**,** 553-562 (2018).10.1007/s10973-017-6909-9.

107. Sharma, R. Sheth, P.N.: Multi reaction apparent kinetic scheme for the pyrolysis of large size biomass particles using macro-TGA. Energy, 151, 1007-1017 (2018).https://doi.org/10.1016/j.energy.2018.03.075.
108. Patra, T.K., Mukherjee, S.Sheth, P.N.: Process simulation of hydrogen rich gas production from producer gas using HTS catalysis. Energy, 173, 1130-1140 (2019).https://doi.org/10.1016/j.energy.2019.02.136.
109. Basu, P.: Biomass Gasification, Pyrolysis, and Torrefaction Practical Design and Theory. Elsevier Inc. (2013).https://doi.org/10.1016/C2011-0-07564-6.
110. Lopez, G., Artetxe, M., Amutio, M., Alvarez, J., Bilbao, J.Olazar, M.: Recent advances in the gasification of waste plastics. A critical overview. Renewable and Sustainable Energy Reviews, 82, 576-596 (2018).https://doi.org/10.1016/j.rser.2017.09.032.
111. Susastriawan, A.A., Saptoadi, H.Purnomo: Small-scale downdraft gasifiers for biomass gasification: A review. Renewable and Sustainable Energy Reviews, 76, 989-1003 (2017).https://doi.org/10.1016/j.rser.2017.03.112.
112. Ramalingam, S., Rajendiran, B.Subramiyan, S.: Recent advances in the performance of Co-Current gasification technology: A review. International Journal of Hydrogen Energy, 45, 230-262 (2020).https://doi.org/10.1016/j.ijhydene.2019.10.185.
113. Patra, T.K. Sheth, P.N.: Biomass gasification models for downdraft gasifier: A state-of-the-art review. Renewable and Sustainable Energy Reviews, 50, 583-593 (2015).https://doi.org/10.1016/j.rser.2015.05.012.
114. Molino, A.J., Iovane, P., Donatelli, A., Braccio, G., Chianese, S.Musmarra, D.: Steam Gasification of Refuse-Derived Fuel in a Rotary Kiln Pilot Plant: Experimental Tests. Chemical engineering transactions, 32, 337-342 (2013).
115. Ribeiro, A., Vilarinho, C., Araújo, J.Carvalho, J.: Refuse Derived Fuel (RDF) Gasification Using Different Gasifying Agents.(2017).10.1115/IMECE2017-71268.
116. Zainal, Z.A., Ali, R., Lean, C.H.Seetharamu, K.N.: Prediction of performance of a downdraft gasifier using equilibrium modeling for different biomass materials. Energy Conversion and Management, 42, 1499-1515 (2001).https://doi.org/10.1016/S0196-8904(00)00078-9.
117. Giltrap, D.L., McKibbin, R.Barnes, G.R.G.: A steady state model of gas-char reactions in a downdraft biomass gasifier. Solar Energy, 74, 85-91 (2003).https://doi.org/10.1016/S0038-092X(03)00091-4.
118. Babu, B.V. Sheth, P.N.: Modeling and simulation of reduction zone of downdraft biomass gasifier: Effect of char reactivity factor. Energy Conversion and Management, 47, 2602-2611 (2006).https://doi.org/10.1016/j.enconman.2005.10.032.
119. Sharma, S. Sheth, P.N.: Air–steam biomass gasification: Experiments, modeling and simulation. Energy Conversion and Management, 110, 307-318 (2016).http://dx.doi.org/10.1016/j.enconman.2015.12.030.
120. Barba, D., Capocelli, M., Cornacchia, G.Matera, D.A.: Theoretical and experimental procedure for scaling-up RDF gasifiers: The Gibbs Gradient Method. Fuel, 179, 60-70 (2016).https://doi.org/10.1016/j.fuel.2016.03.014.
121. Sharma, S. Sheth, P.: Air–steam biomass gasification: Experiments, modeling and simulation. Energy Conversion and Management, 110, 307-318 (2016).10.1016/j.enconman.2015.12.030.

122. Nhuchhen, D., Sit, S.Layzell, D.: Alternative fuels co-fired with natural gas in the pre-calciner of a cement plant: Energy and material flows. Fuel, 295**,** 120544 (2021).10.1016/j.fuel.2021.120544.
123. Wydrych, J. Dobrowolski, B.: Numerical calculations of limestone calcination in cement industry with use of shrink core model. 2078**,** 020034 (2019).10.1063/1.5092037.
124. Mikulcic, H., von Berg, E., Vujanovic, M., Priesching, P., Tatschl, R.Duic, N.: Numerical analysis of cement calciner fuel efficiency and pollutant emissions. Clean Technologies and Environmental Policy, 1-11 (2013).https://doi.org/10.1007/s10098-013-0607-5.
125. Wang, X., Mikulčić, H., Dai, G., Zhang, J., Tan, H.Vujanović, M.: Decrease of high-carbon-ash landfilling by its Co-firing inside a cement calciner. Journal of Cleaner Production, 293**,** 1-11 (2021).https://doi.org/10.1016/j.jclepro.2021.126090.
126. Nakhaei, M., Grévain, D., Jensen, L.S., Glarborg, P., Dam–Johansen, K.Wu, H.: NO emission from cement calciners firing coal and petcoke: A CPFD study. Applications in Energy and Combustion Science, 5**,** 1-13 (2021).https://doi.org/10.1016/j.jaecs.2021.100023.
127. Cristea, E.-D. Conti, P., *Numerical Investigation on Multiphase Reacting/Combusting Turbulent Flows: Aerodynamics, Kinetics, Heat and Mass Transfer Inside a Cement Kiln Precalciner*, in *ASME-JSME-KSME 2019 8th Joint Fluids Engineering Conference*. (2019), ASME: San Francisco, California, USA.https://doi.org/10.1115/AJKFluids2019-5033.
128. Rodríguez Gómez, N., Alonso, M., Grasa, G.Abanades, J.: Heat requirements in a calciner of $CaCO_3$ integrated in a CO_2 capture system using CaO. Chemical Engineering Journal 138**,** 148-154 (2008).https://doi.org/10.1016/j.cej.2007.06.005.
129. Mikulčić, H., von Berg, E., Vujanović, M., Priesching, P., Perković, L., Tatschl, R.Duić, N.: Numerical modelling of calcination reaction mechanism for cement production. Chemical Engineering Science, 69**,** 607-615 (2012).https://doi.org/10.1016/j.ces.2011.11.024.
130. Dou, H., Chen, Z.Huang, J. *Numerical Study of the Coupled Flow Field in a Double-spray Calciner*. in *International Conference on Computer Modeling and Simulation*. (2009). Macau, China: IEEE.https://doi.org/10.1109/ICCMS.2009.45.
131. Qiao, J., Zhao, X.Chai, T. *Soft Measurement Model of Raw Meal Decomposition Ratio Based on Data Driven for Raw Meal Calcination Process*. in *Chinese Control Conference (CCC)*. (2019). Guangzhou, China: IEEE.https://doi.org/10.23919/ChiCC.2019.8866598.
132. Zhang, Y., Cao, S.-X., Shao, S., Chen, Y., Liu, S.-L.Zhang, S.-S.: Aspen Plus-based simulation of a cement calciner and optimization analysis of air pollutants emission. Clean Technologies and Environmental Policy, 13**,** 459-468 (2011).https://doi.org/10.1007/s10098-010-0328-y.
133. Akhtar, S.S., Abbas, T., Goetz, J.Kandamby, N. *A Calciner at its Best*. in *IAS/PCA Cement Industry Conference* (2019). St. Louis, MO, USA: IEEE.https://doi.org/10.1109/CITCON.2019.8729114.
134. Mone, S., Gawali, B.S., Joshi, M.S.Vitankar, V., *Detailed CFD model for predicting combustion, calcination and pollutant formation in calciner*, in *16th NCB International Seminar on Cement, Concrete and Building Materials*. (2019): New Delhi

135. Jianxiang, Z., Yan, W.Xiuli, Z. *Hydrodynamic Modelling of Gas and Solid Flows in the Pre-Calciner*. in *Asia-Pacific Power and Energy Engineering Conference*. (2012). Shanghai, China: IEEE.https://doi.org/10.1109/APPEEC.2012.6307057.

136. Nance, G., Abbas, T., Lowes, T.Bretz, J. *Calciner design for lower CO and NOx using MI-CFD analysis to optimize "Hot-Reburn" Conditions*. in *IAS/PCA 53rd Cement Industry Technical Conference*. (2011). St. Louis, MO, USA: IEEE.https://doi.org/10.1109/CITCON.2011.5934552.

137. Abbas, T., Akritopoulos, M.Akhtar, S.S. *Reducing pressure drop in pyro-processing*. in *IAS/PCA Cement Industry Conference (IAS/PCA)*. (2018). Nashville, TN, USA: IEEE.https://doi.org/10.1109/CITCON.2018.8373111.

138. Nakhaei, M., Grévain, D., Jensen, L.S., Glarborg, P., Dam–Johansen, K.Wu, H.: NO emission from cement calciners firing coal and petcoke: A CPFD study. Applications in Energy and Combustion Science, 5**,** 100023 (2021).https://doi.org/10.1016/j.jaecs.2021.100023.

139. ZhuGang, Y. Hui, L. *Soft sensor for apparent degree of calcination in NSP cement production line*. in *The 2nd International Conference on Computer and Automation Engineering (ICCAE)*. (2010). Singapore: IEEE.https://doi.org/10.1109/ICCAE.2010.5451912.

140. Zhe, S., Zhugang, Y., Qiang, Z., Xianlei, Z.Dezhi, X. *Sliding mode control for calciner outlet temperature via regression modeling*. in *The 27th Chinese Control and Decision Conference (2015 CCDC)*. (2015). Qingdao, China: IEEE.https://doi.org/10.1109/CCDC.2015.7162761.

141. Yu, H., Wang, F., Wang, X.Ma, X. *Study on dynamic models of cement calciner based on typical working conditions*. in *2016 35th Chinese Control Conference (CCC)*. (2016). Chengdu, China: IEEE.https://doi.org/10.1109/ChiCC.2016.7553677.

142. Lin, X., Yang, B.Cao, D. *Multi-Parameter Control for Precalciner Kiln System of Cement Using Adaptive Dynamic Programming*. in *2009 International Workshop on Intelligent Systems and Applications*. (2009). IEEE.https://doi.org/10.1109/IWISA.2009.5072967.

143. Yu, H., Liu, W.Dong, H. *Research on recognition of working condition for calciner and grate cooler based on expert system*. in *12th International Conference on Control Automation Robotics & Vision (ICARCV)*. (2012). Guangzhou, China: IEEE.https://doi.org/10.1109/ICARCV.2012.6485411.

144. Su, Z., Yuan, Z., Zhang, Q.Zhang, X. *An online switching modeling for calciner outlet temperature via grey correlation analysis*. in *2014 IEEE International Conference on Information and Automation (ICIA)*. (2014).10.1109/ICInfA.2014.6932705.

145. Qiao, J. Tian, F. *Abnormal Condition Detection Integrated with Kullback Leibler Divergence and Relative Importance Function for Cement Raw Meal Calcination Process*. in *2nd International Conference on Industrial Artificial Intelligence (IAI)*. (2020). Shenyang, China: IEEE.https://doi.org/10.1109/IAI50351.2020.9262170.

146. Zhang, M., Yan, H.Yu, L. *Adaptive Multi-dimensional Taylor Network Control for Cement Calciner Outlet Temperature*. in *4th Information Technology, Networking, Electronic and Automation Control Conference (ITNEC)*. (2020). IEEE.https://doi.org/10.1109/ITNEC48623.2020.9084964.

147. Zheng, J., Du, W., Lang, Z.Qian, F.: Modeling and Optimization of the Cement Calcination Process for Reducing NOx Emission Using an Improved Just-In-Time

Gaussian Mixture Regression. Industrial & Engineering Chemistry Research, 59, 4987-4999 (2020).https://doi.org/10.1021/acs.iecr.9b05207.

148. Cai, Y.: Modeling for the Calcination Process of Industry Rotary Kiln Using ANFIS Coupled with a Novel Hybrid Clustering Algorithm. Mathematical Problems in Engineering, 2017, 1-9 (2017).https://doi.org/10.1155/2017/1067351.
149. IEA Bioenergy. *The past, present and future for biomass gasification*. in *The IEA Bioenergy Webinar Series* (2020).
150. Chatterjee, A. Sui, T.: Alternative fuels – Effects on clinker process and properties. Cement and Concrete Research, 123, 1-19 (2019).https://doi.org/10.1016/j.cemconres.2019.105777.
151. Wang, C., *Utilization of refuse derived fuel in cement industry - A case study in China*, in *School of Energy Systems* (2017), Lappeenranta University of Technology pp. 1-56
152. Greil, C., Hirschfelder, H.Turna, O., *Operational results from gasification of waste material and biomass in fixed bed and circulating fluidised bed gasifiers*, in *Conference on gasification: the clean choice for carbon management*. (1999): Noordwijk, Netherlands. pp. 1-10
153. Hjuler, K., *Gasification with separate calcination*. (2013), FLSmidth A/S, Valby (DK) Denmark. pp. 1-7
154. Guo, W., Li, S., He, C., Zhang, C., Li, D., Li, Q., Wang, K., Li, Z., Xiao, J., Cheng, X., Yang, C., Hayashi, T., Inoue, E., Katahata, T., Katoh, S., Ichitani, N., Hashmimoto, A.Toshihiro, J., *Waste-processing apparatus*. (2013). pp. 1-42
155. Schuermann, H. Feiss, M., *Plant for producing cement clinker with gasification reactor for difficult fuels*. (2016), KHD Humboldt Wedag GmbH, Koeln (DE). pp. 1-6
156. Weil, S., Hamel, S.Krumm, W.: Hydrogen energy from coupled waste gasification and cement production—a thermochemical concept study. International Journal of Hydrogen Energy, 31, 1674-1689 (2006).https://doi.org/10.1016/j.ijhydene.2005.12.015.
157. Streit, N. Feiss, M., *Pyro-processing*, in *World cement*. (2020), Palladian Publications Ltd. pp. 30-34
158. European cement research academy GmbH: Carbon capture technology - Options and potentials for the cement industry.(2007). pp. 1-96.https://www.vdz-online.de/fileadmin/redaktion/files/pdf/ECRA_Technical__Report_CCS_Phase_I.pdf.
159. Mineral Products Association, Cinar LtdgGmBH, V.: Options for switching UK cement production sites to near zero CO2 emission fuel: Technical and financial feasibility (2019).
160. Talebi, G. Goethem, M.W.M.V.: Synthesis Gas from Waste Plasma Gasification for Fueling Lime Kiln. Italian association of chemical engineering, 37, 1-6 (2014).
161. Hue, F., Pasquier, M., Pasquier, M.Lac, P., *Cement clinker manufacturing plant*. (2016), VICAT, Paris la Defense (FR) pp. 1-9
162. de Lorena Diniz Chaves, G., Siman, R.R., Ribeiro, G.M.Chang, N.-B.: Synergizing environmental, social, and economic sustainability factors for refuse derived fuel use in cement industry: A case study in Espirito Santo, Brazil. Journal of Environmental Management, 288, 112401 (2021).https://doi.org/10.1016/j.jenvman.2021.112401.
163. Yassin, L., Lettieri, P., Simons, S.J.R.Germanà, A.: Techno-economic performance of energy-from-waste fluidized bed combustion and gasification processes in the UK

context. Chemical Engineering Journal, 146**,** 315-327 (2009).https://doi.org/10.1016/j.cej.2008.06.014.
164. Nam–Chol, O., Hyo–Song, P., Yong–Chol, S., Yong–Hyok, R.Yong–Nam, K.: A feasibility study of energy recovery of RDF from municipal solid waste. Energy Sources, Part A: Recovery, Utilization, and Environmental Effects, 40**,** 2914-2922 (2018).10.1080/15567036.2018.1514431.
165. López-Sabirón, A.M., Fleiger, K., Schäfer, S., Antoñanzas, J., Irazustabarrena, A., Aranda-Usón, A.Ferreira, G.A.: Refuse derived fuel (RDF) plasma torch gasification as a feasible route to produce low environmental impact syngas for the cement industry. Waste Manag Res, 33**,** 715-22 (2015).0734242X15586476 [pii]
10.1177/0734242X15586476 [doi].
166. Dejtrakulwong, C. Patumsawad, S.: Four zones modeling of the downdraft biomass gasification process: Effects of moisture content and air to fuel ratio. Energy Procedia, 52**,** 142-149 (2014).https://doi.org/10.1016/j.egypro.2014.07.064.
167. Chen, X., Xie, J., Mei, S., He, F.Yang, H.: RDF pyrolysis by TG-FTIR and Py-GC/MS and combustion in a double furnaces reactor. Journal of Thermal Analysis and Calorimetry, 136**,** 893-902 (2019).10.1007/s10973-018-7694-9.
168. Dou, B., Park, S., Lim, S., Yu, T.-U.Hwang, J.: Pyrolysis Characteristics of Refuse Derived Fuel in a Pilot-Scale Unit. Energy & Fuels, 21**,** 3730-3734 (2007).10.1021/ef7002415.
169. Cerone, N., Contuzzi, L., Barisano, D.Braccio, G.: Biomass/RDF gasification in an updraft reactor: Modelling and analysis of the thermochemical process.(2009).
170. Sharma, A.: Equilibrium modeling of global reductions for a downdraft (biomass) gasifier. Energy Conversion and Management, 49**,** 832-842 (2008).10.1016/j.enconman.2007.06.025.
171. Johansen, J.M., Jakobsen, J.G., Frandsen, F.J.Glarborg, P.: Release of K, Cl, and S during Pyrolysis and Combustion of High-Chlorine Biomass. Energy & Fuels, 25**,** 4961-4971 (2011).10.1021/ef201098n.
172. Bioenergy, I., *Gas analysis in gasification of biomass and waste* (2018). pp. 65-66
173. Barman, N.S., Ghosh, S.De, S.: Gasification of biomass in a fixed bed downdraft gasifier – A realistic model including tar. Bioresource Technology, 107**,** 505-511 (2012).https://doi.org/10.1016/j.biortech.2011.12.124.
174. Rüdiger, H., Kicherer, A., Greul, U., Spliethoff, H.Hein, K.R.G.: Investigations in Combined Combustion of Biomass and Coal in Power Plant Technology. Energy & Fuels, 10**,** 789-796 (1996).10.1021/ef950222w.
175. Rüdiger, H., Kicherer, A., Greul, U., Spliethoff, H.Hein, K.R.G., Pyrolysis Gas from Biomass and Pulverized Biomass as Reburn Fuels in Staged Coal Combustion. in A.V. Bridgwater and D.G.B. Boocock, Developments in Thermochemical Biomass Conversion: Volume 1 / Volume 2. pp. 1387-1398. Springer Netherlands, Dordrecht (1997).10.1007/978-94-009-1559-6_109.
176. Salem, A.M., Zaini, I.N., Paul, M.C.Yang, W.: The evolution and formation of tar species in a downdraft gasifier: Numerical modelling and experimental validation. Biomass and Bioenergy, 130**,** 105377 (2019).https://doi.org/10.1016/j.biombioe.2019.105377.
177. Robert H. Perry, Don W. GreenMaloney, K.O.: Perry's Chemical Engineers' Handbook. McGraw-Hill(1997).

178. Channiwala, S.A. Parikh, P.P.: A unified correlation for estimating HHV of solid, liquid and gaseous fuels. Fuel, 81**,** 1051-1063 (2002).https://doi.org/10.1016/S0016-2361(01)00131-4.
179. Tinaut, F., Melgar, A., Pérez, J.Horrillo, A.: Effect of biomass particle size and air superficial velocity on the gasification process in a downdraft fixed bed gasifier. An experimental and modelling study. Fuel Processing Technology - FUEL PROCESS TECHNOL, 89**,** 1076-1089 (2008).10.1016/j.fuproc.2008.04.010.
180. Taiheiyo Engineering.RSP (Reinforced Suspension Preheater). http://www.taiheiyo-eng.co.jp/en/engineering/rsp-reinforced-suspension-preheater. Accessed June 13 2021
181. Pieper, C., Liedmann, B., Wirtz, S., Scherer, V., Bodendiek, N.Schaefer, S.: Interaction of the combustion of refuse derived fuel with the clinker bed in rotary cement kilns: A numerical study. Fuel, 266**,** 117048 (2020).https://doi.org/10.1016/j.fuel.2020.117048.
182. CRC Handbook of Chemistry and Physics, 84th Edition Edited by David R. Lide (National Institute of Standards and Technology). . Journal of the American Chemical Society, 126**,** 1586-1586 (2004).10.1021/ja0336372.
183. Levenspiel, O.: Chemical Reaction Engineering. Industrial & Engineering Chemistry Research, 38**,** 4140-4143 (1999).10.1021/ie990488g.
184. Rahman, A., Rasul, M.G., Khan, M.M.K.Sharma, S., Cement kiln process modeling to achieve energy efficiency by utilizing agricultural biomass as alternative fuels. Thermofluid Modeling for Energy Efficiency Applications. pp. 197-225. Academic Press(2015).
185. Aspentech, *Getting started modelling processes with solids*. (2001)
186. Aspentech, *User Guide*. (1999)
187. Ergun, R., Guo, J.Huebner-Keese, B., Cellulose. in B. Caballero, P.M. Finglas, and F. Toldrá, Encyclopedia of Food and Health. pp. 694-702. Academic Press, Oxford (2016).https://doi.org/10.1016/B978-0-12-384947-2.00127-6.
188. Dürig, T. Karan, K., Chapter 9 - Binders in Wet Granulation. in A.S. Narang and S.I.F. Badawy, Handbook of Pharmaceutical Wet Granulation. pp. 317-349. Academic Press(2019).https://doi.org/10.1016/B978-0-12-810460-6.00010-5.
189. Baldevraj, R.S.M. Jagadish, R.S., 14 - Incorporation of chemical antimicrobial agents into polymeric films for food packaging. in J.-M. Lagarón, Multifunctional and Nanoreinforced Polymers for Food Packaging. pp. 368-420. Woodhead Publishing(2011).https://doi.org/10.1533/9780857092786.3.368.
190. Joseph, S.M., Krishnamoorthy, S., Paranthaman, R., Moses, J.A.Anandharamakrishnan, C.: A review on source-specific chemistry, functionality, and applications of chitin and chitosan. Carbohydrate Polymer Technologies and Applications, 2**,** 100036 (2021).https://doi.org/10.1016/j.carpta.2021.100036.
191. Bumgardner, J.D., Murali, V.P., Su, H., Jenkins, O.D., Velasquez-Pulgarin, D., Jennings, J.A., Sivashanmugam, A.Jayakumar, R., 4 - Characterization of chitosan matters. in J.A. Jennings and J.D. Bumgardner, Chitosan Based Biomaterials Volume 1. pp. 81-114. Woodhead Publishing(2017).https://doi.org/10.1016/B978-0-08-100230-8.00004-2.
192. Srinivasan, H., Kanayairam, V.Ravichandran, R.: Chitin and chitosan preparation from shrimp shells Penaeus monodon and its human ovarian cancer cell line, PA-1. Int J Biol Macromol, 107**,** 662-667 (2018).10.1016/j.ijbiomac.2017.09.035.

193. Wu, H., Williams, G.R., Wu, J., Wu, J., Niu, S., Li, H., Wang, H.Zhu, L.: Regenerated chitin fibers reinforced with bacterial cellulose nanocrystals as suture biomaterials. Carbohydr Polym, 180**,** 304-313 (2018).10.1016/j.carbpol.2017.10.022.
194. Medina, E., Caro, N., Abugoch, L., Gamboa, A., Díaz-Dosque, M.Tapia, C.: Chitosan thymol nanoparticles improve the antimicrobial effect and the water vapour barrier of chitosan-quinoa protein films. Journal of Food Engineering, 240**,** 191-198 (2019).https://doi.org/10.1016/j.jfoodeng.2018.07.023.
195. Santos, V.P., Marques, N.S.S., Maia, P., Lima, M.A.B., Franco, L.O.Campos-Takaki, G.M.: Seafood Waste as Attractive Source of Chitin and Chitosan Production and Their Applications. Int J Mol Sci, 21**,** (2020).10.3390/ijms21124290.
196. Santos, V.P., Marques, N.S.S., Maia, P.C.S.V., Lima, M.A., Franco, L.D.Campos-Takaki, G.M. *Seafood Waste as Attractive Source of Chitin and Chitosan Production and Their Applications*. International Journal of Molecular Sciences,(2020). 21, DOI.
197. Invixo.Co-polymer of Ethylene & Maleic Anhydride. http://www.invixochemicals.com/co-polymer-of-ethylene-maleic-anhydride.php. Accessed 10 October 2022
198. Klein, R.A., Signal Mountain, Carrier, A.M.Hixson, *Ethylene-maleic anhydride derivatives and their uses* (1999): USA. pp. 15
199. Samide, A., Merisanu, C., Tutunaru, B.Iacobescu, G.E.: Poly (Vinyl Butyral-Co-Vinyl Alcohol-Co-Vinyl Acetate) Coating Performance on Copper Corrosion in Saline Environment. 25**,** 439 (2020).
200. Epple, M., Meyer, F.Enax, J.: A Critical Review of Modern Concepts for Teeth Whitening. Dent J (Basel), 7**,** (2019).10.3390/dj7030079.
201. Xiong, B., Loss, R.D., Shields, D., Pawlik, T., Hochreiter, R., Zydney, A.L.Kumar, M.: Polyacrylamide degradation and its implications in environmental systems. npj Clean Water, 1**,** 17 (2018).10.1038/s41545-018-0016-8.
202. Herth, G., Schornick, G.L. Buchholz, F., Polyacrylamides and Poly(Acrylic Acids). Ullmann's Encyclopedia of Industrial Chemistry. pp. 1-16. https://doi.org/10.1002/14356007.a21_143.pub2.
203. Janajreh, I., Adeyemi, I.Elagroudy, S.: Gasification feasibility of polyethylene, polypropylene, polystyrene waste and their mixture: Experimental studies and modeling. Sustainable Energy Technologies and Assessments, 39**,** 100684 (2020).https://doi.org/10.1016/j.seta.2020.100684.
204. Chen, W.-H., Wang, C.-W., Kumar, G., Rousset, P.Hsieh, T.-H.: Effect of torrefaction pretreatment on the pyrolysis of rubber wood sawdust analyzed by Py-GC/MS. Bioresource Technology, 259**,** 469-473 (2018).https://doi.org/10.1016/j.biortech.2018.03.033.
205. Chen, W.-H., Wang, C.-W., Ong, H.C., Show, P.L.Hsieh, T.-H.: Torrefaction, pyrolysis and two-stage thermodegradation of hemicellulose, cellulose and lignin. Fuel, 258**,** 116168 (2019).https://doi.org/10.1016/j.fuel.2019.116168.
206. Gan, Y.Y., Chen, W.-H., Ong, H.C., Sheen, H.-K., Chang, J.-S., Hsieh, T.-H.Ling, T.C.: Effects of dry and wet torrefaction pretreatment on microalgae pyrolysis analyzed by TG-FTIR and double-shot Py-GC/MS. Energy, 210**,** 118579 (2020).https://doi.org/10.1016/j.energy.2020.118579.

207. Zhou, S., Brown, R.C.Bai, X.: The use of calcium hydroxide pretreatment to overcome agglomeration of technical lignin during fast pyrolysis. Green Chemistry, 17**,** 4748-4759 (2015).10.1039/C5GC01611H.
208. Watkins, D., Nuruddin, M., Hosur, M., Tcherbi-Narteh, A.Jeelani, S.: Extraction and characterization of lignin from different biomass resources. Journal of Materials Research and Technology, 4**,** 26-32 (2015).https://doi.org/10.1016/j.jmrt.2014.10.009.
209. Wu, C.-H., Chang, C.-Y.Tseng, C.-H.: Pyrolysis products of uncoated printing and writing paper of MSW. Fuel, 81**,** 719-725 (2002).https://doi.org/10.1016/S0016-2361(01)00180-6.
210. Pandey, B., Sheth, P.N.Prajapati, Y.K.: Air-CO2 and oxygen-enriched air-CO2 biomass gasification in an autothermal downdraft gasifier: Experimental studies. Energy Conversion and Management, 270**,** 116216 (2022).https://doi.org/10.1016/j.enconman.2022.116216.
211. Tavares, R., Monteiro, E., Tabet, F.Rouboa, A.: Numerical investigation of optimum operating conditions for syngas and hydrogen production from biomass gasification using Aspen Plus. Renewable Energy, 146**,** 1309-1314 (2020).https://doi.org/10.1016/j.renene.2019.07.051.
212. Silva, I.P., Lima, R.M.A., Silva, G.F., Ruzene, D.S.Silva, D.P.: Thermodynamic equilibrium model based on stoichiometric method for biomass gasification: A review of model modifications. Renewable and Sustainable Energy Reviews, 114**,** 1-22 (2019).https://doi.org/10.1016/j.rser.2019.109305.
213. Haydary, J. *Modelling of Gasification of Refuse-derived fuel (RDF) based on laboratory experiments*. (2016).
214. Sarkar, S.: Fuels and Combustion: Third Edition. Universities Press(2010).
215. Kumar, J.N., Suryanarayanan, R., Chitra, P., Dharmalingam, P., Prabhu, H.R.Velayutham, V.: Energy performance assessment for equipment and utility systems. Bureau of Energy Efficiency(2015).
216. FLSmidth, *Burner bibble*. (2003)
217. Kawasaki super green product.CKK System. https://global.kawasaki.com/en/corp/sustainability/green_products/ckk_system.html. Accessed 26 Oct 2022
218. Mittal, A. Rakshit, D.: Utilization of cement rotary kiln waste heat for calcination of phosphogypsum. Thermal Science and Engineering Progress, 20**,** 100729 (2020).https://doi.org/10.1016/j.tsep.2020.100729.
219. Sar, E.: Low Carbon Technology Roadmap for the Indian Cement Sector: Status Review (2018).
220. Moore, D.:White Cement Manufacture. https://www.cementkilns.co.uk/ck_white.html. Accessed 1 October 2022
221. Global Cement.White cement review. https://www.globalcement.com/magazine/articles/890-white-cement-review. Accessed
222. Mishra, N., *J K White Cement's journey of continual improvement*, in *International Cement Review*. (2021). pp. 30-32
223. Herfort, D., Macphee, D.E.Duffy, J.A., *Method for increasing the reflectance of cement*. (2009): Denmark. pp. 9

224. Benmohamed, M., Alouani, R., Jmayai, A., Ben Haj Amara, A.Ben Rhaiem, H.: Morphological Analysis of White Cement Clinker Minerals: Discussion on the Crystallization-Related Defects. International Journal of Analytical Chemistry, 2016**,** 1259094 (2016).https://doi.org/10.1155/2016/1259094.
225. Flenco Fuid systems.Reliance Petcoke Gasification Project – India. https://www.flenco.com/index.php/projects/52-sleipner-oil-field-north-sea-norway-4. Accessed 13 Oct 2022
226. Ultratech Cement Limited.Birla White Cement completes 25 years of operations. https://www.ultratechcement.com/about-us/media/features/birla-white-cement-completes-25-years-of-operations. Accessed 06.07.2022
227. Bureau of Energy Efficiency, Performing financial analysis. Energy performance assessment for equipment and utility systems. pp. 141-153. (2013).
228. S. S. Krishnan, Venkatesh Vunnam, P. Shyam Sunder, A. Murali RamakrishnanRamakrishna, G.: A study for energy efficiency in the Indian cement industry.(2012). pp. 81-82.https://www.cstep.in/drupal/sites/default/files/2019-02/CSTEP_Energy_Efficiency_in_Indian_Cement_Industry_Report_2012.pdf.
229. The C2FO team.How Is the Indian Cement Industry's Supply Chain Tackling Rising Inflation and Input Costs? https://www.c2fo.com/en-in/resources/how-is-the-indian-cement-industrys-supply-chain-tackling-rising-inflation-and-input-costs/. Accessed
230. Peters, M.S., Timmerhaus, K.D.West, R.E.: Plant Design and Economicsfor Chemical Engineers. The McGraw-Hill Companies(1991).
231. Ministry of Labour & Employment, G.o.I., *Order*. (2022): New Delhi
232. Refuse derived fuel. https://dir.indiamart.com/impcat/refuse-derived-fuel.html. Accessed 23 Oct 2022
233. Bureau of Energy Efficiency, M.o.P., Government of India: Pathways for accelerated transformation in industry sector. 10-11 (2020).
234. Ajay Tewari, *Amend the Energy Conservation (Energy Consumption Norms and Standards for Designated Consumers)*, Ministry of power, Editor. (2022)
235. Raj pal, *Amend the Energy Consumption Norms and Standards for Designated Consumers*. (2020). pp. 1-3
236. Indiamart.Bottom ash. https://www.indiamart.com/proddetail/bottom-ash-18788691730.html. Accessed 22 Oct 2022
237. Suhartono, S., Nurhadi, Utomo, Y., Djunaedi, I., Santosa, A.Hidayat, Y.: Design Calculation of a100 kWe Refuse Derived Fuel Gasifier. (2020).
238. Rajakumaran, V., Dillibabu, V.Lakhsmanan, T.: Design and modelling of MSW (RDF) gasifier. IOP Conference Series: Materials Science and Engineering, 1130**,** 012023 (2021).https://doi.org/10.1088/1757-899x/1130/1/012023.
239. Sharma, P., Gupta, B., Pandey, M., Singh Bisen, K.Baredar, P.: Downdraft biomass gasification: A review on concepts, designs analysis, modelling and recent advances. Materials Today: Proceedings, 46**,** 5333-5341 (2021).https://doi.org/10.1016/j.matpr.2020.08.789.

List of Publications

International Journals

1. Sharma, P., S. Sen, P. N. Sheth and B. N. Mohapatra (2022). "Multizone model of a refuse derived fuel gasification: A thermodynamic Semi-empirical approach."**Energy Conversion and Management** 260: 115621.
2. Sharma, P., P. N. Sheth and B. N. Mohapatra (2023). "Co-processing of petcoke and producer gas obtained from RDF gasification in a white cement plant: A techno-economic analysis."**Energy** 265: 126248.
3. Sharma, P., P. N. Sheth and B. N. Mohapatra (2022). "Recent Progress in Refuse Derived Fuel (RDF) Co-processing in Cement Production: Direct Firing in Kiln/Calciner vs Process Integration of RDF Gasification. "**Waste and Biomass Valorization**. 10.1007/s12649-022-01840-8.
4. Sharma, P., P. N. Sheth and S. Sen. "Aspen Plus simulation of an inline calciner for white cement production with a fuel mix of petcoke and syngas" **Energy.** 282: 128892

Full papers communicated

1. Sharma, P., P. N. Sheth (2023). "Air/O_2-enriched air gasification of high ash refuse derived fuel (RDF) and co-gasification with biomass pellets." **Fuel**. **Under review.**
2. Sharma, P., P. N. Sheth, Moon Chourasia, and B. N. Mohapatra (2023). "Chemical Characterization of Refuse Derived Fuel (RDF) using Py-GC/MS." **Journal of Analytical and Applied Pyrolysis. Comments received.**

Book chapter

1. Sharma, P., P. Sheth and B. N. Mohapatra (2019). Waste to energy: Issues, opportunities and challenges for RDF utilization in Indian cement industry. Proceedings of the 7th International Conference on Advances in Energy Research. Mumbai, Springer: 891-900.
2. Sharma, P., B. N. Mohapatra, Ankur Mittal and P.N. Sheth (2022). Futuristic TSR for Indian Cement Industry. Alternative Fuels – A green solution for Indian Cement Industry. National Council for Cement and Building Materials: ISBN:978-81-961444-2-5, 184-191.

International Conference Proceedings

1. Prateek Sharma, Pratik N Sheth & B.N. Mohapatra: Parametric investigation on Refuse derived fuel gasification in a downdraft gasifier, International conference on Sustainable Energy and Clean Technologies (ICSECT-22), Gandhinagar, Gujarat, 2022 **(Received Best paper award)**
2. Prateek Sharma, Pratik N Sheth & B.N. Mohapatra: Chemical Characterization of Refuse Derived Fuel (RDF) using Py-GC/MS, International Conference ontechnological interventions for sustainability (CHEM-CONFLUX22), 2022
3. Prateek Sharma, Pratik N Sheth & B.N. Mohapatra: Modelling and experimental studies for process integration of RDF gasification in cement manufacturing process, 17th NCB International conference on Cement, Concrete and Building Materials, New Delhi, 2022
4. Bibekananda Mohapatra, Prateek Sharma, Kapil Kukreja, S K Chaturvedi & Pratik N Sheth: Potential use of paddy stubble as an energy source in Indian cement industry, 8th International Conference on Advances in Energy Research, IIT Bombay, 2022
5. Prateek Sharma, Pratik N Sheth, B.N. Mohapatra & Rakshit Khandelwal: Thermodynamic stoichiometric equilibrium model for RDF gasification in a fixed bed downdraft gasifier, CHEMCON 2021, Bhubhneshwar, India

Biography

Biography of the candidate

Prateek Sharma completed his B.E. in Chemical Engineering from C.R State College of Engineering, Murthal, Haryana in 2007. He obtained his master's degree in Energy and Environment Management from the Indian Institute of Technology, Delhi in 2017. He joined BITS Pilani as a Part-time Ph.D. student in the Chemical Engineering department in December 2018 and is currently working as Manager and Programme Leader of Advanced Fuel Technology programme in National Council for Cement and Building Materials, Ballabgarh, Haryana. He is an Accredited Energy Auditor of Bureau of Energy Efficiency. He has 14 years of experience in the field of energy audits, process optimization, waste heat recovery, techno-economic feasibility and waste utilization studies for the cement and power sector. He has completed +40 nos. projects related to cement plants and thermal power plants. He has successfully completed international assignments in Oman, Kenya, Spain. He is also course coordinator and faculty for PG Diploma course on Cement technology accredited by AICTE. He has mentored more than ten students of M.Sc and Chemical Engineering backgrounds. Waste heat recovery and waste utilization as alternative fuels in the cement industry are some of his research interests.

Biography of supervisor

Dr Pratik N Sheth is currently working as a Professor and Head- Chemical Engineering Department at Birla Institute of Technology and Science, Pilani, Pilani Campus, Rajasthan. He has over 20 years of teaching, research and academic administration experience. He did his BE (Chemical Engineering) from Government Engineering College, Gandhinagar, Gujarat University , ME (Chemical Engineering) and PhD from Birla Institute of Technology and Science, Pilani, Pilani Campus, Rajasthan.

His current research interests include Pyrolysis, Biomass Gasification, Modeling and Simulation, Computational Fluid Dynamics, and Renewable Energy Sources. He has around 61 research publications including conference proceedings and book chapters to his credit which have been published over the years in various International and National Journals and Conference Proceedings. Dr Sheth has completed four research projects (one funded from Department of Science and Technology, New Delhi; one from Birla Cellulosic, Kharach and two from BITS Pilani). The research publications of Dr Sheth have received the total number of citation of 1960 as per Google scholar website (https://scholar.google.co.in/citations?hl=en&user=S6Im2SYAAAAJ) as on May 02, 2023.

Dr Sheth has guided two PhD students in the area of hydrogen production from biomass and biomass pyrolysis. Dr Sheth has reviewed several research articles of various international journals such as Biomass and Bioenergy, Renewable Energy, Energy, Chemical Engineering Science, Case studies in thermal engineering, Fuel, Energy Conversion and Management, Renewable and Sustainable Energy Reviews, Separation Science and Technology, Journal of water process engineering, Journal of Petroleum technology, Journal of Engineering Tribology, Applied thermal engineering, Waste and Biomass Valorization and African Journal of Agricultural Research.

Dr Sheth is a Life Member of Indian Institute of Chemical Engineers (IIChE) and Institution of Engineers, India. Dr Sheth was Chairman - IIChE - Pilani Regional Centre and has held various positions. He organized a Workshop on Analytical Instruments for Chemical and Environmental Engineers (WAICEE - 2013) during March 22 – 23, 2013. He was the joint organizing secretary for the 8th Annual Session of Students' Chemical Engineering Congress (SCHEMCON - 2012) during September 21 – 22, 2012. Recently, Dr Sheth has organized a Workshop on Analytical Instruments for Chemical and Environmental Engineers (WAICEE - 2017) during Feb 10-11, 2017.

Biography of co-supervisor

Dr B.N. Mohapatra is former Director General of National Council for Cement and Building Materials, Ballabgarh, Haryana, India. He previously, served as Vice President & Corporate Quality Head of Ambuja Cement Limited under the banner of LafargeHolcim and held several key positions in Vikram Cement Works (UltraTech Cement Ltd) under Aditya Birla Group, OCL India Research Institute - Dalmia Institute of Scientific and Industrial Research (DISIR). He is enriched with 13 years of research and over 22 years of industry experience with strong academic relations with premier institutes. He has cross functional experience in development of low carbon cements and clinker, mineralogy & microstructure of cement and concrete, product development & diversification, advanced comminution techniques, energy & environment improvement and Total Quality Management. Previously, Dr Mohapatra made pioneering contribution in the field of co-processing of AF in cement industry in India. He did his M.Sc in Chemistry from Utkal University, Odisha and PhD from Sambalpur University, Odisha.

Dr B.N. Mohapatra has guided one PhD student in the area of Portland Limestone Cement. Dr B.N. Mohapatra was Chairman of Cement Sectoral Committee of Bureau of Energy Efficiency (BEE), Govt. of India, member of Expert Appraisal Committee-Industry-1 sector by Ministry of Environment, Forest and Climate Change (MOEF&CC), Govt. of India, member of Committee for Sustainability of fly ash management system by Central Pollution Control Board (CPCB), nominated by NITI Aayog, Govt. of India as Member of Low Carbon Technology Committee, Circular Economy in Gypsum & handling of waste, member of Research Council of CSIR- National Physical Laboratory (NPL), member of Various Technical Committees of Bureau of Indian Standards (BIS), DISIR, member of Academic Council of AKS University, Satna, member of Board of Studies of Khallikote Autonomous College, Berhampur. He has received Lifetime Achievement Award for the year 2021 by Indian Concrete Institute. He has published more than 130 technical papers in Journals/ conferences. He has authored a book on "Application of X-Ray Diffractometry in Cement Quality Control System".

Appendix I

Fig. I.1 Photograph of downdraft gasifier set up

Fig. I.2 Photograph of Thermo-Gravimetric Analyzer (TGA)

Fig. I.3 Photograph of gas chromatography set up

Fig. I.4 Photograph of Pyrolysis-gas chromatography-mass spectrometry set up

Fig. I.5 Photograph of Palletiser

Appendix II

Gasifier Matlab Code

```
% code for pyrolysis zone by taking 1 kg of RDF as basis%

mc_kg = 0.0357;
ash_kg = 0.3186;

C_kg = 0.3857;

H_kg = 0.0566;% amount of hydrogen present in RDF in kg%

O_kg = 0.1897;% amount of hydrogen present in RDF in kg%

N_kg = 0.007;% amount of hydrogen present in RDF in kg%

S_kg = 0.003;% amount of hydrogen present in RDF in kg%

Cl_kg = 0.00;% amount of hydrogen present in RDF in kg%
C_moles = C_kg/12;% kmoles%
H_moles = H_kg/1;% kmoles%
O_moles = O_kg/16;% kmoles%
N_moles = N_kg/14;% kmoles%
S_moles = S_kg/32;% kmoles%
```

```
Cl_moles = Cl_kg/35.5;% kmoles%
ash_moles = ash_kg/74.31;

% taking basis of 1 kmole/mole of carbon%
C = C_moles/C_moles;
H = H_moles/C_moles;
O = O_moles/C_moles;
N = N_moles/C_moles;
S = S_moles/C_moles;
Cl = Cl_moles/C_moles;
mc_moles = mc_kg/(18*C_moles);
Ash = ash_moles/C_moles;

RDF_Formula =
"C"+""+C+""+"H"+""+H+""+"O"+""+O+""+"N"+""+N+""+"S"+""+S+""+"Cl"+""+Cl+""+
mc_moles+""+"H2O"

Mol_wt = (12*C + H + 16*O + 14*N + 32*S + 35.5*Cl + 74.31*Ash)

symsQ_dryQ_lQ_evapQ_waterQ_RDFCp_liquidwaterC_RDFMSHL
M = (mc_moles)*18;% Moisture content of RDF%
SH = 4.184;% Specific Heat of water in J/gm.K%
L = 2260;% Latent heat of vaporization of water%
Q_l = M*SH*(100-25);% Heat needed to reach the water to its boiling point%
Q_evap = M*L;% Total Latent heat of vaporization%
Q_dry = (Q_l + Q_evap)/10^3;% in KJ%

% pyrolysis zone%
```

```
% temp = input("Enter the reduction zone temperature ");% temp in Kelvin%
Tar = (Mol_wt*0.045*0.55)/18.2283;%
% Tar = (-0.1365*temp + 216.21)/(1000*18.2283);

y = 0.75; x = 0.85;% y = O2 and x = H2%

A = [1, 1, 1, 1, 2, 0, 0, 0, 0, 0, 1;
    0, 0, 0, 4, 4, 2, 2, 0, 2, 1, 1.003;
    0, 1, 2, 0, 0, 0, 1, 0, 0, 0, 0.33;
    0, 0, 0, 0, 0, 0, 0, 0, 0, 0, 1;
    0, 0, 0, 0, 0, 0, 0, 1, 0, 0, 0;
    0, 0, 0, 0, 0, 0, 0, 0, 0, 1, 0;
    0, 0, 0, 0, 0, 0, 0, 0, 1, 0, 0;
    0, 0, 0, 0, 0, 0, 1, 0, 0, 0, Tar*0.33;
    0, 0, 0, 0, 0, 2, x, 0, 0, 0, 0.5*1.003*x;
    0, 28, -44, 0, 0, 0, 0, 0, 0, 0, 0;
    0, 0, 0, 16, -28, 0, 0, 0, 0, 0, 0]

B = [C; H; O; Tar; N/2; Cl; S; 0.8*y*O; (0.5*x*H-x*S-0.5*x*Cl); 0; 0];
comp_mat = inv(A)*B;
nChar = comp_mat(1);
nCO = comp_mat(2);
nCO2 = comp_mat(3);
nCH4 = comp_mat(4);
nC2H4 = comp_mat(5);
nH2 = comp_mat(6);
nH2O = comp_mat(7) + mc_moles;
nN2 = comp_mat(8);
```

```
nH2S = comp_mat(9);
nHCl = comp_mat(10);
nTar = comp_mat(11);
nAsh = Ash;

% Combustion Zone Output%
syms ERKNCONCO2

% mO2_mrdf = input("Enter ratio: ");
% actual_oxygen = (Mol_wt*mO2_mrdf)/32;
ER = input("Enter the ER: ");%
stoichiometric_oxygen = 0.5*(2 + 0.5*H - O);%
actual_oxygen = ER*stoichiometric_oxygen;%
nN2 = nN2 + 3.76*(actual_oxygen);%
K = 0.05;
M = 3.5606;
if actual_oxygen>= 0
    after_comb_H2 = nH2 - 2*(actual_oxygen);
if after_comb_H2 > 0
        nH2O = nH2O + (nH2 - after_comb_H2);
        nH2 = after_comb_H2;
residual_oxygen = 0;
else
        after_comb_H2 = 0
        nH2O = nH2O + nH2;
residual_oxygen = (actual_oxygen - nH2*0.5);
        nH2 = 0;
end
end
```

```
ifresidual_oxygen> 0
after_comb_char = nChar - (2*(M*M*K + 1)/(M*M*K + 2))*residual_oxygen;
ifafter_comb_char>= 0
nCO = nCO + ((M*M*K)/(M*M*K + 2))*residual_oxygen;
        nCO2 = nCO2 + (1/(M*M*K + 2))*residual_oxygen;
residual_oxygen = 0;
nChar = after_comb_char;
else
after_comb_char = 0;
residual_oxygen = residual_oxygen - ((M*M*K + 2)/(2*(M*M*K + 1)))*nChar;
nCO = nCO + ((M*M*K)/(2*M*M*K + 2))*nChar;
        nCO2 = nCO2 + (1/(2*M*M*K + 2))*nChar;
nChar = after_comb_char;
end
end


ifresidual_oxygen> 0
    after_comb_C2H4 = nC2H4 - (residual_oxygen/3);
if after_comb_C2H4 >= 0
        nH2O = nH2O + 2*(nC2H4 - after_comb_C2H4);
        nCO2 = nCO2 + 2*(nC2H4 - after_comb_C2H4);
        nC2H4 = after_comb_C2H4;
else
        nH2O = nH2O + 2*nC2H4;
        nCO2 = nCO2 + 2*nC2H4;
        nC2H4 = 0;
end
end
```

```
nChar

nAsh

nCO;

nCO2;

nCH4;

nC2H4;

nH2;

nN2;

nH2S;

nHCl;

nH2O = nH2O + 0.5;

nTar;


ntotal = nN2+nH2+nCO+nH2O+nCO2+nCH4+nTar;


yN2 = (nN2/ntotal);

yCO = (nCO/ntotal);

yCO2 = (nCO2/ntotal);

yCH4 = (nCH4/ntotal);

yH2 = (nH2/ntotal);

yH2O = (nH2O/ntotal);

yTar = (nTar/ntotal);


mdN2 = (nN2/ntotal)*(101825.625/(8.314*1200));

mdCO = (nCO/ntotal)*(101825.625/(8.314*1200));

mdCO2 = (nCO2/ntotal)*(101825.625/(8.314*1200));

mdCH4 = (nCH4/ntotal)*(101825.625/(8.314*1200));
```

```
mdH2 = (nH2/ntotal)*(101825.625/(8.314*1200));

mdH2O = (nH2O/ntotal)*(101825.625/(8.314*1200));

mdTar = (nTar/ntotal)*(101825.625/(8.314*1200));

range = [0 0.245];

ICs = [101825.625; 1; 1200; mdN2; mdCO2 ;mdCO ; mdCH4; mdH2O ; mdH2; mdTar]
;% P, v, T, N2, CO2, CO, CH4, H2O, H2

[zsol,varsol] = ode45(@red1,range,ICs);
```

REDUCTION ZONE

```
function diffeqs = red(z,var)

P = var(1);
v = var(2);
T = var(3);
n1 = var(4);
n2 = var(5);
n3 = var(6);
n4 = var(7);
n5 = var(8);
n6 = var(9);
n7 = var(10);

EA = 77390.0; EB = 121620.0; EC = 19210.0; ED = 36150.0; EE = 32840; EF =
16736;
AA = 36.161; AB = 15170.0; AC = 0.004189; AD = 0.07301; AE = 2.824*10^-2; AF
= 70;
% Char reactivity factor%
CRF = 500;
Rconst = 8.314;% in   Joules / (mole K)%
```

```
rho_air = 1.1854;% Kg/m^3*%

n = [n1; n2; n3; n4; n5; n6; n7];

Molwt = [28.01; 44.01; 28.01; 16.04; 18.02; 2.02; 18.31];

sum1 = 0;

for i = 1:7

    sum1 = sum1 + n(i);

end

% T = 1200K%

%heat  capacities constants for the gaseous components N2 CO2  CO CH4 H2O H2
Tar respectively%


CA = [3.280; 5.457; 3.376; 1.702; 3.47; 3.249; 10.66];

CB = [0.000593; 0.001047; 0.000557; 0.009081; 0.00145; 0.000422; 0.01452 ];

CC = [0.0; 0.0; 0.0; -0.000002164; 0.0; 0.0; -0.00000153];

CD = [40000.0; -115700.0; -3100.0; 0.0; 12100.0; 8300.0; 441000];


% deltaA,B,C,D for all rxns%

deltaA = [-0.476000; 1.384000; -6.567000; 7.951000; 1.86; -1.187];

deltaB   =   [-7.040001*(10^-4);   -1.240*(10^-3);   7.46600*(10^-3);   -
8.708000*(10^-3); 2.7*10^-4; -15.00*(10^-3)];

deltaC  =  [0.000000;  0.000000;  -2.164000*(10^-6);  2.164000*10^-6;  0;  -
0.00000153];

deltaD    =    [1.962000*(10^5);    7.980000*(10^4);    7.010000*(10^4);
9.700000*(10^3); 58200; 447694];


J  =  [179370.156250;  130546.515625;  -58886.800781;  189433.312500;  -
51443.541780; -7651.45734];

I = [25.655949; 7.642021; 32.541370; -24.899353; 18.007000; 3.34];
```

```
for j=1:6
    K(j) = exp((-J(j)/(Rconst * T)) + ( deltaA(j) * log(T)) + ( (
deltaB(j)/2)*T) + ((deltaC(j)/6)*(T^2)) + ((deltaD(j)/2)*(T^-2)) + I(j)) ;
deltaH(j) = J(j) + Rconst * (( deltaA(j) * T)+(deltaB(j) * (T^2)/2)
+(deltaC(j) * (T^3)/3)-(deltaD(j)/T));
end

avg_mol_wt = 0;

for j = 1:7
    p(j)= n(j)/sum1;
avg_mol_wt = avg_mol_wt + p(j)*Molwt(j);
end

rho_gas = (P*avg_mol_wt)/(Rconst*T*1000);

for k = 1:7
    c(k) = Rconst * ( CA(k) + CB(k) * T + CC(k) * (T^2) + CD(k) * (T^-2));
end

sum = 0; sum2 = 0; sum3 = 0;

rA = sum1 * CRF * AA * exp(-EA/(Rconst * T)) * (p(2) - (p(3)*p(3))/K(1));
rB = sum1 * CRF * AB * exp(-EB/(Rconst * T)) * (p(5)-(p(3) * p(6)/K(2)));
rC = sum1 * CRF * AC * exp(-EC/(Rconst * T)) * ((p(6) * p(6))-(p(4)/K(3)));
rD = sum1 * CRF * AD * exp(-ED/(Rconst * T)) * ((p(4) * p(5))-(p(3) *
p(6)*p(6)*p(6))/K(4));
rE = sum1 * CRF * AE * exp(-EE/(Rconst * T)) * ((p(2) * p(6)) - (p(5)* p(3))/
K(5));
```

```
% rF = sum1 * CRF * AF * exp(-EF/(Rconst * T)) * (p(3) * p(6) - ((p(5)^1.25)
* (p(7)^0.25)/ K(6)));
rF = sum1 * CRF * AF * exp(-EF/(Rconst * T)) * K(6)* (p(5)^1) * (p(7)^1.25)
;

% N2 CO2  CO CH4 H2O H2 Tar respectively%
R = [0; -rA + rE; (2 * rA + rB + rD - rE + rF); rC - rD; - rB - rD - rE -
(0.67 * rF); rB - (2 * rC) + (3 * rD) + rE + (1.18 * rF); -rF ];
sumrdeltaH  = (rA * deltaH(1))  + (rB * deltaH(2)) + ( rC * deltaH(3)) + (rD
* deltaH(4)) + (rE * deltaH(5)) + (rF * deltaH(6));% sum of riHi%

for j = 1:6
sum  = sum + n(j) * c(j);% sum of nxcx%
    sum2 = sum2 + R(j);% sum of Rx%
    sum3 = sum3 + ( R(j) * c(j));% sum of Rxcx%
end

dPdz = ((1183 * rho_gas * (v^2)/rho_air) + (388.19 * v) + 79.896);% dpdz%
dvdz  =  (  (1/(sum  +  sum1  *  Rconst))  *  ((sum*sum2/sum1)-(sumrdeltaH/T)-
dPdz*(v/T + v*sum/P) - sum3) ) ;% dvdz%
dTdz = ( ( (1/(v*sum)) * ( -sumrdeltaH - v * dPdz - P*dvdz - (sum3*T)) ) )
;% dTdz%
dn1dz = ( (1/v)*(R(1) - n(1)*dvdz) ) ;% dn1dz%
dn2dz = ( (1/v)*(R(2) - n(2)*dvdz) ) ;% dn2dz%
dn3dz = ( (1/v)*(R(3) - n(3)*dvdz) ) ;% dn3dz%
dn4dz = ( (1/v)*(R(4) - n(4)*dvdz) ) ;% dn4dz%
dn5dz = ( (1/v)*(R(5) - n(5)*dvdz) ) ;% dn5dz%
dn6dz = ( (1/v)*(R(6) - n(6)*dvdz) ) ;% dn6dz%
dn7dz = ( -(1/v)*(R(7) - n(7)*dvdz) ) ;% dn7dz%
```

```
diffeqs(1,1) = dPdz;

diffeqs(2,1) = dvdz;

diffeqs(3,1) = dTdz;

diffeqs(4,1) = dn1dz;

diffeqs(5,1)= dn2dz;

diffeqs(6,1) = dn3dz;

diffeqs(7,1) = dn4dz;

diffeqs(8,1) = dn5dz;

diffeqs(9,1) = dn6dz;

diffeqs(10,1) = dn7dz;


end
```